2007

Synthesis and functionalizations of tetrapyrrole derivatives

Lijuan Jiao

Louisiana State University and Agricultural and Mechanical College, ljiao1@lsu.edu

SYNTHESIS AND FUNCTIONALIZATIONS OF TETRAPYRROLE DERIVATIVES

A Dissertation

Submitted to the Graduate Faculty of the
Louisiana State University and
Agricultural and Mechanical College
in partial fulfillment of the
requirements for the degree of
Doctor of Philosophy

In

The Department of Chemistry

by
Lijuan Jiao
B.S., Shandong University, China 2000
M. S., University of Science and Technology of China, 2003
December, 2007

DEDICATION

This Dissertation is dedicated to my parents in China for their unconditional love, their continuous support, and their understanding of every decision that I made throughout of my life.

谨以此文献给我远在中国的亲爱的父母，感谢他们这麽多年以来所给予我的无微不至的关爱,默默无闻的支持与理解。

ACKNOWLEDGEMENTS

My last, but not least, appreciation goes to my loved husband, Mr. Erhong Hao. He always stands next to me and supports me. He provides me with the deepest love, the continuous support and encouragement. He offers me his broad shoulder to let my mind rest when I was exhausted from research. It is him who makes chemistry research romantic and attractive. It is him who always believed in me and kept on pushing me to do my best. It is also him who always reminds me to cherish and follow my dreams, so that I will never lose myself. Without him, I would never be able to finish my doctoral research in such a short period. Also, without him, my life will not be so bright, colorful and lovely.

TABLE OF CONTENTS

ABSTRACT

Chapter 1 of this Dissertation presents a brief overview of the history of tetrapyrrole derivatives and of their fundamental properties. Overviews of porphyrins, benzoporphyrins, chlorins and porphycenes are presented.

Work presented in Chapter 2 through Chapter 4 mainly focuses on the syntheses and functionalization of chromophore-extended porphyrin derivatives. Several new synthetic routes for the syntheses and functionalizations of extended porphyrins either at the β-position or at the meso-position of porphyrin are developed. From these improved synthetic routes, the regio-selective syntheses of porphyrin derivatives are described. Chapter 2 mainly focuses on the syntheses of β,β'-fused methylenepropanoporphyrins and related porphyrin dimers. Chapter 3 mainly describes a new synthetic route for selective synthesis of benzoporphyrin regioisomers and Chapter 4 mainly discusses new work on the efficient synthesis of the so-called "Hangman Porphyrin" analogs.

Chapter 5 consists two parts. The first part is devoted results of work on the total synthesis of an important porphycene derivative, 9-capronyl-oxytetrakis(methyoxyethyl)-porphycene, which has already been shown to have attractive potential applications in photodynamic therapy of tumors. The second part of Chapter 5 concerns the improved syntheses of 2,2'-bipyrrole, which is an important part of our effort to improve the synthesis of porphycene and related tetrapyrrole derivatives. The potential utility of these 2,2'-bipyrroles as bio-probes and ion-binding reagents are also tested.

Chapter 6 reports mechanistic studies on the unique regio-selective formation of mono-(L)-aspartylchlorin-e_6. This important photodynamic therapy (PDT) photosensitizer has recently undergone a structural revision, and the work reported in this Chapter provides a rationale for the

formation of the unexpected regioisomeric structure now known to belong to mono-(L)-aspartylchlorin-e$_6$.

CHAPTER 1. INTRODUCTION

1.1 History of Tetrapyrroles

"Tetrapyrrole" is a term widely used to refer to a class of compounds which have four pyrrole type rings linked together, usually through single-atom bridges at the α-positions of the pyrrole rings (see *Figure 1-1* for general examples).
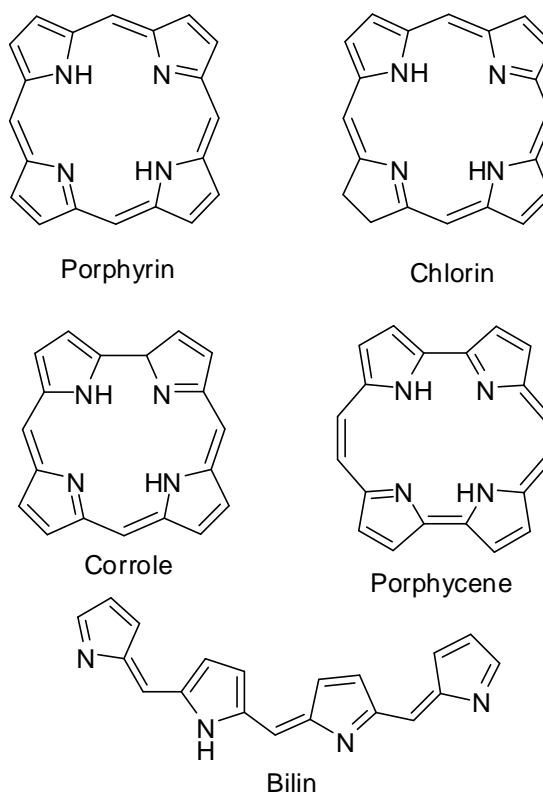
Figure 1-1. Typical tetrapyrrole structures: top and middle, macrocylic structure; bottom, open-chain structure of tetrapyrroles.

Among those, the macrocyclic structure is the most common arrangements for the four pyrrole rings. Porphyrins, chlorins, corroles and porphycenes are representative examples of macrocyclic tetrapyrroles, while bilins represent examples for linear or open-chain tetrapyrroles. Research interests were turned to tetrapyrroles at around 1900. It was found that if the tetrapyrrole derivatives, such as chlorophylls and bilanes, were absent, life would not be able to exist on this

planet[1]. Bile pigments (see *Figure 1-1*) have the bilin carbon skeleton and represent the most common linear tetrapyrroles, play an important role in heme breakdown and the proper functions of algae and plants; examples are bilirubin and phycobilins (see **9** in *Figure 1-2*) in cyanobacteria.
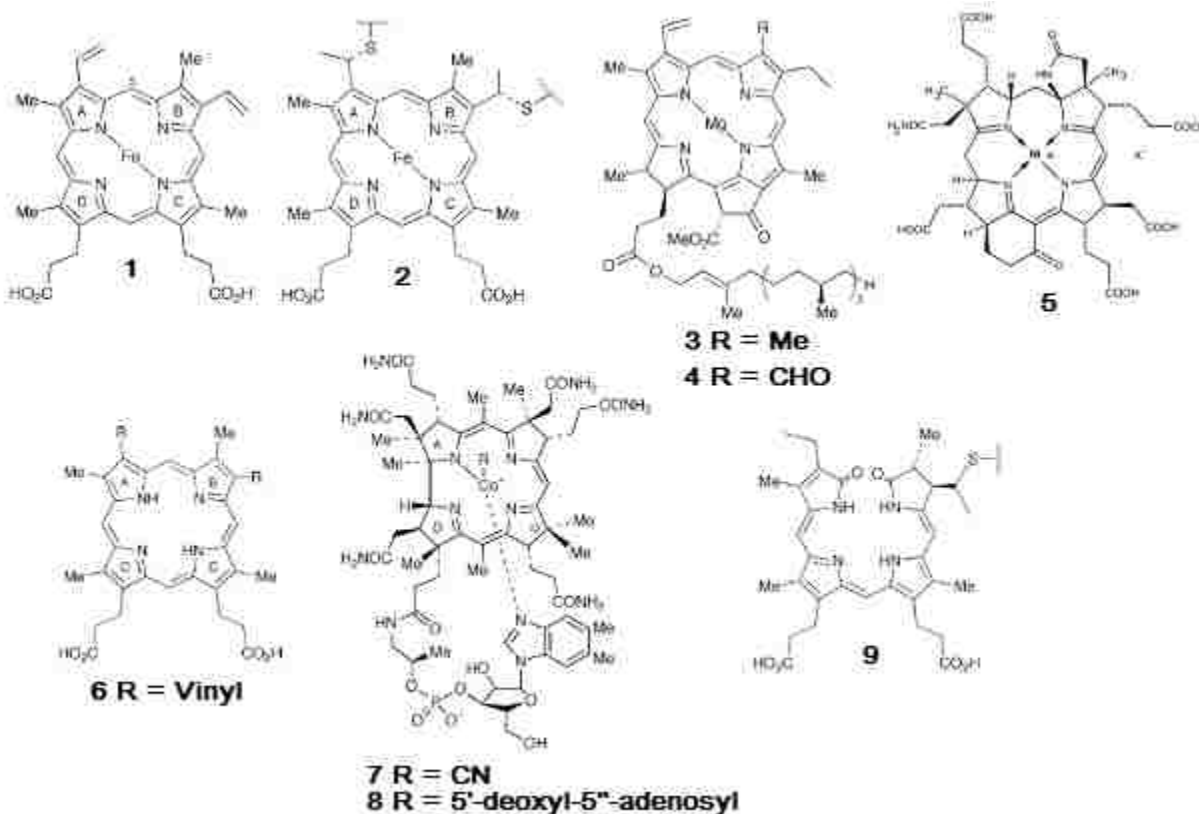
Figure 1-2. Chemical structures of heme (**1**), cytochrome c (**2**), chlorophyll *a* (**3**) and chlorophyll *b* (**4**), coenzyme F430 (**5**), protoporphyrin IX (**6**), vitamin B_{12} (**7** and **8**) and phycobolin (**9**).

As a typical bile pigment, phycocyanin was found to abundantly exist in algae and serve as light-harvesters for the algae. On the other hand, macrocyclic tetrapyrroles play a central and important role as pigments of life; examples are heme and chlorophyll a (see **1** and **3** in *Figure 1-2*) in oxygen storage and transportion and photosynthesis, respectively; cytochrome c (see **2** in *Figure 1-2*) is important in electron transport. Porphyrins, chlorins and corrins possess the basic structure for these biologically important macrocylic tetrapyrrole molecules (see *Figure 1-2*). In biology, these macrocyclic tetrapyrrole structures are usually found associated with different types

2

of metals in order to have proper functionality. The most commonly found metals are iron, magnesium, cobalt and nickel. With the appropriate one of these four metal ions inserted, these different macrocycles are able to properly functionalize in living systems and carry out widely differing biological functions. For example, the well-known heme (see **1** in *Figure 1-2*) and siroheme are the representative examples for iron tetrapyrrole complexes; chlorophylls *a* and *b* (see **3** and **4** in *Figure 1-2*) are the representative examples for magnesium tetrapyrrole; vitamin B_{12} (see **7** and **8** in *Figure 1-2*) and coenzyme B_{12} are the typical examples for cobalt tetrapyrrole; coenzyme F430 (see **5** in *Figure 1-2*) is the representative example for a nickel tetrapyrrole. The fine tuning of the metal reactivity is important to ensure their proper function in biology. For example, chlorophylls possess the appropriate light absorption regions in the biosystem[1]. Meanwhile, phytochrome (see **2** in *Figure 1-2*)[2], which has been found in small amounts in plants, plays vitally important functions by controlling growth and development in plants.

The identification of the macrocylic tetrapyrrole structures had attracted much attention from chemists, especially Hans Fischer. It was in 1864 that Stokes first observed chlorophylls *a* and *b* by using partition methods to isolate the mixture of these two pigments from green leaves[3]. The first synthetic preparation of a porphyrin was reported by Thudichum in 1867[4a]. In 1884, Nencki isolated the first pure porphyrin by preparing hematoporphyrin hydrochloride directly from isolated heme[4b]. It was in 1906 that Willstätter's group eventually separated these two chlorophylls (*a* and *b*) from each other. Their separation was based on Stokes' partition methods; besides that, they also introduced the column chromatography[5] for the separation. After separation, from combustion experiments, Willstätter realized that these chlorophylls contained the metal magnesium. One year later, he confirmed that magnesium was part of the chlorophyll molecule from his experiments and he reported that chlorophylls were organomagnesium

complexes. After that, experiments were performed to remove the magnesium and to generate a metal-free product, named "pheophytin". After chemical manipulation, such as burning, oxidization, reduction, and pyrolysis, many of the degradation products were found to be pyrroles or contain pyrrolic residues. Using less drastic degradation, much of the original molecules were retained and found to be deeply colored stable substances. Then, in 1912, Küster[6] suggested that pheophytin and chlorophylls shared a similar macrocyclic structure, in which four pyrrole derived rings were joined to each other by methane bridges. This structure is now known as the porphyrin macrocycle. Initially, when Küster proposed his suggested structure, Fischer (who was the major porphyrin researcher of the day) doubted his results. It was because Fisher thought there would be a stability problem issue with the large ring-size present in Küster's proposal. Then, in 1925, Keilin[7] discovered that heme (see **1** in *Figure 1-2*) was an organic complex of iron. His discovery was soon confirmed by Fischer and Kämmerer. Also, iron was removed from heme, and protoporphyrin IX was generated. The subsequent chemical manipulation provided similar results as those of pheophytin. One year later, in 1926, Fisher synthesized etioporphyrin-I. From his own synthesis, Fisher also realized the presence of similar aromatic structure as suggested by Küster and accepted Küster's idea. By the late 1930's, Willstätter and Fischer had already worked out the complex structures of both chlorophyll *a* (see **3** in *Figure 1-2*) and heme (see **1** in *Figure 1-2*) from hemoglobin[8]. It was a surprise to discover that although chlorophyll and heme were such difference in their appearances and functionalities, they actually shared a similar basic macrocylic structure and gave similar visible spectra. Later on, the structures of heme (see **1** in *Figure 1-2*) and protoporphyrin IX (**6**) opened the way to understanding how the prosthetic group of the cytochromes *c* isolated from many living things could play a crucially important role in biological electron transport[9].

In the 1940's chromatography became widely used as an important tool in product separation and purification; this provided great opportunities to study the complex structures of tetrapyrroles. It was in 1948 that vitamin B_{12} was first isolated as deep red colored crystals[10]. Its structure was studied in both the USA and Britain, separately by two teams led by Karl Folkers and Sir Alexander Todd. Based on their studies and the efforts of many other research groups, in 1953, cobalt was found in vitamin B_{12}. At that time, even the macrocyclic ligand that held cobalt was identified[11]. It was found that there was a direct link between rings A and D to form a smaller macrocycle in vitamin B_{12}, which is different from heme (**1**) and chlorophyll *a* (**3**). The parent ring system of vitamin B_{12} was named *corrin*. Then, in 1960, Woodward accomplished the first total synthesis of chlorophyll *a*[12].

1.2 Overview of Porphyrins

1.2.1 Introduction
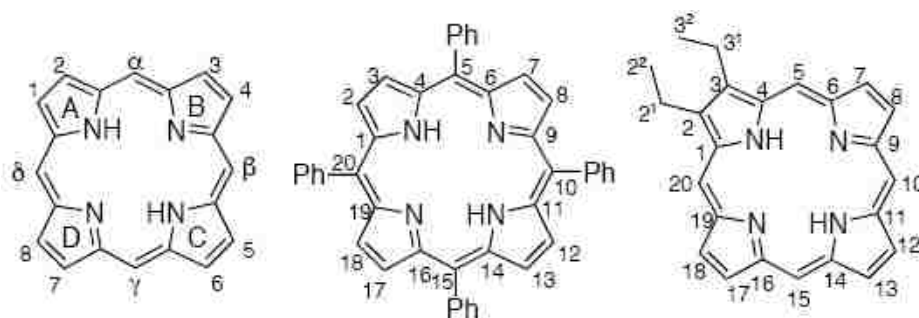
Figure 1-3. Fischer (left) and IUPAC (middle and right) nomenclature systems for porphyrins.

Porphyrin research has been well-established for over a century. It was Thudichum[4a] who first isolated a porphyrin from hemoglobin in 1867. Ever since then, attracted to their interesting physical, chemical, and spectroscopic properties and the essential biological functionalities of porphyrins, scientists from many different areas have devoted themselves to porphyrin research. So far, there has been at least nine Nobel Prizes in Chemistry have been awarded for outstanding

achievements in porphyrin chemistry. Most recently there have also been published the twenty volumes of "The Porphyrin Handbook". Here, only a brief overview of related porphyrins aspects will be discussed, which is intended to help the reader better understand the research projects that will be discussed in detail in the following chapters of this Dissertation.

Porphyrins naturally occur as colored pigments and have been described as "the Pigments of Life"[12]. Porphyrins and their derivatives occur widely in nature and play important roles in biological processes. Representative examples of porphyrin derivatives are hemes, (found in myoglobins, hemoglobins, cytochromes, catalases and peroxidases), chlorophylls and bacteriochlorophylls. Nature uses them in the most important processes of photosynthesis (chlorophylls and bacteriochlorophylls), and in oxygen-transportation, in electron-transfer and also in catalytic oxidations (hemes). For example, heme, the iron(II) complex of protoporphyrin IX, is the prosthetic group in hemoglobins and myoglobins. These heme proteins play the essential roles of transporting and storing molecular oxygen, which is needed for all cellular respiration. Heme can catalyze the oxidation of substrates using hydrogen peroxide in peroxidases, and catalyze the breakdown of hydrogen peroxide to water and oxygen in catalases. Besides these naturally existing porphyrin derivatives, synthetic porphyrins have found important applications in the medical research area. Due to their intriguing physical, chemical and biological properties, porphyrins and their metalated complexes have also attracted lots of interests from various interdisciplinary research areas.

It was in 1912 that Küster first proposed the existence of the intricate porphyrin ring system, which was late confirmed by Fischer. Now it has been well-accepted that the porphyrin macrocycle is an aromatic system, consisting of four pyrrole units which are linked by four sp^2 hybridized meso-carbons and this model has been confirmed by many hundreds of X-ray

structures[6]. Currently there are two nomenclature systems for the numbering of porphyrins and related systems (see *Figure 1-3*). The older one is the so-called the "Fischer system". In this system, the meso positions are labeled by a Greek lettering system, and the four pyrrolic sub-unit rings are also labeled with the capital letters A, B, C, and D. However, the "Fischer system" does not identify all carbons on the porphyrin skeleton. The more modern and more thorough scheme is called the "IUPAC system", which identifies every carbon in the macrocyclic ring. Besides that it also numbered the carbon of the substituents in more complex systems[12a].
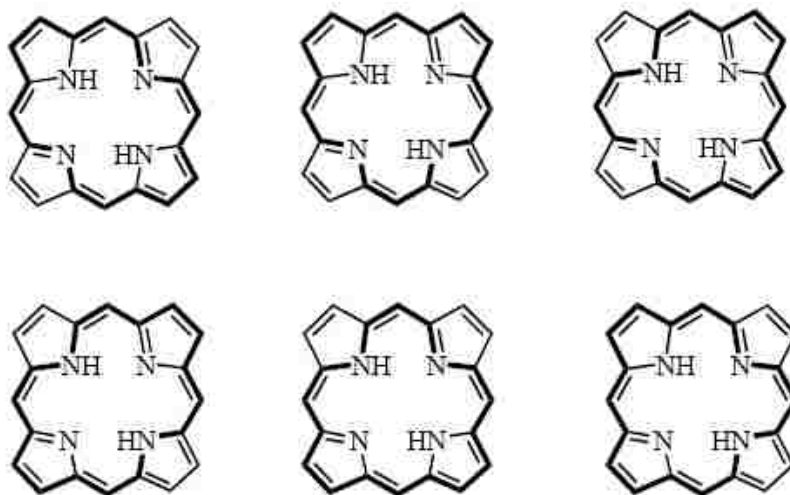
Figure 1-4. The tautamerization of porphyrins, which show the six possible delocalization pathways of porphyrins.

Although there are 22 π-electrons inside the porphyrin macrocyle, only 18 electrons are found to actually participate in any one delocalization pathway, which is consistent with Hückel's [4n+2] rule for atomicity, where n = 4. The different 18 electron-delocalization pathways are shown *Figure 1-4*[13a]. The other four electrons situated outside of the delocalization pathway are located on the two double-bonds opposite to each other at pyrrole rings, which are commonly known as the B and D rings in the Fisher system. The isolation of them from the delocalization pathway, in a cross-conjugated manner, makes these two double bonds easily to

be reduced or oxidized using numerous reactions. Typical examples are: catalytic hydrogenation, reduction with diimide, and hydroboration. The reduction products for porphyrins are usually chlorins or bacteriochlorins. As a typical aromatic system, porphyrin is also able to undergo a number of electrophilic aromatic substitution reactions (EAS), such as nitration, halogenation and formylation on any unsubstituted meso- and/or β-pyrrolic positions[13b-c]. However, the quaternary α-pyrrolic carbons rarely participate in any kind of reactions. It was found that the reducing of the aromatic character from the delocalization pathways can induce dramatic changes in the spectroscopic properties[14].

There are two pyrrolenine nitrogen atoms (pKa~6) and two inner-core NH groups (pKa~16) in porphyrins. The former can act as a base to accept protons and the latter can act as an acid to provide protons. The pyrrolenine nitrogen atoms can be protonated by strong acids, such as sulfuric acid and trifluoroacetic acid (TFA). The inner-core nitrogen protons can be removed by bases and metals. Also the presence of these nitrogen atoms makes most of the porphyrin derivatives amphoteric and shows both acidic and basic behavior[13b-c]. Also they can serve as an inner chelating pocket and provided various opportunities for chemical modifications. In most cases, the insertion of metals into the porphyrin macrocycles is easy and the removal of them can be achieved with Brønsted-Lowry acids without affecting the macrocyclic conjugation. Some represent metalloporphyrins are Cu, Ni, Zn, Fe and Co centered porphyrins.

The NMR spectra of the aromatic tetrapyrrole show anisotropic effects[15]. When there is a magnetic field applied, a ring current is generated and a local magnetic field similar to that in benzene is induced. In the proton NMR spectrum, the interior nitrogen protons normally appear between δ -4 and -2 due to the high shielding by the ring current. The deshielded *meso*-protons usually appear at very low field (δ ~ 10 ppm) and the pyrrolic protons are also deshielded and

tend to resonate at δ 8 to 9, which shows big shift compared to that of pyrrole at δ ~ 6 ppm. However, when there is aggregate formation of these porphyrins, their NMR spectra tends to be hard to assign.

Visible absorption spectroscopy is also a powerful tool to probe the structure of the tetrapyrrole chromophore of porphyrins. The macrocyclic conjugation gives several characteristic weak absorption bands, which are called Q bands and are located between 450-700 nm; there is one major absorption band known as the *Soret* band, which is an intense absorption band ($\varepsilon > 100,000$) located between 400 and 450 nm[16]. The Soret band is characteristic of the macrocyclic conjugation, and it disappears when the aromatic delocalization pathway is disrupted. Porphyrin derivatives show deep colors and have strong absorptions in the visible region near 400 nm, with their molar extinction coefficients to be about 10^5 Mol/L. The color difference among porphyrins is attributed to the different absorption spectra associated with different unique tetrapyrrolic structure. For example, natural porphyrins have dark red colors, but their reduced form, such as chlorins, show dark green or blue green colors. Thus the modification of the peripheral double bond of the porphyrins can cause changes of the absorption spectra, both the intensity and the wavelength. However, as long as the 18 π-electron cyclic pathway remains, the intense Soret band would also remains. The Soret band is absent only when porphyrin macrocyclic conjugation is disrupted. On the other hand, although the chelation, pH and different peripheral substituent arrays change the absorbance energy intensities and even change the color of the compounds, it usually only involves the Q band absorptions, and leaves the Soret band intact.

1.2.2 Synthetic Methodologies:
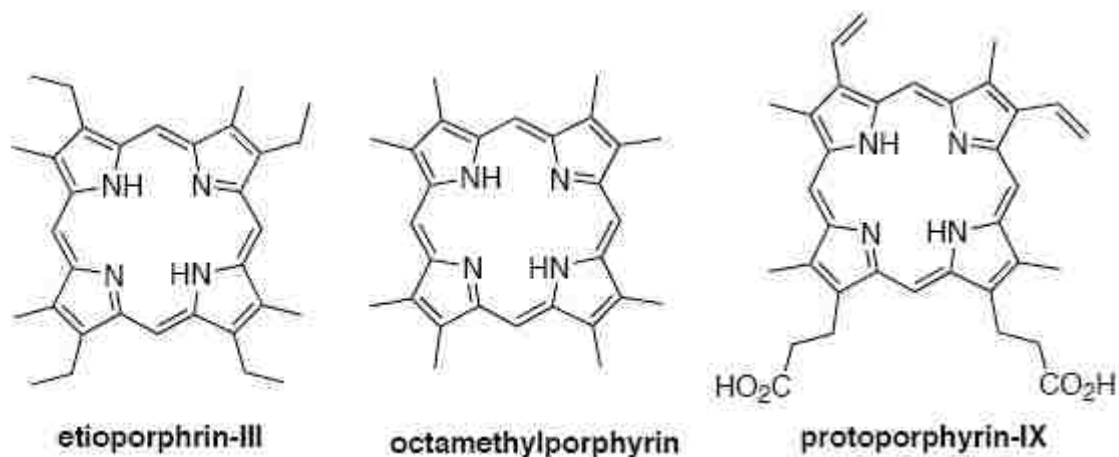
Figure 1-5. Historically and biologically important porphyrins.
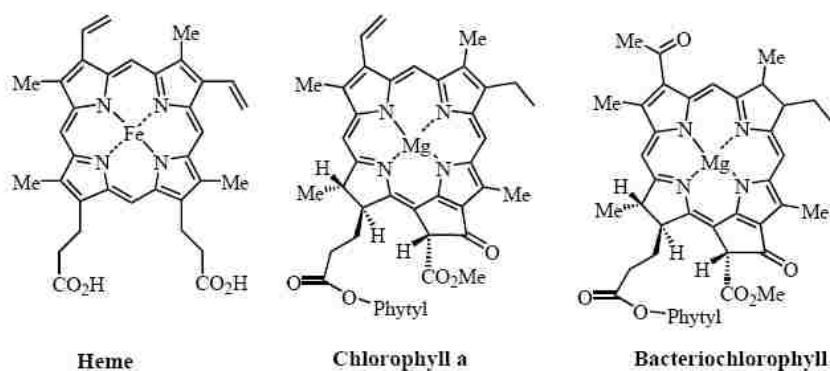
Figure 1-6. Chemical structure of heme, chlorophyll *a* and bacteriochlorophyll.

Fisher, the "father of porphyrin chemistry", reported the first total synthesis of the porphyrins etioporphyrin-III and octamethylporphyrin, in 1926 (see *Figure 1-5*). In 1929 Fischer synthesized and named protoporphyrin-IX (see *Figure 1-5*), which is the free base porphyrin of hemin[17]. Since then, a large number of synthetic routes have been developed for the preparation of both symmetrical and unsymmetrical porphyrin derivatives for structural, mechanistic, synthetic and biological studies. Here, some of the most commonly used synthetic methodologies are described. Porphyrin syntheses often started from the syntheses of a large class of pyrroles. Hans Fischer had already perfected early pyrrole synthetic work and also the syntheses of a

variety of porphyrins[18]. His early research work had inspired many research groups throughout the world to participate and devote their efforts to improve porphyrin synthetic methodology. Now, there are several routes to generate porphyrins. One of them is to modify natural products. For example, the modification of chlorophylls *a* or *b*, bacteriochlorophylls and hemin (see *Figure 1-6*) can be used to generate very desirable porphyrins.

Although porphyrins can be generated from total synthesis starting from monopyrrolic subunits, the types of porphyrins that can be generated are very limited. Recently, many improved synthetic routes have been reported, which now provide easy access to useful porphyrins. Currently the syntheses of symmetric porphyrins including both the octa-ß substituted or tetra-*meso* substituted porphyrins, involve the tetramerization of a suitable monopyrrolic subunit[19]. However, little progress has been made for the unsymmetric porphyrin synthesis.

1.2.2.1 Tetramerization of Pyrroles:

It was Rothemund who first introduced monopyrrole tetramerization to tetra-arylporphyrin syntheses[20]. Rothemund and Menotti who showed that H_2TPP could be slowly generated at high temperature by reacting benzaldehyde with pyrrole in a sealed tube and using pyridine as solvent. This reaction is called the "Rothemund Reaction". The highest yield of H_2TPP obtained from this reaction was about 11% by using $Zn(OAc)_2$ as a metal template in the presence of high pressure. By changing solvents from pure pyridine to a mixture solvent of methanol/pyridine at atmospheric pressure, both H_2TPP and the chlorin (dihydro) form of H_2TPP were obtained. The chlorin obtained is referred to as tetraphenylchlorin (H_2TPC), which can be converted to H_2TPP by oxidization with oxygen or DDQ. Due to the harshness reaction conditions of the Rothemund reaction, only very few benzaldehdes can be used in this reaction.

Thus, it is not practical to prepare H_2TPP and the above route becomes rarely used after the development of Adler-Longo conditions. The Adler-Longo method was developed in 1964, and represents an improvement in H_2TPP synthesis that was achieved by refluxing the mixture of pyrrole and benzaldehyde in propionic acid under open air conditions[21] (see *Scheme 1-7*).
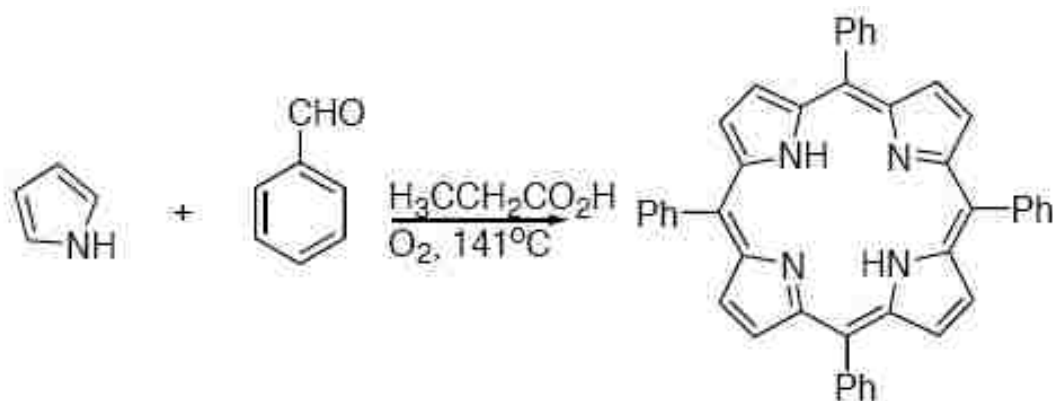
Scheme 1-7. Synthesis of H_2TPP using Adler-Longo conditions.
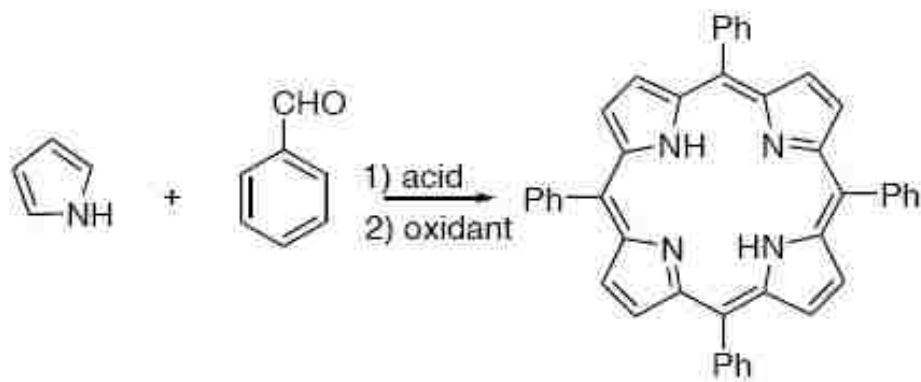
Scheme 1-8. Synthesis of H_2TPP using Lindsey conditions.

Adler and Longo studied many solvent systems with a variety of salts present to enhance the formation of H_2TPP. At atmospheric pressure, by refluxing pyrrole and benzaldehyde in propionic acid, H_2TPP was obtained in up to 20% yield. The reaction conditions were relatively mild, from which a much higher yield was achieved and also it has much faster reaction rate compared with Rothemund conditions. The milder conditions allowed the preparation of

porphyrins with a wide variety of functionalities attached. Although it gave a vast improvement over the Rothemund method, this reaction condition still had its limitations. It was still relative harsh and more sensitive functionalities failed to survive. Also the purifications became more difficult due to the formation of tar. Despite all these drawbacks, it was still the most efficient method for the syntheses of meso-tetra-alkylporphyrins at that time.

In 1986, Lindsey optimized the method and developed an improved synthesis of porphyrins, under so called "Lindsey conditions" (see *Scheme 1-8*). This is by far the most effective route for synthesizing symmetrical porphyrins. For example, the preparation of porphyrins with the same substituents on all four meso-positions, or all eight of β-pyrrolic positions, or a combination of them. Under Lindsey conditions, the synthesis of porphyrin is done in two steps through the formation of porphyrinogen from monopyrrole tetramerization and a subsequent separate oxidation[22].

It was successfully demonstrated by Lindsey that the formation of H_2TPP could be achieved under equilibrium conditions, and under this situation many functional groups could survive. A colorless porphyrinogen was first formed, followed by a subsequent oxidation step with *p*-chloranil or DDQ. H_2TPP was formed by dissolving benzaldehyde and pyrrole in dichloromethane in a 10^{-2} M solution. The acid catalyst ($BF_3 \cdot Et_2O$ or TFA) was typically added at a dilution of 10^{-3} M. The yields of porphyrins generated under these conditions were improved to around 30-40%. It was found that the use of *p*-chloranil for the oxidation typically gave higher yields than the case when DDQ was used as oxidation reagent. Lindsey and coworkers discovered that not only the oxidation reagent, but the reaction time, the concentration of starting materials and the acid catalyst could also affect the reaction. It was found by altering the concentration of acid, the yield was only slightly affected. However, the yields of H_2TPP were

decreased a lot by varying the reagent concentrations to ten-fold higher and ten-fold lower than 10^{-2} M. The oxidation rate depended on the oxidizing agent. For example, the oxidation can finish within minutes by using DDQ, while it requires an hour to complete the oxidation when *p*-chloranil was used. The efficiency of Lindsey conditions have been proved for both tetra-arylporphyrins and *meso*-tetra-alkylporphyrins, giving unprecedented yields.

1.2.3 Applications of Synthetic Porphyrins

Porphyrins play vital roles in biological systems, not only in nature but also in applications in material science and medicine areas.

1.2.3.1 Applications in Material Science

Porphyrins-based molecular wires are appealing because polyporphyrin systems containing redox active and/or photoactive units, which allows the long-distance delocalization of electron density, thus makes them ideal systems for electron- or energy- transfer[23]. Earlier research using porphyrins and related compounds to study electron transfer was focused on modeling the photosynthetic reaction center and on a better understanding of the complex mechanism of photosynthesis[23a]. Covalently-linked bisporphyrins and quinine-substituted porphyrin dimers and trimers were built and used to mimic the electron transfer process in biological systems. Recently, more study has been focused on using supramolecular porphyrin arrays as potential photonic molecular wires.

Certain heme-containing enzymes such as cytochrome P450 have been found to perform hydroxylation of alkanes and epoxidation of unfunctionalized alkenes[24]. Noncovalent hydrogen-bonding interactions have been found to be the most important factor in dynamically regulating the active site for PCET (Proton-Coupled Electron Transfer) reactivity inside some of these enzyme systems. As a result, a lot of research has been developed to design porphyrin molecules

for biomimetic models for heme-containing enzymes. Recently, porphyrins functionalized with hydrogen-bond synthons have been widely studied because they could be used as efficient building blocks for construction of supramolecules with appealing structural and electronic properties. Among these, the so-called "Hangman Porphyrins" have attracted much recent interest, because of the prospective application they have for unraveling the hydrogen bonding effect on energy and electron-transfer reaction. Due to the rigidity of the spacer used in these systems, a side-to-side arrangement of the porphyrin macrocycle and hydrogen-bond functionality has been shown. These hangman porphyrins have simplified the construction of biomoleculaes with engineered distal sites as platforms able to control both proton and electron transfer, which provides the opportunity to precisely control the functional nature of a hydrogen-bonding group[25]. Despite these advantages, the elucidation of structure/reactivity relationships of PCET catalysis is difficult in porphyrin systems. Significant challenges are posed by the lengthy total synthesis and tedious purification of porphyrin platforms and their intractability to modular modifications[26]. In the meanwhile, heteroatom-bridged calixarenes, such as the oxygen-bridged calix[4]arenes, are easy to access and modify and also display unique chemical and physical properties[27]. Inspired by the easy availability and the unique discrete 1,3-alternate conformations of oxacalix[4]arenas, the design and synthesis of hangman porphyrin analogs with oxacalix[4]arene as spacer to hang hydrogen synthons over porphyrin macrocycle[28] become very attractive, and this will be discussed in Chapter 4.

1.2.3.2 Biological Applications of Porphyrins - Photodynamic Therapy (PDT)

PDT is a binary therapy which combines light and a photosensitizer in the presence of oxygen to destroy tumors or unwanted tissues[29] (see *Figure 1-9*). It has been found that many
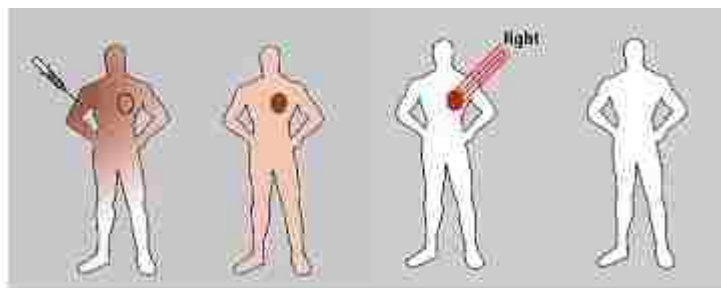
Figure 1-9. How photodynamic therapy works. Copy from website (2007) (http://www.bmb.leeds.ac.uk/pdt/images/4man/).

porphyrin derivatives are effective photosensitizers for PDT treatment of cancers. Due to their selectively accumulation ability in tumor tissues, retain for relatively long periods, low-dark toxicity, high chemical stability, high affinity for serum proteins, ability to form stable complexes with variety of metal ions, fluoresce, and absorb strongly in the visible region of the optical spectrum, porphyrin derivatives are also the most widely explored sensitizer/tumor active compounds[30].

$$^1P + h\nu \rightarrow {}^1P*$$

$$^1P* \xrightarrow{ISC} {}^3P*$$

$$^3P* + {}^3O_2 \rightarrow {}^1P + {}^1O_2$$
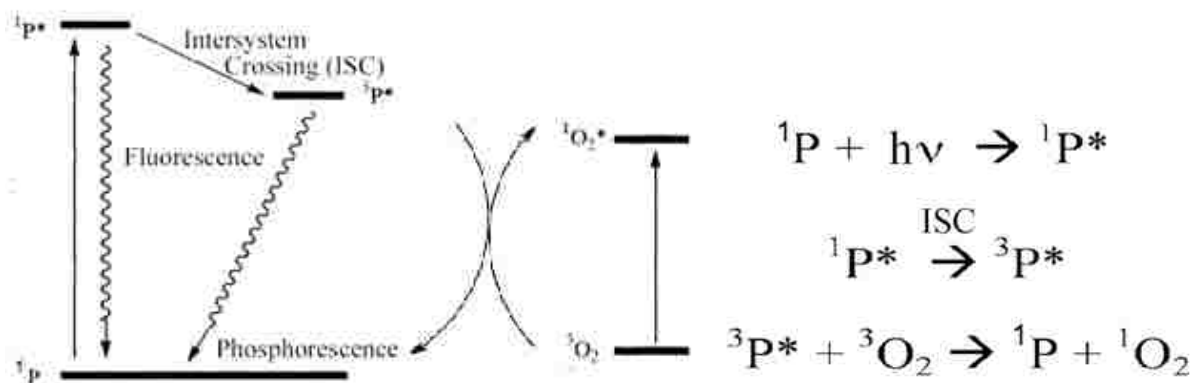
Figure 1-10. How toxic singlet oxygen generated.

Although the distribution of porphyrin based sensitizers in the body is still under investigation, it is believed that some structural features, such as the nature of peripheral groups, coordinated metal ions and accompanying axial ligands will affect the uptake and retention of porphyrin-molecules in tumors[31]. In PDT, the photosensitizer has a negligible dark toxicity to the body while it is accumulated preferentially in the rapidly dividing cells[32]. Also, it has been

hypothesized that porphyrins have the tendency of association with plasma proteins, particularly low density lipoproteins (LDL), while the increasing level of LDL receptors has been found in cancer cells[33]. Usually, photosensitizers are injected into the bloodstream and it is generally believed that amphiphilic molecules that bear both hydrophobic sites and hydrophilic sites should improve tumor-specificity (see *Figure 1-9*). At the absence of light, the photosensitizer is harmless and has no effect to either healthy or abnormal tissue. When exposed to a carefully regulated specific light dose, it becomes activated and can rapidly destroy the tissue irradiated with the light. Compared to the other currently available cancer therapeutic methods, such as chemotherapy, radiotherapy and surgery (or a combination of these methods), PDT has the advantage of preferential accumulation of the photosensitizer in the target tissue and precise selectivity of the treatment by controlling the illumination[34]. Figure **1-10** shows a modified Jablonski diagram of the mechanism for PDT. After the light penetrates the tissue, the photosensitizer is excited and reacts with other substrates, mainly the molecular oxygen to generate highly cytotoxic species, including singlet oxygen, superoxide anion and hydroxyl radicals, which can cause irreversible damage to the tumor cells[34]. Ground state (^{1}S) is the stable electronic configuration of photosensitizers[35]. With an appropriate wavelength of light irradiation, the photosensitizer is excited to its singlet excited state (^{1}S*). When it decays to the ground state, the fluorescence radiation enables the identification of tumor tissue. Meanwhile, it can also undergo a nonradiative process of inter-system crossing (ISC) to convert the photosensitizer from a singlet state to a triplet excited state (^{1}T*) or through internal conversion to release the energy as heat. The relaxation of photosensitizer from the triplet excited state to the ground state usually through two pathways: release of phosphorence radiation, or non-radiatively transferring its energy to another molecule with a triplet ground state. ISC involves a change in the electron

spin, thus it is a spin-forbidden pathway and imposes a relatively long time on the triplet state, allowing interaction with adjacent molecules of the photosensitizer. Molecular oxygen has a triplet ground state and is abundant in tissue. It can interact with the triplet state photosensitizer to generate highly cytotoxic species. A good photosensitizer can go through this pathway with high efficiency.
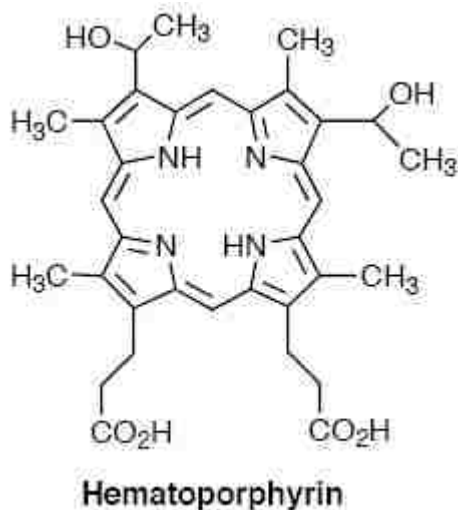
Figure 1-11. Chemical structure of hematoporphyrin.

Hematoporphyrin (see *Figure 1-11*) was the first evaluated porphyrin for PDT and it is readily available from blood. Back to the early 1960s, Lipson et al. had already prepared a derivative of hematoporphyrin (HPD) which displayed an enhanced selectivity for PDT. HPD is a mixture of hematoporphyrin, protoporphyrin-IX, hydroxyethylvinylporphyrin and other complex compounds containing dimeric and oligomeric derivatives of hematoporphyrin[36]. In 1981, Dougherty et al. prepared a more purified form of HPD, known today as Photofrin®, from gel exclusion chromatography. Photofrin® was approved in the USA by the Food and Drug Administration (FDA) and it also is now approved in eleven European countries. Over the last two decades, Photofrin® has been used successfully in the treatment of both early and advanced stages of the lung cancer. Although it has shown curative for a range of cancers, Photofrin® has

some well-documented drawbacks for the PDT treatment: First of all, it is a complex mixture of HPDs and there are reproducibility problem associated with both the synthesis and its pharmacological benchmarking; second, Photofrin® absorbs weakly in the therapeutic window, thus there is limited usage of this compound in treating deep-seated tumors; third, there is long retention time of this drug in normal skin and thus Photofrin® induces prolonged skin sensitivity[37]. Due to these problems associated with Photofrin®, many research efforts have been devoted to the development of new or improved compounds for PDT since the early 1980s.

An ideal PDT photosensititizer should have good pharmacokinetic properties, fluorescence, and an increased absorbance in the red region of the optical spectrum; it should have a high quantum yield of the triplet state, efficient generation of cytotoxic oxygen species, appreciable selectivity for malignant tissue over normal tissue, and low dark toxicity[38]. Among these, the most important issue is the strong absorption in the therapeutic window (between 650-750 nm) to ensure the deep penetration of light through tissue and with minimal light scattering. Over the last decades, research to develop new photosensitizers has been mainly focused on the synthesis of porphyrin based sensitizers and on their structure-functionality relationships. Among those, chlorins, benzoporphyrins, phthalocyanines, and expanded porphyrin analogs have been found to be strong long wavelength absorbers[39]. Mono-L-aspartyl chlorin e_6 (MACE, NPe6, Talaporfin, LS-11) and mono-carboxylic acid (BPD-MA, Visudyne™), which are obtained either from chlorophyll or from protoporphytin, are important naturally derived second generation photosensitizers. These two, as PDT photosensitizers, are currently undergoing human clinical trials for the treatment of various cancers and age-related macular degeneration[40]. In the meanwhile, synthetically derived second generation photosensitizers, such as the symmetric

meso-tetra(*m*-hydroxyphenyl)chlorin (m-THPC, Foscan®) and Sn(IV)-etiopurpin (SnET2, PuryltinTM), are in their early clinical trials for the treatment of various cancers[41].

1.3 Benzoporphyrins

1.3.1 Overview of Benzoporphyrins

Benzoporphyrin refers to the type of porphyrin that has aromatic subunits fused at the β-pyrrolic positions (see *Figure 1-12*). When there are four aromatic subunits fused at the β-pyrrolic positions of porphyrin, they are called tetrabenzoporphyrins (TBPs) (see **1-10** in *Scheme 1-9*).[42] TBPs are chemically stable compounds, and have unique chemical, physical and spectroscopic properties. Among those, their absorption spectra are significantly shifted to the infrared region due to the extended π-conjugation. Different from porphyrin derivatives, which can absorb light between 380-400 and 500-560 nm, TBPs have absorbance in the near IR region, which allows deep light penetration into tissue and they are therefore suitable photosensitizers in photodynamic therapy (PDT) of cancer[43]. They can act as models for naturally occurring tetrapyrrole derivatives. They have similar physical properties compared with phthalocyanine, which is one of the most widely studied organic pigments, having many applications in industry as dyes, inks, catalysts, electrical conductors and other optical materials. Similarly, TBPs have found applications as opto-electronic materials, nonlinear optical materials, and luminescent markers for oxygen, near-IR labeling dyes, and pH sensors in biomedical imaging[44]. Benzoporphyrins were first discovered in trace amounts in various oil shales and petroleum[45]. Despite the increasing interests in their syntheses and characterization, researches on tetrabenzoporphyrins (TBPs) have progressed slowly due to the difficult synthetic access to these compounds. Above all, unsymmetrical (non-tetra) benzoporphyrins such as the

monobenzoporphyrins and dibenzoporphyrin (see *Figure 1-12)*, have proven to be very difficult

to synthesize**.**
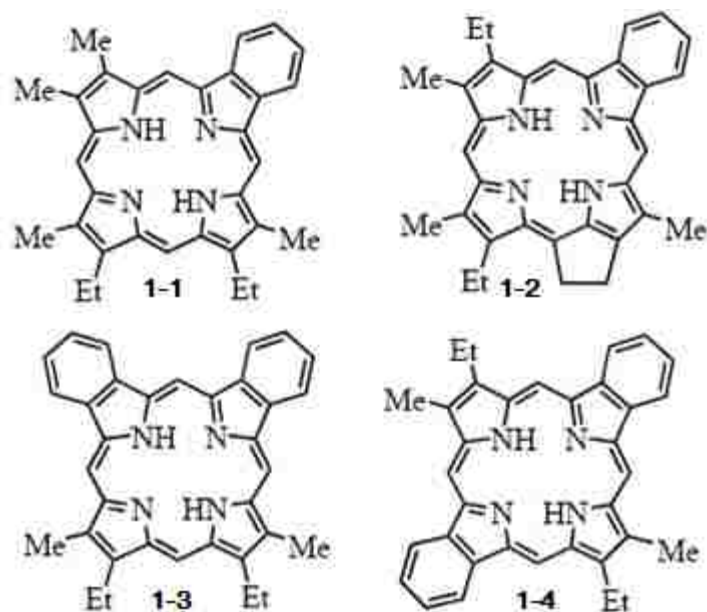
Figure 1-12. Chemical structures of unsymmetrical benzoporphyrins.

1.3.2 Syntheses of Benzoporphyrins
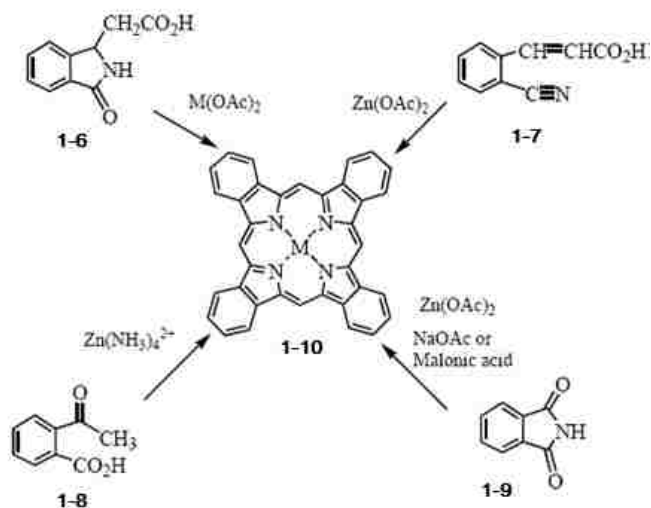
Scheme 1-9. Previous symmetrical benzoporphyrin synthetic routes.

Helberger and coworkers first described the syntheses of TBPs from *o*cyanoacetophenone and various phthalimidines[46]. Back then, there were two main approaches for the synthetic development of benzoporphyrins: The first approach was the high temperature condensation using phthalimidine derivatives at the presence of a metal template; the second approach was the condensation of pyrroles with mesocarbon donors[47]. Later on, many improved syntheses of benzoporphyrin were reported (see *Scheme 1-9*).

The initial improvement of TBP synthesis was made by Linstead's group, in which TBPs were prepared by high temperature condensation (350-400 °C) of **1-6** or **1-7** (see *Scheme 1-9*) in the presence of metal salts, such as iron, zinc, magnesium, cadmium, or metallic acetates[48]. The metalated symmetrical benzoporphyrins thus obtained were usually very impure and required extensive purification processes. Later on, Vogler and Kunkely used the template reaction of 2-acetylbenzoic acid (see **1-8** in *Scheme 1-9*) with zinc(II) acetate in the presence of aqueous ammonia and molecular sieves at 400 °C to improve the reaction efficiency and simplify the purification process[49]. Also, they found that the condensation of phthalimide or its potassium salt with sodium acetate or malonic acid (see **1-9** in *Scheme 1-9*) in the presence of zinc(II) acetate at 360 °C could afford TBPs. Vogler and Kunkley's synthesis affords the corresponding **1-10** in a more pure form in 17% yield[50].

Metalated symmetrical benzoporphyrins can also be synthesized using Rothemund conditions, in low yields, from unstable isoindoles through inert atmosphere pyrolysis in the presence of metals or metal salts, or from refluxing in a high-boiling solvent (1,2,4-trichlorobenzene or 1-chloronapthalene). Remy improved the synthesis of metalated symmetrical benzoporphyrins by high temperature condensations of isoindole (see **1-15** in *Scheme 1-10*) and formaldehyde in the presence of a metal or metal salt[51]. It was found that metal salts play an

important role in Remy's method. In the presence of metal salts the yield achieved for the target compound was 53%. In the absence of the metal salt, only very low yields were achieved. Under similar condition, when changing from formaldehyde to benzaldehyde, the metalated tetraphenyltetrabenzoporphyrin was obtained as the major product together with a mixture of partially *meso*-substituted metallo-TBPs[52].
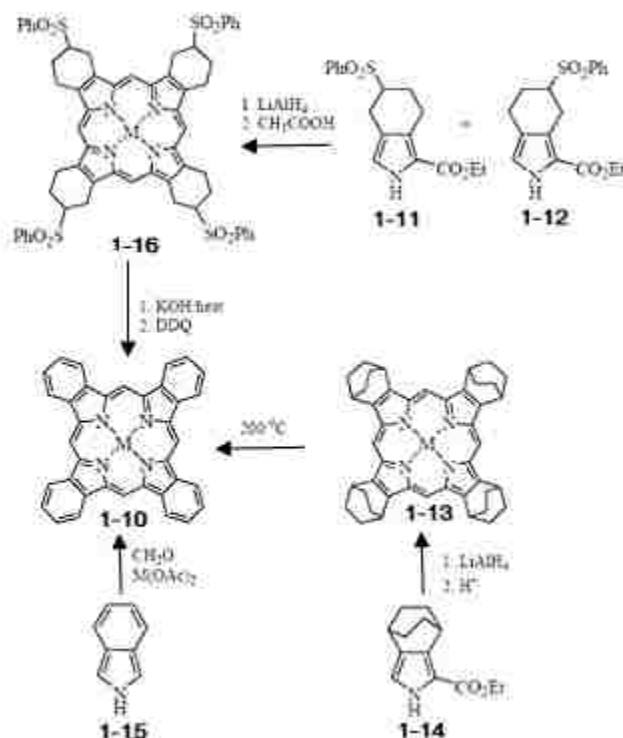
Scheme 1-10. Recently improved syntheses of benzoporphyrins

Recently, Vicente et al. developed milder and more modern synthetic methods to prepare metalated symmetrical benzoporphyrins (see *Scheme 1-10*)[53]. Starting from pyrroles (**1-11** and **1-12** in *Scheme 1-10*), which can be obtained from classical Barton-Zard conditions[54], firstly the reduction with lithium aluminum hydride was performed; subsequently cyclotetramerization was performed in acetic acid, and finally oxidation was achieved by using DDQ. The mixtures of isomers of phenylsulfonyl-substituted porphyrins were separated in 60% yield from this reaction. The elimination of the phenylsulfinate units was achieved under basic condition and subsequent

23

oxidation was performed by using DDQ. After isolation, the target metalated symmetrical benzoporphyrins **1-10** were obtained in 53% overall yield. Meanwhile, Ono et al. avoided the use of instable isoindole in the preparation of **1-10** by generating a masked isoindole **1-14** and subsequently using it for the reaction[55]. Ono's improvement was performed by reducing **1-14** with lithium aluminum hydride, then acid catalyzed cyclotetramerization, and eventually oxidation with DDQ. After isolation, **1-13** was obtained in 30% yield. The eventual generation of tetrabenzoporphyrin **1-10** was achieved in very pure form in quantitative yield through a retro-Diels-Alder reaction by just simply heating **1-13** at 200 °C.

The condensation of benzodipyrromethene hydrobromides and Diels-Alder type reaction involving β-vinyl porphyrins and activated dienophiles can also be used to generate benzoporphyrins[56]. Compared with porphyrins, unsubstituted TBP has very poor solubility due to its extended, planar, π-conjugated system and high π-π stacking (aggregation) tendency. Thus, the physicochemical property evaluation of these compounds has been slow. However, the tetraaryl substituted tetrabenzoporphyrins have enhanced solubility due to their significantly non-planar structure due to the steric hindrance effect generated from the four meso-aryl substituents.

1. 4 Overview of Chlorin-e$_6$ as a PDT Sensitizer

The development of the so-called "2nd-generation" of photosensitizers is aimed to increase the efficiency of photosensitizers in PDT, expand their applications in PDT, and maintain the advantages of currently approved photosensitizers. Current research has focused on the improvement of their photophysical and pharmacokinetic properties. Chlorins have strong absorptions at the ideal part of the therapeutic region. The electron delocalization pathway of chlorins is shown in *Figure 1-13*. Unlike the porphyrins, there are no chlorin-based photosensitizers that have been approved in the United States by the FDA. However, mono-(L)-

aspartylchlorin-e$_6$ is currently in advanced-stages of clinical trials as a 2nd-generation of photosensitizer.

Figure 1-13. The tautomeric structure of chlorins.
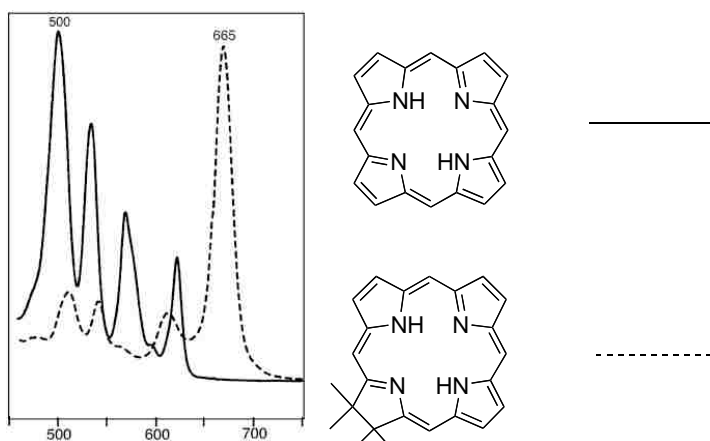
Figure 1-14. The comparation of the UV-vis absorption spectra of porphyrin (top) and chlorin (bottom).

Mono-(L)-aspartylchlorin-e$_6$, known as talaporfin or NPe6 or LS-11 is a derivative of chlorophyll *a*. More specifically, NPe6 is an aspartic acid conjugate of chlorin-e$_6$[57]. It was prepared from pheophorbide *a,* which was prepared by transesterification of chlorophyll *a* with a methyl ester group at the phytyl ester position[58]. The isocyclic ring-opening reaction of pheophorbide *a*, followed by saponification of the methyl esters, and subsequent coupling with a protected aspartic acid; after final step deprotection, NPe6 was obtained[59]. As a chlorin derivative, NPe6 has characteristic long wavelength absorption at 666 nm (see *Figure 1-14*), which allows for greater light penetration, thus increasing the utility of photons compared to Photofrin®. Upon irradiation, NPe6 gives good yields of long-lived triplets with the lifetimes

25

ranges from 500 to 800 μs, thus giving high yields of cytotoxic singlet oxygen. Furthermore, it can rapidly clear from normal tissue, having negligible residual photosensitivity in tissues. Compared with Photofrin® in PDT of cholangiocarcinoma, NPe6 (see *Figure 1-15*) shows many advantages: it can reduce tumor volume, inhibit tumor re-growth, and increase depth of tissue injury up to 67%. Also, the undesired side effect of residual skin photosensitization has been found to be decreased[60].
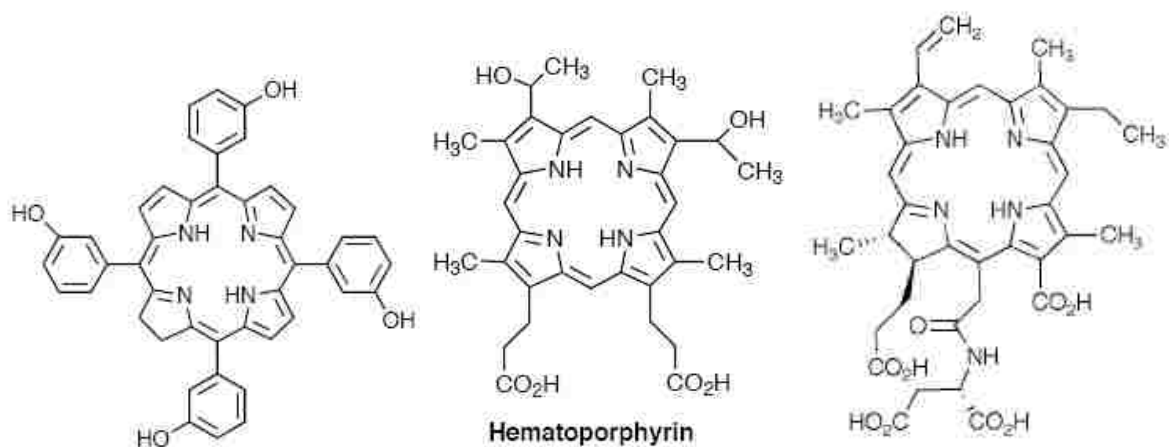
Figure 1-15. Chemical structures of temoporfin (left), the main component (hematoporphyrin) of Photofrin® (middle) and NPe6 (right).

In the binary treatment modalities, stability is especially significant. Degradation products will shift the light absorbtion wavelength outside of the laser therapy window and makes the treatment ineffectual. Chlorophyll *a* derivatives have increased stability due to their unusual structural characteristics, which is hard to access from current synthetic methods[61]. As a chlorophyll-*a* derivative, NPe6 has increased stability compared to the other chlorin photosensitizers, such as temoporfin (*Figure 1-15*, left), which can readily oxidize back to porphyrin. In order to improve the efficiency of photosensitizers in PDT, amphiphilicity is required[62]. Recently, it was found that small differences in photosensitizer structure, even involving regioisomerism of substituents, can bring the huge functional differences, for example

26

in subcellular localization, which has already been demonstrated as a factor in the mode of cell damage (i.e., necrosis vs. apoptosis)[63]. Chlorophyll *a* derivatives related to chlorin e_6 have three carboxylic side chains, thus providing synthetic handles for easy access for modifications to generate novel amphiphilic photosensitizers. The success of NPe6 as a photosensitizer has attracted much interest in the optimization of its synthesis.

Ironically, despite its interesting properties and the increasing attention to its synthesis, there was a great amount of ambiguity associated with the structure identification for NPe6. The first report of NPe6 came from a patent filed in 1987, in which it was claimed that NPe6 was probably a mixture of regioisomers. With isolation from HPLC a pure compound was achieved, and it was called NPe6[64]. Ever since then, all academic publications shared the idea that NPe6 was the 17^3-position regioisomer of mono-(L)-aspartylchlorin-e_6. Although none had shown any convincing evidence of this structure, everybody accepted this theoretically favored structure. In 1998 a Japanese research group proposed an alternative view of the structure of NPe6 in the journal *Heterocycles*; they claimed that NPe6 was actually the 15^2-position regioisomer. This conclusion was based on a 2D-NMR study result obtained in D_2O. The results on this paper were not accepted by the porphyrin community due to the seriously complicated NMR analysis associated with chlorin aggregations in water[65]. Moreover, the new result was counterintuitive from a mechanistic perspective, which was the main reason for ambiguous structure analysis. Since no protecting group strategies had been employed during the synthesis, with three carboxylic acids at the chlorin periphery readily available for coupling, it was expected that the 17^3-position coupling product would be the major product if the coupling mechanism is through the classic carboxylic acid activation with DCC. In 2006, our group reported the X-ray structure of the tetramethyl ester of authentic NPe6, which was achieved from methylation of commercial

27

available NPe6 with diazomethane[66]. This clealy showed that authentic NPe6 is the 15^2-aspartyl regioisomer. The unambiguous syntheses of all three NPe6 regioisomers and the difunctional NPe6 "DACE" were also reported by our group[67]. Since the formation of the new NPe6 (the 15^2-regioisomer) structure was hard to explain thus it became necessary to discover the underlying mechanism for the unique formation of this structure. Chapter 6 will present the related mechanism study results.

1.5 Overview of Porphycene
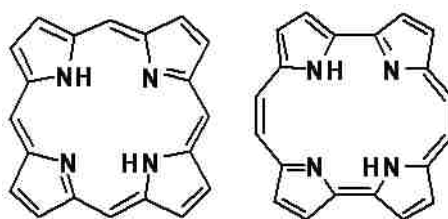
Figure 1-16. Chemical structure of porphycene (right) and porphyrin (left).

The name of porphycene combines both porphyrin and acene together, in order to describe its unique structural constitution (see *Figure 1-16*)[68]. The increasing interests in porphyrin researches led to the discovery of porphyrin isomers such as porphycene in 1986 by Vogel[68]. Two years later, in 1988, he also reported the first heteroporphycene[69a]. In 1993, Merz and coworkers reported the synthesis of tetrathiaporphycenes[69b]. One year later, Cava and coworkers also reported their independent synthesis of this type of porphycene[69c]. Following these initial reports, the synthesis of corrphycene[70a] and hemiporphycene[70b] were report in 1994, and the synthesis of isoporphycene[71] was reported in 1996. The preparation of porphycenes usually starts from a 5,5'-diformyl-2,2'-bipyrrole. A low-valent titanium coupling reaction was used for the final step cyclization reaction, often the McMurry coupling[72]. Shortly after the synthesis of porphycene, Vogel and his coworkers realized that porphycenes possess a strong intense absorption at the phototherapeutic window for PDT (between 600 and 800 nm), and that

this was red-shift compared to porphyrin systems. Thus they proposed that porphycenes might serve as an important photosensitizer in the photodynamic therapy of cancers.[72,73] Ever since then, many porphycene derivatives have been synthesized. It was found that the peripheral substitutents of porphycenes can affect the photoexcited triplet states of free-base porphycenes. Richert et al. prepared the tetramethoxy- and dimethoxy-porphycenes and subsequently converted them into their 9-acetoxy-substituted derivatives. Among these, 9-acetoxy-2,7,12,17-tetrakis (β-methoxyyethyl)porphycene has been used for PDT of psoriatic lesions. Also, extensive preclinical and phase I /II clinical trials with this dye have been performed[74].

Considering the dominant role that metalloporphyrins play in porphyrin chemistry, the metalation of porphycene also attracted lots of interests. Due to the strong intra-core NH-N hydrogen bonding and the rectangular shape of the four central nitrogen atoms, the metalation of porphycene is relatively difficult compared to porphyrins, and the type of metalloporphycenes that have been reported[71a,72, 75] are limited. There are several other ways to modify porphycenes, which mainly involve: 1) modification at the pyrrolic nitrogens[76]; 2) catalytic hydrogenation; 3) post-synthetic skeletal modification[77].

The characteristic spectrum properties of porphyrinoid aromatic system can be found in the absorption spectra of porphycenes. There is one split Soret-like band around 370 nm and three enhanced Q-band absorptions in their UV-vis spectra. With the higher intensity of Q-band absorption compared to those of porphyrins, porphycenes are more attractive compared with porphyrin derivatives for application in PDT of cancers[72,73]. Compared to porphyrins, the NMR spectra of porphycene shows great high field shift of the internal NH protons, from around -2~-4ppm to around +3ppm[78].

1.6 References

1 Battersby, A. R. *Nat. Prod. Rep.*, **2000**, *17*, 507.

2 Fischer, H.; Hess, R.; *Hoppe-Seyler's Z. Physiol. Chem.*, **1931**, *194*, 195; b) Siedel, W.; Fischer, H.; *Hoppe-Seyler's Z. Physiol. Chem.*, **1933**, *214*, 145.

3 Stokes, G. G. *J. Chem. Soc.*, **1864**, *17*, 304.

4 Thudichum; J. L. W. *Report Med. Off. Privy. Council*, **1867**, *Appendix 710,* 152; b) Nencki, M., *Arch. Exptl. Path. Parmakol.* **1888**, *24*, 430.

5 Robinson, R., *Obituary Notices of Fellows of the Royal Society*, **1953**, *8*, 609.

6 Küster, W., *Hoppe-Seyler's Z. Physiol. Chem.*, **1912**, *82*, 463.

7 Keilin, D., *Proc. R. Soc. London*, *B*, **1925**, *98*, 312.

8 Fischer, H.; Stern, A., *Die Chemie des Pyrrols*, Vol. 2, Part 2, Akad Verlag, Leipzig, **1940**; b) Willstätter, R.; Stoll, A., *Investigations on Chlorophyll*, Science Press, Lancaster, Ohio, **1928**.

9 Lemberg, R.; Barrett, J. *Cytochromes*, Academic Press, London and New York, **1973**.

10 Todd, A. R. in *Vitamin B$_{12}$*, Zagalak B.; Friedrich, W. Eds., de Gruyter, Berlin, **1979**, Page 1; b) Folkers, K. in *Vitamin B$_{12}$*, Zagalak, B.; Friedrich, W. Eds., de Gruyter, Berlin, **1979**, Page 7.

11 Hodgkin, D. C., in *Vitamin B$_{12}$*, Zagalak, B.; Friedrich, W. Eds., de Gruyter, Berlin, **1979**, Page 19.

12 Vicente, M. G. H.; Smith, K. M. *Curr. Org. Chem.* **2000**, *4*, 139; b) Milgrom, L. R. in *The Colors of Life*, Oxford University Press, Oxford, New York and Tokyo, **1997**.

13 Abraham, R. J.; Medforth, C. J.; Mansfield, K. E.; Simpson, D. J.; Smith, K. M. *J. Chem. Soc. Perkin Trans*. *2*, **1988**, 1365; b) Smith, K. M. in *The Porphyrins*, Elsvier Press, **1975**, pp 9; c) Boucher, L. J.; Katz, J. J. *J. Am. Chem. Soc.* **1967**, 89,4703.

14 Abraham, R. J.; Medforth, C. J.; Mansfield, K. E.; Simpson, D. J.; Smith, K. M. *J. Chem. Soc. Perkin Trans*. *2*, **1988**, 1365.

15 Smith, K. M.; Goff, D. A.; Abraham, R. J. *J. Org. Magn. Reson*. **1984**, 22, 779; b) Kenner, G. W.; McCombie, S. W.; Smith, K. M., *J. Chem. Soc. Perkin Trans 1,* **1973**, 21, 2517; c) Senge, M. O.; Smith, K. M. *Photchem. Photobiol.* **1991**, 54, 841; d) Smith, K. M.; Unsworth, J. F. *Tetrahedron,* **1975**, 31, 367.

16 Soret, J. L. *Compt. Rend.* **1883**, 97, 1267; b) Weiss, C. J. *J. Mol. Spectrosc*. **1972**, 44, 37.

17 Fischer, H.; Klarer, J. *Liebigs Ann. Chem*. **1929**, 98, 468.

18 Kim, J. B.; Adler, A. D.; Longo, F. R. in "*The Porphyrins*", Dolphin, D. Ed. Academic Press, New York, **1978**, Vol. I, Part A, p. 85.

19 Smith, K. M. in "*Porphyrins and Metalloporphyrins*", Smith, K. M. Ed., Elsevier, Amsterdam (**1975**), p. 32; b) Adler, A. D.; Longo, F. R.; Finarelli, J. D.; Goldmacher, J.; Assour, J.; Korsakoff, L. *J. Org. Chem.* **1967**, 32, 476.

20 Rothemund, P.; Menotti, A. R. *J. Am. Chem. Soc.* **1939**, *61*, 2912.

21 Adler, A.; Longo, F. R.; Finarelli, J. O.; Goldmacher, J.; Assour, J.; Korsakoff, L. *J. Org. Chem.* **1967**, *32*, 476.

22 Lindsey, J. S.; Hsu, H. C.; Schreiman, I. C. *Tetrahedron Lett.* **1986** , *27* , 4969; b) Rao, P. D.; Dhanalekshmi, S.; Littler, B.; Lindsey, J. S., *J. Org. Chem.* **2000**, *65*,7323; c) Geier, G. R.; Lindsey, J. S. *Tetrahedron* **2004**, *60*, 435; d) Rao, P. D.; Littler, B. J.; Geier, G. R.; Lindsey, J. S. *J. Org. Chem.* **2000**, *65*, 1084.

23 Paolesse, R.; Jaquinod, L.; Sala, F. D.; Nurco, D. J.; Prodi, L.; Montali, M.; Natale, C. D.; D'Amico, A.; Carlo, A. D.; Lugli, P.; Smith, K. M., *J. Am. Chem. Soc.* **2000**, *122*, 11295; b) Wagner, R. W.; Johnson, T. E.; Lindsey, J. S., *J. Am. Chem. Soc.* **1996**, *118*, 11166; c) Anderson, H. L., *Inorg. Chem.* **1994**, *33*, 972; d) Lin, V. S. −Y.; Dimagno, S. G.; Therien, M. J., *Science*, **1994**, *264*, 1105.

24 Dawson, J. H. *Science* **1988**, *240*, 433; b) Dismukes, G. C. *Science* **2001**, *292*, 447; c) Tommos, C.; Babcock, G. T. *Acc. Chem. Res*. **1998**, *31*, 18; d) Yocum, C. F.; Pecoraro, V. L. *Curr. Opin. Chem. Biol*. **1999**, *3*, 182; e) Sono, M.; Roach, M. P.; Coulter, E. D.; Dawson, J. H. *Chem. Rev.* **1996**, *96*, 2841; f) Ozaki, S.-I.; Roach, M. P.; Matsui, T.; Watanbe, Y. *Acc. Chem. Res.* **2001**, *34*, 818.

25 Chang, C. J.; Chng, L. L.; Nocera, D. G. *J. Am. Chem. Soc.* **2003**, *125*, 1866; b) Momenteau, M.; Reed, C. A. *Chem. Rev.* **1994**, *94*, 659; b) Chang, C. J.; Brown, J. D. K.; Chang, M. C. Y.; Baker, E. A.; Nocera, D. G. *Electron Transfer in Chemistry*; Balzani, V., Ed.; Wiley-VCH: Weinheim, Germany, **2001**; Vol. 3.2.4, pp 409; c) Cukier, R. I.; Nocera, D. G. *Annu. Rev. Phys. Chem.* **1998**, *49*, 337.

26 Liu, S. Y.; Nocera, D. G. *J. Am. Chem. Soc.* **2005**, *127*, 5278.

27 Hao, E.; Fronczek, F. R.; Vicente, M. G. H. *J. Org. Chem*. **2006**, *71*, 1233; b) Sommer, N.; Staab, H. A. *Tetrahedron Lett.* **1966**, *25*, 2837; c) Katz, J. L.; Feldman, M. B.; Conry, R. R. *Org. Lett*. **2005**, *7*, 91; d) Katz, J. L.; Geller, B. J.; Conry, R. R. *Org. Lett*. **2006**, *8*, 2755; e) Katz, J. L.; Selby, K. J.; Conry, R. R. *Org. Lett*. **2005**, *7*, 3505; f) Maes, W.; Rossom, W. V.; Hecke, K. V.; Meervelt, L. V.; Dehaen, W. *Org. Lett*. **2006**, *8*, 4161; g) Konishi, H.; Tanaka, K.; Teshima, Y.; Mita, T.; Morikawa, O.; Kobayashi, K. *Tetrahedron Lett*. **2006**, *47*, 4041.

28 Jiao, L.; Hao, E.; Fronczek, F. R.; Smith, K. M.; Vicente M. G. H. *Tetrahedron,* **2007**, *63*, 4011.

29 Vicente, M. G. H. *Curr. Med Chem.-Anti-Cancer Agents*, **2001**, *1*, 175; b) Henderson, B. W.; Dougherty, T. J. *Photochem Photobiol*. **1992**, *55*, 145; c) Dougherty, T. J; Comer, C. J; Henderson, B. W. *J Nat. Cancer Inst.* **1998**, *90*, 889; d) Tappeiner, H. V., Jesionek, A. *Munch. Med. Wochenschr* **1903**, *50*, 3042; e) Kaye, A. H.; Morstyn, G.; Apuzzo, M. L. J. *J. Neurosurg*. **1988**, 69, 1; f) Hausman, W. *Biochem. Z.* **1909**, 14, 275; g) Lipson, R. L.; Baldes E. J.; Gray, M. J. *Cancer* **1967**, *20*, 2255; Dougherty, T. J.; Grindley, G. E.; Fiel, R., et al. *J Natl Cancer Inst.* **1975**, *55*, 115.

30 Woodburn, K. W.; Vardaxis, N. J.; Hill, J. S.; Kaye, A. H.; Phillips, D. R; *Photochem. Photobiol*. **1992**, *54*, 725; b) Woodburn, K. W.; Vardaxis, N. J.; Hill, J. S.; Kaye, A. H.; Phillips, D. R. *Photochem. Photobiol*. **1992**, *55*, 697; c) Boyle, R. W.; Dolphin, D. *Photochem. Photobiol*. **1996**, *64*, 469; d) Jori, G.; Reddi, E. *In Photodynamic Therapy of Neoplastic Disease,* Vol. 2, Kessel, D. Eds., **1990**; pp117; e) Jori, G. *J. Photochem. Photobiol*. B **1996**, *36*, 87; f) Soncin, M.; Busetti, A.; Reddi, E.; Jori, G.; Rither, B. D.;Kenney, M. E.; Rodgers, M. A. J. *J. Photochem. Photobiol*. B **1997**, *40*, 163; g) Peng, Q.; Moan, J.; Nesland, J. M. *Ultrastruct. Pathol*. **1996**, *20*, 109.

31 Berg, K.; Western, A.; Bommer, J. C.; Moan, J. *Photochem. Photobiol*. **1990**, *52*, 481; b) Ambroz, M.; MacRobert, M. J.; Morgan, J.; Rumbles, G.; Foley, M. S. C.; Phillips, D. *J. Photochem. Photobiol*. B **1994**, *22*, 105; c) Peng, Q.; Moan, J.; Farrants, G.; Danielson, H. E.; Rimington, C. *Cancer Lett*. Shannon, Irel. **1991**, *58*, 17; d) Bottriroli, G.; Croce, A. C.; Ramponi, R.; Vachi, P. *Photochem. Photobiol*. **1992**, *55*, 575; e) Merchat, M.; Spikes, J. D.; Bertoloni, G.; Jori, G. *J. Photochem. Photobiol*. B **1996**, *35*, 149; g) Margaron, P.; Gregoire, M-J.; Scasnar, V.; Ali, H.; van Lier, J. E. *Photochem. Photobiol*. **1996**, *63*, 217.

32 Bonnett, R. *Rev. Contemp. Pharmacother*. **1999**, *10*, 1.

33 Kongshaug, M. *Int. J. Biochem*. **1992**, *24*, 1239; b) Maziere, J. C.; Morliere, P.; Santus, R. *J. Photochem. Photobiol*. B. Biol. **1991**, *8*, 351; c) Obochi, M. O. K.; Boyle, R. W.; vanLier, J. E. *Photochem. Photobiol*. **1993**, *57*, 634; d) Korbelik, M.; Krosol, G.; Olive, P. L.; Chaplin, D. J. *Br. J. Cancer*, **1991**, *64*, 508-512; e) Krosl, G.; Korbelik, M.; Dougherty, T. J. *Br. J. Cancer*, **1995**, *71*, 549; f)Hamblin, M. R.; Newman, E. L. *J. Photochem. Photobiol*. B: Biol. **1994**, *23*, 3; g) Brasseur, N.; Langlois, R.; Lamadeleine, C.; Ouellet, R.; vanLier, J. E. *Photochem. Photobiol*. **1999**, *69*, 345; h) Thomas, J. P.; Girotti, A. W. *Photochem. Photobiol*. **1989**, *49*, 241; e) Brault, D. *J. Photochem. Photobiol*. B: Biol. **1990**, *6*, 79; f) Peng, Q.; Moan, J.; Cheng, L. S. *Cancer, Lett*. **1991**, *58*, 29; g) Jori, G.; Reddi, E. *Int. J. Biochem*. **1993**, *25*, 1369.

34 Chaber, B, A. in *Present status and future prospects for treatment of metastatic cancer.*; Honn, K. V.; Powers, W. E.; Sloane, B. F.; Martinus, N.; Eds, **1986**, pg 15; b) Liotta, L. A. *Cancer Res*. **1986**, 46, 1.

35 Vicente, M. G. H. *Rev. Port. Quím*. **1996**, *3*, 47; b) Stenberg, E. D.; Dolphin, D.; Brückner, C. *Tetrahedron,* **1998**, *54*, 4152; c) Pandey, R. K.; Zheng, G. Porphyrins as Photosensitizers in Photodynamic therapy, in *The Porphyrin Handbook*, Kadish, K. M.; Smith, K. M. Guilard, R. Eds. Academic press, **2000**; d) Dougherty, T. J.; Gomer, C. J.; Henderson, B. W.; Jori, G.; Kessel, D.; Korberlik, M.; Moan, J.; Peng, Q. *J. Natl. Cancer Inst*. **1998**, *90*, 889; e)

Schnitmaker, J. J.; Bass, P.; van Leengoed, M. L. L. M.; van der Meulen, F. W.; Star, W. M.; van Zaudwijk, N. J. *Photochem. Photobiol. B. Biol*. **1996**, *34*, 3; f) Hahn, S. M.; Glatstein, E. *Rev. Contemp. Pharmacother*. **1999**, *10*, 69; g) Hsi, R. A.; Rosenthal, D. I.; Glastein, E. *Drugs,* **1999**, *57*, 725; h) Webber, J.; Herman, M.; Kessel, D.; Fromm, D. *Annals Surg*. **1999**, *230*, 12; i) Webber, J.; Herman, M.; Kessel, D.; Fromm, D. *Langenbeck's Arch. Surg*. **2000**, *385*, 299; j) Mason, M. D. Rev. *Contemp. Pharmother*. **1999**, *10*, 25.

36 Lipson, R. L.; Baldes, E. J.; Olsen, A. M. *J. Natl. Cancer Inst*. **1961**, 26, 1-12

37 Dougherty, T. J. *Photochem. Photobiol*. **1983**, *38*, 377; b) Pandey, R. K.; Majchzycki, D. F.; Smith, K. M. *Proc. SPIE* **1989**, *1065*, 164; c) Bonett, R.; Berenbaum, M. C. *Adv. Exp. Biol. Med*. **1983**, *160*, 241; d) Pandey, R. K. Dougherty, T. J. *Photochem. Photobiol*. **1988**, *47*, 769; e) Kessel, D. *Photochem. Photobiol*. **1986**, *44*, 193.

38 Bonnett, R. *Chem. Soc. Rev*. **1995**, *24*, 19; b) Fisher, A. M. R.; Murphree, A. L.; Gomer, C. J. *Lasers Surg. Med*. **1995,** *17*, 2; c) Sternberg, E. D.; Dolphin, D.; Bruckner, C. *Tetrahedron,* **1998**, *54*, 4151; d) Pandey, R. K. *J. Porphyrins Phthalocyanines*, **2000**, *4*, 368; e) Ali, H.; van Lier, J. E. *Chem. Rev*. **1999**, *99*, 2379.

39 Pandey, R. K.; Zheng, G. In *The Porphyrin Handbook*, Vol. 6, Kadish, K. M.; Smith, K. M. Guillard R. Eds. Academic Press: San Diego, **2000**; pp 157.

40 Kessel, D. *J. Photochem. Photobiol. B: Biol*. **1997**, *39*, 81; b) Spikes, J. D.; Bommer, J. C. *J. Photochem. Photobiol. B: Biol*. **1993**, *17*, 135; c) Peyman, G. A.; Kazi, A. A.; Moshfeghi, D.; Unal, M.; Khoobehi, B.; Yoneya, S.; Mori, K.; Rivera, I. *Ophthal. Surg. Lasers*, **2000**, *31*, 323.

41 Glanzmann, T.; Forrer, M.; Blant, S. A.; Woodtli, A.; Grosjean, P.; Braichotte, D.; van den Bergh, H.; Monnier, P.; Wagnieres, G. *J. Photochem. Photobiol. B: Biol*. **2000**, *57*, 22; b) Garbo, G. M. *J. Photochem. Photobiol. B: Biol*. **1996**, *34*, 109.

42 Martinsen, J.; Pace, J. L.; Phillips, B.M.; Ibers, A. J. *J. Am. Chem. Soc*. **1982,** *104*, 83.

43 Lash, T. D. *J. Porph. Phthal*, **2001**, *5*, 267; b) Wolford, S. T.; Novicki, D. L.; Kelly, B. *Fundam. Appl. Toxicol*. **1995**, *24*, 52; c) Sessler, J. L.; Seidel, D. *Angew. Chem. Int. Ed*. **2003**, *42*, 5134; d) Brown, S. B.; Truscott, T. G. *Chem. Br*. **1993**, *29*, 995; e) Bonnett, R. *Chem. Rev*. **1994**, *24*, 19.

44 Leznoff, C. C., *Phthalocyanines: Properties and Applications*; VCH Publishers: New York, **1990-1996**; Vol. 1-4; b) Volger, A.; Rethwisch, B.; Hutterman, J.; Bensenhard, J. O. *Angew. Chem. Int. Ed. Engl*. **1978**, *17*, 951; c) Vogler, A.; Kunkley, H. *Inorg. Chim. Acta*. **1980**, *44*, L 211; d) Nguyen, K. A.; Pachter, R. *J. Chem. Phys*. **2001**, *114*, 10757; e) Hanack, M.; Zipplies, T. *J. Am. Chem. Soc*. **1985**, *107*, 6127; f) Remier, K. J.; Remier, M. M.; Still, M. J. *Can. J. Chem*, **1981**, *59*, 1388; g) Carlson, J. B.; Vouros, P. *J. Mass. Spectrosc*. **1996**, *31*, 1403.

45 Baker, E. W., *J. Am. Chem. Soc*. **1966**, *88*, 2311; b) Baker, E. W.; Yen, T. F.; Dikie, J. P.; Rhodes, R. E.; Clarke, L. F. *J. Am. Chem. Soc*. **1967**, *89*, 363; c) Kaur, S.; Chicarelli, M. I.;

Maxwell, J. R. *J. Am. Chem. Soc*. **1986**, *108*, 1347; d) Kaur, S.; Gill, J. P.; Evershed, R. P.; Eglinton, G.; Maxwell, J. R. *J. Chromatogr*. **1989**, *473*, 135; e) Quirke, J. M. E.; Dale, T.; Britton, E. D.; Yost, R. A.; Trichet, J.; Belayouni, H. *Org. Geochem*. **1990**, *15*, 1969.

46 Helberger, J. H.; *Ann*. **1937**, *529*, 205; b) Helberger, J. H.; von Rebay, A. *ibid*. **1937**, *531*, 279; c) Helberger, J. H.; von Rebay, A.; Hever, D. B. *ibid*. **1938**, *533*, 197; c) Helberger, J. H.; Hever, D. B. *ibid*. **1938**, *536*, 173.

47 Kopranenkov, V. N.; Takhanova, E. A.; Lukyanets, E. A. *Zh. Org. Khim*. **1979**, *15*, 642; b) Kopranekov, V. N.; Makaranova, E. A.; Lukyanets, E. A. *Zh. Obshch. Khim*. **1981**, *51*, 2727; c) Bender, C. O.; Bonnett, R.; Smith, R. G. *J. Chem. Soc*. **1969**, 345; d) Bender, C. O.; Bonnett, R.; Smith, R. G. *J. Chem. Soc*. **1970**, 1251; c) Bender, C. O.; Bonnett, R.; Smith, R. G. *J. Chem. Soc*. **1972**, 771; d) Bornstein, J.; Remy, D. E.; Sheilds, J. E. *J. Chem. Soc.* **1972**, 1149.

48 Barrett, P. A.; Linstead, R. P.; Rundall, F. G.; Tuey, G. A. P. *J. Chem. Soc*. **1940**, 1079; b) Linstead, R. P.; Weiss, F. T. *J. Chem. Soc*. **1950**, 2975.

49 Vogler, A.; Kunkely, H. *Angew. Chem. Int. Ed. Engl*. **1978**, *17*, 760; b) Kopranenkov, V. N.; Vorotnikov, A. M.; Ivanova, T. M.; Luk'yanets, E. A. *Chem. Heterocyclic Comp*. **1988**, *24*, 1120; c) Kopranenkov, V. N.; Makarova, E. A.; Dashkevich, S. N.; Luk'yanets, E. A. Chem. *Heterocyclic Comp*. **1988**, *24*, 630.

50 Vogler, A.; Kunkley, H.; Rethwisch, B. *Inorg. Chim. Acta*, **1980**, *46*, 101.

51 Remy, D. *Tetrahedron Lett*. **1983**, *24*, 1451.

52 Cheng, R.-J.; Chen, Y.-R.; Chuang, C.-E. *Heterocycles*, **1992**, *34*, 1; b) Cheng, R.-J.; Chen, Y.-R.; Chuang, C.-E. *Polyhedron*, **1993**, *12*, 1353; c) Yasuike, M.; Yamaoka, T.; Ohno, O.; Ichimura, K.; Morii, H.; Sakuragi, M. *Inorg. Chim. Acta*. **1991**, *182*, 83.

53 Vicente, M. G. H.; Tome, A. C.; Walter, A.; Cavaleiro, J. A. S. *Tetrahedron Lett*. **1997**, *38*, 3639.

54 Arnold, D. P.; Burgess-Dean, L.; Hubbard, J.; Rahman, M. A. *Aust. J. Chem*. **1994**, *47*, 969; b) Haake, G.; Struve, D.; Montforts, F.-P. *Tetrahedron Lett*. **1994**, *35*, 9703.

55 Ito, S.; Murashima, T.; Ono, N. *Chem. Commun*. **1998**, 1661.

56 Bonnett, R.; McManus, K. A. *J. Chem. Soc. Chem. Commun*. **1994**, 1129; b) Morgan, A. R.; Pangka, V. S.; Dolphin, D. *J. Chem. Soc. Chem. Commun*. **1984**, 1047; c) Yon-Hin, P.; Wijesekera, T. P.; Dolphin, D. *Tetrahedron Lett*. **1989**, *30*, 6135.

57 Spikes, J. D.; Bommer, J. C. In *Chlorophylls;* Scheer, H. Eds., CRC Press: Boston, **1996**, p 1188.

58 Smith, K. M.; Goff, D. A.; Simpson, D. J. *J. Am. Chem. Soc.* **1985**, *107*, 4946; b) Weller, A.; Livingston, R. *J. Am. Chem. Soc.* **1954**, *76,* 1575; c) Wasielewski, M. R.; Svec, W. A. *J. Org. Chem*. **1980**, *45*, 1969.

59 Cox, M. T.; Jackson, A. H.; Kenner, G. W.; McCombie, S. W.; Smith, K. M. *J. Chem. Soc., Perkin Trans. 1,* **1974**, 516; b) Fischer, H.; Orth, H. *Die Chemie Pyrrols* Akademische Verlag: Liepzig, vol II, part 2, **1940**, p 206.

60 Song, L. M. W.; Wang, K.K.; Zinmeister, Alan R. *Cancer* **1998**, *82* (2), 421.

61 Woodward, R. B. *Pure Appl. Chem*. **1961**, *2*, 383; b) Smith, K. M., *J Chem Soc. Perk Trans.* 1, **1988**, 3119.

62 Vicente, M.G. H. *Curr. Med Chem.-Anti-Cancer Agents*, **2001**, *1*, 175.

63 Kessel, D. H; Luguya, R.; Vicente, M. G. H. *Photochem. Photobiol*. **2003**, *78*, 431-435; b) Krieg, R. C.; Messmann, H.; Schlottman, K.; Enlicher E.; Seeger, S.; Scholmerich, J.; Knuechel, R. *Photochem. Photobiol*. **2003**, *78*, 393.

64 Bommer, J., Ogden, B. F., *Tetrapyrrole Therapeutic Agents*, U. S. Patent 4,693,885, Sept 15, **1987**.

65 Gomi, S.; Nishizuka, T.; Ushiroda, O.; Takahashi, H.; Sumi, S. *Heterocycles* **1998**, *48*, 2231; b) Abraham, R. J.; Rowan, A. E. In *Chlorophylls;* Scheer, H. Ed.; CRC Press: Boston, **1996**; pp 797.

66 Hargus, J. A., in Master Dissertation, Louisiana State University, Baton Rouge, **2005**.

67 W. G. Roberts, F. -Y. Shiau, J. S. Nelson, K. M. Smith and M. W. Berns. *J. Natl. Cancer Inst*. **1988**, *80,* 330; b) W. G. Roberts, K. M. Smith, J. L. McCullough and M. W. Berns. *Photochem. Photobiol.* **1989**, *49*, 431.

68 Vogel, E.; Köcher, M.; Schmickler, H.; Lex, J. *Angew. Chem. Int. ed. Engl*. **1986**, *25*, 257.

69 Vogel, E.; Sicken, M.; Röhrig, P.; Schmickler, H.; Lex, J.; Ermer, O. *Angew. Chem. Int. ed. Engl*. **1988**, *27*, 411.

70 Aukauloo, M. A.; Guilard, R. *New. J. Chem.* **1994**, *18*, 1205; b) Callot, H. J.; Rohrer, A.; Tschamber, T. *New. J. Chem.* **1995**, *19*, 155; c) Vogel, E.; Bröring, M.; Scholz, P.; Deponte, R.; Lex, J.; Schmickler, H.; Schaffner, K.; Braslavsky, S. E.; Müller, M.; Pörting, S.; Weghorn, S. J.; Fowler, C. J.; Sessler, J. L. *Angew. Chem. Int. ed. Engl*. **1997**, *36*, 1651.

71 Vogel, E. *Heterocycl. Chem*. **1996**, *33*, 1461; b) Vogel, E.; Bröring, M.; Erben, C.; Demuth, R.; Lex, J.; Nendel, M.; Houk, K. N. *Angew. Chem. Int. ed. Engl*. **1997**, *36*, 353.

72 Vogel, E.; Balci, M.; Pramod, K.; Koch, P.; Lex, J.; Ermer, O. *Angew. Chem. Int. ed. Engl*. **1987**, *26*, 928.

73 Wehrle, B.; Limbach, H.-H.; Köcher, M.; Ermer, O.; Vogel, E. *Angew. Chem. Int. ed. Engl*. **1987**, *26*, 934.

74 Jux, N.; Koch, P.; Schmickler, H.; Lex, J.; Vogel, E. *Angew. Chem. Int. ed. Engl*. **1990**, *29*, 1385.

75 Richert, C.; Wessels, J. M.; Mueller, M.; Kisters, M.; Benninghaus, T.; Goetz, A. E. *J. Med. Chem.,* **1994**, 37, 2797.

76 Chang, C. K.; Morrison, I.; Wu, W.; Chern, S.-S.; Peng, S.-M. *J. Chem. Soc., Chem. Commun*. **1995**, 1173; b) Vogel, E.; Köcher, M.; Balci, M.; Teichler, I.; Lex, J.; Schmickler, H.; Ermer, O. *Angew. Chem. Int. ed. Engl*. **1987**, *25*, 931.

77 Vogel, E. *Pure Appl. Chem*. **1990**, *62*, 557; b) Vogel, E. *Pure Appl. Chem*. **1993**, *65*, 143; c) Vogel, E. *Pure Appl. Chem*. **1996**, *68*, 1335; d) Sessler, J. L. *Angew. Chem. Int. ed. Engl*. **1994**, *33*, 1348; e) Toporowicz, M.; Ofir, H.; Levanon, H.; Vogel, E.; Köcher, M.; Pramod, K.; Fessenden, R. W. Photochem. Photobio. **1989**, *50*, 37.

CHAPTER 2. β,β'-FUSED METHYLENEPROPANOPORPHYRINS

2.1 Introduction

Porphyrins can be used as chemical sensors[1-3], catalysts[4,5], and as molecular devices[6,7]. Among those, porphyrin systems functionalized with redox groups, such as ferrocene, have been reported in the last decades and have found potential applications in solar energy conversion[1-3]. It was found that the properties of these systems depended on the efficient π-overlap between the central porphyrin unit and the peripheral substitutents. Lately metallocene-modified porphyrins, as charge-transfer materials, have also attracted much attention due to their wide applications as molecular conductors and molecular magnets. Metallocene-modified porphyrin complexes have been studied over the last decades[8-9]. In most cases, the metallocene fragments were connected to the porphyrin through various spacers at meso- or at β- position of porphyrins. For example, the direct connection of the metallocene to the meso-positions of porphyrins through a single C-C bond, an aromatic system, or via conjugated double or triple bonds[1,10,11] have been reported. However, the spectroscopic and electrochemical results indicate negligible strong communications between the two fragments. This is attributed to the poor overlap (if any) between the two aromatic π-systems.

In the meanwhile, the design and synthesis of covalently linked multiporphyrin arrays became a frontier research area in porpyrin chemistry. These multiporphyrin arrays[12] have unique photo-electronic properties[13-16], and have attracted much recent interest because they play important roles in many areas such as in light harvesting,[17] energy and electron transfer,[18] and multielectron redox catalysis[19]. The construction of these multiporphyrin arrays also required an extended π-electron network. Among the fused porphyrin dimers and oligoporphyrins being reported, significant novel spectroscopic properties[20-21] were observed; in particular, the

formation of bisporphyrin sandwich complexes has been shown to dramatically change the redox properties of porphyrins. It was found that in bis(porphyrin) sandwich complexes, the porphyrin complexes acted as both the electron-donor and electron-acceptor species[22]. The initial study in our group had shown that the fusion of two porphyrins at β-positions could enhance the overlap of the two π-systems, and enhance the interactions between the redox moieties. The formation of sandwich complexes can enhance the overlap of porphyrin HOMOs to assist the energetic situation of both the porphyrin-porphyrin bonding and anti-bonding orbitals. It is reported that the large metal ion in these bis(porphyrin) sandwich complexes are generally much easier to oxidize than the corresponding monoporphyrin[23-24], since the large metal ion is able to hold two porphyrin macrocycles close enough to raise the HOMO energy level. For the metallocene-containing bisporphyrin and oligoporphyrins, there is long distance communication from frameworks that should find attractive applications in nanoelectronics.

On the other hand, the covalently linked porphyrin arrays, especially cofacial porphyrins[25,26] have been widely studied in the past two decades because of their unique photo-electronic properties. Particularly, these cofacial porphyrins have found potential applications as electron-energy transfer moieties in molecular wires[21,27]. So far, several fused bisporphyrins and oligoporphyrins have been synthesized[28]. Among these, the most successful cofacial porphyrins are the so-called "Pacman Porphyrin" systems, which consist of two octa-alkylporphyrins held almost cofacial through a single rigid bridge.[25] However, the synthesis of cofacial porphyrins has been, and will still remain, a challenge.[29]

The development of new methods for carbon-carbon bond formation is at the heart of organic synthesis. The most desirable methods are those that are easily accomplished in large scale, operate near ambient temperature, and do not require drastic reaction conditions. Usually,

the construction of carbocyclic rings requires the preparation of highly functionalized intermediates. The reactions of atomic oxygen with unsaturated organic compounds have demonstrated that the primary reactive intermediates can undergo extensive rearrangement before forming isolable oxygenated products[30,31]. The reactions of triplet oxygen atoms with olefins[32], methylenecycloalkanes[31], and phenylethylenes[33] have been reported.

The construction of these bisporphyrins and oligoporphyrins required efficient syntheses of mono-methylenepropanoporphyrins and bismethylenepropanoporpyrins. In this Chapter, the efficient synthesis of these porphyrin monomers will be discussed. Based on these monomers, the construction of novel bisporphyrins will also be discussed.

2.2 Results and Discussion

2.2.1 Syntheses of β,β'-Fused Methylenepropanoporphyrins

The tandem carbon-carbon bond formation catalyzed by Pd(0) through [3+2] cycloaddition has been reported[34-37]. In most cases, a strongly electron-withdrawing group, such as ester, nitrile, nitro, ketone or sulfone, is required to activate the double bond towards the cycloaddition. In the meanwhile, there are few reports about the reactivity of the activated double bonds toward this [3+2] cycloaddition[38]. Also it is required that the Pd(0) be generated *in situ* for the 1,3-dipolar cycloaddition. Solvents also found an important role in this type reaction. For example, the substitution of toluene with THF could greatly shorten the reaction time and enhance the cycloaddition yield[39]. When considering the readily available selective nitration of porphyrin, the Pd(0) catalyzed [3+2] cycloaddition reaction of 2-[(trimethylsilyl)methyl]-2-propen-1-yl acetate with electron-deficient double bonds are very attractive in building methylenepropanoporphyrins[38]. A Michael-addition, followed by the ring-closure reaction, is believed to be the mechanism[40-42] for this reaction.

2.2.1.1 Synthesis of β,β'-Fused Mono-methylenepropanoporphyrins

It's well known, that although there are a total of 22π-electrons in the porphyrin system, only 18 of them are involved in any of the delocalization pathways (see *Figure 2-1*). The other four electrons that are not participating in the delocalization are located at the opposite two peripheral double bonds. These two cross-conjugated double bonds have isolated alkene properties. It was found that when there was a nitro group attached at the β-position of a porphyrin, as in 2-nitro-5,10,15,20-tertraphenylporphyrins, the nucleophilic addition to that specific position became very easy. Thus, based on the nitroporphyrins, a range of β-substituted porphyrins could be obtained. Our group previously had reported the utility of 2-nitro-5,10,15,20-tertraphenylporphyrins for double-bond activation on the periphery of porphyrins due to the readily available preparation of 2-nitroporphyrins in large scale and without the requirement for chromatography purification[43, 44].

Free Base Porphyrin   Metalloporphyrin or Porphyrin Dication
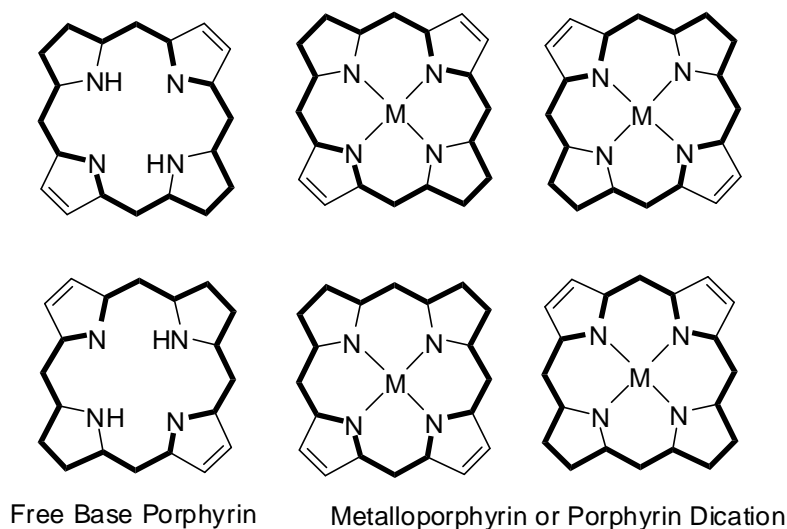
Figure 2-1. Tautomerism of free base porphyrin (left) and metalloporphyrin (middle to right).

Here, nickel(II) and copper(II) were chosen as the central metal of the porphyrin, due to the facts that nickel(II) porphyrins are robust, can survive both the strong acidic and basic conditions, and could be used directly for NMR study. On the other hand, it is easy to generate

free base porphyrin from copper(II) porphyrins and subsequently other types of metal salts can be inserted to form various types of metalloporphyrin.

M=Cu, Ni
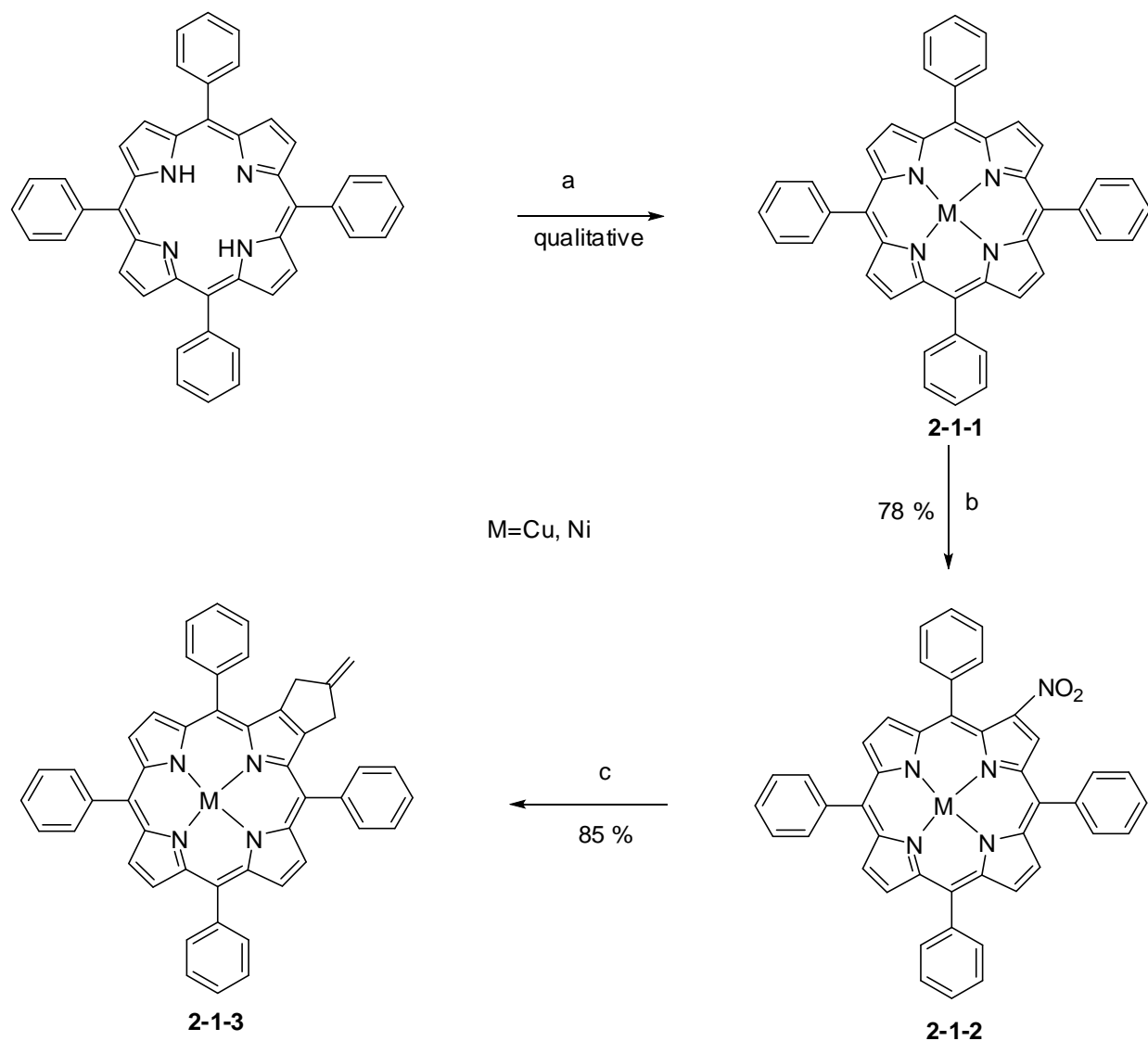
Scheme 2-1. Methylenepropanoporphyrin synthetic route. Reaction conditions: a) M(acac)$_2$, MeOH/CHCl$_3$ = 1/3, reflux; b) LiNO$_3$, AcOH / Ac$_2$O / CHCl$_3$, reflux; c) Pd(OAc)$_2$, (i-PrO)$_3$P, 2-[(trimethylsilyl)methyl]-2-propen-1-yl acetate, THF, Argon, reflux.

The syntheses of β,β'-fused methylenepropanoporphyrin monomers **2-1-3** (see *Scheme 2-1*) were started from 5,10,15,20-tertraphenylporphyrin (H$_2$TPP), which was easily synthesized from the Adler-Longo condensation of pyrrole and benzaldehyde[45]. Considering the

41

regioselectivity differences between free-base porphyrin and the metalloporphyrin for the nitration reaction, the insertion of metal before nitration was mandatory[46, 47].

Quantitative metalation of porphyrin to generate **2-1-1** was performed at refluxing temperature by dissolving H_2TPP in methanol/chloroform (v/v = 1/3) in the presence of 10 equivalents of metal acetylacetonate [$M(acac)_2$]. After filtration to remove the excess amount of $M(acac)_2$, the desired product **2-1-1** was obtained. Further recrystallization was performed from MeOH/DCM. The subsequent mono-nitration to generate **2-1-2** was performed in chloroform/acetic acid (AcOH); acetic anhydride (Ac_2O) and lithium nitrate ($LiNO_3$) was used as the nitration-reagent. The resulting **2-1-2-Cu** was isolated in 78% yield and a similar yield was obtained for **2-1-2-Ni**. The preparation of mono-methylenepropanoporphyrin **2-1-3** was achieved by Pd(0) catalyzed [3+2] cycloaddition reaction as described in the literature[38]. The catalyst, Pd(0), was prepared *in situ* by reacting of $Pd(OAc)_2$ with triisopropylphosphite [$(i-PrO)_3P$] in THF under strict air-free conditions at room temperature. It generally took 30 minutes for the generation of Pd(0). It was found that even a minute amount of air could ruin the generation of the Pd(0) catalyst. The solution changed color from yellow to colorless with the generation of Pd(0). To this colorless THF solution of Pd(0), was added solid **2-1-2**, and followed by 2-[(trimethylsilyl)methyl]-2-propen-1-yl acetate with exclusion of air. Immediately, this reaction mixture was placed in a preheated (90 ^{o}C) oil bath and refluxed for a period of 2 days. TLC was used to follow the reaction. Upon the complete consumption of the starting material, the reaction temperature was raised to 100 ^{o}C, and the mixture was refluxed for an additional period of 2 days. After the reaction mixture was cooled to room temperature, the desired **2-1-3** was purified using a silica gel column eluted with DCM/hexane (v/v = 1/10). After removing the solvent under

vacuum, **2-1-3-Cu** was obtained as a reddish brown solid in 85% yield; **2-1-3-Ni** was obtained in similar yield.

It was found that the presence of metal at the porphyrin central was very necessary for ensuring the success of this Pd(0) catalyzed cycloaddition reaction. The use of free-base porphyrin for this coupling reaction failed to generate the desired product. The nature of the metal also played an important role for the success of this reaction. It was noticed that despite the fact that the Pd(0) catalyzed cyclization reaction works well for both **2-1-2-Cu** and **2-1-2-Ni,** it can only generate tiny amounts of **2-1-3-Zn** when **2-1-2-Zn** was used.
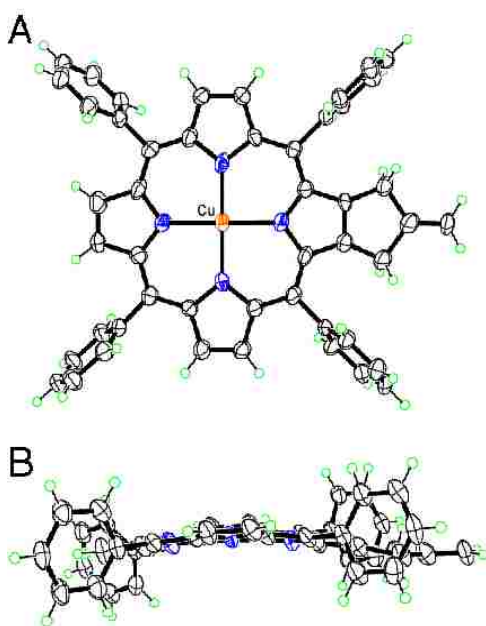
Figure 2-3. X-Ray structure of **2-1-3-Cu** (CuTPPCp): A) top-view, B) side-view.

Figure 2-3 shows the X-ray structure of **2-1-3-Cu**. The crystal was obtained by diffusion of hexane into a concentrated DCM solution of **2-1-3-Cu**. The 24-atom porphyrin ring system has a flattened saddle conformation, with mean out-of-plane deviation 0.18 Å and maximum 0.417(9) Å. The Cu atom lies 0.017(1) Å from this plane and forms Cu-N distances in the range 1.975(7) - 2.006(6) Å. The five-membered ring carrying the exocyclic C=C bond is nearly

43
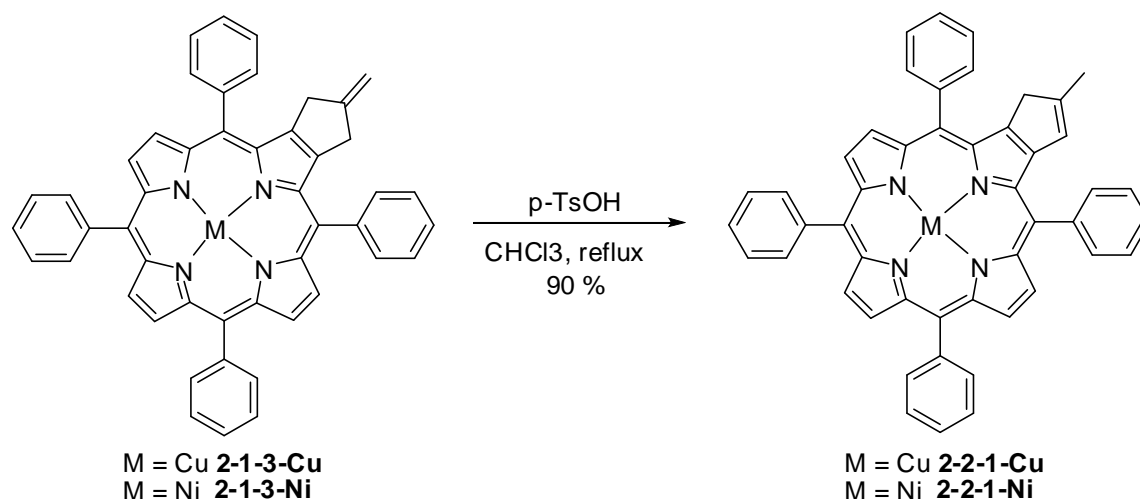
Scheme 2-2. Double-bond migration under weak acid catalytic condition.
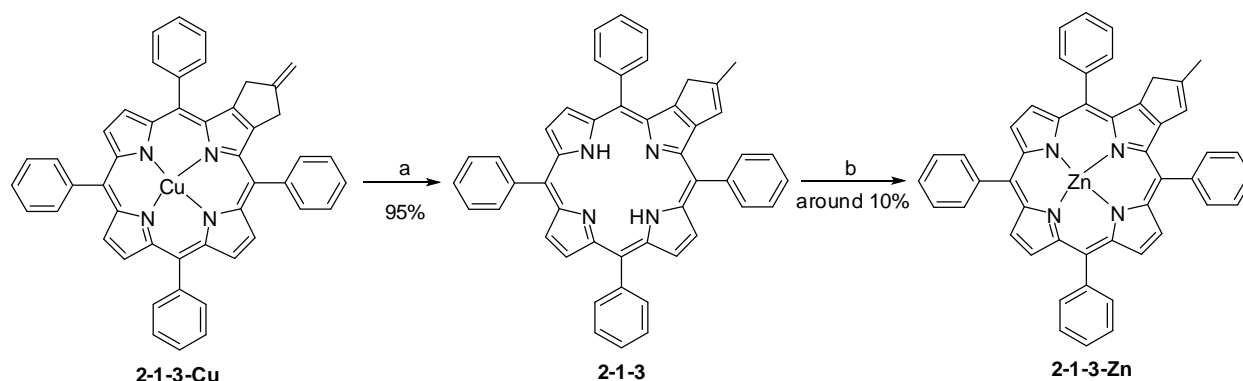
Scheme 2-3. ZnTPPCp synthesis. Reaction conditions: a) 5% H_2SO_4/TFA; b) Zn(OAc)$_2$, MeOH/CHCl$_3$ = 1/3, reflux.

planar, with mean deviation 0.03 Å, and it is coplanar with the pyrrole ring fused to it. In the presence of p-toluenesulfonic acid (p-TsOH) as a weak acid catalyst, **2-1-3-M** (M = Cu, Ni) was successfully converted into its regioisomer **2-2-1-M** (M = Cu, Ni) (see *Scheme 2*-2) in around 90% yield in refluxing CHCl$_3$ solution after a period of one day. It was not possible to obtain the desired **2-2-1-Zn** from the Pd(0) catalyzed [3+2] reaction with znic(II)porphyrin. An alternative route to prepare **2-2-1-Zn** from demetalation of **2-1-3-Cu** and subsequent insertion of zinc(II) also failed. The demetalation works well and generated a 95% yield of free-base porphyrin;

however the metalation reaction using the zinc(II)-salt was only performed in extremely low yield (see *Scheme 2-3*). It was found that most of the starting material free-base porphyrin was converted into extreme polar mixtures with a green color. This is attributed to the easy photo-oxidation properties in the presence of air due to the photosensitizing properties of **2-1-1-Zn**. After this, porphyrin **2-1-3-Cu** was treated with lithium diisopropylamide (LDA)[48-50] at 0 °C (see *Scheme 2-4*). The color of the solution changed from red to green, which indicated deprotonation of the fused cyclopentadienide ring system. This color change is attributed to the delocalization of electrons from the porphyrin π-system of **2-1-3-Cu** with the aromatic cyclopentadienide. After adding FeCl$_2$ to the reaction mixture under strict air-free conditions, it was allowed to continue stirring at room temperature for an additional period of one day.
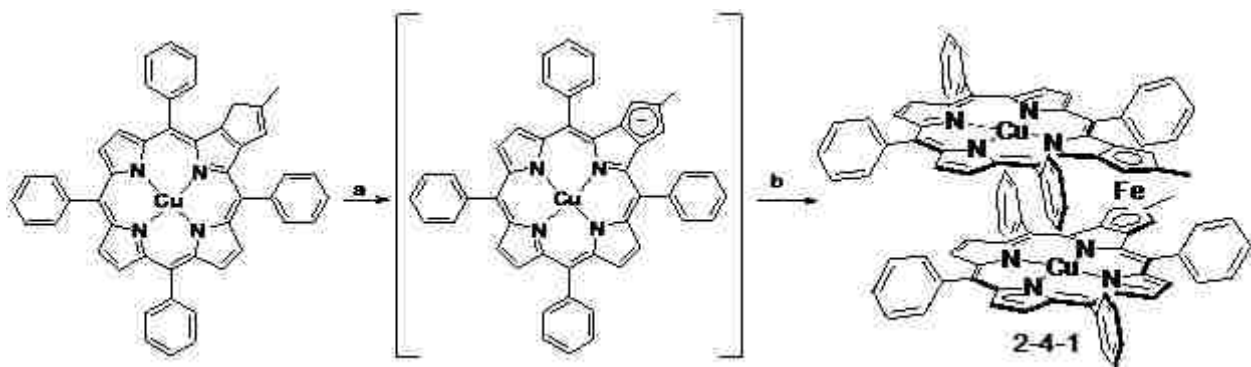
Scheme 2-4. Bis-copper(II) porphyrinatoferrocene complex synthesis. Reaction conditions: a) LDA, THF, 0 °C~r.t.; b) FeCl$_2$, THF, reflux; 7.5 % yield.

MALDI-TOF mass spectrometry gave a peak at MW 1510.1 corresponding to the formation of **2-4-1**. Silica gel plates were used for the purification, eluted with DCM/cyclohexane (v/v = 15/1). In the optical spectrum for **2-4-1**, there was a broad Soret band [UV-vis: λ$_{max}$ CH$_2$Cl$_2$ (log ε) 410 nm (5.04)] and no well-defined Q bands were observed.

2.2.2 Synthesis of β,β'-fused Bis-methylenepropanoporphyrins.

Selective Synthesis of cis-Bis(methylenepropano)porphyrins
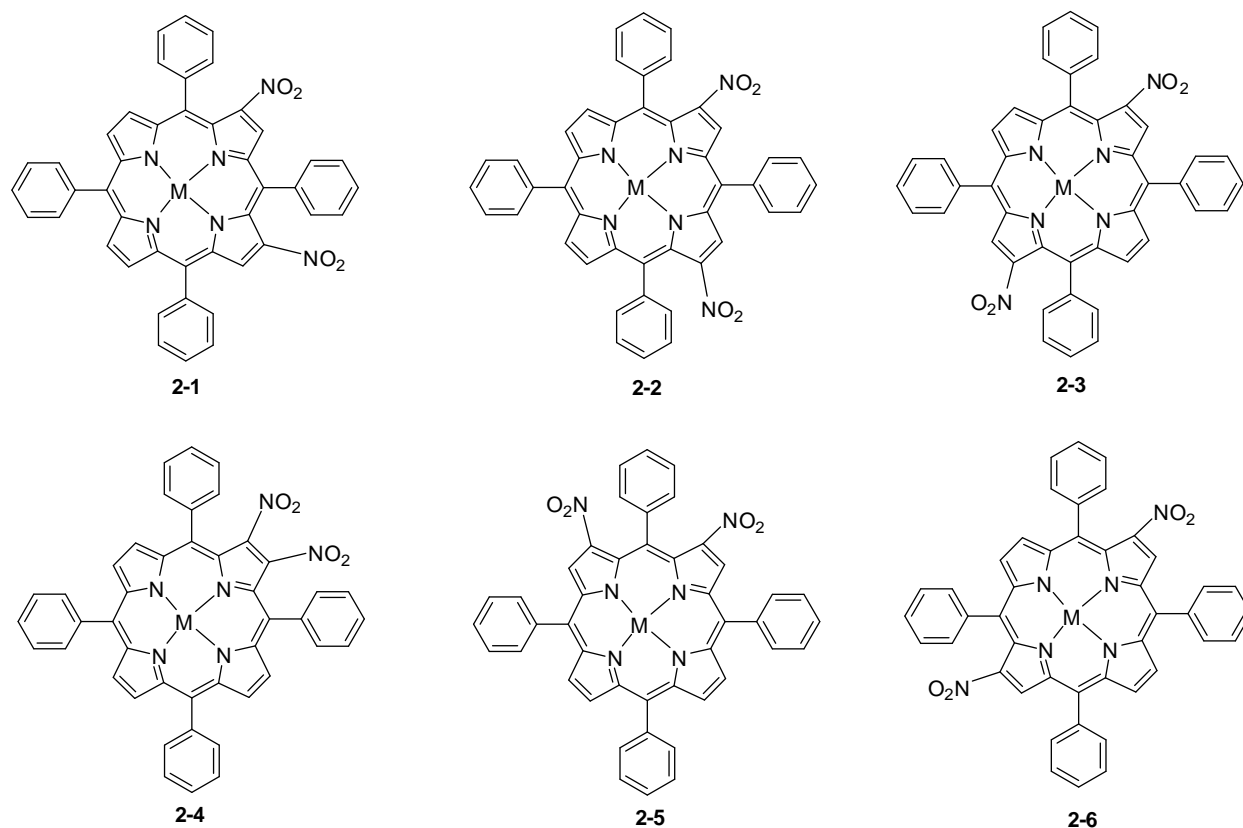
Figure 2-4. Six regioisomers of the di-nitro-5,10,15,20-tetraphenylporphyrin.

It was considered, in the planning of this project, that *opp*-bis(methylenepropano) porphyrins might eventually yield *opp*-bis(cyclopentadienide)porphyrins that could be used for construction of novel conducting redox materials. The syntheses of these bis(methylenepropano)porphyrins involved the preparation of **2-n** (n = 1-6) (see *Scheme 2-5* and *2-6*), which was prepared from extending the reaction time of the mono-nitration reaction and with the use of excess amounts of nitration reagents (see *Scheme 2-1*). The six regioisomers of dinitroporphyrin **2-1** to **2-6** were obtained as a mixture in around 60% total yield. Only a tiny amount of the mono-nitro-product and trinitro-products were obtained. After a short silica gel

column separation, the six regioisomers of dinitroporphyrin **2-1** to **2-6** (see *Figure 2-4*) were separated as a mixture from the other nitro-products.
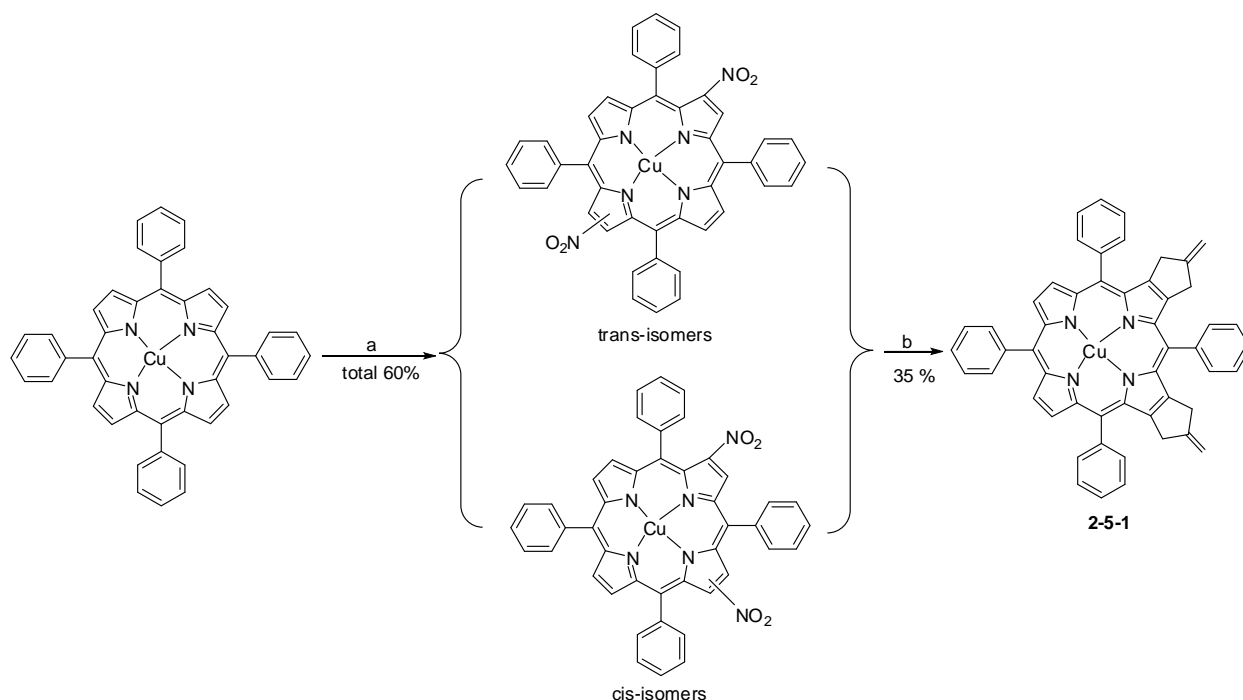
Scheme 2-5. Selective cis-Bis(methylenepropano)copper(II)-porphyrin dsynthesis. Reaction conditions: a) LiNO₃, AcOH/Ac₂O/CHCl₃, reflux; b) Pd(OAc)₂, (i-PrO)₃P, 2-[(trimethylsilyl)methyl]-2-propen-1-yl acetate, THF, argon, reflux.
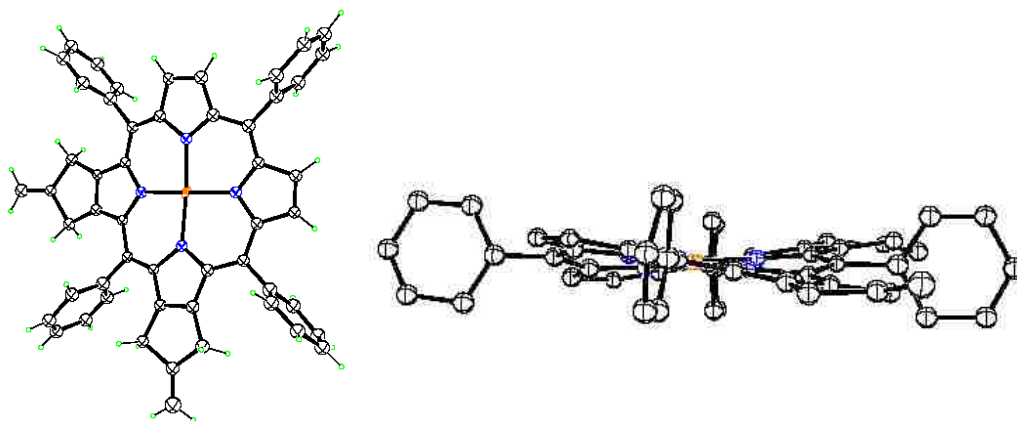
Figure 2-5. X-Ray structure of **2-5-1**: top-view (Left); side-view (right).

Without further purification, this mixture was used directly for the subsequent [3+2] cyclolization reaction to prepare bis(methylenepropano)metal(II)-porphyrins **2-5-1** and **2-6-1**. Surprisingly, it was found that in both cases, only the cis-regioisomer of the bis(methylenepropano)porphyrin (**2-5-1** and **2-6-1**) was obtained from this reaction and that was no trans-regioisomer (based on TLC and ^{1}H-NMR spectroscopy).
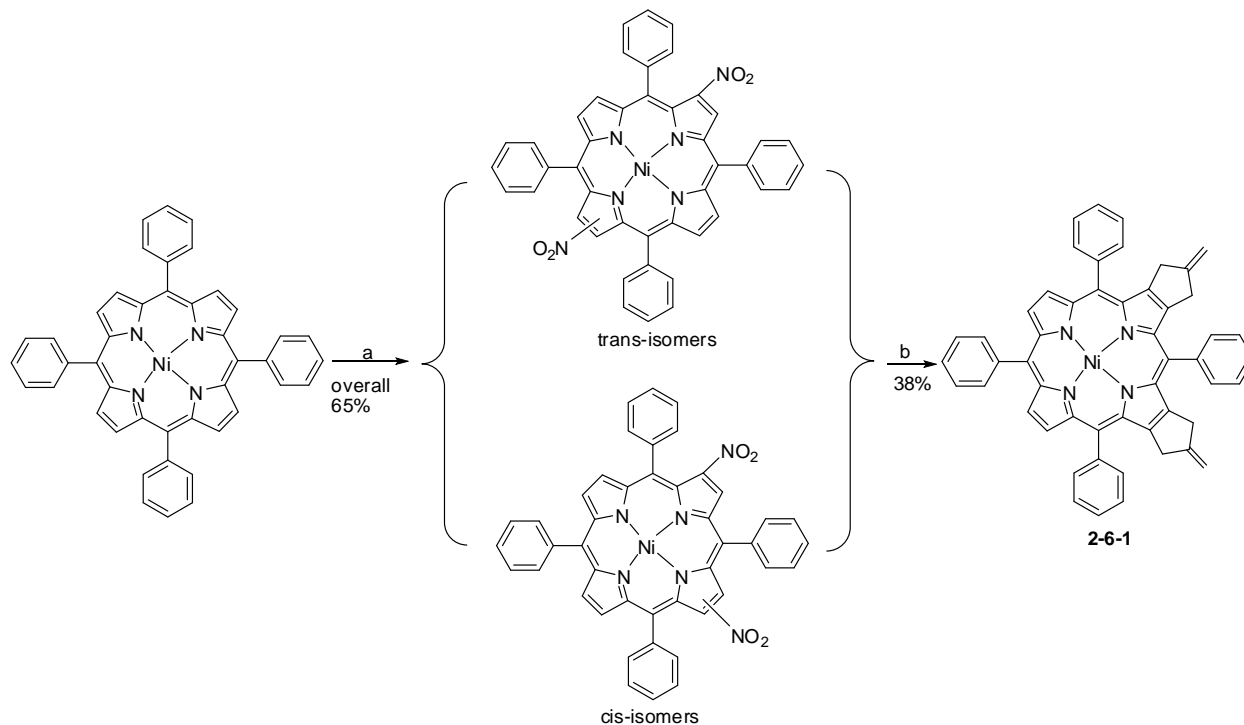
Scheme 2-6. Selective synthesis of **2-6-1**. Reaction conditions: a) LiNO$_3$, AcOH/Ac$_2$O/ CHCl$_3$, reflux; b) Pd(OAc)$_2$, (i-PrO)$_3$P, 2-[(trimethylsilyl)methyl]-2-propen-1-yl acetate, THF, argon, reflux.

This selective formation of the cis-regioisomer during the Pd(0) catalyzed cycloaddition of dinitroporphyrin was first observed for the preparation of **2-5-1** from CuTPP(NO$_2$)$_2$, as shown in *Scheme 2-5*. It was surprising to find that the Pd(0) catalyzed cycloaddition of dinitroporphyrin [**2-n** (n = 1-6)] was faster than the cyclization of the mono-nitro-porphyrin (**2-1-2**). Separation was performed on a silica gel column eluted with DCM/hexane (v/v = 1/10).

Although the reaction for the preparation **2-5-1** was faster, as indicated from the color-change during the reaction (from green to reddish brown), the isolated yield was lower - only a 35% yield was obtained. The X-ray structure of **2-5-1** is shown in *Figure 2-5*. The crystal was grown by diffusion of hexane into a concentrated chloroform solution of **2-5-1**. The molecule has two cis-oriented exocyclic double bonds as shown in the X-ray structure. The reproducibility of this regioselectivity was tested by using the mixture of dinitro-Ni(II)-porphyrins (**2-1-Ni** to **2-6-Ni**). MALDI-TOF mass spectrometry gave a peak at MW 774.2 corresponding to the formation of the bis-cycloaddition product **2-6-1** (see *Figure 2-6*).
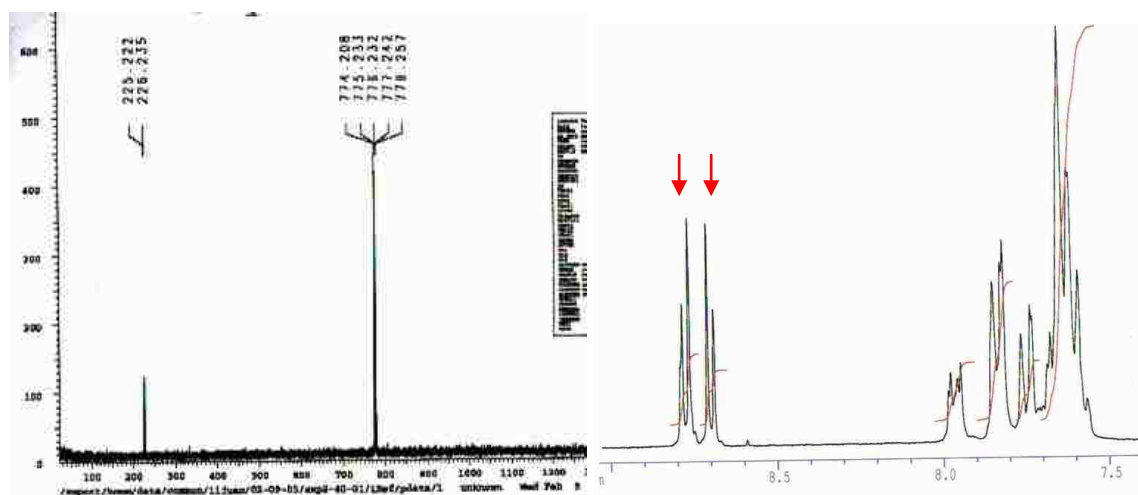
Figure 2-6. Characterizations of **2-6-1**. MALDI-TOF (left) and ^{1}H-NMR spectra (right); red-arrows indicate the β-proton position of porphyrin in the NMR.

The ^{1}H-NMR spectrum (see *Figure 2-6*) gave a split peak for the porphyrin β-protons, which corresponds to the formation of the cis-regioisomer of the bis-cycloaddition product **2-6-1**. At first, we attributed the selective formation of the cis-regioisomer to a different reaction pathway of the two regio-isomer formations. We assumed the cis-regioisomer was formed through a kinetic process while the trans-regioisomer was formed from a thermodynamic process. In that case, the extended reaction time would help the generation of the trans-regioisomer. Efforts to achieve the trans-regioisomer failed. Even when the reaction time was increased to two

weeks, still no trans-regioisomer formation was detected. We attributed this to release of a proton and NO_2 during the reaction which was poisoning the Pd(0) catalyst. Thus extra amounts of catalyst were also added (two equivalents) and still only a trace amount of trans-regioisomer was detected after extension of the reaction time to two weeks.

Seletively Synthesis of trans-Bismethylenepropanoporphyrins:
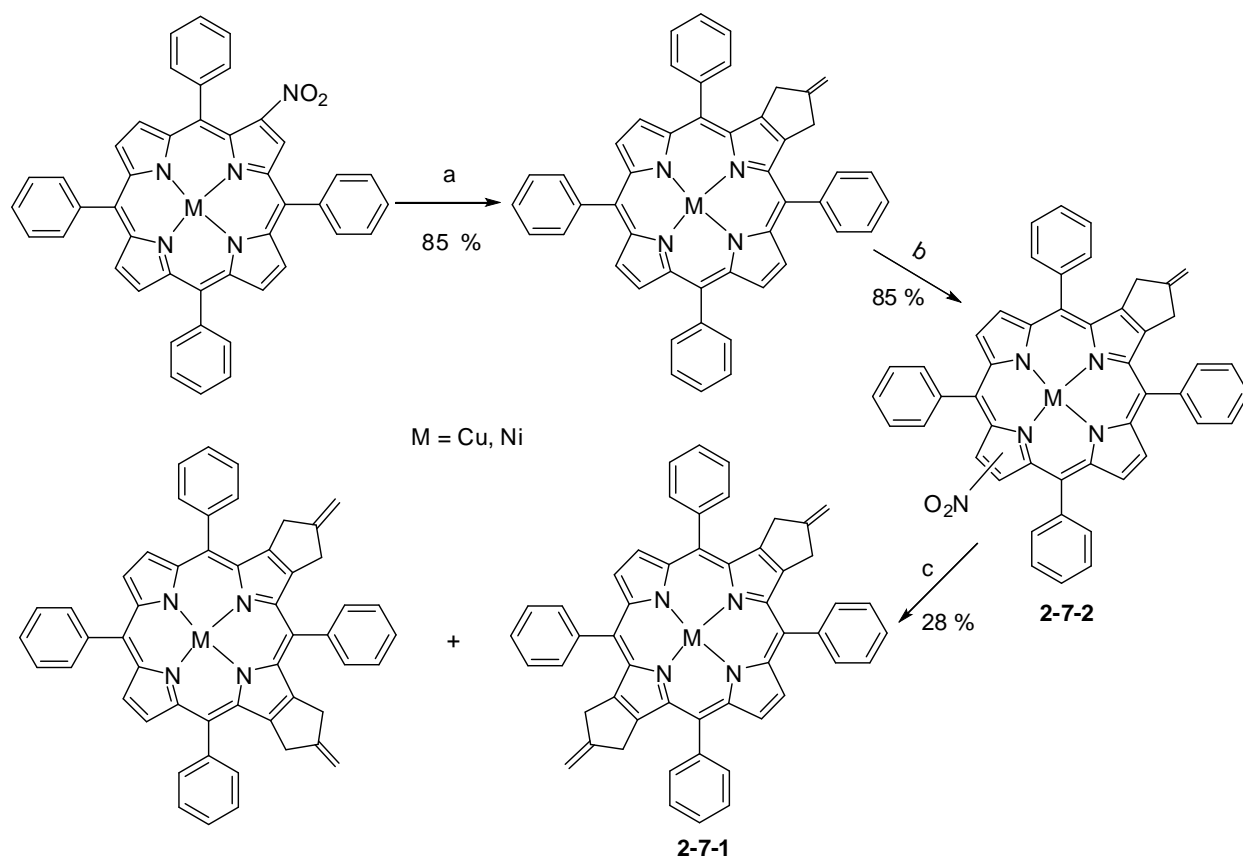
Scheme 2-7. First approach to the trans-bis(methylenepropano)porphyrin. Reaction conditions: a) Pd(OAc)$_2$, (i-PrO)$_3$P, 2-[(trimethylsilyl)methyl]-2-propen-1-yl acetate, THF, argon, reflux; b) LiNO$_3$, AcOH/Ac$_2$O/CHCl$_3$, reflux; c) Pd(OAc)$_2$, (i-PrO)$_3$P, 2-[(trimethylsilyl)methyl]-2-propen-1-yl acetate, THF, argon, reflux.

After failing to generate the trans-regioisomer of **2-7-1** from the Pd(0) catalyzed cyclization reaction of the mixture of dinitro-porphyrin of regioisomers, alternative routes were tried. The first approach was to follow the previous synthetic route of a former group member (see *Scheme 2-7)*. For this approach, the mono-methylenepropanoporphyrin was used as starting

material; after one nitration compound **2-7-2** was generated. After a subsequent Pd(0) catalyzed cyclization reaction, the mixture of regioisomers of bis(methylenepropano)porpyrins (**2-5-1** and **2-7-1**) was obtained in 28% overall yield. Despite the fact that the yield was acceptable, the separation was extremely difficult. Instead of column separation, silica gel plates were required for the separation, which limited the scale of the desired product prepared and made it unpractical. In this case, attracted to the selective synthesis of cis-regioisomer of bismethylenepropanoporphyrins (**2-5-1** and **2-6-1**), we began to seek the alternative synthetic route for the selective synthesis of the trans-regioisomer of bis(methylenepropano)porphyrin (**2-7-1**). It was noticed that there was different electron delocalization pathway between metal-porphyrin and free-base porphyrin, and so we expected to achieve the selective formation of the trans-regioisomer (**2-8-1**) from Pd(0) catalyzed cycloaddition of the mixture of trans-regioisomers of dinitroporphyrins. In other words, we selected to drive the formation of the trans-regioisomer by forcing the initial nitro groups to give the trans-dinitroporphyrin. The preparation of trans-dinitroporphyrin was achieved from reactions shown in *Scheme 2-8*. The demetalation reaction to remove copper(II) from **2-1-2-Cu** was performed using 5% H_2SO_4 in 95% TFA, from which **2-1-2-2H** was achieved in 98% yield. Subsequently, we wanted to insert metal and then subject it to the Pd(0) catalyzed cyclization reaction. However, the nitration of **2-1-2-2H** failed to generate the desired trans-regioisomer of dinitro-product **2-8-1**; instead only the mixture of tri-nitroporphyrins (**2-8-3**) was obtained (see *Scheme 2-8*). To achieve the selective formation of the trans-dinitroporphyrins, four groups were introduced to the opposite four β-positions of the starting porphyrin. The main idea was to block the formation of the cis-dinitroporphyrin. Upon selective formation of the mixture regioisomers of trans-dinitroporphyrin **2-9-4**, we expected to obtain the desired trans-bis(methylenepropano)porphyrin **2-7-1** after Pd(0)

51
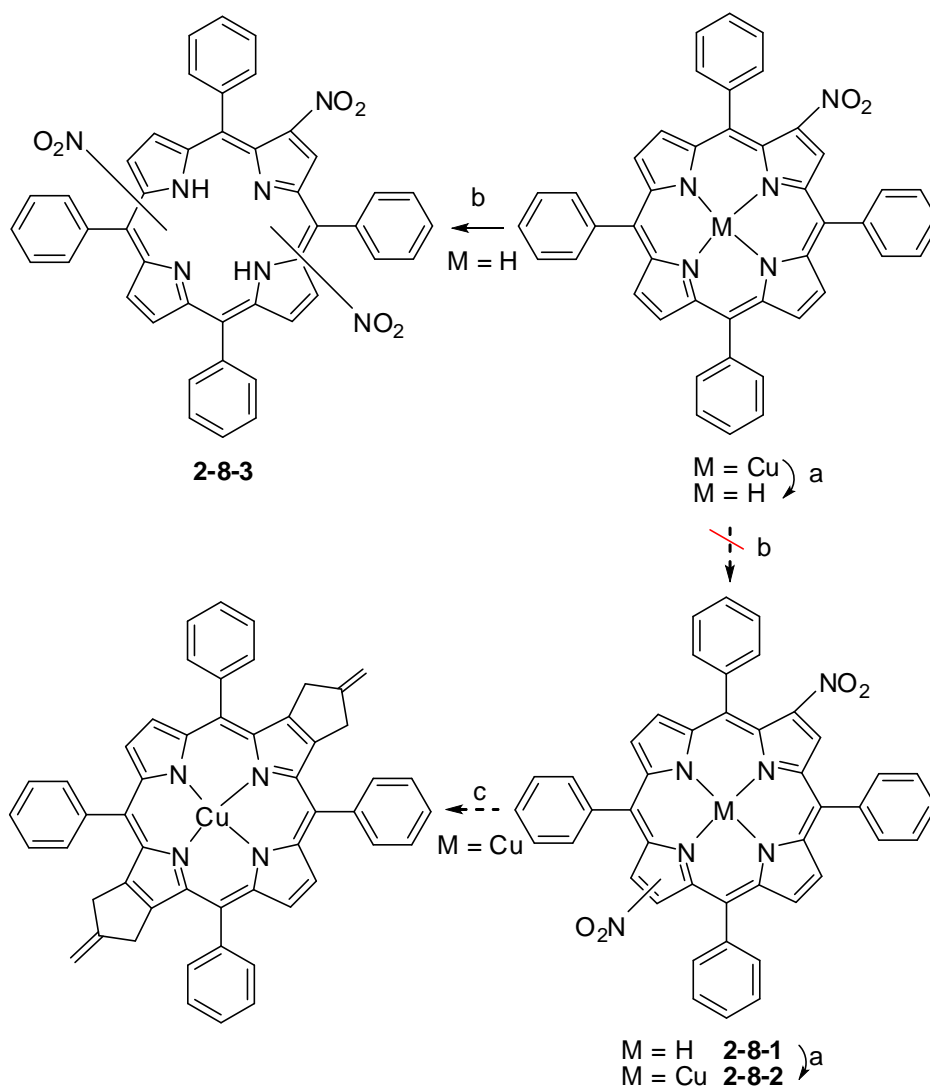
Scheme 2-8. Second approach for the selective syntheses of trans-bis(methylenepropano)porphyrin. Reaction conditions: a) 5% H_2SO_4/TFA, r.t.; b) $LiNO_3$, AcOH/Ac_2O/$CHCl_3$, reflux.

catalyzed cyclization. The regioselectivetertrabromination of free-base porphyrin H_2TPP was performed in chloroform and excess NBS was used. To avoid the potential dehalogenation reaction in the following nitration and Pd(0) catalyzed reaction associated with the presence of these bromines, four methyl groups were introduced from the Suzuki-coupling reaction, to form **2-9-2**. As shown in *Scheme 2-9*, **2-9-1** was obtained by refluxing the free-base porphyrin (H_2TPP) with 6.7 equivalents of NBS in $CHCl_3$[51] for 4 hours.

Scheme 2-9. Third approach for the selective formation of trans-bis(methylenepropano)porphyrin **2-9-5**. Reaction conditions: a) NBS, CHCl₃, reflux 4 hrs; b) Pd(PPh₃)₄, CH₃B(OH)₂, THF/toluene, argon, reflux; c) Ni(acac)₂, MeOH/CHCl₃ = 1/3, reflux; d) LiNO₃, AcOH /Ac₂O/CHCl₃, refluxing; e) Pd(OAc)₂, (i-PrO)₃P, 2-[(trimethylsilyl)methyl]-2-propen-1-yl acetate, THF, argon, refluxing for 5 days.
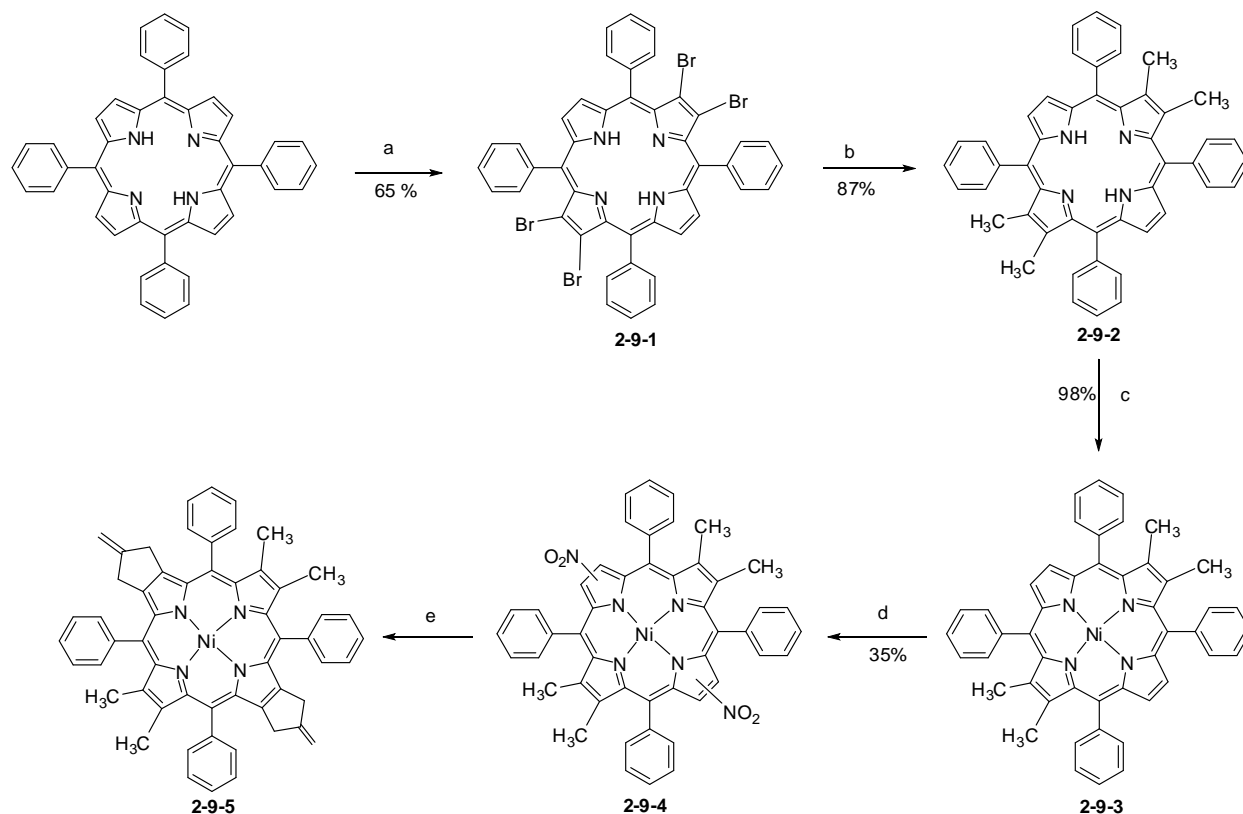
TLC and UV-vis were used to follow this reaction. The reaction was stopped when TLC indicated no starting material left and the Soret band shifted to 430 nm in the UV-vis spectra. After stopping this reaction, it was cooled to room temperature and cleaned up using a short silica gel plug to remove excess NBS, washing with DCM to collect the desired product. After removing the solvent under vacuum, the solid was washed with methanol three times, and **2-9-1** was obtained in 65% yield as a purple solid. No further purification was performed. The Suzuki-coupling reaction between **2-9-1** and CH₃B(OH)₂ was performed by refluxing them in THF/toluene (v/v = 3/2) under argon. It took a period of two days under strict air-free condition[52] to finish this reaction. Pd(PPh₃)₄ was used as catalyst, and **2-9-2** was obtained in 87%

yield after separation. Because of the huge polarity differences between the starting material **2-9-1** and the desired product **2-9-2**, the separation was very convenient. Only a very short silica gel plug was required. Pure DCM was used to elute down the small amount of starting material **2-9-1**. After that, the eluting solvent was changed to the mixture solvents of DCM/ethyl acetate (v/v = 10/1). **2-9-2** was obtained as a green fraction from the column and after removing the solvents under vacuum it was obtained as purple microcrystals. The high polarity of **2-9-2** is attributed to the nonplanar distortion of porphyrin macrocycle to form the saddle conformation associated with the presence of the tetra-methyl groups at the β-positions.

The insertion of Ni(II) was performed by refluxing **2-9-2** with an excess amount of Ni(acac)$_2$ in chloroform/methanol (v/v = 1/3) overnight. After filtration, **2-9-3** was obtained in 98% yield. Although the mono-nitration of **2-9-3** was completed within 0.5 hour and the yield was around 90%, the dinitration to generate **2-9-4** by simply extending the nitration time and increasing the amount of nitration reagent used, was slower. After separation, only 35% yield of **2-9-4** was obtained, with large amounts of the trinitro-porphyrins as byproducts. No further purification was performed before submitting the mixture of regioisomers of **2-9-4** to the Pd(0) catalyzed cycloaddition reaction. Unfortunately, the cyclization reaction of **2-9-4** was found to be extremely slow. According to TLC, only a small amount of **2-9-5** was obtained after refluxing it for five days.

Faced with all the problems associated with either the selective dinitration or the final step cyclization, finally, the selective formation of **2-7-1** was approached from the Pd(0) catalyzed cycloaddition of free-base nitroporphyrin. Encouraged by the fact that the Pd(0) catalyzed cyclization of metal(II) porphyrin **2-8-2** predominantly gave the cis-regioisomer ,a literature search presented an interesting selectivity associated with "chlorin formation"[53]
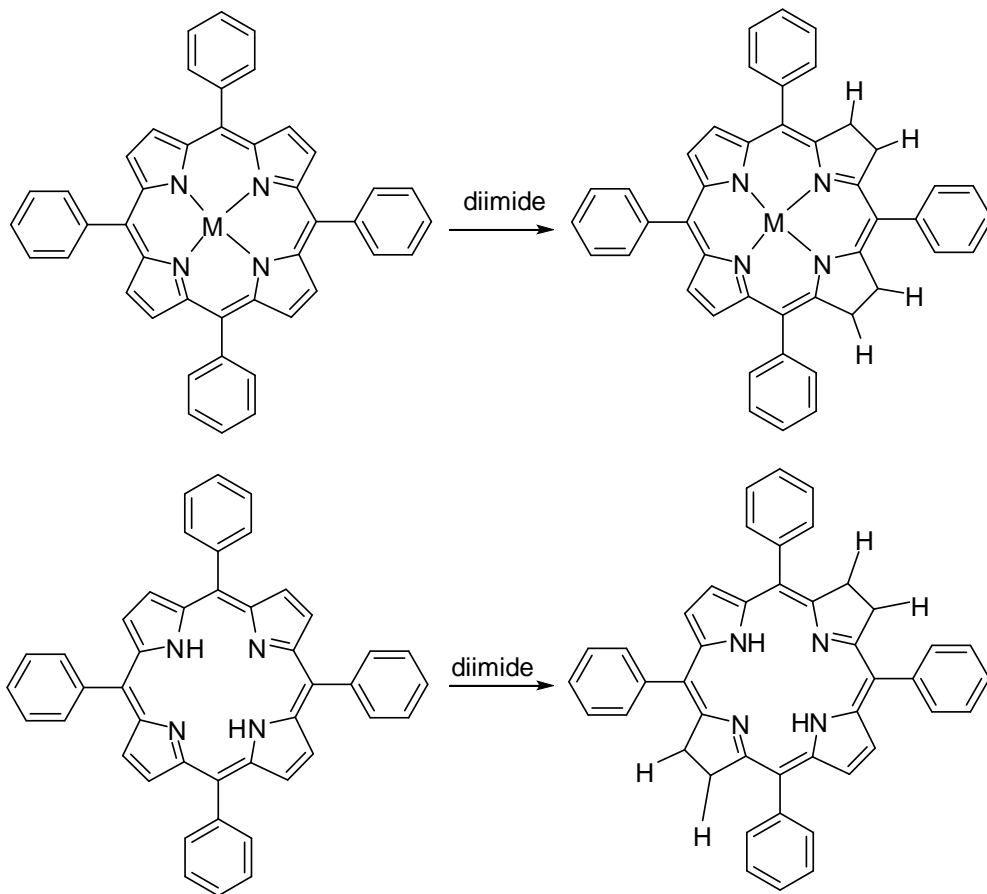
Scheme 2-10. Selective formation of chlorins from porphyrins: top, isobacteriochlorin; bottom, bacteriochlorin.
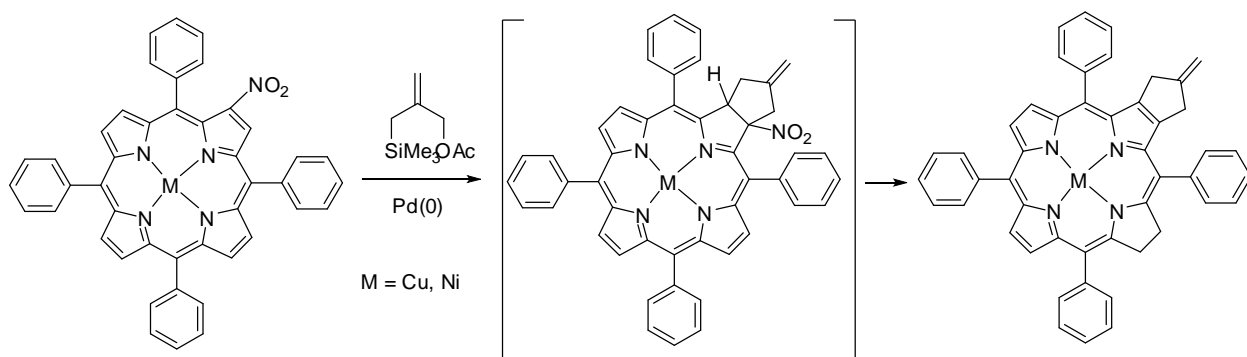
Scheme 2-11. The chlorin intermediate directs the formation of bis(methylenepropano)porphyrin processes.

In the literature, it was found that in either oxidation or reduction of the β-position double-bond of porphyrins, there was a preferential formation of bacteriochlorins for the free-

base porphyrin, and isobacteriochlorins for the metal-porphyrin (see *Scheme 2-10*). We attributed the selective formation of the cis-regioisomers for the metal-porphyrin to the formation of chlorin-intermediate (see *Scheme 2-11*). Since the cyclization of the dinitro-metal(II) porphyrin had been found result in the selective formation of cis regioisomer, it would be very reasonable for the achievement of the trans-regioisomer when dinitrated free-base porphyrin was used for the cyclization.
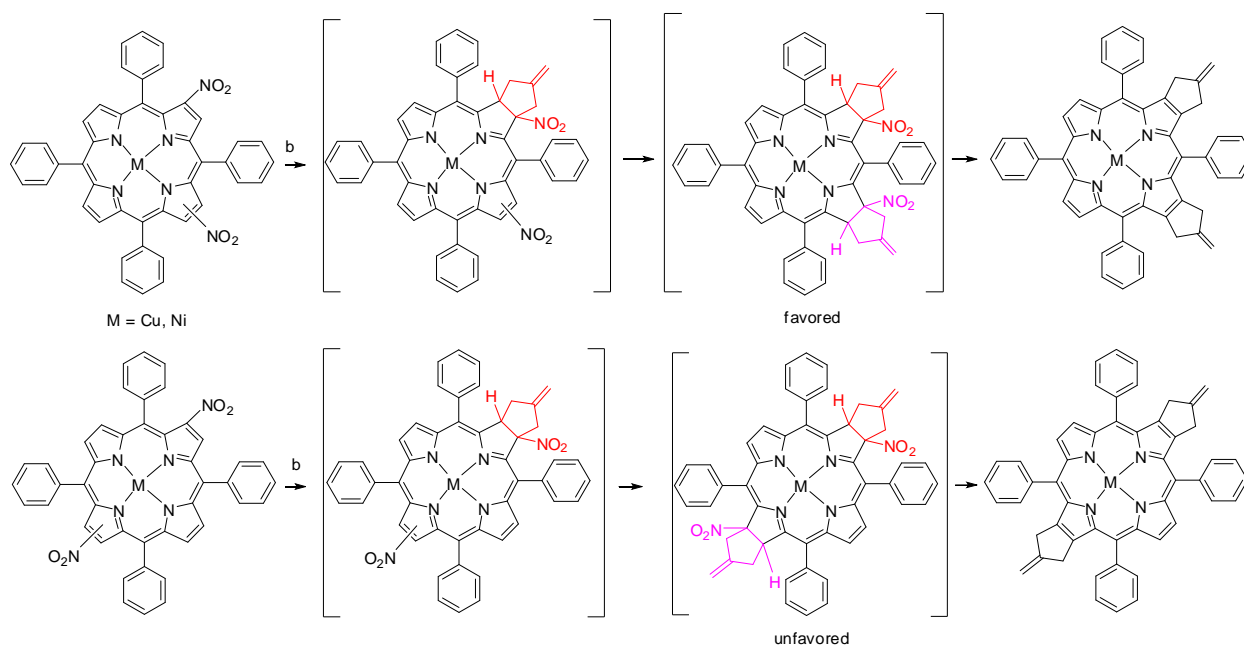
Scheme 2-12. Chlorin induces the regioselectivity for the formation of bis(methylenepropano)porphyrins.

The chlorin intermediate was observed in the formation of the **2-1-3** and could even be isolated when performing the cyclization reaction at low temperatures. It was converted into porphyrin by increasing the temperature from 90 °C to 100 °C over 24 hours or even a longer period. Two modified routes were planned to improve the synthesis rate and yield. The first modification was based on reaction shown in *Scheme 2-9*. It was started from **2-9-4**, after performing the mononitration and by the Pd(0) catalyzed cyclization reactions; the second nitration was performed and followed by the second Pd(0) catalyzed cyclization reaction.

Another modification route was designed to introduce copper(II) instead of nickel(II) into the porphyrin before dinitration, and then removal of the copper(II) before the final Pd(0) catalyzed cyclization reaction. By doing this, we envisioned the Pd(0) catalyzed cyclization of the free-base porphyrin might be able to generate the desired trans-isomers of bis(methylenepropano)_porphyrin. In the second improved approach, copper(II) was first removed under acidic condition to obtain the free-base dinitrated porphyrin; then under strictly air-free condition the Pd(0) catalyzed reaction was performed. Unfortunately, the trans-bis(methylenepropano)porphyrin was obtained, but in extremely low yield. MALDI-TOF mass spectrometry gave a peak at 718 corresponding to the formation of **2-13-1**, the ^{1}H-NMR spectrum indicated the formation of this trans-isomer.

2-13-1
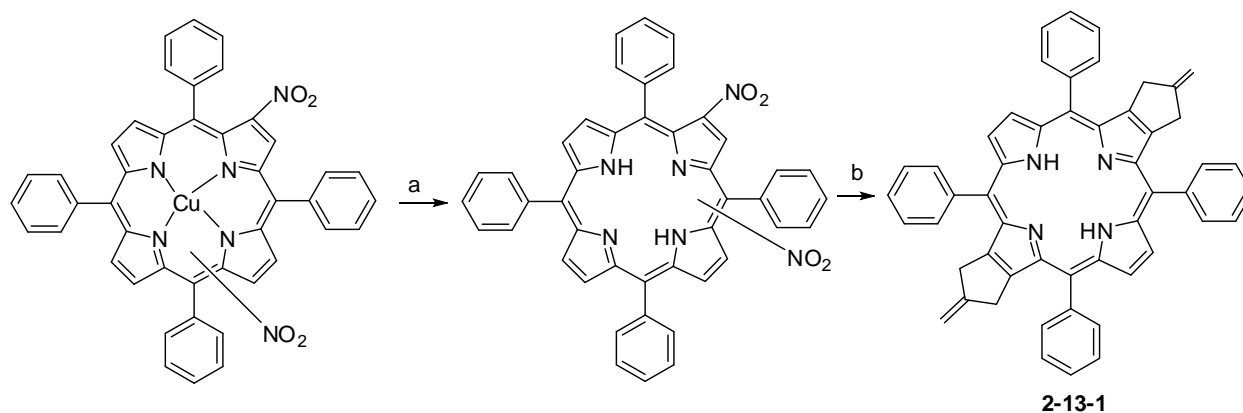
Scheme 2-13. Forth approach in the selective formation of the trans-bis(methylenepropano)porphyrin. Reaction conditions: a) 5% H_2SO_4/TFA, DCM, r.t.; b) Pd(OAc)$_2$, (i-PrO)$_3$P, 2-[(trimethylsilyl)methyl]-2-propen-1-yl acetate, THF, argon, reflux.

2.2.3. Construction of Cofacial Bisporphyrins

Our group has previously synthesized several fused metallocenoporphyrin derivatives and bisporphyrin-metallocenes.[24] An unexpectedly efficient synthesis of a cofacial metallo-bisporphyrin was found from a simple DBU catalyzed carbon-carbon bond formation followed by a self-sensitized oxygenation reaction at room temperature. The β,β'-fused

57

methylenepropanoporphyrin **2-1-3** served as a key precursor in the construction of both cofacial bisporphyrin and the metallocenoporphyrins.[24] In particular, we made use of literature observations that methylene cycloalkanes can be oxygenated to give very useful intermediates[21], and in this particular case, formation of cofacial bis-porphyrin systems.
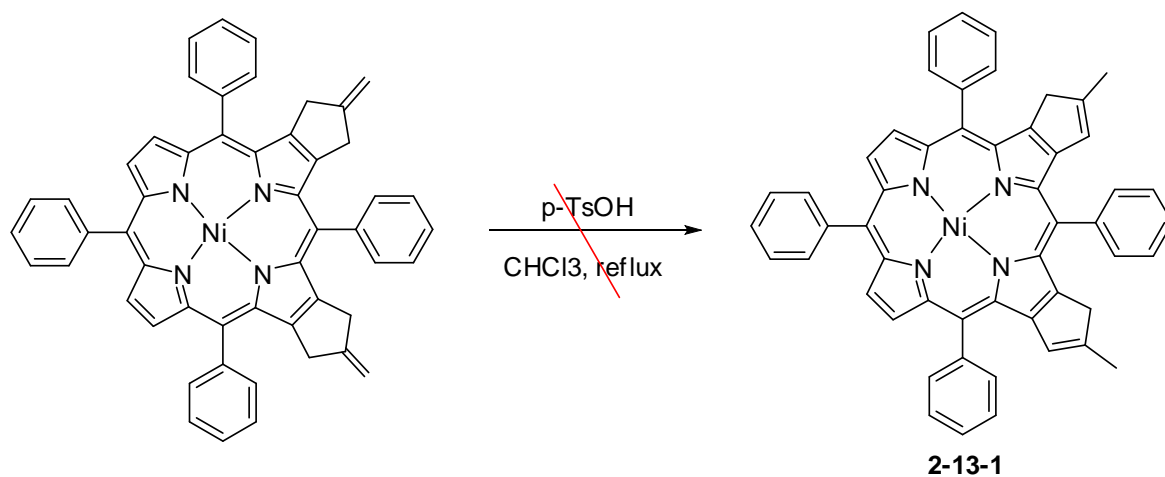
Scheme 2-13. Double-bond migration under acidic condition failed to generate **2-13-1**.
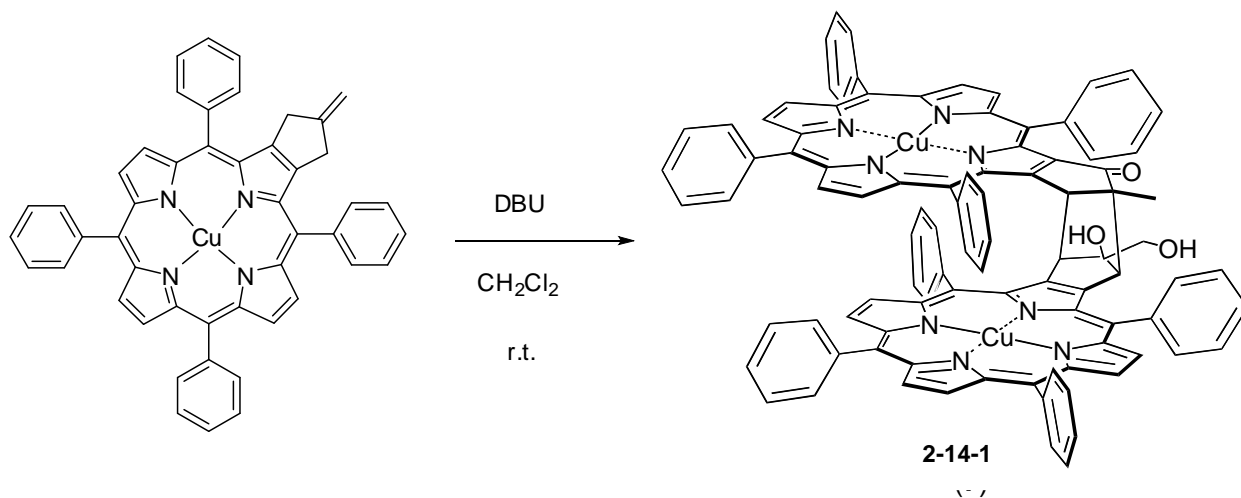
Scheme 2-14. Formation of **2-14-1** under DBU catalyzed reaction in DCM at room temperature.

By using a weak acid catalyst (p-TsOH), **2-1-3** had been successfully converted into its regioisomers **2-2-1** with the formation of an endo-position double bond in 90% yield (see *Scheme 2-2*) [16]. Despite the high yield of the endocyclic double bond formation under weakly

acidic condition, with the presence of two methylenepropano groups at **2-6-1**, only extremely low yields of **2-13-1** were generated from this p-TsOH-catalyzed double-bond migration reaction (see *Scheme 2-13*). Since weakly acidic condition failed to generate the desired product **2-13-1** in acceptable yield, a base-catalyzed migration reaction was performed by using DBU as the base catalyst. At first, **2-1-3-Cu** was used, with DBU as base and DCM as solvent. Surprisingly, it was found after the reaction mixture had stirred for 52 hours at room temperature under air in the presence of light, no desired product **2-13-1** was generated from **2-1-3-Cu.** Instead an interesting porphyrin dimer **2-14-1** was obtained in 60% yield after chromatographioc separation using DCM/EtOAc (see *Scheme 2-14*).
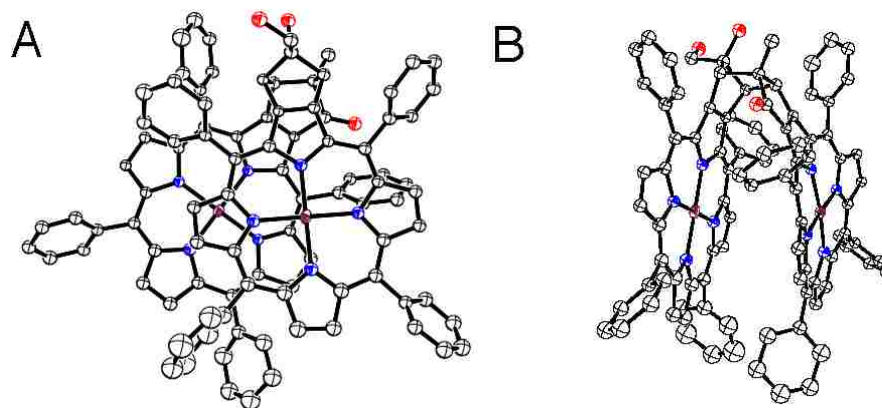
Figure 2-7. X-Ray structure of **2-14-1**: A, top-view; B, side-view.

Fortunately, we were ale to obtain the crystal from the diffusion of hexane to a concentrated DCM solution of **2-14-1**. The X-ray structure is shown in *Figure 2-7*. The two porphyrin macrocycles are partially overlapped as shown from the top-view of the X-ray; the side-view clearly indicates the cofacial arrangement of these two porphyrin macrocyles with approximately parallel porphyrin planes [dihedral angle 4.1(5)º], and a perpendicular distance

59

between coordination planes of approximately 4.2Å. The Cu–Cu distance is 5.290(4) Å, and Cu–N distances fall within the range 1.942(8) - 2.002(8) Å.
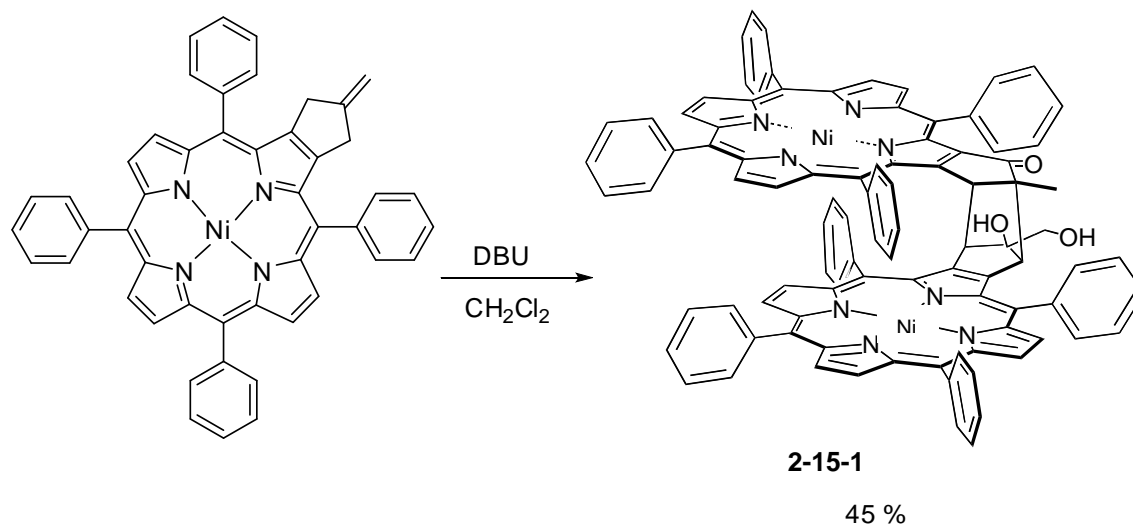
Scheme 2-15. Formation of **2-15-1** under DBU catalyzed condition in DCM at room temperature.
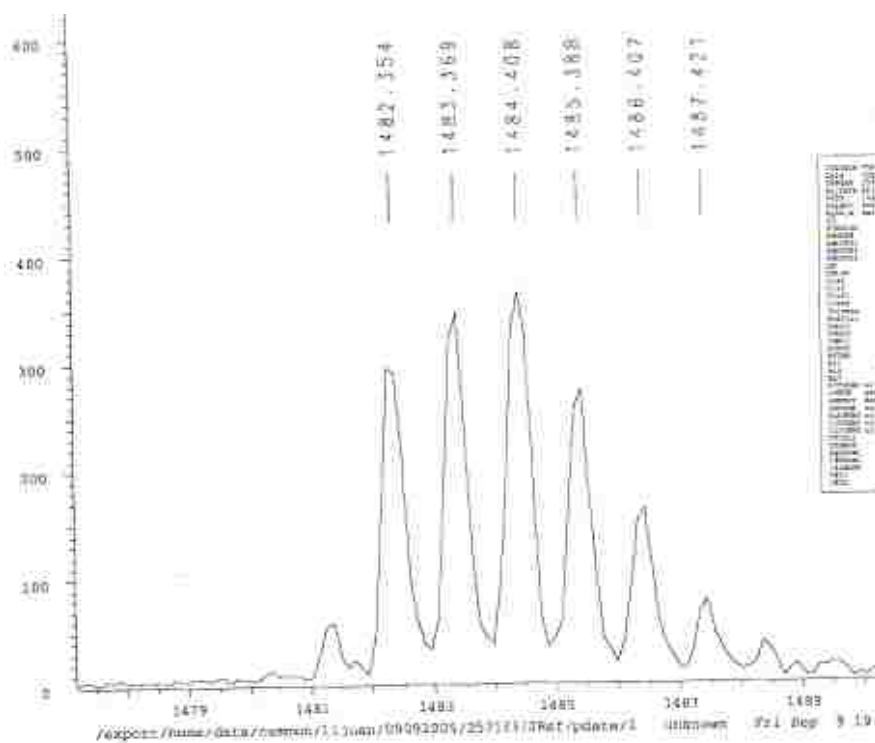
Figure 2-8. MALDI-TOF mass spectrum of **2-15-1**.

The effort of removing copper(II) from **2-14-1** to generate free-base porphyrin dimers using 95% TFA and 5% H_2SO_4 only caused decomposition. In the meanwhile, **2-1-3-Ni** was also used in the same reaction condition, and **2-15-1** was obtained in 45% yield after a silica gel column separation (see *Scheme 2-15*). MALDI-TOF mass spectrometry gave a peak at 1482.2 corresponding to the losing of one water molecule from **2-15-1** (see *Figure 2-8*). Surprisingly, with the presence of an additional substituent group at the meso-position of the porphyrin, no reaction was detected based on TLC and MALDI-TOF and all starting materials were recovered (see *Scheme 2-15*). This result indicated that the electron delocalization of porphyrin macrocyle might be the cause of the formation of porphyrin dimers. Several reactions were designed and performed to search for the underlying mechanism for this reaction (see *Scheme 2-16* and *Scheme 2-17*). In the absence of either light or air, or both of them, no desired porphyrin dimers were formed, with only a small amount of intermediate being detected. Thus both the light and air were critical for this reaction. Already many metalloporphyrin are known as photosensitizers[55-57], and used as catalysts for the oxidation of the isolated double bonds of small molecules at the presence of air and light[58].
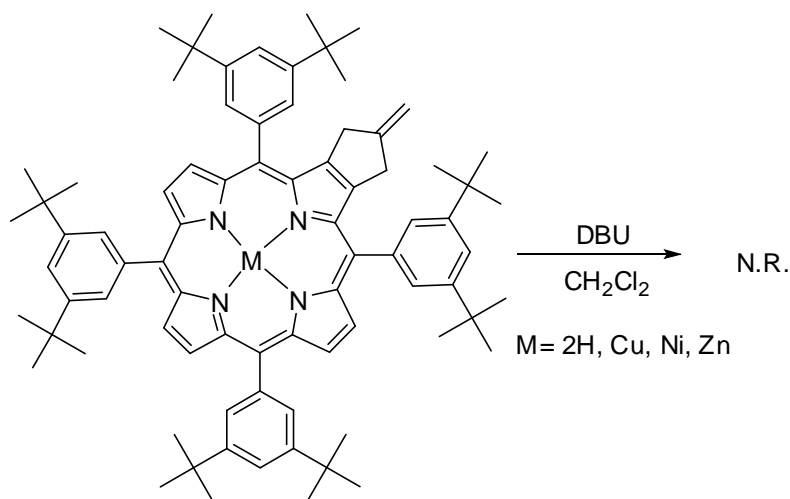
Scheme 2-15. With the presence of bulky t-butyl group at the meso-position of porphyrins, no reaction occurs.
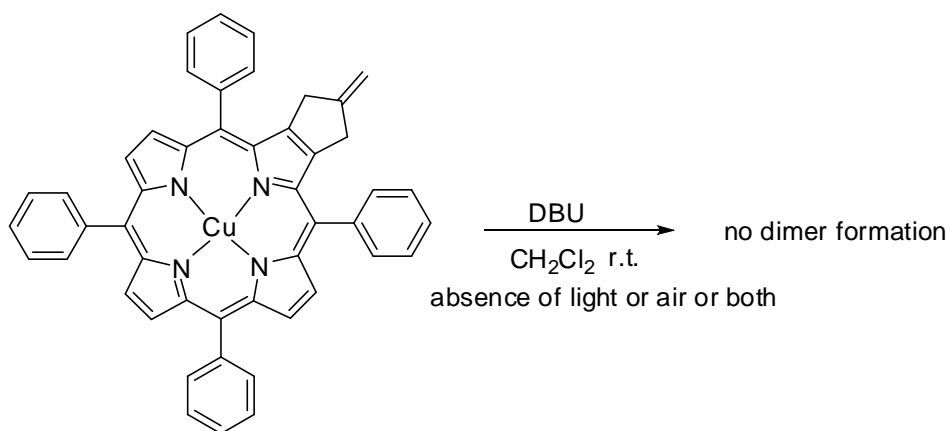
Scheme 2-16. Designed reaction eliminating either light or air or both of them; no desired porphyrin dimers were detected.

Thus, we rationalized that this reaction occurred through a self-photooxidation process. Although photosensitization by *paramagnetic* copper(II) porphyrins is unusual, it is not unique. Skalkos and coworkers have shown that some copper(II) porphyrins can be used in photodynamic therapy[56], and Chandrasekhar et al. have shown that a copper(II) porphyrin can be used to promote cleavage of DNA[57]. Furthermore, several copper(II) porphyrins have shown applications in the oxidation of alkenes to ketones, alcohols and related compounds[58].
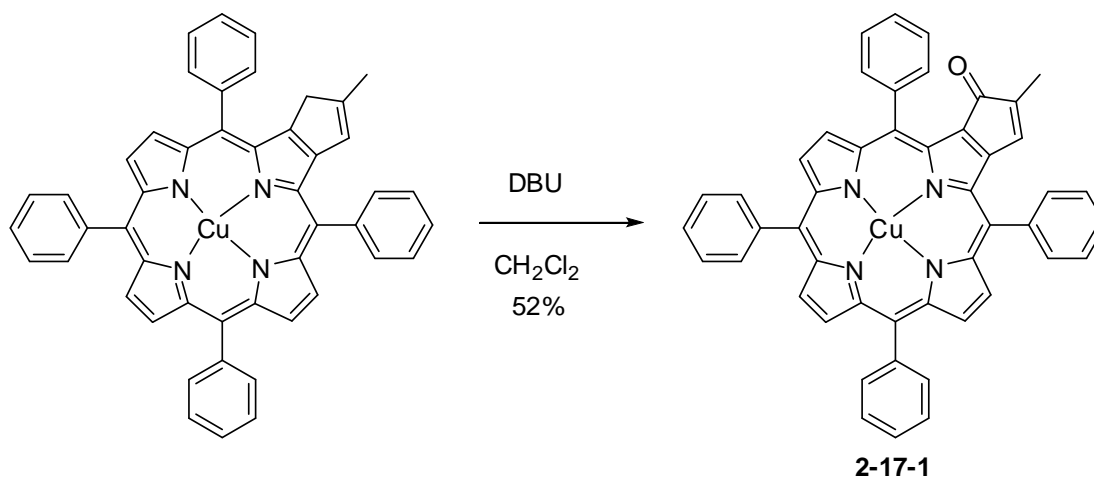
2-17-1

Scheme 2-17. With the double-bond migrated **2-2-1-Cu** as the starting material, the oxidized product **2-17-1** was formed in 52% isolated yield, which serves as key intermediate for the formation of porphyrin dimer **2-14-1**.
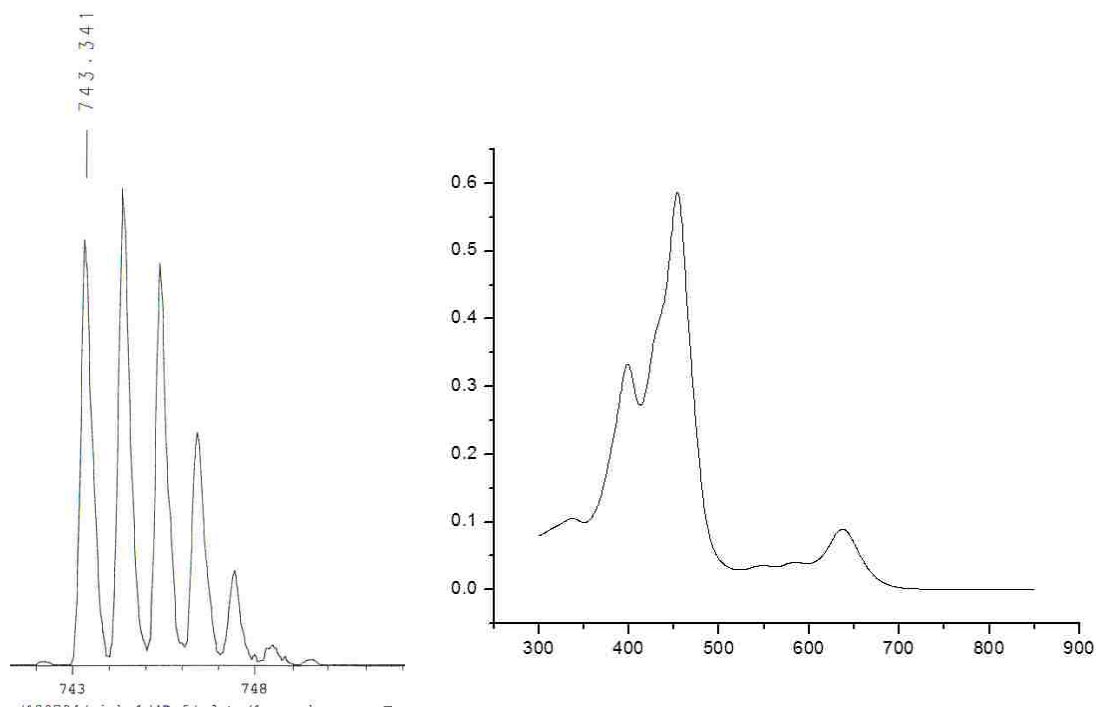
Figure 2-9. MALDI-TOF mass spetrum (left) and UV-vis spectrum (right) of **2-17-1**.

With the presence of the endo-cyclic double bond of **2-2-1-Cu**, when DBU as base in DCM at room temperature in the presence of both light and air, a new green spot was detected on TLC after letting the reaction mixture stir for 5 hours. Upon separation using a silica gel column, **2-17-1** was isolated in 52% yield. MALDI-TOF mass spectrometry gave a peak at 743.3 corresponding to the formation of **2-17-1** and confirmed the addition of one oxygen atom to the starting material (see *Figure 2-9*). FT-IR spectroscopy gave a peak at 1738 cm^{-1} corresponding to the presence of a ketone in the target compound **2-17-1**. The UV-visible spectrum of **2-17-1** displayed a split Soret band and relatively intense Q bands (see *Figure 2-9*). The splitting of the Soret band has been observed on unsymmeterical porphyrins and is from charge-transfer within this molecule.

In summary, both **2-1-3** and **2-2-1** were stable in the solid state. However, while handling their solutions in air, it became apparent that they were being converted into the

63

oxidized byproducts from TLC and MALDI-TOF. In the dark, in solution under argon, both **2-1-3** and **2-2-1** were perfectly stable. Also, with the separate presence of either air or light, both **2-1-3** and **2-2-1** were stable. However, once exposed to both light and air, they were rapidly converted into the oxidized byproducts. The presence of conjugated endocyclic double bond made **2-2-1** more unstable when exposed to light and air. The major product was an α,β-unsaturated ketone **2-17-1**, which was isolated in 52% yield. Based on these experimental results, we propose a self-photooxidation mechanism for the formation of these porphyrin dimers (see *Figure 2-10*). A literature search revealed numerous examples of photooxygenation of organic molecules bearing exo-cyclic alkenes. Of particular relevance was the work of Havel[21] who showed that methylenecycloalkanes react with triplet oxygen. Methylenecycloalkanes were shown to yield epoxides, and alkenones among other oxygenated products. In other work, alkenyl-linked [60]fullerene derivatives have been shown to self-photooxygenate to give allylic alcohols,[58] and Saracoglu et al.[55] have shown, for example, that cycloheptatriene derivatives can be photooxygenated in the presence of H$_2$TPP (**2**) as a singlet oxygen sensitizer, to give the norcaradiene endoperoxides and bis-epoxide derivatives. The relevance of this literature became apparent when, upon treatment with DBU, porphyrin **2-1-3** afforded a 60% yield of the oxygenated bis-porphyrin **2-14-1** (see *Figure 2-11*). As shown in *Figure 2-11*, we propose compound **2-1-3** undergoes photooxidation with triplet oxygen to generate epoxide 2-**8**, from which the diol **2-9** and allylic alcohol **2-10** is subsequently formed. Meanwhile, the endocyclic alkene compound **2-2-1** is photo-oxidized to give the epoxide **2-11** and then converted into the diol **2-12**, from which the allylic alcohol **2-13** is generated. Then the Michael addition generates intermediates **2-17-1** and **2-14.** The subsequent Michael addition reaction between anion **2-14**
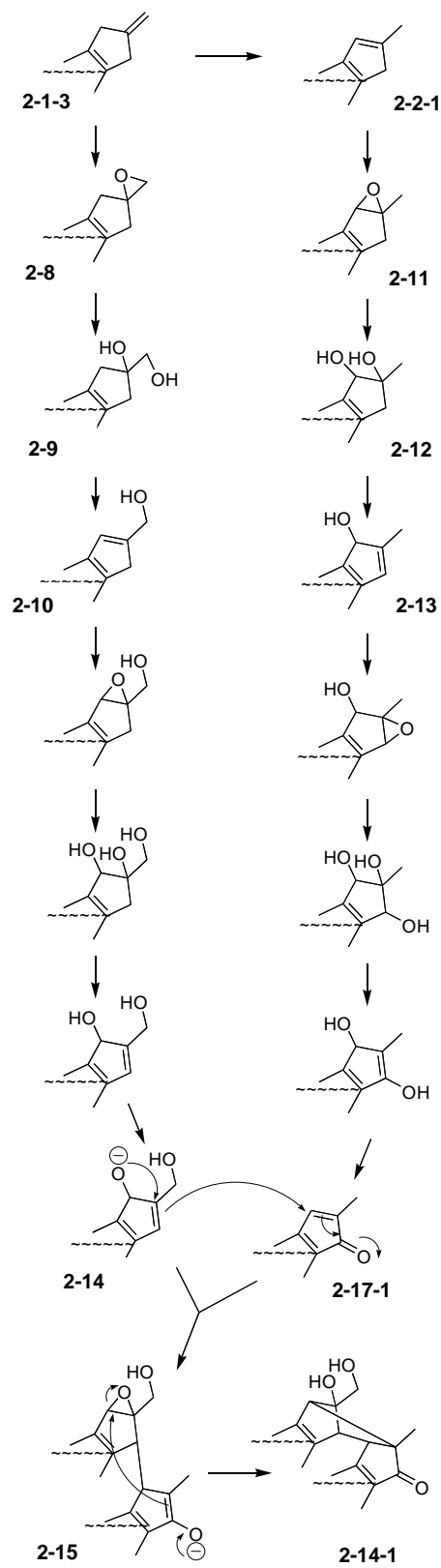
Figure 2-11. Proposed mechanism for the formation of cofacial bisporphyrin dimers from **2-1-3** and **2-2-1**.

and α,β-unsaturated ketone **2-17-1** generates the epoxide **2-15,** from which the ring-opening reaction was performed and **2-14-1** was obtained.

The optical spectrum of **2-14-1** is shown in *Figure 2-12,* and is dramatically different from the conjugated ferrocene sandwich porphyrin dimer **2-4-1** (see *Figure 2-12*). The characteristic red-shifted of Q-bands shown by **2-14-1**, indicate π-stacking between the two porphyrins. On the other hand, the decreasing intensity of the Soret band together with the disappearance of Q-bands of **2-4-1**, indicate a direct electronic communication between the two porphyrin systems associated through the ferrocene.
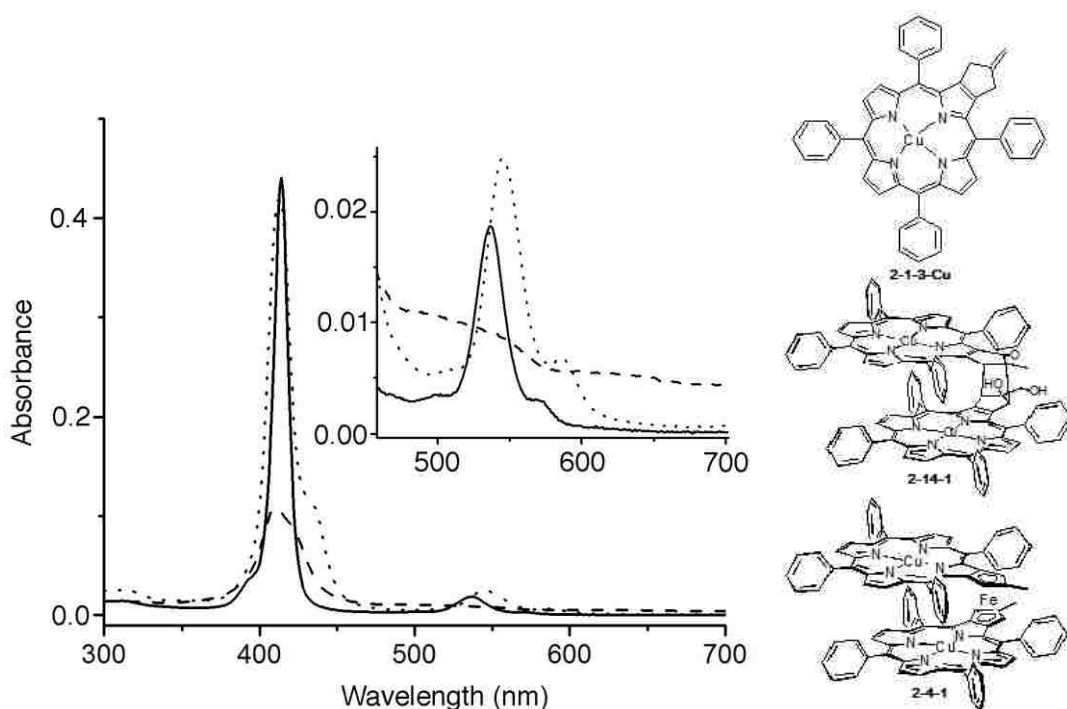
Figure 2-12. UV-Vis spectra in dichloromethane at 1 x 10^{-6} M. **2-1-3-Cu** (solid line), **2-14-1**(dotted line) and **2-4-1**(dashed line).

Besides the identification of intermediate **2-17-1**, there is also other preliminary evidence to support the proposed mechanism for the generation of **2-14-1** (see *Figure 2-11*).

66

When DBU was replaced with a weak Lewis acid (silica gel), a small amount of **2-14-1** was also

detected from the refluxing of **2-1-3-Cu** in THF for a period of 2 days (see *Scheme 2-18*).
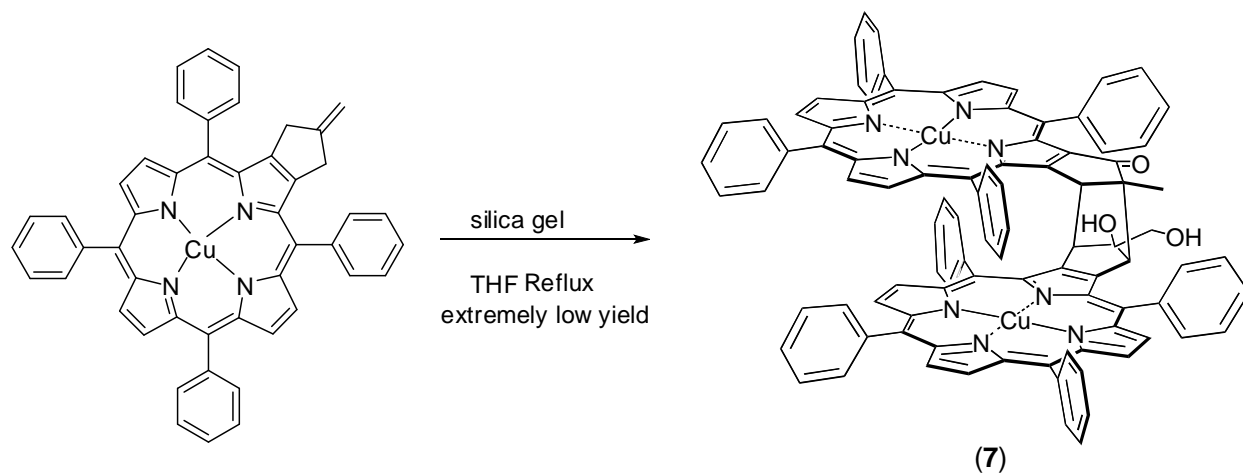
Scheme 2-18. The self-photooxidation of **2-1-3-Cu** under weakly acidic conditions.
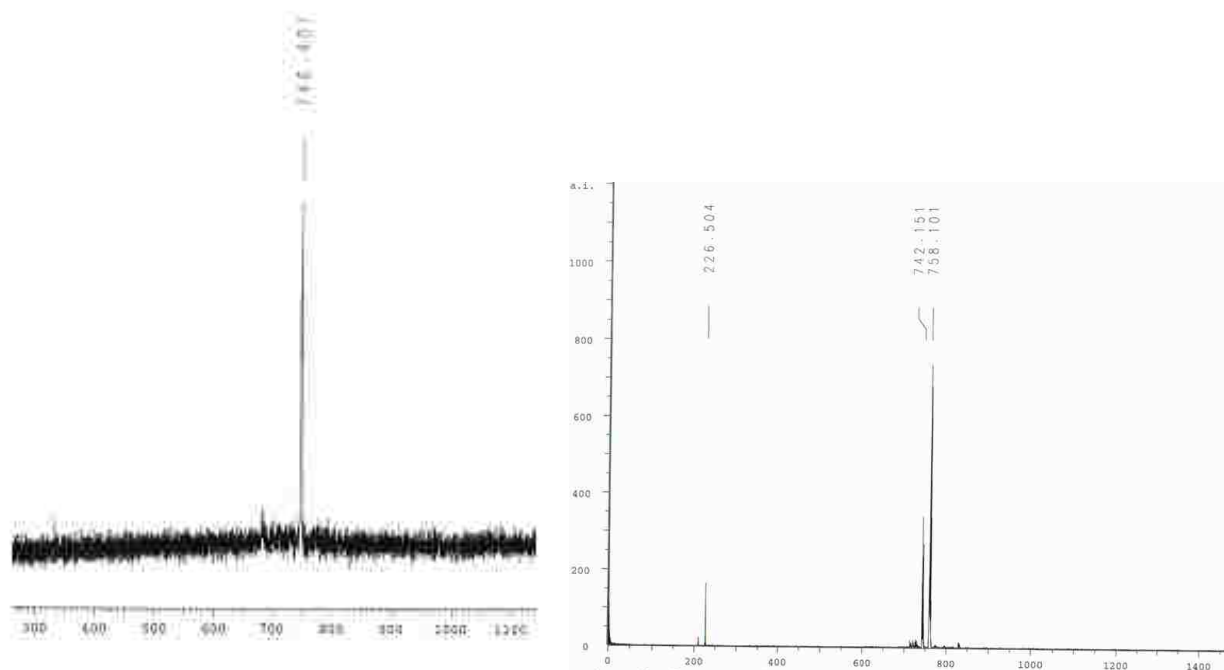
Figure 2-13. MADLI-TOF of the two major intermediates from reaction shown in *Scheme 2-18*.

The yield of **2-14-1** was admittedly low compared to that under basic conditions; however, two additional porphyrins were isolated as major products. MALDI-TOF mass spectrometry gave a peak at 743.341 for the less polar one, and another peak at 758.101 for the more polar porphyrin (see *Figure 2-13*).

The MALDI-TOF results indicated one or two oxygen atoms have been added to the starting material **2-1-3-Cu**. For the more polar product, besides the 758.101 peak, there was also another peak at 742.2 shown in the MALDI spectrum, indicating that a facile loss of one oxygen atom had taken place. The molecular weights of these two products were well in agreement with the two important intermediates (**2-17-1** and **2-14**) as proposed in *Figure 2-11*. We believe that these two reactions (DBU and/or silica gel) might share similar reaction mechanisms. The slight difference happened at the nucleophilic addition step: under basic conditions, it was the hydroxyl group that acted as the nucleophilic reagent while under Lewis acid catalyst conditions, water was the nucleophilic reagent. The different nucleophilic ability of these two reagents made high temperature necessary for the acidic condition reaction and explained why a very low yield of **2-14-1** was obtained under these conditions. The whole mechanism (see *Figure 2-11*) involves several mono oxidations of double bonds to form epoxide intermediates. These critically important major intermediates, epoxides and spiro-epoxides, had been previously reported in the literature associated with the reactions of methylenecycloalkanes with triplet oxygen[11]. In our case, the triplet oxygen was generated *in situ* from dioxygen activated by **2-1-3-Cu**.

2.3 Experiment

2.3.1 General Information

All reactions were monitored by TLC using 0.25 mm silica gel plates with or without UV indicator (60F-254). Silica gel (Sorbent Technologies 32-63 m) was used for flash column

chromatography. ^{1}H- and ^{13}C-NMR spectra were obtained on either a DPX-250 or an ARX-300 Bruker spectrometer. Chemical shifts (δ) are given in ppm relative to residual CHCl$_3$ (7.26 ppm, 1H), or DCM (5.32 ppm, 1H) unless otherwise indicated. Electronic absorption spectra were measured on a Perkin Elmer Lambda 35 UV-Vis spectrophotometer. MALDI-TOF mass spectra were obtained on an Applied Biosystems QSTAR XL, using positive method with dithranol as matrix. Materials obtained from commercial suppliers were used without further purification.

2. 3.2 Procedure for the Synthesis of 2-14-1

A mixture of β,β'-fused copper(II) methylenepropanoporphyrin **2-1-3-Cu** (100 mg, 0.14 mmol) and DBU (100 mL, 0.67 mmol) was dissolved in CH$_2$Cl$_2$ (20 mL) and stirred at room temperature in air for 52 hours. Upon the completion of the reaction, the separation was performed on a silica gel column using CH$_2$Cl$_2$ as eluting solvent. The title porphyrin **2-14-1** was obtained in 60% yield (63 mg, 0.042 mmol). UV/Vis: λ_{max} CH$_2$Cl$_2$ (log ε) 413 nm (5.62), 545 (4.40), 585 (3.83); MS (HR-MALDI-TOF) C$_{96}$H$_{62}$Cu$_2$N$_8$O$_3$ (M$^+$): Calcd m/z for 1502.3553; Found 1502.1324. A crystal of **2-14-1** (See *Figure 2-7*) was grown by slow diffusion of hexane into the concentrated dichloromethane solution of **2-14-1**.

2.3.3 Procedure for synthesis of porphyrin **2-17-1**

A mixture of endocyclic alkene porphyrin **2-2-1** (100 mg, 0.14 mmol) and DBU (100 mL, 0.67 mmol) was dissolved in CH$_2$Cl$_2$ (20 mL) and was stirred at room temperature under air for 5 hours. The separation was performed on a silica gel column using CH$_2$Cl$_2$ /hexane (v/v =1/2) as eluting solvent. The tile green porphyrin **2-17-1** was obtained in 52% yield (54 mg, 0.072 mmol). UV/Vis: λ_{max} CH$_2$Cl$_2$ (log ε) 338 nm (4.72), 399 (5.22), 454 (5.47), 549 (4.25), 584 (4.30), 637 (4.65); MALDI-TOF C$_{48}$H$_{30}$CuN$_4$O (M+H): Calcd m/z for 742.2; Found 742.5.

2.3.4 Procedures for synthesis of 2-1-3

The preparation of **2-1-3-Ni** was performed under strictly air-free conditions. The Pd(0) catalyst was prepared *in suit* by reacting Pd(OAc)$_2$ (113 mg, 0.5 mmol) with triisopropylphosphate (3 mmol) in 100 ml dry THF. The reaction mixture was stirred at room temperature for a period of 30 minutes. Porphyrin **2-1-2-Ni** (1.42 g, 2 mmol) was weighed and added directly into a Schlenck reaction flask. Subsequently 2-[(trimethylsilyl)methyl]-2-propen-1-yl acetate (0.5 mmol) was added. Then the reaction temperature was raised to 90 $^{\circ}$C and the mixture was refluxed at this temperature for 2 days. TLC and MALDI-TOF were used to follow this reaction. When most of the starting material was consumed, the reaction temperature was raised to 100 $^{\circ}$C and the mixture was refluxed at this temperature for an additional period of 2 days. Solvent was removed under vacuum and the residue was applied to a silica gel column for separation; hexane/DCM was used as eluting solvent. After removing the solvent under vacuum, the desired product **2-1-3-Ni** was obtained as a reddish brown solid in 82% yield (1.19 g). MP > 300°C; ^{1}H-NMR (250 MHz, CDCl$_3$) ppm: 8.75-8.72 (m, 6H), 8.01-7.97 (m, 4H), 7.87-7.83 (m, 4H), 7.70-7.63 (m, 12H), 4.99-4.98 (m, 2H), 3.48-3.46 (m, 4H).

2-1-3-Cu was prepared in a similar procedure as described above for 2-1-3-Ni. MALDI-TOF Calcd. for C$_{48}$H$_{32}$N$_4$Cu, 728.3. Found, 728.1. Anal. Calcd for C$_{48}$H$_{32}$CuN$_4$.C$_6$H$_{14}$: C, 79.62; H, 5.69; N, 6.88. Found: C, 79.22; H, 5.72; N, 7.05. UV/vis: λmax DCM (log ε) 414 nm (5.64), 536 (4.27), 568 (3.49).X-Ray data: C$_{48}$H$_{32}$CuN$_4$HCl$_3$, triclinic space group P-1, a = 12.940(4), b = 13.185(5), c = 13.694(7) A$^{\circ}$, a = 108.12(2), b = 117.71(2), c = 90.22(2), V = 1935.0(14) A$^{\circ}$ ^{3}, T = 110 K, Z = 2, R = 0.094 (F2 > 2r), Rw = 0.271 (all F2) for 5879 unique data and 514 refined parameters. CCDC 280898.

2.3.5 Procedures for synthesis of 2-2-1

The preparation of **2-2-1-Cu** was performed by mixing of porpyrin **2-1-3-Cu** (432 mg, 0.6 mmol) with p-TsOH (17 mg, 0.1 mmol) in 15 mL of chloroform and then refluxed for a period of 24 hours. After cooling down to room temperature, excess of p-TsOH was filtered off. The remained solution was washed with saturated aqueous Na_2CO_3 and water. Solvent was removed under vacuum and the residue was submitted to silica gel column separation. The eluting solvent was hexane/DCM. The desired product was obtained in 90% yield (390 mg) after recrystallization from MeOH/DCM. MALDI-TOF: calcd m/z for $C_{48}H_{32}CuN_4$ 728.3; found 727.9; UV/vis λmax DCM (log ε) 411 nm (5.51), 540 (4.36).

2-2-1-Ni was prepared similar to **2-2-1-Cu** as described above from **2-1-2-Ni**. ^{1}H-NMR (250 MHz, CDCl3) ppm 8.78-8.73 (m, 6H), 8.03-7.97 (m, 8H), 7.71-7.66 (m, 12H), 5.57 (s, 1H), 3.10 (s, 2H), 2.10 (s, 3H). MALDI-TOF Calcd. for $C_{52}H_{36}N_4Ni$, 775.6. Found, 775.6.

2-1-2-Ni: ^{1}H-NMR (CDCl3, 250 MHz) ppm 8.99 (s, 1H), 8.71-8.65 (m, 6H), 8.00-7.96 (m, 8H), 7.72-7.62 (m, 12H). MALDI-TOF Calcd. for $C_{44}H_{27}N_5NiO_2$, 716.4. Found 716.4.

2.3.6 Procedures for synthesis of **2-6-1** and related Compounds

The preparation of **2-6-1** was similar to that of **2-1-3-Ni**. After the *in situ* preparation of the Pd(0) catalyst, the mixture of isomers of dinitro-Ni(II)TPP (383 mg, 0.5 mmol) was added into the reaction mixture and allowed to stir at 90 °C for a period of 2 days. Then the temperature was raised to 100 °C for an additional 2 days. TLC and MALDI-TOF indicated the selective formation of cis-isomer **2-6-1-Ni**. After separation using silica gel TLC, the desired **2-6-1-Ni** was obtained in 35% yield (134 mg). ^{1}H-NMR (CDCl3, 250 MHz) ppm 8.79 (d, 2H, J = 5.0 Hz), 8.72 (d, 2H, J = 5.0 Hz), 7.93-7.98 (m, 2H), 7.86 (d, 4H, J = 7.5 Hz), 7.77 (d, 2H, J = 7.5 Hz), 7.69-

71

7.60 (m, 12 H), 4.97 (s, 4H), 3.48 (d, 8H, J = 10.0 Hz). MALDI-TOF Calcd. for $C_{52}H_{36}N_4Ni$, 775.6. Found, 775.1. m.p. > 300 °C.

2-5-1 was prepared in a similar procedure as described for **2-6-1-Ni**, with a similar yield 33%. MALDI-TOF Calcd. for $C_{52}H_{36}N_4Cu$, 780.4. Found, 780.0.

2-7-2-Cu: MALDI-TOF Calcd. for $C_{96}H_{62}N_8Ni_2O_3$ [M-H_2O], 1475.0. Found, 1474.7.

2.3.7 Procedure for preparation of 2-9-1

Recrystallization of NBS was performed in hot water followed by drying at 80 °C under vacuum for a period of 6 h. H_2TPP (600 mg, 1.0 mmol) was dissolved in $CHCl_3$ (120 mL) and freshly recrystallized NBS (1.0 g, 6.0 mmol) was added into the solution which was refluxed for a period of 4 h. After cooling to room temperature, $CHCl_3$ was removed under vacuum. The residue was then washed with methanol (2×40 mL) to remove the succinimide impurities. Then the residue as a purple solid was dissolved in $CHCl_3$ and purified on a silica gel column with $CHCl_3$ as the eluting solvent. The first fraction from the column was collected and the solvent was removed under vacuum. The solid was further recrystallized from $CHCl_3$ /CH_3OH (1:3). After filtration and removal of the solvent under vacuum, **3-2** was obtained in 66% yield (600 mg). ^{1}H NMR ($CDCl_3$, 250 MHz): ppm 8.70 (s, 4H), 8.20-8.17 (m, 8H), 7.80-7.78 (m, 12H), −2.90 (s, 2H). UV–vis (DCM): λmax (nm) (log ε): 437 (5.50), 535 (4.34), 613 (3.60), 687 (4.12). MALDI-TOF Calcd for $C_{44}H_{26}Br_4N_4$: 930.3. Found 930.4.

2.3.8 Procedures for Preparation of 2-9-3

The preparation of **2-9-2** was achieved from Suzuki-coupling reaction[52]. **2-9-1** (465 mg, 0.5 mmol), Pd(PPh$_3$)$_4$ (225 mg, 0.02 mmol) anhydrous K_2CO_3 (1.2 g, 8 mmol),and $CH_3B(OH)_2$ (120 mg, 2 mmol) in THF/toluene (v/v = 3/2) 100 ml. The reaction mixture was degassed and then let it stirred at 90 °C under argon atmosphere for 3 days. After completion of reaction, the solvent

was removed under vacuum. The crude product was dissolved in $CHCl_3$ and washed with saturated aqueous $NaHCO_3$ solution followed by saturated aqueous NaCl solution, and the organic layer was dried over anhydrous Na_2SO_4. After reducing the solvent under vacuum, the reaction mixture was loaded on a silica gel column. Only a very short silica gel plug was required. Pure DCM was used to elute down the small amount of starting material **2-9-1**. After that, the eluting solvent was changed to the mixture solvents of DCM/ethyl acetate (v/v = 10/1). **2-9-2** was obtained as a green fraction from the column and after removing the solvents under vacuum it was obtained as purple microcrystals in 87% yield (292 mg). ^{1}H NMR ($CDCl_3$, 250 MHz) ppm: 7.94 (m, 8H), 7.58 (m, 4H), 7.47 (m, 8H), 6.76 (m, 20H), 1.84 (s, 12H), -1.68 (s, 2H). MALDI-TOF Calcd for $C_{48}H_{36}N_4$ 668.8. Found 668.7. The insertion of Ni(II) was performed by refluxing **2-9-2** (268 mg, 0.4 mmol) with an excess amount of $Ni(acac)_2$ (4mmol) in chloroform/methanol (v/v = 1/3) overnight. After filtration, **2-9-3** was obtained in 98% yield (285 mg). ^{1}H-NMR ($CDCl_3$, 250 MHz) ppm 7.47 (m, 8H), 7.12 (m, 4H), 7.02 (m, 8H), 6.68 (m, 20H), 1.58 (s,12H). MALDI-TOF Calcd. for $C_{48}H_{36}N_4Ni$, 727.5. Found, 727.8.

2.3.8 Procedure for Preparation of 2-17-1

A mixture of endocyclic alkene porphyrin **2-2-1-Cu** (100 mg, 0.14 mmol) and DBU (100 μL, 0.67 mmol) in DCM (20 mL) was stirred at room temperature under air for 5 h. The mixture was purified by column chromatography on silica gel using DCM/hexane (v/v = 1/2) as eluent, giving the green porphyrin **2-17-1** in 52% yield (54 mg, 0.072 mmol). UV/vis: λmax DCM (log ε) 338 nm (4.72), 399 (5.22), 454 (5.47), 549 (4.25), 584 (4.30), 637 (4.65); MALDI-TOF $C_{48}H_{30}CuN_4O$ [M+H]: Calcd m/z for 742.2. Found 742.5.

2.3.9 Procedures for Preparation of 2-14-1, 2-15-1 and Related Compounds

A mixture of β,β'-fused copper(II) methylenepropanoporphyrin **2-3-1** (100 mg, 0.14 mmol) and DBU (100 μL, 0.67 mmol) in DCM (20 mL) was stirred at room temperature in air for 52 h. The mixture was purified by column chromatography on silica gel using DCM as eluent, giving the title porphyrin **2-14-1** in 60% yield (63 mg). UV/vis: λmax DCM (log ε) 413 nm (5.62), 545 (4.40), 585 (3.83). MS (HRMALDI-TOF) $C_{96}H_{62}Cu_2N_8O_3$ (M+): Calcd m/z for 1502.3553. Found 1502.1324. The crystal of 7 was grown by slow diffusion of hexane into dichloromethane solution. X-ray data for Compound **2-14-1**, $C_{96}H_{60}Cu_2N_8O_3$, triclinic space group P-1, a = 14.174(6), b = 16.881(8), c = 17.876(10) A °, a = 99.97(3),b = 101.23(3), c = 99.171(17), V = 4048(3) A° ^{3}, T = 110 K, Z = 2, R = 0.101 (F2 > 2r), Rw = 0.278 (all F2) for 100,38 unique data and 448 refined parameters. CCDC 280897.

2-16-1 was obtained in a similar procedure as described above. MALDI-TOF Calcd. for $C_{96}H_{62}N_8Ni_2O_3$ [M-H_2O]$^+$, 1475.0. Found, 1474.7.

2-4-1: MALDI-TOF: calcd m/z for $C_{96}H_{62}Cu_2FeN_8$ 1510.5. Found 1510.1. UV/vis: λmax DCM (log ε) 410 nm (5.04).

2.4 Conclusions and Future Work

Using Pd(0) catalyzed [3+2] cyclization reactions, under strictly air-free conditions, a series of mono-methylenepropanoporphyrins and bis(methylenepropano)porphyrins had been synthesized. The selective formation of both cis-bis(methylenepropano)porphyrins and trans-bis(methylenepropano)porphyrins has been accomplished from the corresponding nitroporphyrins. Starting from mono-methylenepropanoporphyrins, a new type of self-sensitized photooxidation reaction was accidently discovered, from which β,β'-cofacial porphyrin dimers were built. The mechanism for this reaction was also studied in some detail.

Future research will be focused on the use of the bis(methylenepropano)porphyrins to build either ferrocenoporphyrin monomers with two ferrocenes in each structure, and the building of sandwich ferrocenoporphyrin trimers.

2.5 References

1   Plenoio, H.; Diodone, R. *J. Organomet. Chem.* **1995**, *492*, 73.

2   Burrell, A. K.; Campbell, W. M.; Officer, D. L.; Scott, S. M.; Gordon, K. C.; MaDonald, M. R. *J. Chem. Soc. Dalton Trans.* **1999**, 3349.

3   Beer, P. D. *Chem. Soc. Rev.* **1989**, *18*, 409.

4   Beer, P. D.; Kurek, S. S. *J. Organomet. Chem.* **1989**, *366*, C6-C8.

5   Ryabov, A. D.; Goral, V. N.; Gorton, L.; Csoregi, E. *Chem. Eur. J.* **1999**, *5*, 961.

6   Thornton, N. B.; Wojtowicz, H.; Netzel, T.; Zixton, D. W. *J. Phys. Chem. B.* **1998**, *102*, 2101.

7   Boyd, P. D. W.; Burrel, A. K.; Campbell, W. M.; Cocks, P. A.; Gordon, K. C.; Jameson, G. B.; Officer, D. L.; Zhao, Z. *Chem. Commun.* **1999**, 637.

8   Nemykin, V. N.; Kobayashi, N. *Chem. Commun.* **2001**, 165.

9   Wagner, R. W.; Brown, P. A.; Johnson, T. E.; Lindsey, J. S. *J. Chem. Soc., Chem. Commun.* **1991**, 1463.

10 Rhee, S. W.; Park, B. B.; Do, Y.; Kim, J. *Polyhedron* **2000**, *19*, 1961.

11 Wollmann, R. G.; Hendrickson, D. N. *Inorg. Chem.* **1977,** *16*, 3079.

12 Burrell, A. K.; Officer, D. L.; Plieger, P. G.; Reid, D. C. W. *Chem. Rev.* **2001**, *101*, 2751; (b) Harvey, P. D. In *The Porphyrin Handbook,* Kadish, K. M.; Smith, K. M.; Guilard, R. Eds.; Academic Press: San Diego, CA; **2003**; vol. 18, pp 63; (c) Vicente, M. G. H.; Jaquinod, L.; Smith, K. M. *Chem. Commun.* **1999**, 1771.

13 Wagner, R. W.; Johnson, T. E.; Lindsey, J. S. *J. Am. Chem. Soc.* **1996**, *118*, 11166.

14 Anderson, H. L. *Inorg. Chem.* **1994**, *33*, 972.

15 Lin, V. S.-Y.; DiMagno, S. G.; Therien, M. J. *Science* **1994,** *264*, 1105.

16 Lin, V. S.-Y.; Therien, M. J. *Chem. Eur. J.* **1995**, *1*, 645.

17 Recent example: Kuramochi, Y.; Satake, A.; Kobuke, Y. *J. Am. Chem. Soc.* **2004**, *126*, 8668.

18 Recent examples: Faure, S.; Stern, C.; Guilard, R.; Harvey, P. D. *J. Am. Chem. Soc.* **2004**, *126*, 1253.

19 Recent examples: Chang, C. J.; Loh, Z.-H.; Shi, C.; Anson, F. C.; Nocera, D. G. *J. Am. Chem. Soc.* **2004**, *126*, 10013.

20 Collman, J. P.; Kendall, J. L.; Chen, J. L. *Inorg. Chem.* **2000,** *39*, 1661.

21 Anderson, H. L.; Martin, S. J.; Bradley, D. D. C. *Angew. Chem. Int. Ed. Engl.* **1994,** *33*, 655.

22 Wilson, G. S.; Anderson, H. L. *Chem. Commun*. **1999**, 1539.

23 Buchler, J. W.; De Cian, A.; Fischer, J. ; Hammerschmitt, P. ; Loffler, J.; Scharbert, B.; Weiss, R. *Chem. Ber.* **1989**, *122*, 2219.

24 Bilsel, O.; Rodriguez, J.; Milam, S. N.; Gorlin, P. A.; Girolami, G. S.; Suslick, K. S.; Holten, D. *J. Am. Chem. Soc.* **1992**, *114*, 6528.

25 Bilsel, O.; Rodriguez, J.; Milam, S. N.; Gorlin, P. A.; Girolami, G. S.; Suslick, K. S.; Holten, D. *J. Am. Chem. Soc.* **1992**, *114*, 6528.

26 Collman, J. P.; Wagenknecht, P. S.; Hutchison, J. E. *Angew. Chem. Int. Ed. Engl.* **1994,** *33,* 1537.

27 Clement, T. E.; Nurco, D. J.; Smith, K. M. *Inorg. Chem.* **1998**, *37*, 1150.

28 Wagner, R. W.; Johnson, T. E.; Lindsey, J. S. *J. Am. Chem. Soc.* **1996,** *118*, 11166; (b) Anderson, H. L. *Inorg. Chem.* **1994**, *33*, 972; (c) Lin, V. S.–Y; Therien, M. J. *Chem. Eur. J.* **1995**, *1*, 645.

29 Anderson, H. L.; Martin, S. J.; Vradley, D. D. C. *Angew. Chem. Int. Ed. Engl*. **1994**, *33*, 655. (b) Wilson, G. S.; Anderson, H. L. *Chem. Commun*. **1999**, 1539.

30 Sanders, J. K. M. In *The Porphyrin Handbook*; Kadish, K. M.; Smith, K. M.; Guilard, R. Eds.; Academic Press: San Diego, CA; **2000**; vol. 3, pp 347.

31 Cvetanovic, R. J.; Singleton, D. L. *Rev. Chem. Intermed*. **1984**, *5*, 183.

32 Havel, J. J. *J. Org. Chem*. **1978**, *43*, 762.

33 Tanner, D. D.; Kandanarachchi, P.; Das, N. C.; Brausen, M.; Vo, C. T.; Camaioni, D. M.; Franz, J. A. *J. Org. Chem*. **1998**, *63*, 4587.

34 Zadok, E.; Rubinraut, S.; and Mazur, Y. *J. Org. Chem.* **1987,** *52*, 385.

35 Holzapfel, C. W.; Van der Merwe, T. L. *Tetrahedron Lett.* **1996**, *37*, 2303.

36 Schimizu, I.; Ohashi, Y.; Tsuji, J. *Tetrahedron Lett.* **1984,** *25*, 5183.

37 Ejiri, S.; Yamago, S.; Nakamura, E. *J. Am. Chem. Soc.* **1992,** *114*, 8707.

38 Trost, B. M.; Matelich, M. C. *J. Am. Chem. Soc.* **1991**, *113*, 9007.

39 Holzapfel, C. W.; Van der Merwe, T. L. *Tetrahedron Lett*. **1996**, *37*, 2307.

40 Schimizu, I.; Ohashi, Y.; Tsuji, J. *Tetrahedron Lett.* **1984**, *25*, 5183.

41 Trost, B. M.; Chan, D. M. T. *J. Am. Chem. Soc.* **1979**, *101*, 6429.

42 Trost, B. M.; Chan, D. M. T. *J. Am. Chem. Soc*. **1981**, *103*, 5972.

43 Trost, B. M.; Miller, M. L. *J. Am. Chem. Soc*. **1988**, *110*, 3687.

44 Shea, K. M.; Jaquinod, L.; Khoury, R. G.; Smith, K. M. *Chem. Commun.* **1998**, 759.

45 Krattinger, B.; Nurco, D. J.; Smith, K. M. *Chem. Commun.* **1998**, 757.

46 Adler, A. D. et. al. *J. Org. Chem*. **1967,** *32*, 476.

47 Shine, H. J.; Padilla, A. G.; Wu, S.-M. *J. Org. Chem*. **1979**, *44*, 4069.

48 Wickramasinghe, A.; Jaquinod, L.; Nurco, D. J.; Smith, K. M. *Tetrahedron* **2001**, *57*, 4261.

49 Dailey, K. K.; Yap, G. P. A.; Rheingold, A. L.; Rauchfuss, T. B. *Angew. Chem. Int. Ed. Engl.* **1996**, *35*, 1833.

50 Lichtenberger, D. L.; Elkadi, Y.; Gruhn, N. E. *Organometallics* **1997**, *16*, 5209.

51 Beck, C. U.; Field, L. D.; Hambley, T. W.; Humphrey, P. A.; Masters, A. F.; Turner, P. *J. Organomet. Chem.* **1998**, *565*, 283.

52 Kumar, P. K.; Bhyrappa, P.; Varghese, B. *Tetrahedron Lett.* **2003**, *44*, 4849.

53 Zhou, X.; Zhou, Z. Y.; Mak, T. C. W.; Chan, K. S. *J. Chem. Soc. Perkin. Trans. 1*, **1994**, 2519.

54 Whitlock, H. W.; Hanauer, Jr. R.; Oester, M. Y.; Bower, B. K. *J. Am. Chem. Soc.* **1969**, *91*, 7485.

55 Wang, H. J. H.; Jaquinod, L.; Nurco, D. J.; Vicente, M. G. H.; Smith, K. M. *Chem. Commun.* **2001**, 2646.

56 Saracoglu, N.; Talaz, O.; Azizoglu, A.; Watson, W. H.; Balci, M. *J. Org. Chem*. **2005**, *70*, 5403.

57 Selman, S. H.; Hampton, J. A.; Morgan, A. R.; Keck, R. W.; Balkany, A. D.; Skalkos, D. *Photochem. Photobiol.* **1993**, *57*, 681. (b) Hampton, J. A.; Skalkos, D.; Taylor, P. M.; Selman, S. H. *Photochem. Photobiol.* **1993**, *58*, 100.

58 Chandrasekhar, V.; Nagendran, S.; Azhakar, R.; Kumar, M. R.; Srinivasan, A.; Ray, K.; Chandrashekar, T. K.; Madhavaiah, C.; Verma, S.; Priyakumar, U. D.; Sastry, G. N. *J. Am. Chem. Soc.* **2005**, *127*, 2410.

59 Chronakis, N.; Vougioukalakis, G. C.; Orfanopoulos, M. *Org. Lett.*, **2002**, *4*, 945.

60 Suslick, K. S.; Acholla, F. V.; Cook, B. R. *J. Am. Chem. Soc.,* **1987**, *109*(9), 2818.

CHAPTER 3. BENZOPORPHYRINS FROM THE RING-CLOSING-METATHESIS

3.1 Introduction

Chemical modification of natural and synthetic porphyrin macrocycles and their peripheral substituents have attracted intense interests for a number of years. By developing new methodologies for easy access to functionalized porphyrins and their derivatives, the tedious total synthesis of porphyrins can be avoided and a variety of new porphyrin derivatives can be efficiently synthesized[1]. Among the chemical modifications, the functionalization of tetrapyrroles at their β-pyrrolic positions is particularly attractive because of the potential applications involving addition of new bonds to directly conjugate the porphyrin macrocycle[2].

Porphyrins with extended π-conjugated systems are always attractive because of their potential applications in the medicinal area, such as the photodynamic therapy treatment of cancers (PDT) and in material science, such as electric and electro-optic materials of use in a number of commercial areas[3]. Theoretically, the most obvious way to extend the π-conjugation is to convert porphyrins into the corresponding benzoporphyrins[4]. However, the efficiency and selectivity of benzoporphyrin syntheses to achieve pure regioisomers are still problems.

The synthesis of benzoporphyrins has been limited to a number of methods, most of which are based on either the total synthesis of porphyrins or the Diels-Alder reaction of intact porphyrins[5]. Among those, the total syntheses of benzoporphyrins usually require high temperature, the product is generated in low yield, and tedious separation was invariably required. Furthermore, the regioselective synthesis remains a challenge. In most cases, total synthesis of porphyrin can only generate symmetrical benzoporphyrins[5b-5f]. Although mono-benzoporphyrins have been obtained from Diels-Alder reactions, still the yields were very low and the separation was still hard[5g]. Thus, currently even the synthesis of symmetrical TBPs

(tetrabenzoporphyrin) is still a challenge[6], not to mention the regioselective synthesis of unsymmetrical benzoporphyrins.
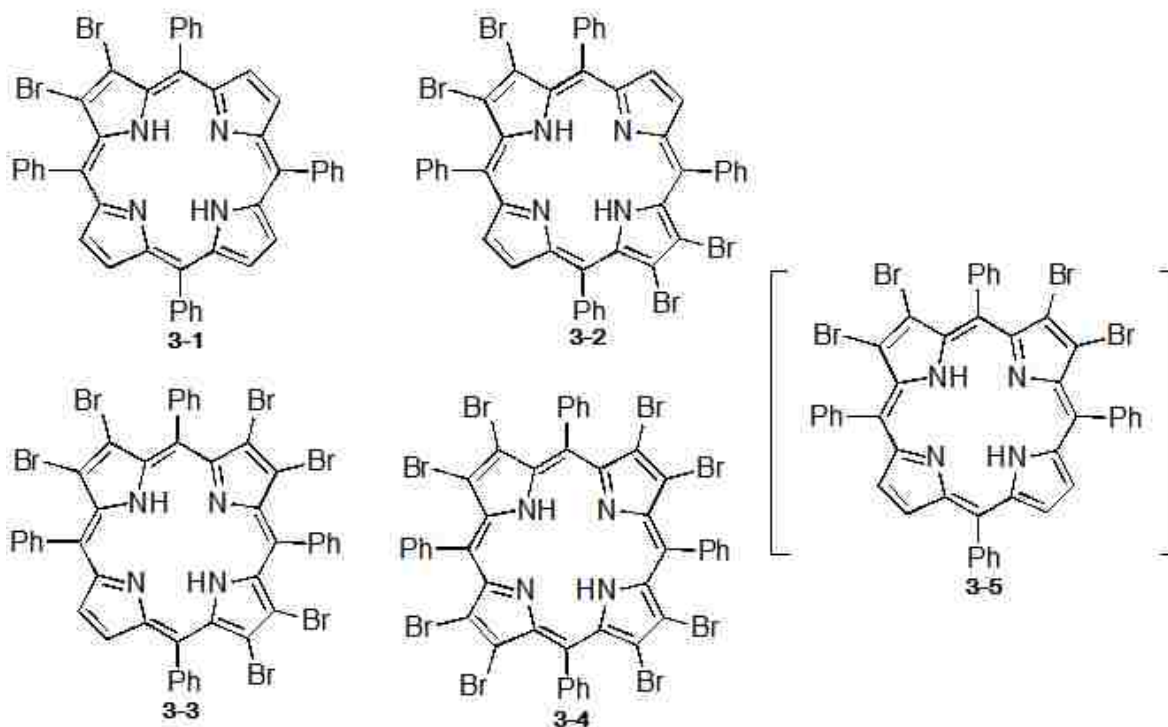
Figure 3-1. Selective brominations at the β-positions of porphyrins.

The efficiency of the regioselective β-bromination of porphyrins (see *Figure 3-1*) has been reported[7], which provided the opportunity to selective modify porphyrins at the β-position. So far, with the exception of **3-5**, all the other β-brominated porphyrins **3-1** to **3-4** have been synthesized. The insertion of metal into these halogenated porphyrins resulted in an increase of their stability towards strong oxygen donors. Partially substituted bromoporphyrins have been used as important precursors for the synthesis of synthetically inaccessible porphyrins. Nowadays, various metal-catalyzed reactions have been widely used to efficiently construct carbon-carbon bonds. Among these, the Suzuki-coupling reaction is a very powerful tool in organic synthesis. It is suitable to introduce various functional groups, such as aryl, alkyl, allyl,

and alkyl, to the β-position of porphyrin macrocycle by coupling halide-substituted porphyrins with the corresponding boronic acids or esters[8].

Recently, with the advent of efficient catalysts, the olefin metathesis has emerged as a powerful tool for the formation of C-C bonds. *Figure 3-2* shows the chemical structure of the common catalyst used for metathesis, the so-called "Grubbs' 2nd generation catalyst". Olefin metathesis has many advantages, including the high activity, durability and excellent tolerance toward functional groups. In the past decades, it has been widely used in advanced organic and polymer chemistry in synthesis of both natural and artificial products[9].
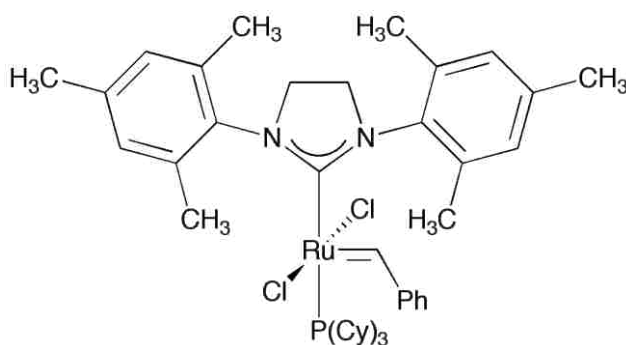
Figure 3-2. Chemical structure of Grubbs' 2nd generation catalyst.

Being aware of the importance and challenge of benzoporphyrin synthesis, and with the consideration of the readily available regioselectively brominated porphyrin at the β-position, plus the efficiency of Suzuki-coupling and olefin metathesis, we designed a new synthetic route to improve the synthetic efficiency and selectivity of benzoporphyrin regioisomer syntheses.

3.2 Results and Discussion

The general synthetic approach to benzoporphyrin regioisomers starts with the syntheses of bromoporphyrins. Among those, the tetrabromoporphyrin **3-2** was the easiest one to access. The synthesis of **3-2** is very straightforward (see *Figure 3-0*)[7], and was first reported by Crossley

and coworkers. The product was indentified by UV–vis, ^{1}H NMR and MALDI-TOF mass spectrometry.
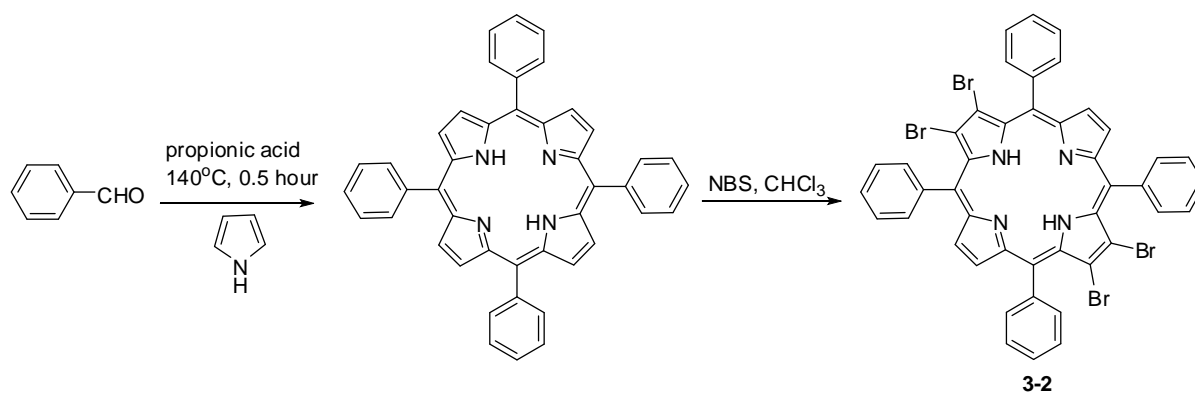
Scheme 3-0. Regioselective tetrabromination of H_2TPP to generate **3-2**.
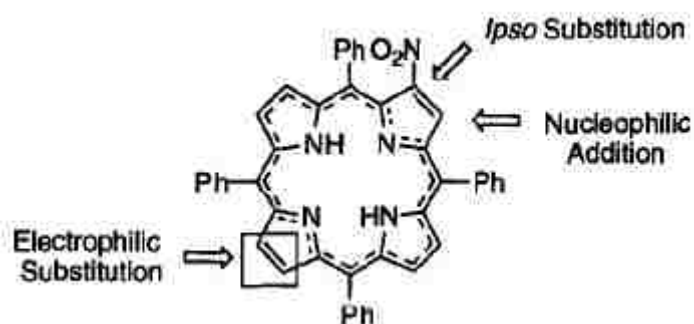
Figure 3-3. Reactivities of **3-2-3**.

The starting material, H_2TPP, was obtained by Adler-Longo condensation reaction as described in Chapter 2. The mixture of H_2TPP and 6.0 equivalents of N-bromosuccinimide (NBS) were dissolved in dry $CHCl_3$ and allowed to reflux for a period of 4 hours. After cooling it to room temperature, the $CHCl_3$ was removed under vacuum. The residue was then washed with methanol to remove the succinimide impurities. Then the residue was dissolved in $CHCl_3$ and purified on a silica gel column with $CHCl_3$ as the eluting solvent. The first fraction from the column was collected and the solvent was removed under vacuum. The solid was further

recrystallized from CHCl$_3$/CH$_3$OH (1/3). After filtration and removal of the solvent under vacuum, **3-2** was obtained in 66% yield.
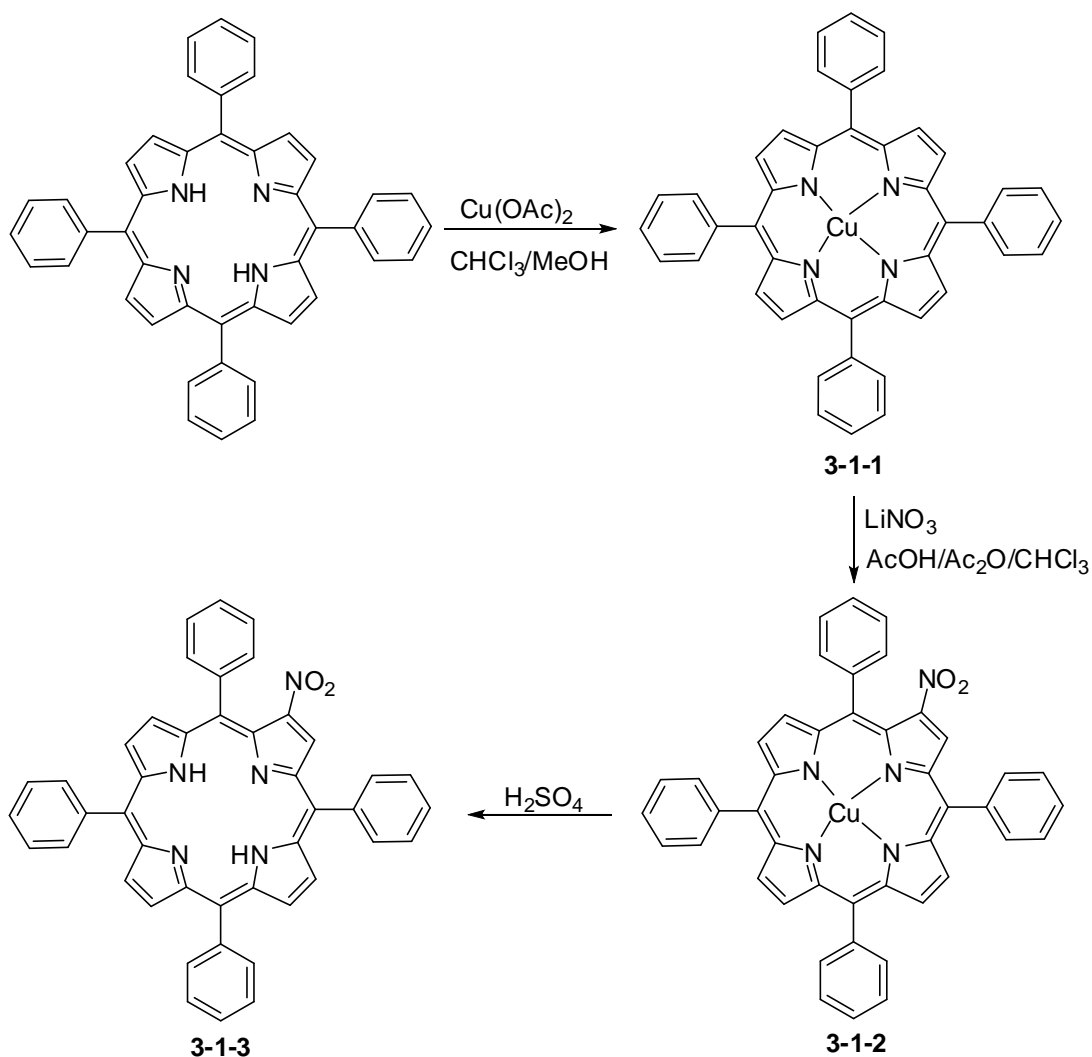
Scheme 3-1. Preparation of β-nitro metalloporphyrin and free-base porphyrin.

With increasing amounts of NBS, the yields became lower and no higher brominated TPP products were observed from UV-vis, MALDI-TOF, and NMR even with NBS excesses up to 12 equivalents. It was found that the presence of nitro group at the β-position of porphyrins assisted the electrophilic substitutions to be selectively performed on the double bond at the antipodal pyrrole ring. The directing effect of the nitro group in the regioselective functionalization of

porphyrin is shown in *Figure 3-3*. Thus the nitro group was introduced to assist the regioselectively synthesize of both the hexabromoporphyrin **3-3** and dibromotetraphenylporphyrin **3-1**.

In the meanwhile, the nitro group displayed unique reactivity in peripheral functionalizations of porphyrins. By introducing the nitro group at the β-position of porphyrins to generate **3-2-2** and **3-2-3**, we also envisioned a subsequent easy access to the further functionalized of porphyrin β-positions. The preparation of nitro-functionalized porphyrins is shown in *Scheme 3-1*.
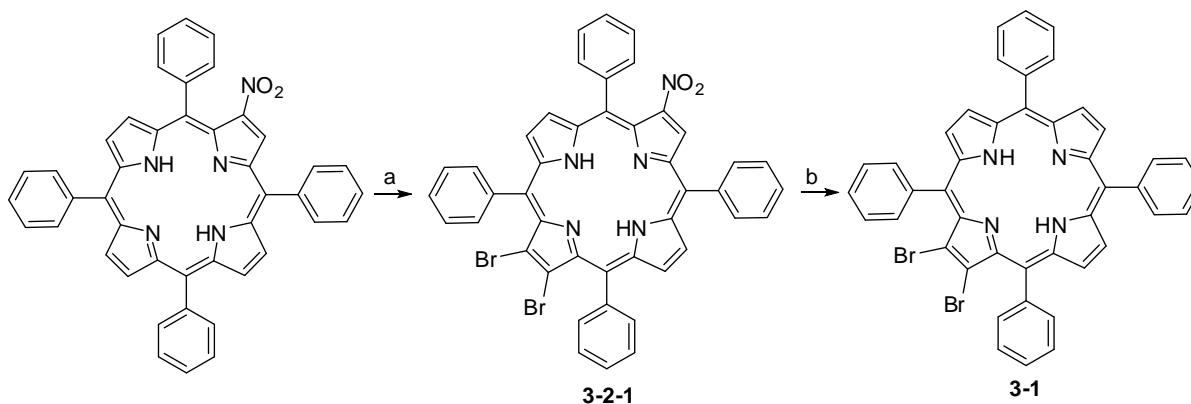
Scheme 3-2. Regioselective dibromination of **3-1-3** to generate **3-2-1** and **3-1**. Reaction conditions: a) NBS, CHCl$_3$; b) toluene, heat.

2-Nitroporphyrins **3-1-2** and **3-1-3** presented a reactivity profile that is similar to simple nitroalkenes. A wide range of nucleophiles can react with the β-position of porphyrins, through Michael additions, to generate new β-substituted porphyrins and functionalized chlorins. The β-nitro group can also undergo S$_N$2 type electrophilic substitution with softer nucleophiles such as thiolates with no requirement for activation assistance from other electron-withdrawing functional groups. The synthesis of both dinitro-tertraphenylporphyrin and hexanitro-tetraphenylporphyrin started from the synthesis of the corresponding nitroporphyrins either in

metalated form **3-1-2** or metal-free form **3-1-3** (see *Scheme 3-1*). As described in Chapter 2, these nitroporphyrins were obtained in high yields with simple purification due to the huge polarity difference generated before and after the introduction of the nitro group to the porphyrin. The demetalation of **3-1-2** to generate **3-1-3** was achieved by using concentrated H_2SO_4. Porphyrin **3-1-2** was dissolved in a minimum amount of concentrated sulfuric acid with alternating stirring and sonication for a period of 1 hour. After this it was poured into a mixture of ice/water and the **3-1-3** was extracted with $CHCl_3$. The organic phase was subsequently washed with water and saturated aqueous $NaHCO_3$. After drying over Na_2SO_4, the solvent was removed under vacuum. Recrystallization from $CHCl_3$ /MeOH gave **3-1-3** as a dark purple powder in 74% yield.

The dibromoporphyrin **3-2-1** was obtained from the bromination of metal-free nitroporphyrin **3-1-3** with 2.4 equivalents of NBS in ethanol-free chloroform (see *Scheme 3-2*). The reaction mixture was left to reflux for a period of 12 hours. After cooling it to room temperature, the reaction mixture was poured through an alumina plug (Grade III) and eluted with $CHCl_3$. After removal of solvent under vacuum, the resulting solid was further recrystallized from $CHCl_3$/MeOH. The desired **3-2-1** was eventually obtained as a brown powder in 80% yield. The nitro group was compatible with the demetalation process. The removal of the nitro group was performed with $NaBH_4$ as a reducing reagent to generate **3-1** through the corresponding nitrochlorin (2,3-dihydro-2-nitroporphyrin) intermediate, which was readily converted into tetraphenylporphyrins by refluxing in chloroform with the assistance of silica gel or in toluene at high temperature (around 100 ^{o}C). Porphyrin **3-2-1** was dissolved in cold dry THF placed in an ice-salt bath and 1.8 equivalents of $NaBH_4$ were added into the solution under argon. After the reaction mixture was left stir for a period of 1 hour, the ice bath
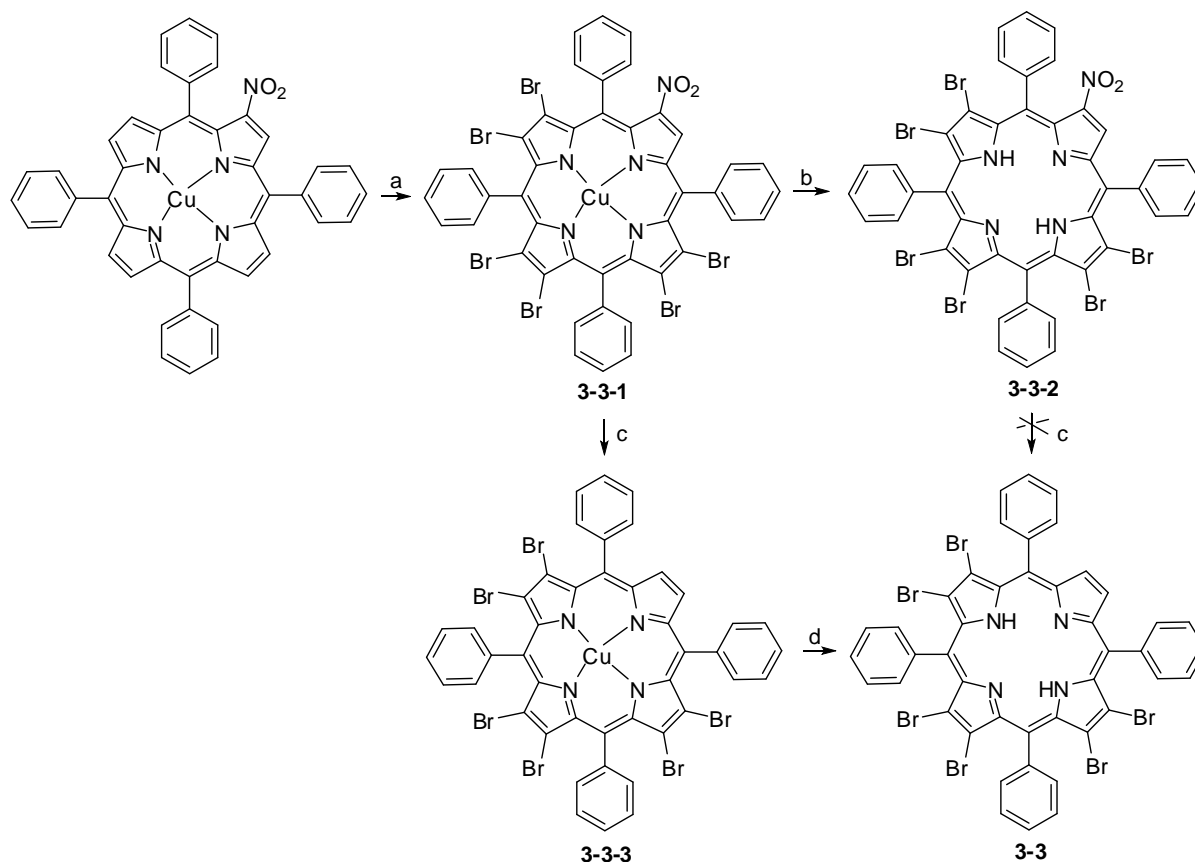
Scheme 3-3. Regioselective hexabromination to generate **3-3-1**, **3-3-2**, **3-3-3** and **3-3**. Reaction conditions: a) NBS, 1,2-dichloroethane, reflux; b) and d) H_2SO_4; c) NaBH$_4$, DMSO.

was removed and stirring was continued at room temperature for an additional 1 hour. The reaction was monitored by UV-vis spectra. When the Soret band was blue-shifted from 436 to 424 nm, the reaction was stopped, DCM was added and then the reaction mixture was poured into water. The separated organic phase was then washed twice with water, dried over Na_2SO_4 and the solvent was removed under vacuum. The residual solid was dissolved in CHCl$_3$ and filtered through a short alumina plug (Grade III) and eluted with CHCl$_3$. After reducing the solvent volume under vacuum, silica gel was added into the reaction mixture and refluxing under argon was continued for an additional period of 1 day. Then it was cooled to room temperature, the silica gel was removed by filtration thoroughly washed with CHCl$_3$. After removing solvent

under vacuum and subsequent recrystallization from CHCl$_3$/MeOH, **3-1** was obtained as a purple powder in 83% yield. Hexabromoporphyrin **3-3-1** was obtained from the hexabromination of **3-1-2** with excess amounts of NBS in boiling 1,2-dichloroethane (see *Scheme 3-3*). To the 1,2-dichloroethane solution of **3-1-2** was added 10 equivalents NBS and it was refluxed for a period of 16 hours under argon. After cooling to room temperature, the reaction mixture was poured into a silica gel plug and eluted with CHCl$_3$. After removal of the solvent under vacuum and subsequent recrystallization from CHCl$_3$/MeOH, **3-3-1** was obtained as a dark green powder in 68% yield. This reaction was careful monitored by UV-vis spectrophotometry. Extended refluxing times should be avoided because of the slow degradation of the desired product and a concomitant decrease in the yield. The demetalation of **3-3-1** to generate **3-3-2** was achieved with concentrated H$_2$SO$_4$. A minimal amount of DCM was added to dissolve **3-3-1** into a suitable round bottom flask. After slow removal of the solvent by rotation under vacuum, an oily film was formed on the inner surface of the flask. Then a minimal amount of concentrated sulfuric acid was added to the flask to dissolve the film, followed by alternating stirring and sonication for a period of 1.5 hours. After pouring the mixture into ice/water, **3-3-2** was extracted with CHCl$_3$. The organic phase was subsequently washed with water and saturated aqueous NaHCO$_3$. After drying over Na$_2$SO$_4$ the solvent was removed under vacuum. Subsequent recrystallization from CHCl$_3$/MeOH and filtration gave **3-3-2** as a green powder in 95% yield. The removal of the nitro group from **3-3-1** to generate **3-3-3** and **3-3** was achieved with NaBH$_4$ as the reducing reagent. To a dry DMSO solution of **3-3-1** under argon was added 1.8 equivalents of NaBH$_4$ and the reaction mixture was stirred at room temperature. The solution was initially green and soon turned brown in color. Stirring was continued for around 2 hours and then the reaction was stopped (when the Soret band gave a 22 nm blue-shift). After adding DCM, the reaction mixture

was poured into water. The organic phase was then washed several times with water. After reducing the solvent volume under vacuum, the solution was placed in the refrigerator for around 3~6 hours. After filtration, pure **3-3-3** was obtained as a dark brown precipitate, in 55% yield. Compared to the metalated porphyrin **3-3-1**, the green solution of **3-3-2** easily underwent slow decomposation under even slightly basic conditions. Thus the reduction of **3-3-2** with NaBH$_4$ failed to generate **3-3**. Instead, **3-3** was obtained from the demetalation of **3-3-3** with concentrated H$_2$SO$_4$ in a method similar to the generation of **3-3-2**. **3-3-3** was dissolved in concentrated H$_2$SO$_4$ for a period of 1 hour with alternating stirring and sonication. After it was poured into the mixture of ice/water and **3-3** was extracted with CHCl$_3$. The organic phase was subsequently washed with water and saturated aqueous NaHCO$_3$. After drying over Na$_2$SO$_4$, the solvent was removed under vacuum. Recrystallization from CHCl$_3$/MeOH gave **3-3** as a dark purple powder in 74% yield.

The Suzuki-coupling reactions were performed in toluene at 100 ºC (see *Scheme 3-4*). The mixture of bromoporphyrin (**3-1** to **3-4**), Pd(PPh$_3$)$_4$ (5 mmol % catalyst /Br) and K$_2$CO$_3$ were dissolved in freshly distilled toluene, to which 2-allyl-4,4,5,5-tetramethyl-1,3,2-dioxaborolane was added through a syringe. This coupling reaction required strictly air free conditions. TLC and MALDI-TOF mass spectrometry were used to follow the reaction. When most of the bromoporphyrin had been consumed, the reaction was stopped. After diluting with DCM, the solution was poured into water. The organic layer was separated and dried over anhydrous Na$_2$SO$_4$. After reducing the solvents under vacuum, the solution was applied to a silica gel column and separated with DCM/hexane as eluent. After removing solvent under vacuum, **3-4-n** (n = 1 ~ 5) were achieved in 49% ~ 84% yields. The solution was found to have a dramatic color and polarity change associated with this coupling reaction; the color of the starting materials was

reddish brown while it was green for **3-4-n** (n = 2,3). The starting materials showed low polarity, while **3-4-n** (n = 2,3) showed very high polarity.
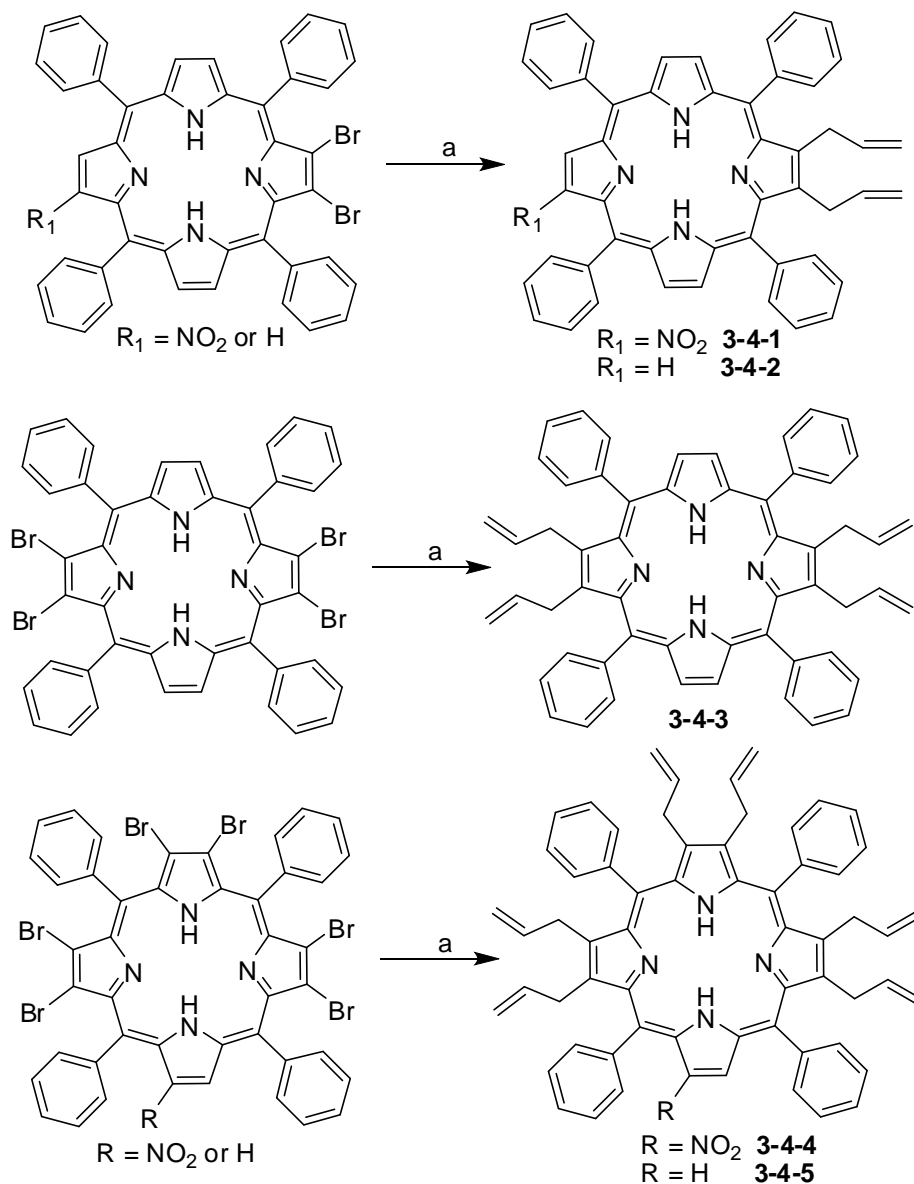
Scheme 3-4. Suzuki-coupling to generate metathesis precursors. Reaction conditions: a) 2-allyl-4,4,5,5-tetramethyl-1,3,2-dioxaborolane, anhydrous potassium carbonate, 100 ºC.

Thus, the separation was easily performed. It is surprising to see that the use of 2-allyl-4,4,5,5-tetramethyl-1,3,2-dioxaborolane in the Suzuki-coupling reaction had indeed provided high yields. Boron-esters, such as 2-allyl-4,4,5,5-tetramethyl-1,3,2-dioxaborolane, have been

reported in the literature to have very limited reactivity in the Suzuki-coupling reaction. Thus it usually required to convert them into the corresponding boronic acid before coupling to achieve efficiency and high yields[10].
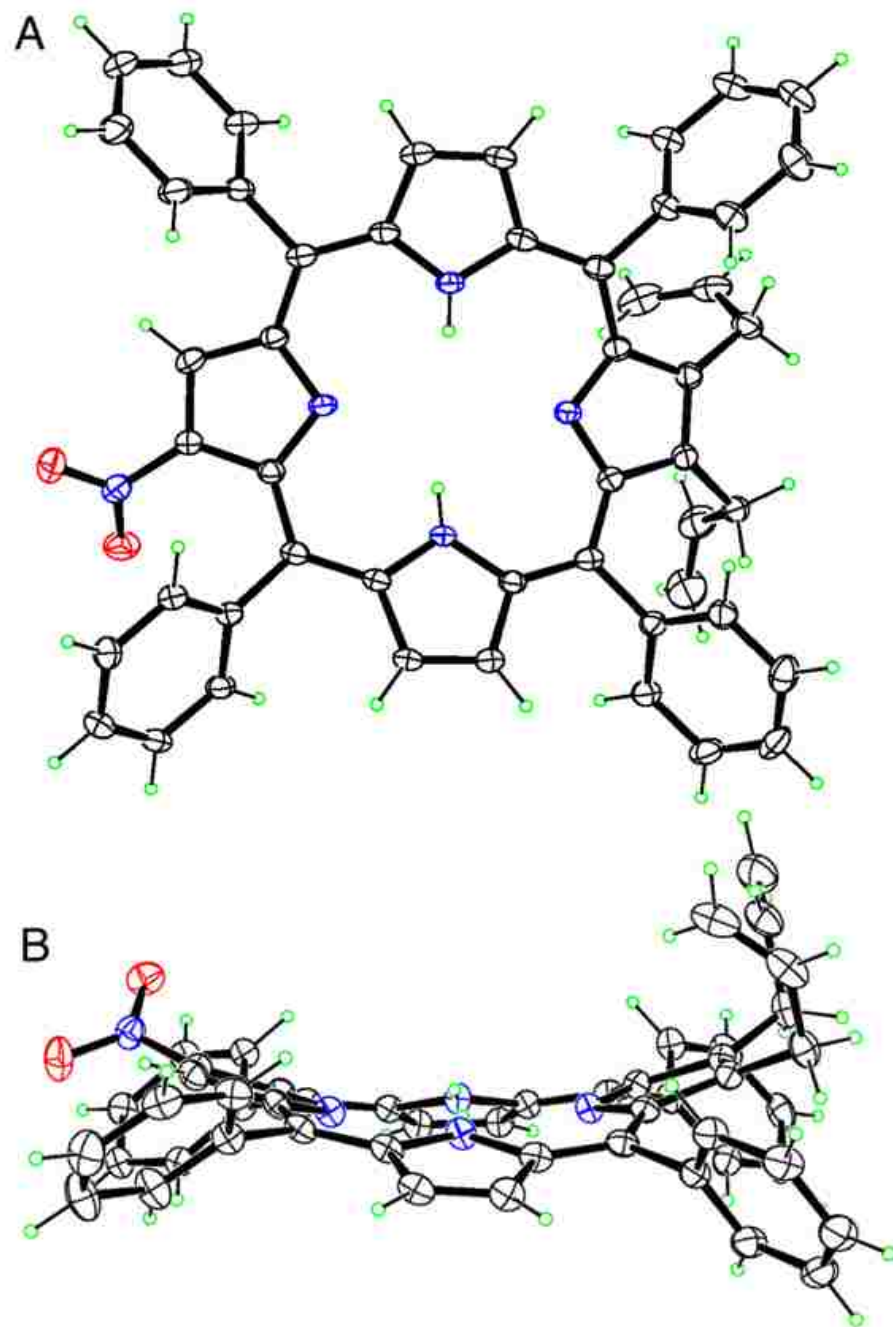
Figure 3-4. X-Ray structure of **3-4-2**: above, top view; bottom, side view.
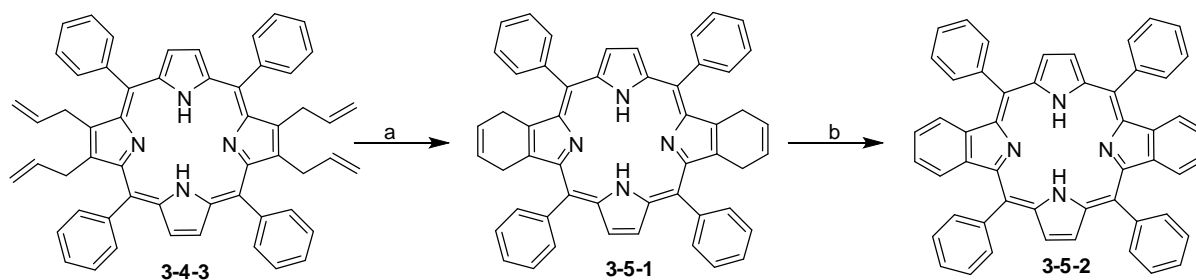
Scheme 3-5. Metathesis followed by oxidation to generate dibenzoporphyrin **3-5-2**. Reaction conditions: a) 10% Grubbs' 2nd generation catalyst, dry DCM, 40 ºC; b) DDQ, THF.

The X-ray structure of the RCM (ring-closing-metathesis) reaction precursor **3-4-1** is shown in *Figure 3-4*. The side view clearly shows the two allyl groups pointing toward each other, which facilitate the metathesis reaction process. The RCM reaction to form the benzoporphyrin precusors was performed in dilute DCM (10^{-2} M concentration) to avoid any intermolecular olefin metathesis reactions. The allyl-substituted porphyrins **3-1-n** (n = 1 ~ 5, 0.1 mmol) from the various Suzuki-coupling reactions were dissolved in anhydrous DCM. Grubbs' II catalyst (0.0025 mmol/allyl group) in anhydrous DCM was added dropwise into the above porphyrin solutions. The solution was then heated under reflux overnight in an atmosphere of argon. TLC and MALDI-TOF mass spectrometry were used in monitoring progress of the reaction. When all starting material had been consumed, the reaction was stopped. After cooling to room temperature and concentration, a silica gel column was used for purification, using DCM/hexane as the mobile phase. After a short silica gel column separation, **3-5-1** was obtained in 91% yield. DDQ was subsequently used to oxidize **3-5-1** to the corresponding benzoporphyrins in almost qualitative yield. A dramatic color change was ssociated with the oxidation: **3-5-1** gives a reddish solution while **3-5-2** is green solution. Following the same procedure, monobenzoporphyrins (see *Scheme 3-6*) were obtained in 87% yield (**3-6-1**) and 85%

yield **(3-6-2)**. Also, tribenzoporphyrin**s** (see *Scheme 3-7*) were obtained in 83% **(3-7-1)** and 82%

yield **(3-7-2)**.
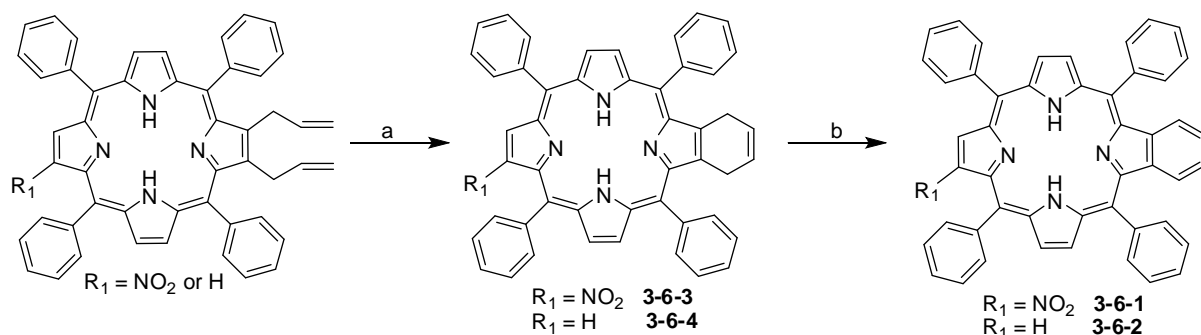
Scheme 3-6. Metathesis followed by oxidation to generate monobenzoporphyrin **3-6-1** and **3-6-2**. Reaction conditions: a) Grubbs' 2nd generation catalyst, dry DCM, 40 ºC; b) DDQ, THF.
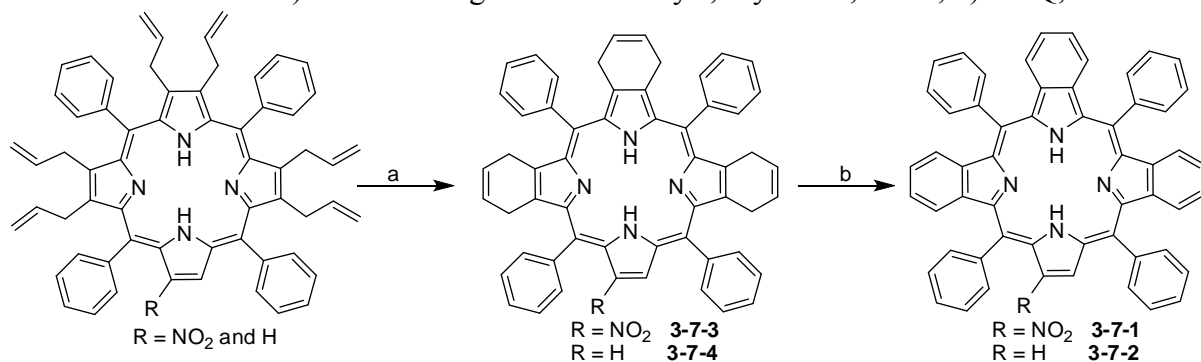
Scheme 3-7. Metathesis followed by oxidation to generate tribenzoporphyris **3-7-1** and **3-7-2**. Reaction conditions: a) Grubb's 2nd generation catalyst, dry DCM, 40 ºC; b) DDQ, THF.

The X-ray structure of **3-5-2** was shown in *Figure 3-5*. The porphyrin macrocycle was

adopted a saddle conformation, which was attrictuted to the presence of four phenyl group at the

meso-position of porphyrin. The UV-vis spectra of monobenzoporphyrin (**3-6-2**),

dibenzoporphyrin (**3-5-2**) and tribenzoporphyrin (**3-7-2**) are plotted in *Figure 3-6*. With the

increase in of the number of benzo-groups attached to the porphyrin macrocycle, there was a clear

red shift of both the Soret band and the Q-bands. This confirmed that the presence of benzo-

groups provides extended conjugation to the porphyrin macrocyle.
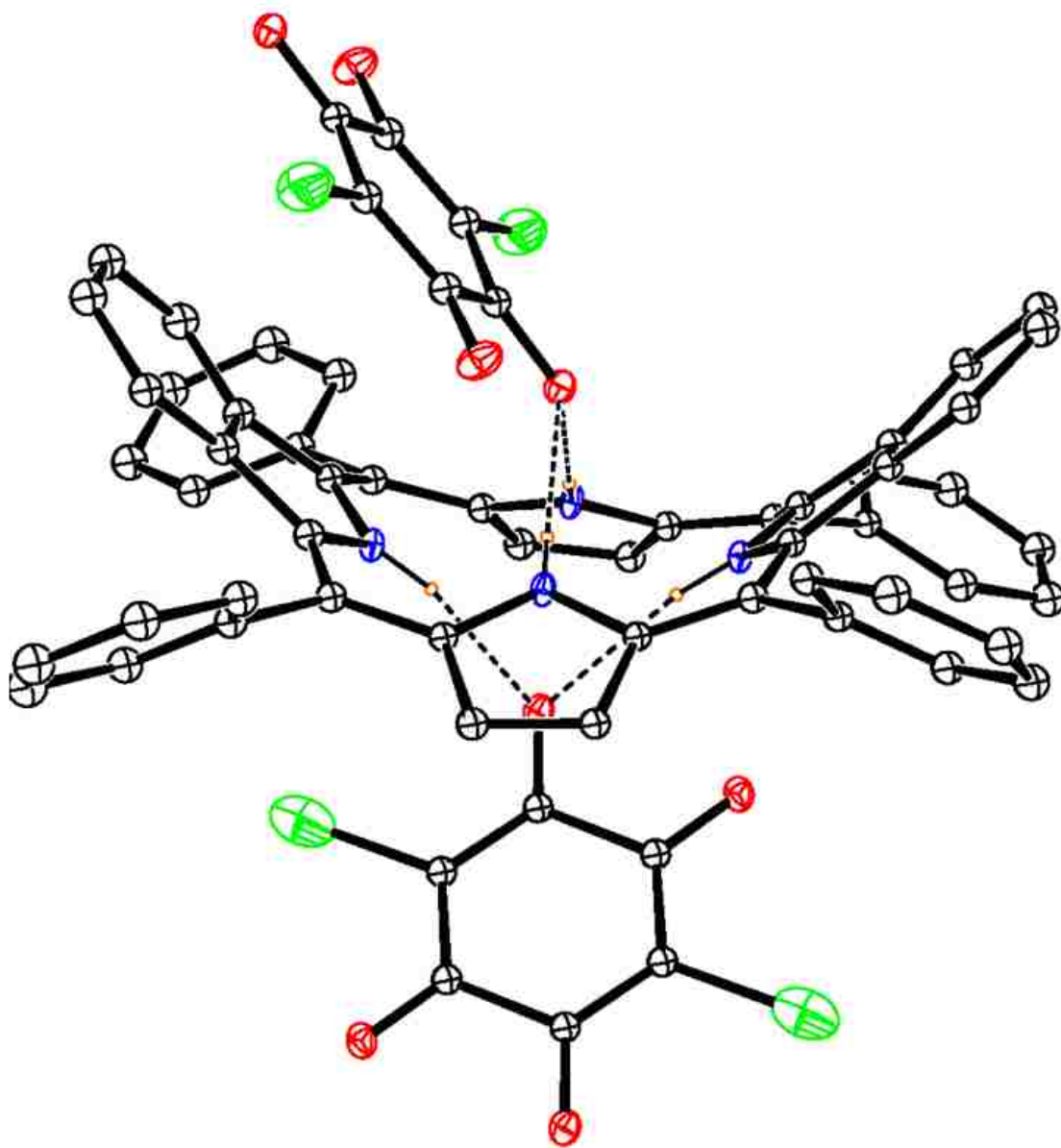
Figure 3-5. X-ray Structure of **3-5-2**.

Following the generation of benzoporphyrin precursor **3-5-1**, the Diels-Alder reaction was performed upon it. We envisioned the generation a more extended π-conjugated porphyrin system from this reaction - the so called "anthracenoporphyrin" **3-8-2** (see *Scheme 3-8*). The diene precursor used in this Diels-Alder reaction, 1,4-dihydro-2,3-benzoxathiin-3-oxide was generated as a liquid according to the literature[11]. The preparation of **3-8-2** was performed by mixing 1,4-dihydro-2,3-benzoxathiin-3-oxide with **3-5-1** at the ratio of 3/1 in toluene and
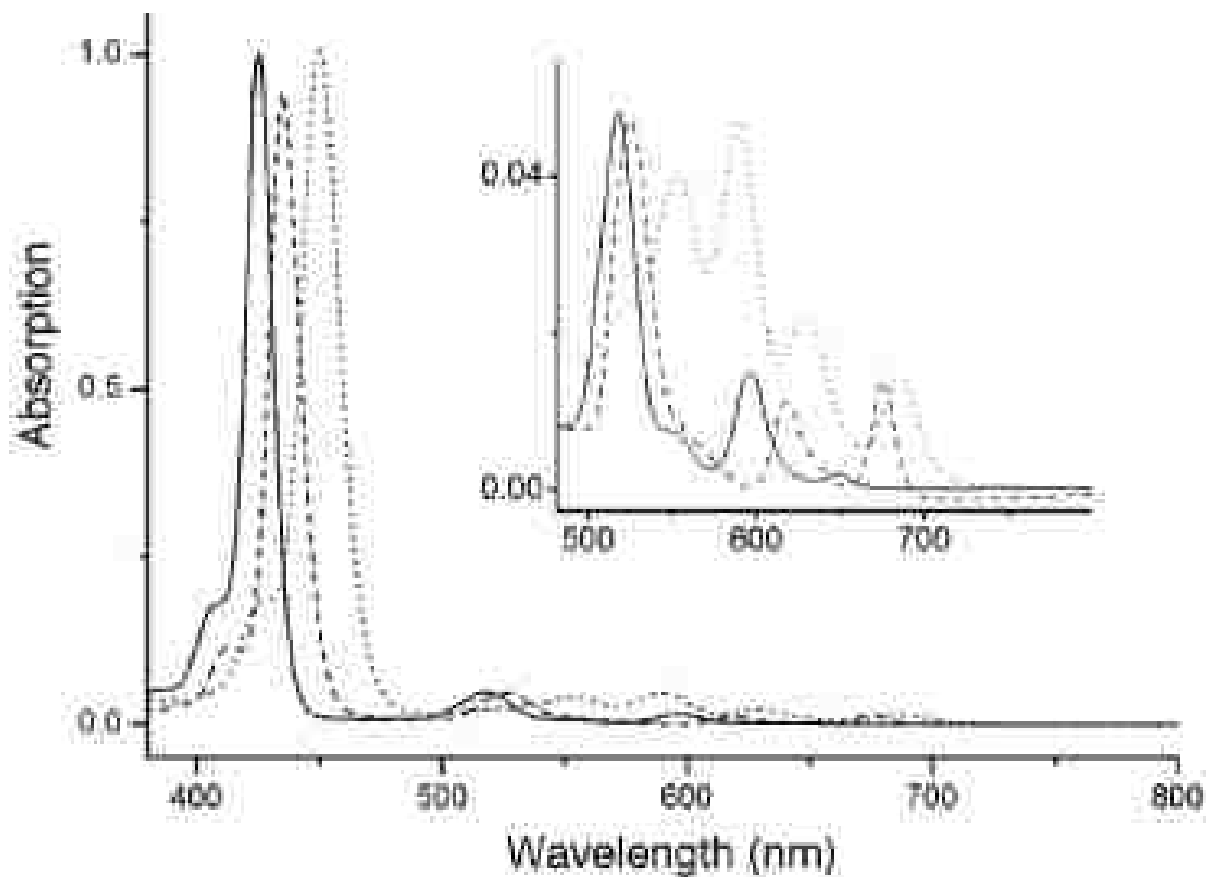
Figure 3-6. UV-vis spectra of benzoporphyrins in DCM: **3-5-2** (dash), **3-6-2** (solid) and **3-7-2** (dot).

subsequently refluxing the reaction mixture at 120 ℃ under argon. TLC was used to follow the progress of the reaction. The reaction was stopped when most of the starting material had been consumed. After separation on a silica gel column, **3-8-1** was obtained in 58% yield. However, the oxidation of **3-8-1** to generate **3-8-2** was problematic. Firstly, the direct use of **3-8-1** in the DDQ oxidation in THF resulted in no generation of **3-8-2** both after a long period of room temperature reaction or at refluxing conditions over 24 hours. Both MALDI-TOF and ^{1}H-NMR spectra indicated partial oxidation of **3-8-1**, as shown in *Figure 3-7*. The UV-vis spectra gave absorption peaks (λmax) at 426, 459, 545, 640 and 696 nm. Secondly, the metal zinc was inserted into the porphyrin central cavity using Zn(OAC)$_2$ in hot MeOH/CHCl$_3$ overnight.
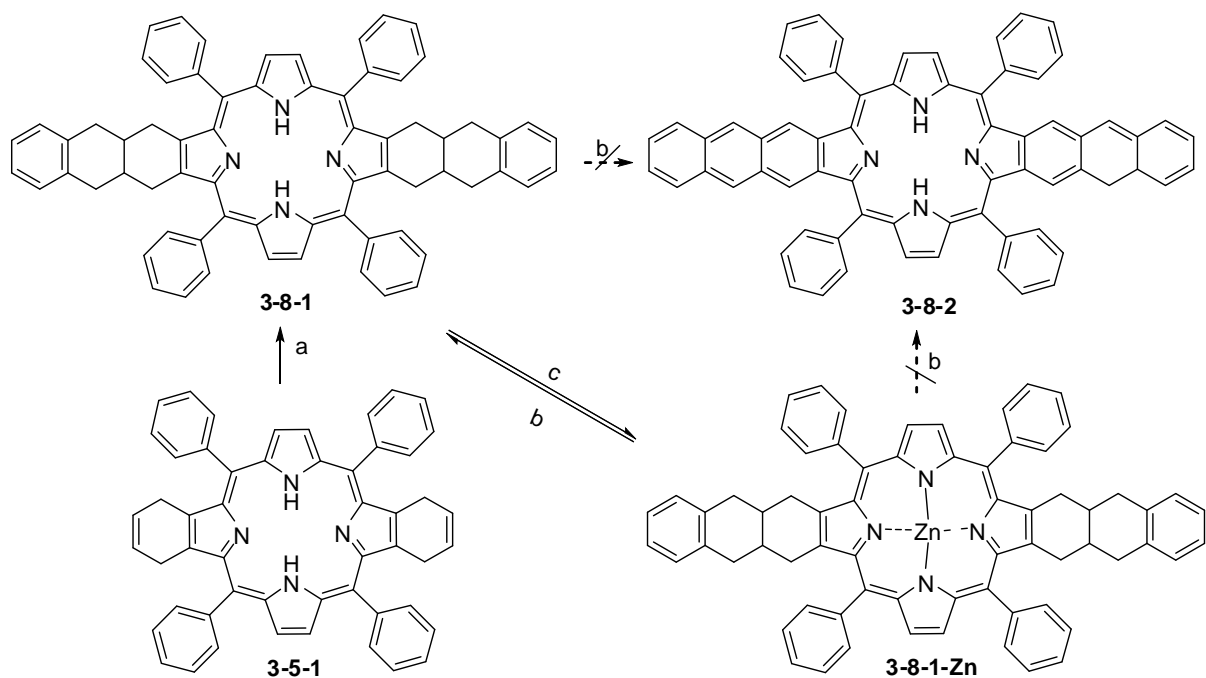
Scheme 3-8. The approach to generate anthracenoporphyrins. Reaction conditions: a) 1,4-dihydro-2,3-benzoxathiin-3-oxide, toluene, 120 ºC; b) DDQ, THF; c) Zn(OAc)$_2$, MeOH/CHCl$_3$.
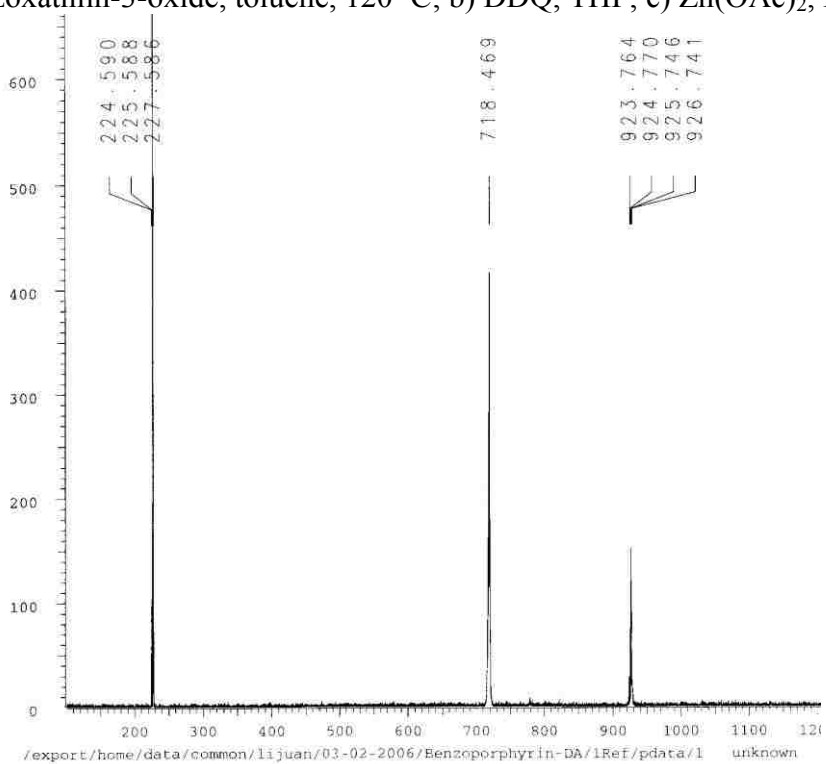
Figure 3-7. MALDI-TOF mass spectrum of **3-8-1**.

95
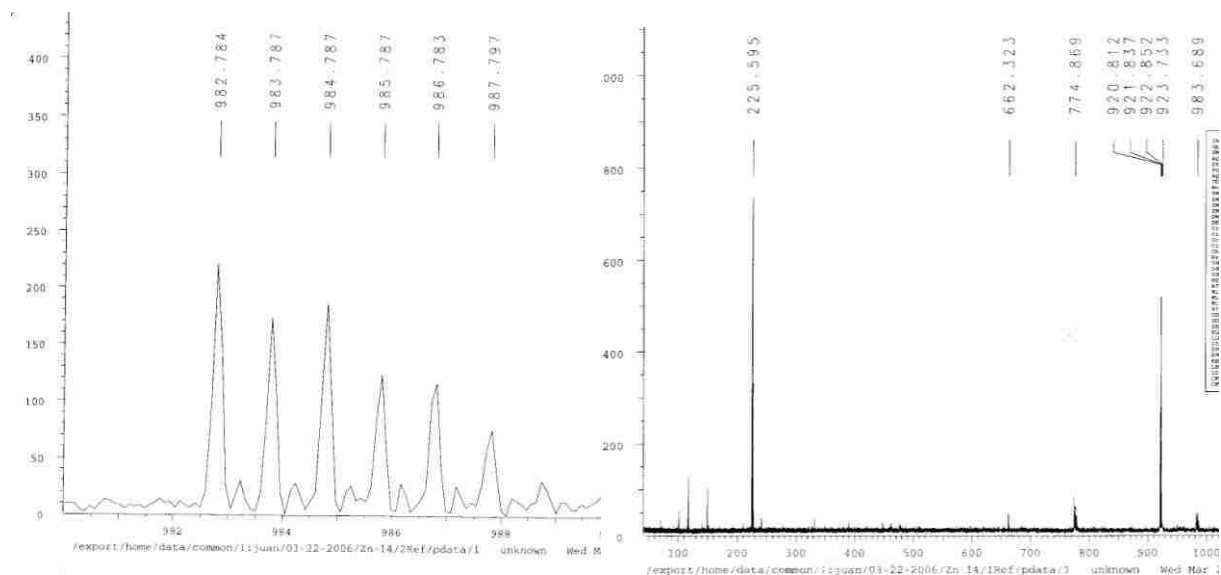
Figure 3-8. MALDI-TOF spectra of **3-8-1-Zn** (left) and **3-8-1** (right) regenerated upon DDQ oxidation.
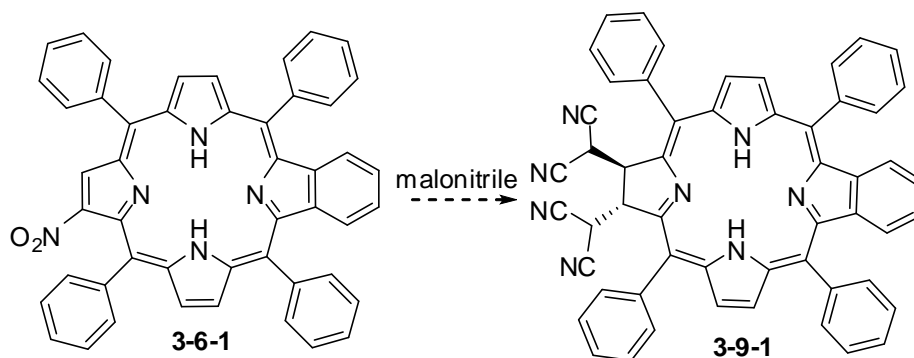
Scheme 3-9. The approach to generate benzochlorin **3-9-1**. Reaction conditions: malononitrile, reflux, K$_2$CO$_3$ in dry THF, followed by DDQ oxidation in toluene at 120 ºC.

After separation of **3-8-1-Zn** through filtration, DDQ was used for the oxidation. Still no desired **3-8-2** was obtained from this reaction; instead MALDI-TOF spectra indicated the use of DDQ only resulted in the regeneration of **3-8-1** by removing the metal zinc from the porphyrin central cavity (see *Figure 3-8*). Change of chelated metal to copper(II) before DDQ oxidation also failed to generate the desired compound **3-8-2**. The Diels-Alder reactions were therefore abandoned.The modification of nitro-monobenzoporphyrins to generate benzochlorins was performed by reaction of **3-6-1** with malononitrile at 65 °C in THF with K$_2$CO$_3$ as base (see

96

Scheme 3-9)[2]. The mixture of K_2CO_3 and 1.3 equivalents of malononitrile in dry THF were refluxed for a period of 1 hour under argon. After cooling to room temperature, 0.4 equivalents of **3-6-1** were added to the mixture. The temperature was slowly increased to 65 °C and stirring was continued for an additional 6 hours. Using TLC to follow the reaction and stopped it upon the disappearance of **3-6-1** on TLC. Again the reaction mixture was cooled to room temperature and diluted with DCM. After washing with water, and drying over anhydrous Na_2SO_4, the solvent was removed under vacuum. The crude chlorin was purified by chromatography on a short silica gel column eluted with DCM/EtOAc. Instead of a red fraction usually observed for the chlorins, an unexpected product was obtained in 68% yield.
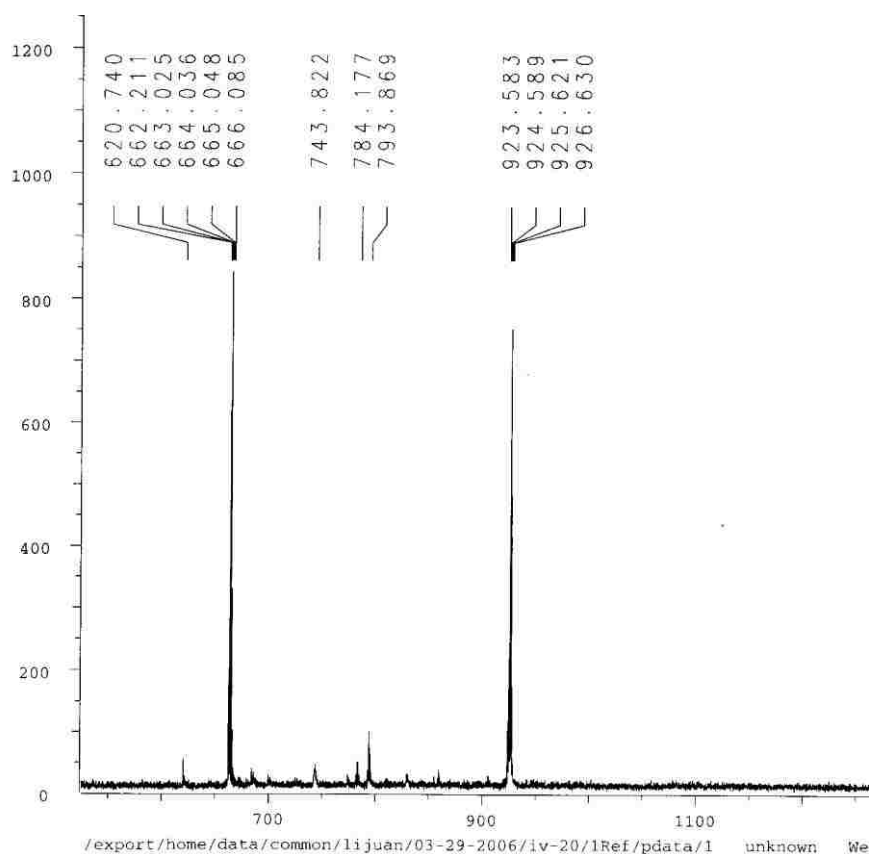
Figure 3-9. MALDI-TOF spectrum of the product generated from reaction shown in *Scheme 3-9*.

97

Instead of adding two malonoitrile groups to porphyrin, MALDI-TOF showed a peak at MW 923.6, corresponding to the addition of four malononitrile groups to the porphyrin macrocycle (see *Figure 3-9*). In the meanwhile, it gave a characteristic chlorin band on UV-vis spectra, which indicated the formation of a chlorin. However, the color of the solution was deep green instead of red often observed for most of the chlorin system.

3.3 Conclusions

An efficient transition catalyzed synthetic route was developed for the selective syntheses of the benzoporphyrin regio-isomers. This synthetic route avoided the total synthesis route for making benzoporphyrin and achieved the high regio-selectivity in generation of benzoporphyrin regio-isomers. The further usage of the synthetic precursors for the generation of the other type of extended porphyrin system will also be studied in our group in the future.

3.4 Experiment

3.4.1 General information

All reactions were monitored by TLC using 0.25 mm silica gel plates with or without UV indicator (60F-254). Silica gel (Sorbent Technologies 32-63 m) was used for flash column chromatography. ^{1}H- and ^{13}C-NMR spectra were obtained on either a DPX-250 or an ARX-300 Bruker spectrometer. Chemical shifts (δ) are given in ppm relative to residual $CHCl_3$ (7.26 ppm, 1H), or DCM (5.32 ppm, 1H) unless otherwise indicated. Electronic absorption spectra were measured on a Perkin Elmer Lambda 35 UV-Vis spectrophotometer. MALDI-TOF mass spectra were obtained on an Applied Biosystems QSTAR XL, using positive method with dithranol as matrix. Materials obtained from commercial suppliers were used without further purification.

3.4.2 Syntheses and Characterization

General procedure for metathesis and subsequent oxidation

The allyl-substituted porphyrins **3-1-n** (n = 1 ~ 5, 0.1 mmol) from the various Suzuki-coupling reactions were dissolved into anhydrous DCM. Grubbs II catalyst (0.0025 mmol/allyl group) in anhydrous DCM was added dropwise into the above porphyrin solutions. The solution was then heated under reflux overnight in an atmosphere of argon. TLC and MALDI-TOF spectra were used in monitoring the reaction. When all starting material had been consumed, the reaction was stopped. After cooling to room temperature and concentration, a silica gel column was used for purification, using a mixture of DCM/hexane as the mobile phase. After the short silica gel column separation, **3-5-1** was obtained in 91% yield. DDQ (182 mg, 0.8 mmol) was subsequently used to oxidize **3-5-1** to the corresponding benzoporphyrin (64 mg, 0.09 mmol) in almost qualitative yield. The solution was again found to undergo a dramatic color change associated with the oxidation: **3-5-1** was reddish in solution while **3-5-2** gave a green solution.

3-6-1: 87% yield. MALDI-TOF Calcd for $C_{48}H_{33}N_5O_2$ [M+H]$^+$ 712.271, found 712.149. UV-vis (DCM) λmax (nm): 383 (log ε 5.10), 439 (5.72), 536 (4.64), 614 (4.11), 680 (4.32). ^{1}H-NMR (300 MHz, CDCl3) 8.97 (1H, s), 8.85-8.88 (2H, m), 8.63-8.67 (2H, m), 8.21-8.25 (4H, m) 8.09-8.12 (4H, m), 7.68-7.81 (12H, m), 5.73 (2H, s), 3.27 (4H, s), -2.62 (2H, s). Mp >300 ºC.

3-5-1: 91 % yield. MALDI-TOF Calcd for $C_{52}H_{38}N_4$ [M]$^+$ 718.9, found 718.9. ^{1}H–NMR (250 MHz, CDCl$_3$): ppm 8.50 (s, 4H), 8.15-8.0 (d, 8H, J = 7.5), 7.77-7.66 (m, 12 H), 5.85 (s, 4H), 3.50 (s, 8H), -2.83 (s, 2H). Mp >300 ºC.

3-6-2: 85% yield. MALDI-TOF Calcd for $C_{48}H_{33}N_4$ [M+H]$^+$ 665.271, found 665.201. UV-vis (DCM), λmax (nm): 407 (log ε 4.95), 425 (5.70), 518 (4.38), 596 (3.88) and 650 (3.01). δH (300

MHz, CDCl3) 8.87 (2H, d, J = 5.9 Hz), 8.77 (2H, d, J = 5.9 Hz), 8.71 (2H, s), 8.19-8.24 (8H, m), 7.74-7.93 (12H, m), 7.36-7.39 (2H, m), 7.12-7.16 (2H, m), -2.61 (2H, s). Mp > 300 ºC.

3-5-2: MALDI-TOF Calcd for $C_{52}H_{35}N_4$ $[M+H]^+$ 715.286, found 715.798. UV-vis (DCM) λmax (nm): 413 (log ε 4.76), 435 (5.67), 525 (4.37), 618 (3.75) and 675 (3.85). δH (300 MHz, CD2Cl2) 8.76 (4H, d, J = 7.38 Hz), 8.53 (4H, d, J = 6.99 Hz), 8.28 (4H, s), 8.12-8.17 (4H, m), 8.00-8.05 (4H, m), 7.84-7.89 (4H, m), 7.56 (8H, s). Mp > 300 ºC.

3-7-1: 83% yield. MALDI-TOF Calcd for $C_{56}H_{35}N_5O_2$ $[M+H]^+$ 809.279, found 809.422. UV-vis (DCM) λmax (nm): 394 (log ε 5.02), 448 (5.73), 543 (4.62), 615 (4.26), 682 (4.09). δH (300 MHz, CD_2Cl_2) 8.93 (1H, s), 8.88-8.92 (2H, m), 8.71-8.73 (2H, d, J = 6.03 Hz), 8.16-8.27 (8H, m), 7.73-7.91 (12H, m), 7.30-7.34 (2H, d, J = 11.0 Hz), 7.08 (2H, s), -2.35 (2H, s). Mp > 300 ºC.

3-7-2: 82% yield. MALDI-TOF Calcd for $C_{56}H_{37}N_4$ $[M+H]^+$ 765.302, found 765.670. UV-vis (DCM) λmax (nm): 428 (log ε 4.97), 450 (5.70), 553 (4.31), 590 (4.37), 628 (4.04), 685 (3.86). δH (250 MHz, CD_2Cl_2) 8.44 (2H, s), 8.21-8.30 (10H, m), 7.82-7.97 (12H, m), 7.42-7.45 (2H, m), 7.30-7.34 (2H, m), 7.14-7.20 (4H, m), 7.02-7.05 (1H, m), 6.93 (1H, d, J = 7.24 Hz), -1.2 (2H, brs). Mp >300 ºC.

3-6-3: UV-vis (λmax nm/DCM): 394, 448, 543, 615, 682. ^{1}H-NMR (250 MHz, CDCl_3) 8.99 (s, 1H), 8.87-8.82 (m, 2H,), 8.64-8.61 (m, 2H), 8.28 (d, 2H, J = 5.0 Hz), 8.22 (d, 2H, J = 5.0 Hz), 8.13-8.10 (m, 4H), 7.83-7.70 (m, 12H), 5.30 (s, 4H), 3.26 (s, 8H), -2.62 (2H, s). Mp >300 ºC.

3-2-3: ^{1}H-NMR (250 MHz, CDCl_3): ppm 9.06 (s, 1H), 9.02 (s, 1H), 8.95 (s, 1H), 8.91 (s, 2H), 8.73 (s, 2H), 8.21 (br, 8H), 7.80 (s, 12H), -2.61 (s, 2H). MALDI-TOF Calcd for $C_{44}H_{29}N_5O_2$, 659.7. Found 659.8. Mp >300 ºC.

General Procedure for Diels-Alder Reaction

The Diels-Alder reaction was typically performed on **3-5-1**. The diene precursor used in this Diels-Alder reaction, 1,4-dihydro-2,3-benzoxathiin-3-oxide was generated as a liquid according to the literature[11]. The preparation of **3-8-2** was performed by mixing 1,4-dihydro-2,3-benzoxathiin-3-oride with **3-5-1** in the ratio of 3/1 in toluene and subsequently refluxing the reaction mixture at 120 ºC under argon. TLC was used to follow the reaction. **3-8-1**: UV-vis (λmax DCM /nm) 427, 456, 545, 584, 642, 698. MALDI Calcd. for $C_{68}H_{46}N_4$, 919.1. Found, 918.6. **3-8-1-Zn**: UV-vis (λmax DCM /nm) 440, 470, 579, 641, 732.

The preparation of Benzochlorin 3-9-1.

A mixture of K_2CO_3 (34 mg, 0.25mmol) and malononitrile (20 µL, 0.3 mmol) in dry THF (1 mL) was stirred for 1 h at reflux under argon. The reaction mixture was cooled to room temperature, and **3-6-1** (21 mg, 0.03 mmol) was added to the mixture. The temperature was slowly increased to 65 °C and the mixture was allowed to stir for 6 h until all starting material and intermediate cyclopropylchlorin had disappeared (monitored by TLC). The reaction mixture was cooled, diluted with DCM (20 mL), washed with H_2O, dried over anhydrous Na_2SO_4, filtered, and evaporated to dryness. The crude chlorin was purified by chromatography on a short silica gel column eluted with DCM/cyclohexane (2/1), and the red band was collected. UV-vis (λmax DCM /nm) 424, 481, 515, 547, 629, 686.

Genral procedure for Suzuki-Coupling Reaction

The mixture of bromoporphyrin (**3-1** to **3-4**) (0.1 mmol) with $Pd(PPh_3)_4$ (57.8 mg/Br, 0.05 mmol /Br) and K_2CO_3 were dissolved in freshly distilled toluene, to which 2-allyl-4,4,5,5-tetramethyl-1,3,2-dioxaborolane (33.6 mg/Br, 0.2 mmol/Br) was added through a syringe. Strictly air free

conditions was required. TLC and MALDI-TOF were used to follow the reaction. When most of the bromoporphyrin had been consumed, the reaction was stopped.

3-4-3: ^{1}H NMR (250 MHz, CDCl$_3$): ppm 8.37 (s, 4H), 8.15-8.09 (m, 8H), 7.75-7.63 (m, 12 H), 5.69 -5.64 (s, 4H), 4.76 (d, 4H, J = 10.0 Hz), 4.47 (d, 4H, J = 7.5 Hz), 3.51 (s, 8H), -2.50 (s, 2H). MALDI-TOF Calcd for C$_{56}$H$_{46}$N$_4$:775.0. Found 775.8.

3-4-4: ^{1}H NMR (250 MHz, CDCl$_3$): ppm 8.33-8.22 (m, 9H), 7.76-7.71 (m, 12H), 5.35-5.12 (m, 6H), 4.65-4.42 (m, 8H), 4.11-3.97 (m, 4H), 3.40-3.18 (m, 8H), 2.82 (s, 4H), -1.94 (s, 2H). MALDI-TOF Calcd for C$_{62}$H$_{53}$N$_5$O$_2$: 900.1. Found 901.7.

3-4-1: MALDI-TOF Calcd for C$_{50}$H$_{37}$N$_5$O$_2$: 740.0. Found 740.0.

General procedures for Bromination

3-2-1: A mixture of **3-2-3** (2.0 g, 3.0 mmol) and N-bromosuccinimide (1.4 g, 2.4 equiv) in dry chloroform (ethanol free, 250 mL) was refluxing for a period of 12 h. After being cooled to room temperature, the reaction mixture was poured into an alumina plug (Grade III) and eluted with CHCl$_3$. After removing of solvent under vacuum, the resulting solid was further recrystallized from CHCl$_3$/MeOH. The desired **3-2-1** was eventually obtained as a brown powder in 80% yield (1.97 g). UV-Vis (λmax nm): 442, 543, 695; MALDI-TOF Calcd for C$_{44}$H$_{27}$Br$_2$N$_5$O$_2$, 817.5. Found 817.8.

3-1: NaBH$_4$ (80 mg, 2.2 mmol) was added to a cold solution (ice/NaCl) of **3-2-1** (1.0 g, 1.2 mmol) in dry THF (50 mL) under argon. After allowing the reaction mixture to stir for a period of 1 h, the ice bath was removed and the mixture was stirred for an additional 1 h. This reaction was monitored by UV-vis spectrophotometry. When the Soret band was blue shifted from 436 to 424 nm, the reaction was stopped, DCM (200 mL) was added and then the reaction mixture was poured into water (around 200 mL). The separated organic phase was washed twice with water

(200 mL each), and after drying over anhydrous Na_2SO_4, the solvent was removed under vacuum. The residual solid was dissolved in DCM and filtered through a short alumina plug (Grade V) and eluted with $CHCl_3$. After reducing the volume of solvent under vacuum to around 400 mL, the silica gel (80 g) was added into the reaction mixture and it was refluxed under argon for a period of 1 d. It was cooled to room temperature and the silica gel was removed by filtration, followed by a thorough washing with $CHCl_3$. After removing the solvent under vacuum and subsequent recrystallization from $CHCl_3$/MeOH, **3-1** was obtained as a purple powder in 83% yield (782 mg). UV-Vis (λmax nm /DCM): 431, 534, 601, 652; MALDI-TOF Calcd for $C_{44}H_{28}Br_2N4$, 772.5. Found m/z 772.5.

3-3-1: The mixture of **3-1-2** (3.0 g, 4.25 mmol) and NBS (7.5 g, 10 equiv) was dissolved in 1,2-dichloroethane (300 mL) and was refluxed for a period of 16 h under argon. After cooling to room temperature, the reaction mixture was poured into a silica gel plug and eluted with $CHCl_3$. After removing the solvent under vacuum and subsequent recrystallization from $CHCl_3$/MeOH, the desired product **3-3-1** was obtained as a dark green powder in 68% yield (3.4 g). This reaction was careful monitored by UV-vis spectrophotometry. Extension of the reflux times should be avoided in order to prevent the slow degradation of the desired product and a concomitant decrease in the yield. UV-Vis (λmax nm/DCM): 465 nm, 591, 635; MALDI-TOF Calcd. for $C_{44}H_{21}Br_6CuN_5O_2$, 1194.6. Found 1194.9.

3-3-2: Porphyrin **3-3-1** (1.2 g, 1.0 mmol) was placed in a 200 mL round bottom flask and a minimal amount of DCM was added to dissolve it. After slow removal of the solvent by rotation under vacuum, an oily film was formed on the surface of the flask. Then concentrated sulfuric acid (40 mL) was added and the mixture was alternately stirred and sonicated for a period of 1.5 h. It was poured into a mixture of ice/water, and the demetalated product was extracted with

CHCl$_3$. The organic phase was subsequently washed with water (40 mL), and saturated aqueous NaHCO$_3$ (40 mL). After drying over Na$_2$SO$_4$ and reducing the solvent volume to around 50 mL under vacuum, 50 mL of MeOH was added. After subsequent further concentration, and filtration, **3-3-2** was obtained as a green powder in 95% yield (1.1 g). UV-Vis (λmax nm /DCM), 472, 579, 635, 751; MALDI-TOF Calcd for C$_{44}$H$_{23}$Br$_6$N$_5$O$_2$, 1133.1. Found 1133.0.

3-3-3: Porphyrin **3-3-1** (1.2 mg, 1.0 mmol) was dissolved in dry DMSO (30 mL) under argon, and NaBH$_4$ (66 mg, 1.8 mmol) was added into the solution with stirring. The solution was initially green and soon turned into brown. Stirring was continued for around 2 h. When the Soret absorption band showed a 22 nm blue-shift, the reaction was stopped. After adding 500 mL of DCM, the reaction mixture was poured into 500 mL of water. The organic phase was washed several times with water (500 mL each). After reducing the solvent volume to around 30 mL under vacuum, the solution was placed in the refrigerator for around 3~6 hours. After filtration, pure **3-3-3** was obtained as a dark brown precipitate in 55% yield (650 mg). MALDI-TOF Calcd for C$_{44}$H$_{22}$Br$_6$N$_4$Cu: 1149.6. Found 1149.6.

3-3. Compared to the metalated starting material, the green solution of **3-3-2** was relatively unstable even under slightly basic conditions. Thus the reduction of **3-3-2** was not tried. The desired free-base hexabromotetraphenylporphyrin was obtained from the demetalation of the corresponding metallo-hexabromotetraphenylporphyrin **3-3-3** using concentrated H$_2$SO$_4$. **3-3-3** (350 mg, 0.3 mmol) was dissolved in 50 mL concentrated sulfuric acid for a period of 1 h with alternating stirring and sonication. After this it was poured into ice/water, and the demetalated product was extracted with 50 mL of CHCl$_3$. The organic phase was subsequently washed with water (50 mL), and saturated aqueous NaHCO$_3$ (50 mL). After drying over anhydrous Na$_2$SO$_4$, the solvent was removed under vacuum. Recrystallization from CHCl$_3$/MeOH gave **3-3** as a dark

purple powder in 74% yield (230 mg). UV-Vis (λmax nm /DCM) 473, 548, 634, 728; MALDI-TOF Calcd for $C_{44}H_{24}Br_6N_4$: 1088.1. Found 1088.2.

3-2: Recrystallization of NBS was performed in hot water followed by drying at 80 °C under vacuum for a period of 6 h. H_2TPP (600 mg, 1.0 mmol) was dissolved in $CHCl_3$ (120 mL) and freshly recrystallized NBS (1.0 g, 6.0 mmol) was added into the solution which was refluxed for a period of 4 h. After cooling to room temperature, $CHCl_3$ was removed under vacuum. The residue was then washed with methanol (2×40 mL) to remove the succinimide impurities. Then the residue as a purple solid was dissolved in $CHCl_3$ and purified on a silica gel column with $CHCl_3$ as the eluting solvent. The first fraction from the column was collected and the solvent was removed under vacuum. The solid was further recrystallized from $CHCl_3$ /CH_3OH (1:3). After filtration and removal of the solvent under vacuum, **3-2** was obtained in 66% yield (0.6 g). ^{1}H NMR ($CDCl_3$, 250 MHz): ppm 8.70 (s, 4H), 8.20-8.17 (m, 8H), 7.80-7.78 (m, 12H), −2.90 (s, 2H). MALDI-TOF Calcd for $C_{44}H_{26}Br_4N_4$: 930.3. Found 930.4.

3.5 References

1   Smith, K. M. In Rodd's Chemistry of the Carbon Compounds; Sainsbury, M., Ed.; Elsevier: Amsterdam; 1997; Chapter 12, Suppl. to Vol. IVB.; 1997; pp 277.

2   Shea, K. M.; Jaquinod, L.; Smith, K. M.; *J. Org. Chem.*, **1998**, *63*, 7013.

3   Pandey, R. K.; Zheng, G. In *The Porphyrin handbook*; Kadish, K. M.; Smith, K. M.; Guildard, R.; Eds.; Academic Press: San Diego, **2000**; Vol. 6, pp. 157. b) Hoffman, B. M.; Ibers, J. A.; *Accounts Chem. Res.* **1983**, *16*, 15. c) Nevin, W. A.; Chamberlain, G. A.; *J. Appl. Phys.* **1991**, *69*, 4324. d) Rao, D. V. G. L. N.; Aranda, F. J.; Roach, J. F.; Remy, D. E. *Appl. Phys. Letters* **1991**, *58*, 1241.

4   Whitlock, H. W.; Hanauer, R.; Oester, M. Y.; Bower, B. K. *J. Am. Chem. Soc.* **1969**, *91*, 7485.

5   Senge, M. O. In *The Porphyrin handbook*; Kadish, K. M.; Smith, K. M.; Guildard, R.; Eds.; Academic Press: San Diego, **2000**; Vol. 1, pp. 284. b) Kopranenkov, V. N.; Dashkevich, S. N.; Kukyanets, E. A. *J. Gen. Chem. USSR.* **1981**, *51*, 2513. c) Remy, D. E. *Tetrahedron Lett.* **1983**, *24*, 1451. d) Ichimura, K.; Sakuragi, M.; Morii, H.; Yasuike, M.; Toba, Y. ; Fukui, M. ; Ohno, O. *Inorg. Chim. Acta* **1991**, *186*, 95. e) Ichimura, K.; Sakuragi, M.; Morii, H.; Yasuike,

M.; Fukui, M. ; Ohno, O. *Inorg. Chim. Acta* **1991**, *182*, 83. f) Vinogradov, S. A.; Wilson, D. F. J. Chem. Soc., *Perkin Trans. 2* **1995**, 103. g) Ito, S.; Murashima, T.; Uno, N. *Chem. Commun.* **1998**, 1661. h) Tomé, A. C.; Lacerda, P. S. S.; Neves, M. G. P. M. S.; Cavaleiro, J. A. S. *Chem. Commun.,* **1997**, 1199. i) Silva, A. M. G.; Tomé, A. C.; Neves, M. G. P. M. S.; Cavaleiro, J. A. S. ; Kappe, C. O. *Tetrahedron Lett*. **2005**, *46*, 4723.

6   Bonnett, R.; McManus, K. A. *J. Chem. Soc. Perkin Trans. 1*, **1996**, 2461. b) Vicente, M. G. H.; Tome, A. C.; Walter, A. ; Cavalerio, J. A. S. *Tetrahedron Lett.* **1997**, *38*, 3639. c) Martinsen, J.; Pace, J. L.; Phillips, B. M.; Ibers, A. J. *J. Am. Chem. Soc.* **1982**, *104*, 83.

7   Jaquinod, L. In *The Porphyrin handbook*; Kadish, K. M.; Smith, K. M.; Guildard, R.; Eds.; Academic Press: San Diego, **2000**; Vol. 5, pp. 202. b) Crossley, M. J.; Burn, P. L.; Chew, S. S.; Cuttance, C. F.; Newsom, I. A. *J. Chem. Soc., Chem. Commun.* **1991**, 1564. c) Kumar, P. K.; Bhyrappa, P.; Varghese, B. *Tetrahedron Lett.* **2003**, *44*, 4849. d) Mandon, D.; Ochsenbein, P. ; Fischer, J.; Weiss, R.; Jayaraj, K.; Austin, R. N.; Gold, A. White, P. S.; Brigaud, O.; Battioni, P.; Mansuy, D. *Inorg. Chem.,* **1992**, *31*, 2044. e) Jaquinod, L.; Khoury, R. G.; Shea, K. M.; Smith, K. M. Tetrahedron, 1999, 55, 13151.

8   Suzuki, A. *Pure Appl. Chem.,* **1994**, *68*, 213. b) Chan, K. S.; Zhou, X.; Lou, B.-S.; Mak, T. C. W. *J. Chem. Soc., Chem. Commun.***1994**, 271. c) Zhou, X.; Zhou, Z.-Y.; Mak, T. C. W.; Chan, K. S. *J. Chem. Soc., Perkin Trans.1*, **1994**, 2519.

9   Fürstner, A. *Angew. Chem. Int. Ed.,* **2000**, *39*, 3012. b) Ivin, K. J. *J. Mol. Catal. A-Chem.* **1998**, *133*, 1. c) Grubbs, R. H.; Chang, S. *Tetrahedron* **1998**, *54*, 4413. d) Randall, M. L.; Snapper, M. L. *J. Mol. Catal. A-Chem*. **1998**, *133*, 29.

10 Occhiato, E. G.; Trabocchi, A.; Guarna, A. *J. Org. Chem.* **2001**, *66*, 2459.

11 Hoey, M. D.; Dittmer, D. C.; *J. Org. Chem.* **1991**, *56*, 1947.

CHAPTER 4. "HANGMAN PORPHYRIN" ANALOGS

4.1 Introduction

The mechanisms of proton-coupled electron transfer (PCET) processes occur in many natural systems[1–3]. It has been the subject of several investigations using model porphyrin-based compounds[4, 5]. Such studies indicate that either a face-to-face or side-to-side arrangement of the acid–base and redox sites are crucial for efficient proton and electron transfers[6]. On the other hand, the hydrogen-bond framework in heme model systems has served as a determinant in the heme structure and function. Thus the targeted synthesis of model systems containing one or more hydrogen-bond functionalities attracts much of research interest[7–10]. Porphyrins have interesting structural and electronic properties, especially the so-called "hangman porphyrins" (see *Figure 4-1*).
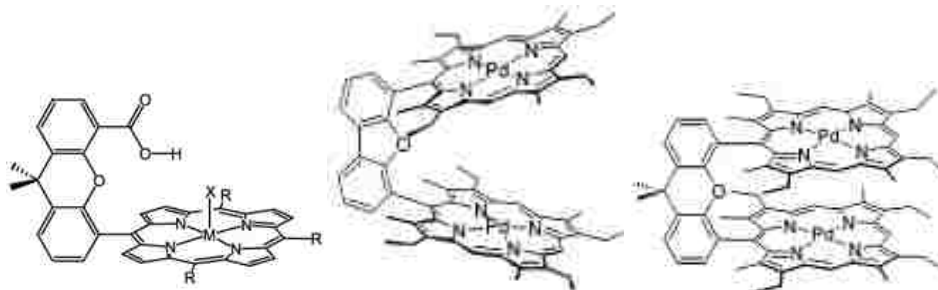
Figure 4-1. Chemical structures of Hangman Porphyrins (left) and related cofacial bisporphyrins (middle to right).

Hangman porphyrins serve as attractive PCET model systems and allow the control of both the proton and electron transfers. In the meanwhile, they also provide methods to the specific modification of PCET model system with specific proton-donating group and specific arranging it to the special region of metalloporphyrin redox site[6]. As a potential model system for investigations of hydrogen-bond frameworks and the related energy transfer in natural systems[6,11–19], Hangman porphyrins bearing hydrogen synthons with different pKa values have been reported[6, 13–19]. The acidity of these systems was found to influence the PCET rate and the

stability of the catalyst during PCET process[6, 15c]. However, the synthesis of such models presents several challenges due to very long synthetic routes and tedious separation using currently available methods. Furthermore, routes lack susceptibility to modular modifications of the target systems[14]. Calixarenes have been extensively studied in recent years because of their interesting chemical and physical properties[20–32]. Among these, heterocalixarenes are far less prevalent in the chemical literature, especially the oxacalixarenes. Although the modest yield synthesis of oxacalixarene was first reported in 1966, their further studies are especially scarce[26]. Previous synthesis of oxacalixarene was based on a nucleophilic aromatic substitution and this had been used to efficiently synthesize highly functionalized oxacalixarenes. However, this requires high temperature and extended reaction times. Recently, Katz et al.[30] made a significant improvement in oxacalixarene synthesis. This improved synthesis selectively chose bases and solvents and allowed the reaction to proceed at room temperature with high yields (*Scheme 4-1*).
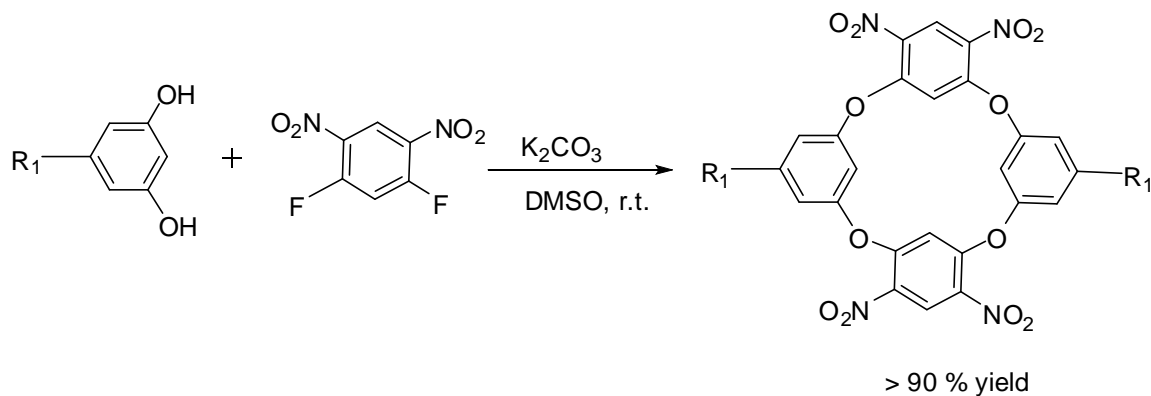
Scheme 4-1. Recent improved synthesis of the symmetrical oxacalix[4]arenes from literature.

Based on this improved synthesis, Vicente's research group have recently reported the synthesis of oxacalix[4]arene-linked bisporphyrins (see *Figure 4-2*) through nucleophilic aromatic substitution reaction of 1,5-difluoro-2,4-dinitrobenzene with a 3,5-dihydroxyphenyl-containing porphyrin[33]. Despite these advances in recent research aspects of heterocalixarenes,

the efficient synthesis of unsymmetric heterocalixarenes remains a challenge, especially for the case of oxacalixarenes.
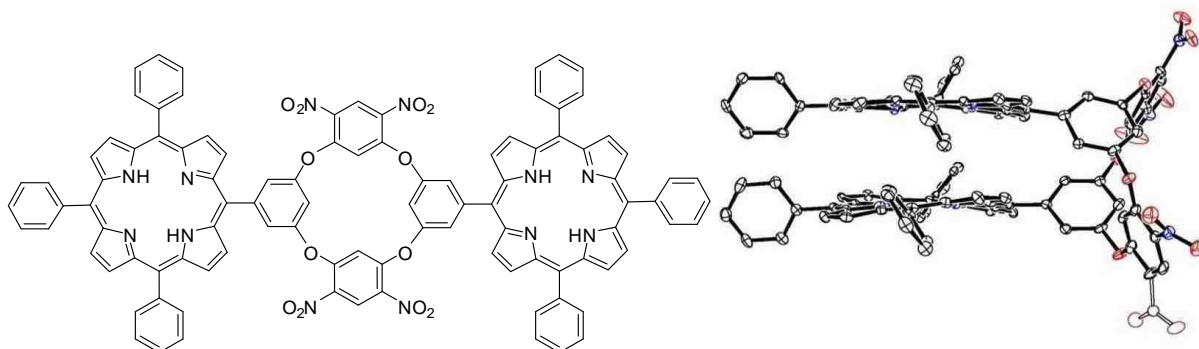
Figure 4-2. The X-ray structure of oxacalix[4]arene-linked cofacial porphyrin, which clearly shows the 1,3-alternative conformation (Left, chemical structure; Right, X-ray) from the literature.
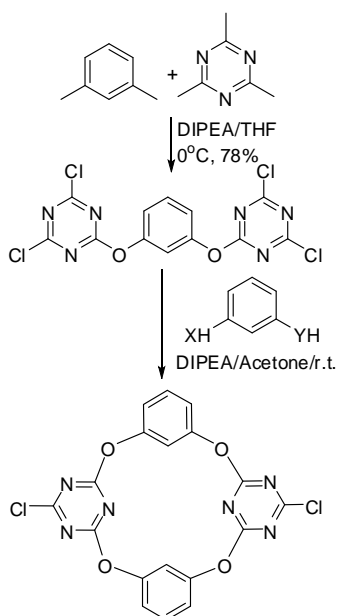
Figure 4-3. Recent improved synthesis of unsymmetrical heterocalix[4]arenes from literature.

Recently, Wang and Yang[24] developed a fragment-coupling approach to the O- and N-bridged calixarenes based on triazine fragment. Still this reaction needs long reaction times in general (see *Scheme 4-3*). Attracted to the unique discrete 1,3-alternating conformations of oxacalix[4]arenes[20–33], we envisioned to design and synthesize porphyrin containing oxacalix[4]arenes with hydrogen synthons being suspended over the porphyrin macrocycle. We

109

believed that the compounds would be useful in PCET as heme model systems and also serve as efficient synthetic approaches to unsymmetrical oxacalixarene and heterocalixarene in organic synthesis.

4. 2 Results and Discussion
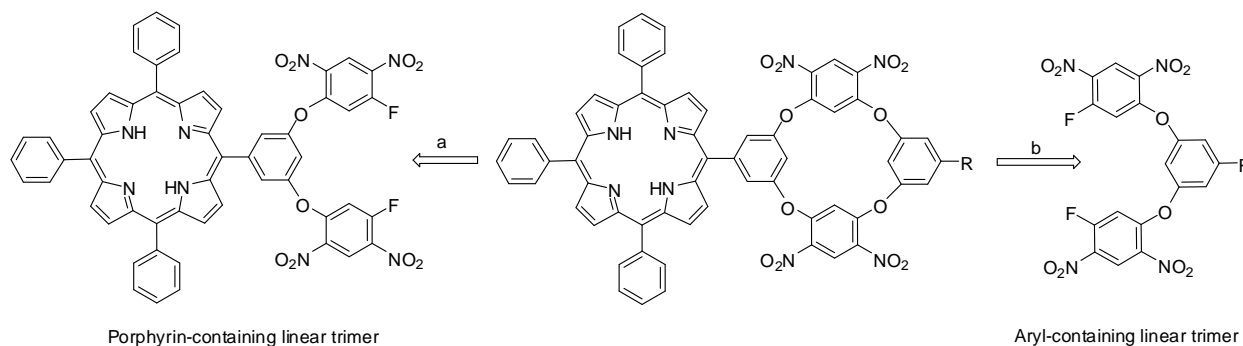
Scheme 4-2. Retro-synthetic analysis of the designed unsymmetrical porphyrin-oxacalix[4]arenes.

Our synthetic strategy is shown in *Scheme 4-4.* Inspired by the fragment coupling reaction in the unsymmetrial heterocalixarene synthesis, our synthesis used a [3+1] fragment coupling reaction, from which a series of novel unsymmetrical oxacalix[4]arenes were achieved from the nucleophilic aromatic substitution of functionalized meta-dihydroxybenzenes with 1,5-difluoro-2,4-dinitrobenzene. The target compound could be synthesized either from the porphyrin-containing linear trimer or from the aryl-containing linear trimer, as shown in *Scheme 4-2*. Either way, the efficient preparation of the linear trimer was required. Attracted to the convenience to react the porphyrin containing linear trimer with different readily available dihyroxybenzenes in the formation the target compounds, we started to use the approach as shown in *Scheme 4-2*.

The synthesis of the 5-(3,5-dihydroxyphenyl)-triphenylporphyrin (**4-3-1**) was shown in *Scheme 4-3*. A mixture of 1 equivalent of 5-(3,5)-dimethylbenzaldehyde, 3 equivalents of benzaldehyde and 4 equivalents of freshly distilled pyrrole was dissolved in dry DCM. The

solution was stirred for 10 minutes under argon. Subsequently, a catalytic amount of a DCM solution of 2.5M BF$_3$·OEt was added to the reaction mixture. The reaction mixture was stirred under argon with avoidance of light. TLC was used to follow the reaction. After adding DDQ to the reaction mixture, stirring was continued for an additional 45 minutes. Then the volume of solvent was reduced and the residue was applied to a silica gel column using hexane and DCM as eluting solvents. After removal of solvent under vacuum, **4-3-2** was obtained as purple powder in 8.5% yield.
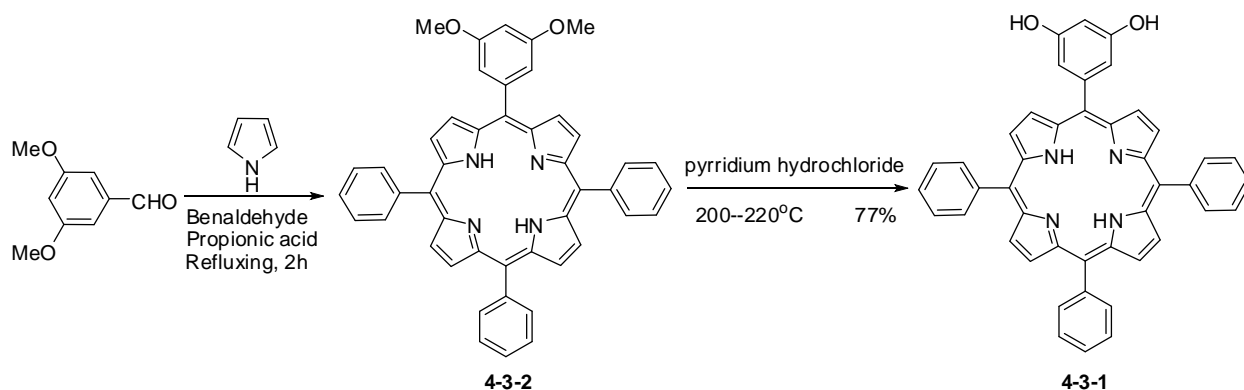
Scheme 4-3. Synthesis of 3, 5-dihydroxy-tetraphenylporphyrin **4-3-1**.

The hydrolysis of **4-3-2** to obtain 5-(3,5-dimethoxyphenyl)-10,15,20-triphenylporphyrin (**4-3-1**) was performed at 220 °C using an oil bath. A mixture of 1 equivalent of **4-3-2** and 140 equivalents of pyridine hydrochloride was added to a round-bottom flask and heated to 220 °C in an oil bath. Upon the melting of the pyridium hydrochloride at 170 °C, the solution turned green in color. TLC was used to follow the reaction and the reaction was stopped when most of the starting materials had been consumed. After cooling to room temperature, the reaction mixture was poured into cold water and extracted with ethyl acetate. The combined organic layers were washed with aqueous 0.1 M HCl and saturated aqueous NaHCO$_3$. After drying over anhydrous Na$_2$SO$_4$, the solvent was removed under vacuum. The residue was separated using a silica gel column eluted with chloroform/ethyl acetate (1:1). The major fraction was collected and was

111

further purified by recrystallization from DCM/hexane. After filtration and removal of the solvent under vacuum, the target porphyrin **4-3-1** was obtained as a purple powder in 84% yield.
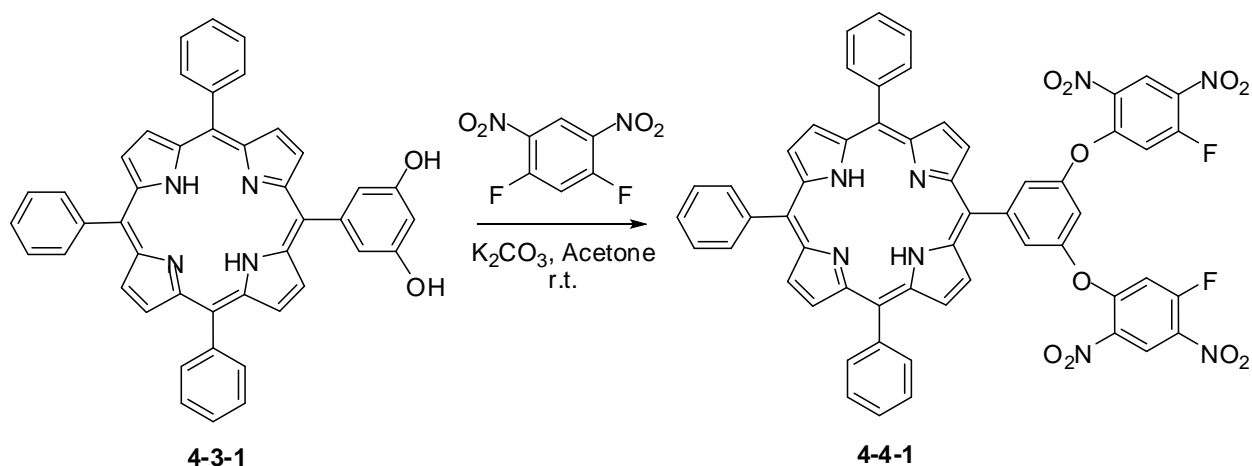
Scheme 4-4. Synthesis of porphyrin containing linear trimer **4-4-1**.
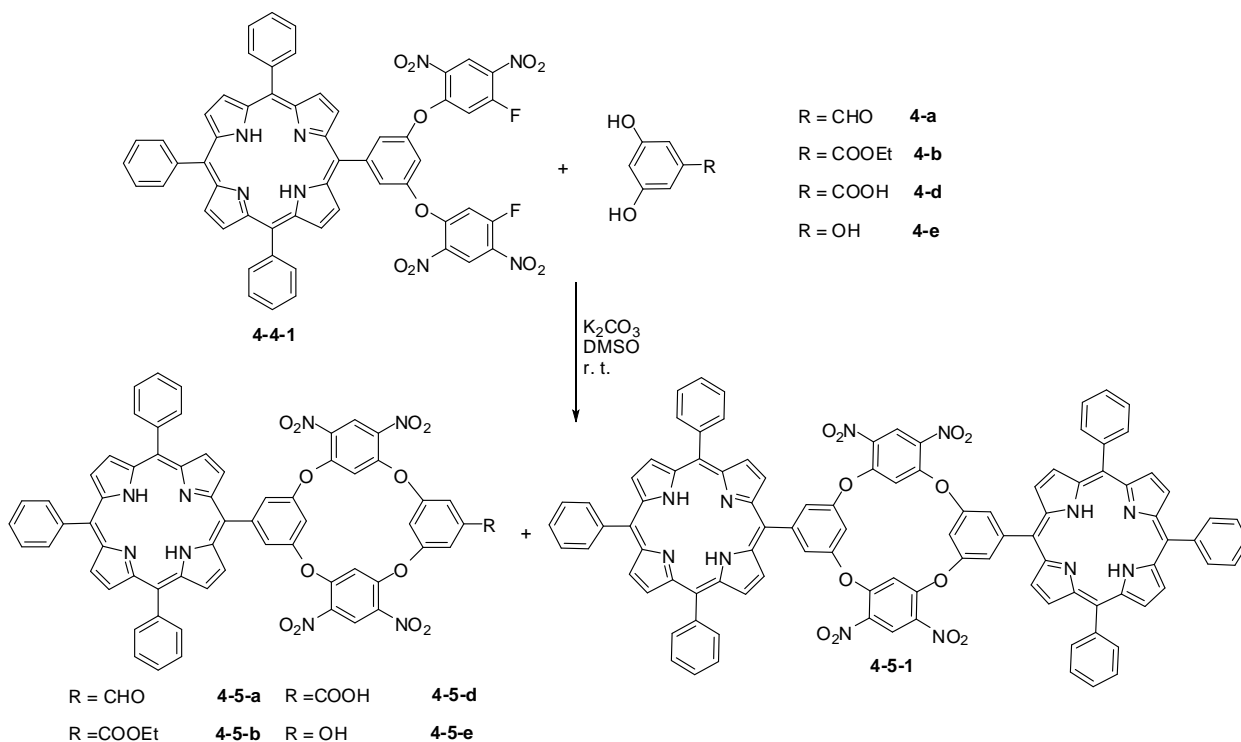
Scheme 4-5. The synthesis of unsymmetrical porphyrin-oxacalix[4]arenes from the porphyrin-containing linear trimer **4-4-1**.

The synthesis of the porphyrin containing the linear trimer **4-4-1** is shown in *Scheme 4-6*.

A mixture of 1 equivalent of **4-3-1**, 4 equivalents of 1,5-difluoro-2,4-dinitrobenzene and eight
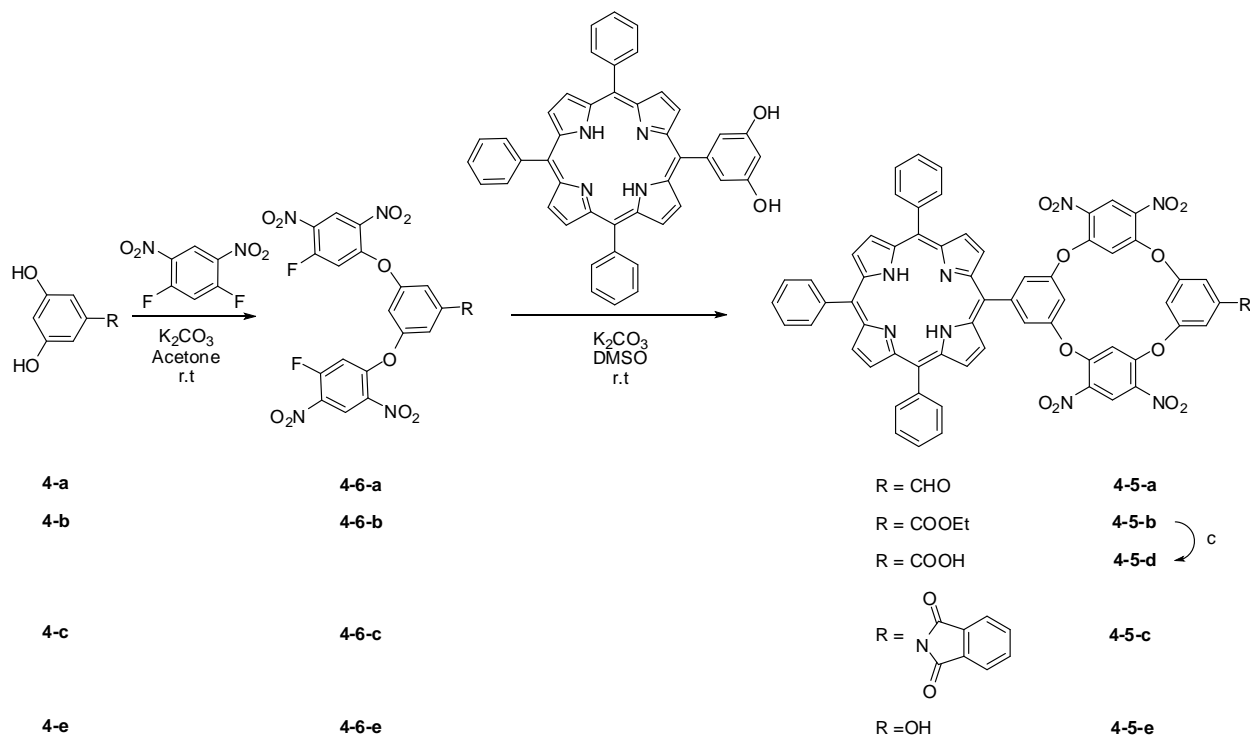
Scheme 4-6. The efficient synthesis of unsymmetrical oxacalix[4]arene **4-5-n** (n = a-e).

equivalents of K_2CO_3 was dissolved in phenol-free acetone. The reaction mixture was stirred at room temperature under air. After this, acetone was removed under vacuum. The residue was separated using a silica gel column eluted with DCM/hexane. After removing solvents under vacuum and subsequent recrystallization from hexane/DCM, compound **4-4-1** was isolated in 80% yield. The synthesis of functionalized oxacalix[4]arene porphyrins **4-5-n** (n = a, b, d, e) from the coupling reaction between **4-4-1** and readily available dihydroxybenzenes **4-n** (n = a, b, d, e) is shown in *Scheme 4-5*. This reaction was performed in DMSO in the presence of finely ground K_2CO_3. Despite the different type of 3,5-dihydroxybenzene reagents used in this reaction, the yields of the desired products **4-5-n** (n = a, b, d, e) were low (10–25%). The major product from these reactions was invariably the symmetric oxacalix[4]arene bisporphyrin **4-5-1**[33]. The generation of **4-5-1** under these reaction conditions is attributed to the scrambling of the porphyrin containing linear trimer **4-4-1**. The thermodynamic reversibility of oxacalixarene formation during nucleophilic substitution has been studied and confirmed recently by Katz et

al.[30], which is also in agreement with studies reported for thiocalixarenes[34] and with the invariable formation of symmetrical **4-5-1** and the absence of **4-3-1** in our case. To solve the scrambling problem of the porphyrin containing linear trimer, the aryl-containing linear trimer was used for the [3+1] fragment coupling reaction (see *Scheme 4-6*).

A mixture of 1 equivalent of **4-n** (n = a–c, e), 3 equivalents of 1,5-difluoro-2,4-dinitrobenzene and 4 equivalents of finely ground K_2CO_3 (<80 mm) was dissolved in acetone at room temperature. The reaction mixture was stirred for around 1–2 hours at room temperature under air. TLC was used to follow the reaction. When the reaction was complete, acetone was removed under vacuum. The residue was separated using a silica gel column eluted with DCM. After removal of the solvent and washing with hexane (2×10 mL), linear trimer **4-6-n** (n = a-c, e) was obtained as a white solid in 75–85% yields on multi-gram scale. By simply choosing acetone as solvent and 3 equivalents (rather than two) of 1,5-difluoro-2,4-dinitrobenzene, the formation of symmetrical oxacalix[4]arene **4-5-1** as a scrambling byproduct was reduced to a minimal amount. The linear trimers **4-6-n** (n = a–c, e) were then used to generate the target functionalized oxacalix[4]arene porphyrins **4-5-n** (n = a-e) in 80–86% yields (see *Scheme 4-6*). A mixture of 1 equivalent **4-3-1**, 1.2 equivalents of **4-6-n** (n = a-c, e) and 4 equivalents of finely ground K_2CO_3 was dissolved in DMSO. The reaction mixture was stirred at room temperature for a period of 30 minutes or up to 3 hours. TLC was used to follow this reaction, and the reaction was stopped upon complete disappearance of the starting materials. These fragment-coupling reactions are very efficient and no higher analogs were detected, compared with other fragment-coupling reactions reported in the literature[20–25]. Thus the yields were higher and the separations were easier. Using DMSO as the solvent in place of acetone in the ring-closure fragment coupling

114

reaction improved the yields of the reaction. However, the use of DMSO instead of acetone resulted in lower yields of linear trimer formation.
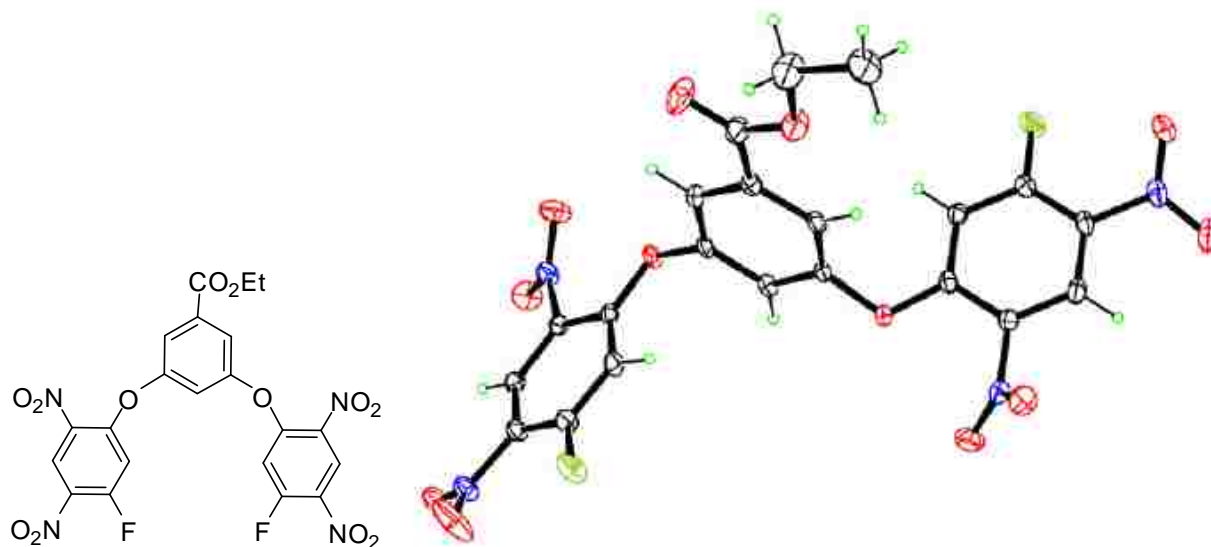
Figure 4-4. Chemical structure (left) and X-ray structure (right) of **4-6-b.**

The generation of **4-5-d** was achieved by hydrolysis of the ester functionality in **4-5-b**. The hydrolysis under basic conditions by using NaOH aqueous solution failed to generate the desired product; instead the starting material decomposed under these conditions, in agreement with the scrambling that occurred in the generation of **4-5-1**. The hydrolysis under dilute acidic condition also failed, leaving the starting material intact. The final successful hydrolysis of **4-5-b** was accomplished by refluxing it in a mixture of THF/4 M aqueous HCl (v/v = 1/2) for a period of 3 days. After separation, **4-5-d** was obtained as a purple powder in 95% yield. The functionalized oxacalix[4]arenoporphyrins **4-5-n** (n = a–e, 1) were characterized by HRMS, UV–vis, fluorescence, and ^{1}H NMR spectroscopy. The structure of trimer **4-6-b** was also confirmed by X-ray crystallography at T=150K (see *Figure 4-4*). The crystals of **4-6-b** were destroyed by cooling to temperatures lower than 150K, apparently as a result of a phase change. The C–F distances are 1.331(2) and 1.334(2) A°.

The linear trimers **4-6-n** (n = a–c, e) shared characteristic ^{1}H NMR spectra, with two downfield singlets (around 8.9 ppm) for the protons adjacent to the carbons bearing the NO_2 groups, and two upfield singlets (around 6.9 ppm) for the protons adjacent to the carbons bearing the F groups. Based on the characteristic upfield chemical shifts observed in the ^{1}H NMR spectra of oxacalix[4]arenes for the interior protons on the electrophilic (NO_2-bearing) aromatic rings[28], it is believed that these compounds adopt 1,3-alternating structures in solution[20–33]. Recent X-ray structures[26–33] have confirmed this conformation of oxacalix[4]arenes in the solid state.

Table 4-1. ^{1}H NMR shifts for the interior protons on the NO_2-bearing benzene rings of porphyrins **4-5-n** (n = a–e, 1).

Porphyrins	**4-5-a**	**4-5-b**	**4-5-d**	**4-9-1**	**4-5-e**	**4-5-c**
δ (ppm)	6.77	6.43	6.70	6.87	6.70	6.49

Table 4-1 shows the ^{1}H NMR chemical shifts observed for these protons on porphyrins **4-5-n** (n = a–e) and **4-9-1** (see Scheme 4-9). These results suggest that our functionalized oxacalix[4]arene porphyrins also adopt 1,3-alternating conformations in solution, in agreement with results reported for symmetrical oxacalix[4]arenes[26–33]. Furthermore, computer calculations using the AM1 theoretical model incorporated into the Spartan program were performed to determine the minimum energy conformations for oxacalix[4]arene porphyrins **4-5-n** (n = a-e), **4-9-1**. Such calculations have been found reliable for the determination of geometrical parameters in porphyrin arrays[37–40]. Similar optimized geometries were found for all oxacalix[4]arene porphyrins (see *Figure 4-5*) and the calculated structure obtained for bisporphyrin **4-5-1** was in agreement with the crystal data[33]. These results suggest, as seen in *Figure 4-5*, favorable 1,3-alternating conformations for all oxacalix[4]arene porphyrins, with the hydrogen-bond synthons hanging over an adjacent pyrrole ring. Such a conformation would
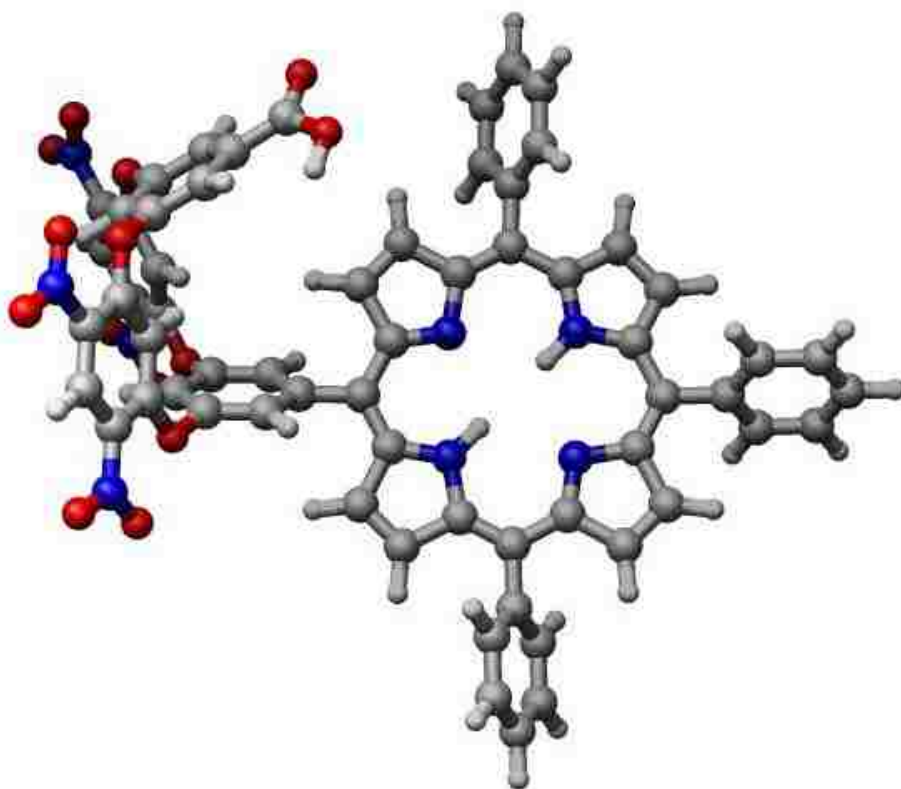
Figure 4-5. AM1 calculated conformation of **4-5-d**.

R = H   **4-7-3**
R = t-butyl **4-7-4**

R = H   **4-7-1**
R = t-butyl **4-7-2**
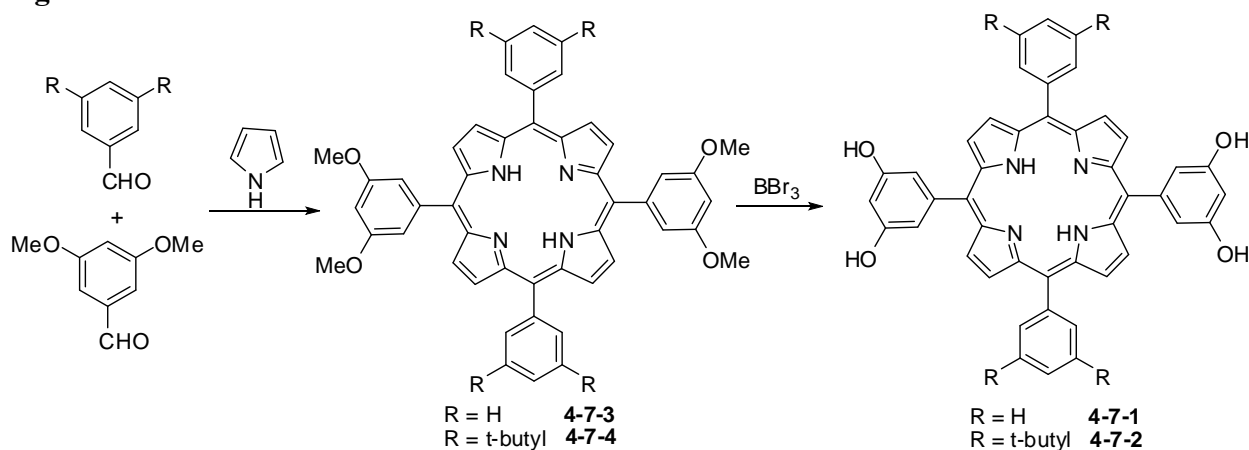
Scheme 4-7. Synthesis of tetrahydroxyporphyrins **4-7-1** and **4-7-2**.

provide a face-to-face structural arrangement for the porphyrin macrocycles and hydrogen-bond

synthons, therefore making these compounds suitable as model systems for PCET and hydrogen-

bond investigations. The preparation of **4-7-4** was achieved from a mixed aldehyde condensation
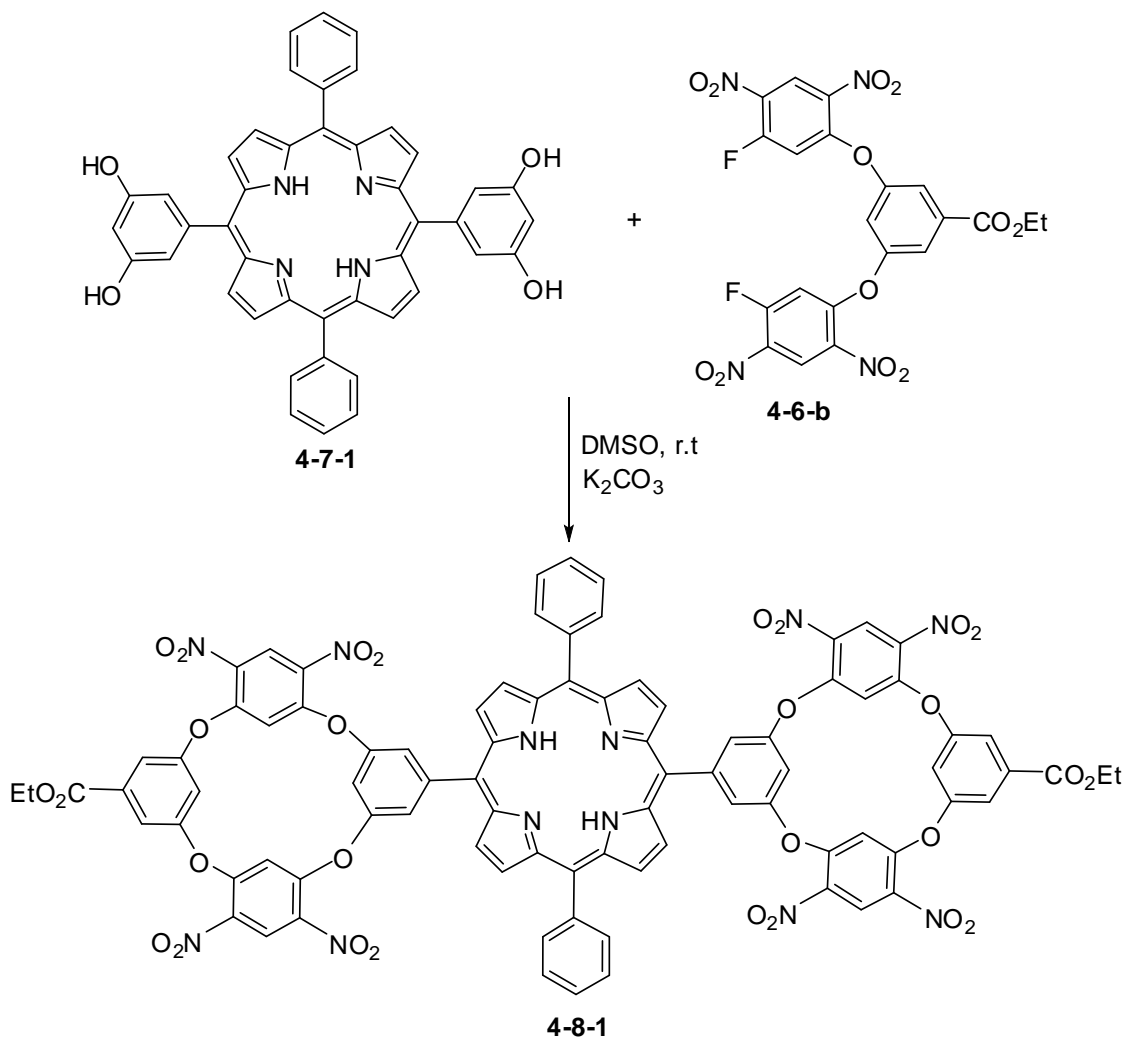
Scheme 4-8. Synthesis of symmetrical porphyrin-bisoxacalix[4]arene **4-8-1**.

similar to the preparation of **4-3-1**[36]. A mixture of 1 equivalent of 3, 5-dimethylbenzaldehyde, 1

equivalent of 3, 5-di-tert-butylbenzaldehyde and 2 equivalents of pyrrole was dissolved in dry

DCM. The reaction mixture was stirred for around 10 minutes under argon before adding a DCM

solution of 2.5 M $BF_3 \cdot OEt$. The reaction mixture was stirred under argon and in the dark. TLC

was used to follow this reaction. After addition of DDQ, the reaction mixture was left to stir for

an additional 45 minutes. After reducing the solvent under vacuum, the residue was applied to

silica gel column for separation, eluted with hexane/DCM. The third purple fraction was

collected. After removal of solvent under vacuum, **4-7-4** was obtained as a purple powder in
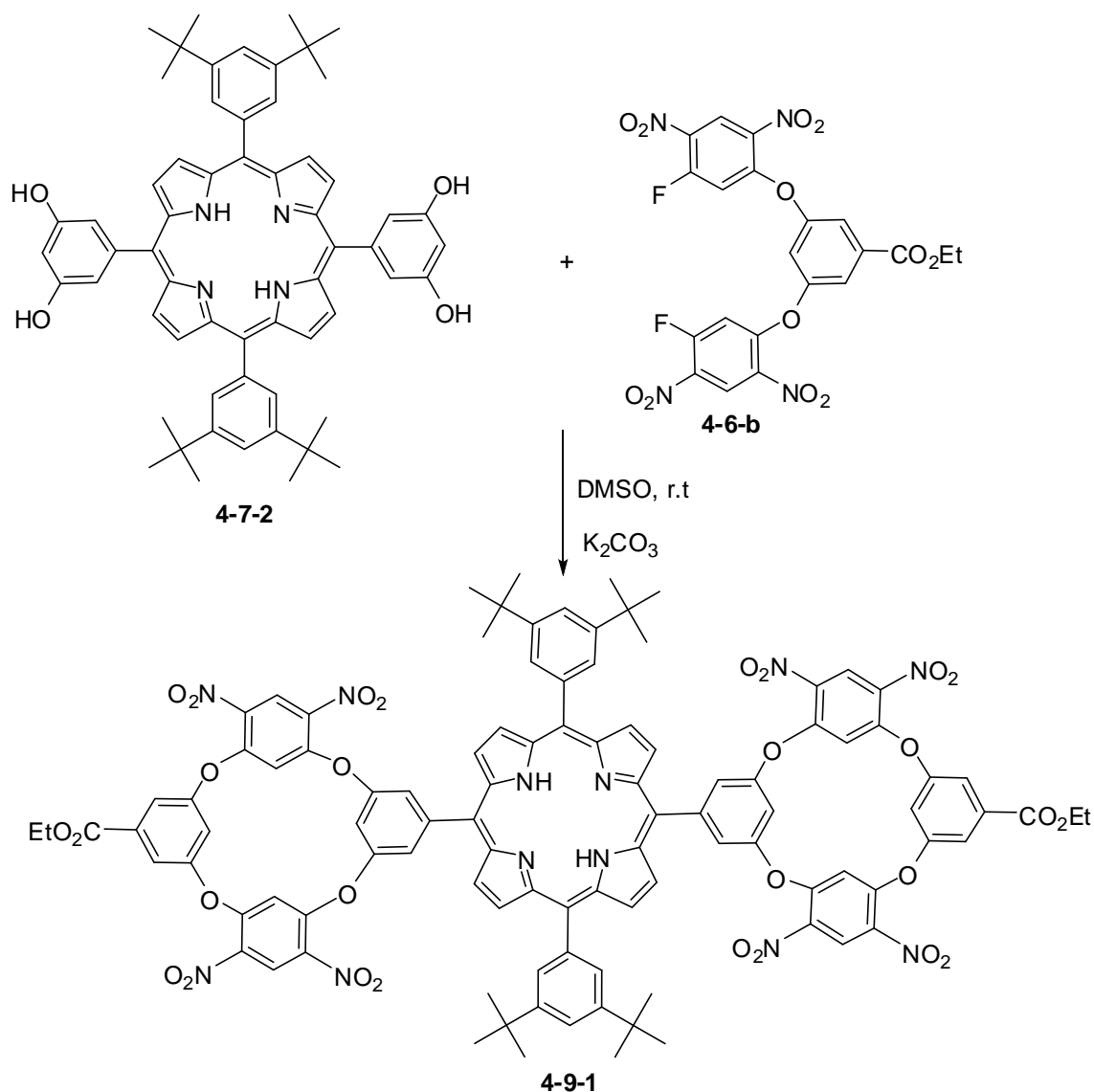
Scheme 4-9. Synthesis of symmetrical porphyrin-oxacalix[4]arene **4-9-1**.

7.9% yield. Compound **4-7-2** was obtained from the subsequent demethylation reaction using

BBr$_3$[35], similar to the demethylation of **4-3-2**, to generate **4-3-1**. Compound **4-7-1** was then used

for the subsequent preparation of bis(oxacalix[4]areno)porphyrin 5,15-di(3,5-

hydroxyphenyl)porphyrin **4-8-1**. This ring closure fragment coupling reaction was performed by

mixing 1 equivalent of **4-7-1** with 2 equivalents of linear trimer **4-6-b** and 6 equivalents of

K$_2$CO$_3$ in DMSO at room temperature under air for a period of 3 hours. Dilute 0.1 M aqueous

HCl was used to quench the reaction, followed by addition of ethyl acetate to extract the reaction

mixture from the water. The resulting organic phase was dried over anhydrous Na_2SO_4 and purified by alumina column chromatography using DCM/ethyl acetate (v/v = 100/1) as eluting solvents. After removal of the solvent under vacuum, the major product was obtained in 54% yield. Although MALDI-TOF mass spectroscopy gave a peak corresponding to the desired compounds **4-8-1**, and TLC always gave one spot for the desired compound, efforts to obtain a decent NMR spectrum for **4-8-1** failed. We attribute this to the poor solubility of this compound, which easily formed aggregates in most organic solvents. Meanwhile, we thought that it might also be attributed to rapid conformational changes of this compound in solution from which broad NMR signals were observed.

To solve this problem, we introduced bulky groups into the meso-position of porphyrins, to increase the solubility and help reduce aggregation. The generation of **4-9-1** was from a similar fragment coupling reaction as in the preparation of **4-8-1**, with the substitution of porphyrin **4-7-1** to **4-7-2**. The desired **4-9-1** was obtained as a purple powder in 84% yield. The presence of the four tert-butyl groups at the meso-position of porphyrin **4-7-2** induced high solubility of this compound in organic solvents, and its structure, was confirmed by HRMS (a molecular ion peak was observed at 1923.5460), UV–vis, fluorescence, and ^{1}H NMR spectroscopy. Based on the characteristic upfield chemical shifts observed in the ^{1}H NMR spectra of oxacalix[4]arenes for the interior protons on the electrophilic (NO_2-bearing) aromatic rings[28], it is believed that these compounds adopt 1,3-alternating structures in solution[20–33]. The photophysical properties of porphyrins **4-5-n** (n= a-e) and **4-9-1** are summarized in *Table 4-2*. The long wavelength absorption and fluorescence emission bands for all porphyrins except **4-5-d** were observed between 646–652 and 652–658 nm. The carboxyl group in porphyrin **4-5-d** is probably involved in intermolecular hydrogen-bonding, resulting in its distinct absorbance and

emission spectra compared with the other porphyrins, as well as its reduced fluorescence quantum yield (0.03). All other oxacalix[4]arene porphyrins showed quantum yields between 0.13 and 0.22.

Table 4-2. Spectral properties of porphyrins **4-5-n** (n = a–e) and **4-9-1** in degassed DCM at room temperature. [a] Excitation at 415 nm. [b] Calculated using 5,10,15,20-tetraphenylporphyrin as the standard.

Porphyrin	Absorption λ_{max} (nm)	Emission[a] λ_{max} (nm)	Fluorescence[b] quantum yield
4-5-a	418, 514, 548, 591, 647	652	0.13
4-5-c	418, 515, 550, 591, 652	658	0.15
4-5-b	418, 513, 548, 591, 649	652	0.13
4-5-e	417, 513, 548, 591, 646	655	0.17
4-5-d	418, 514, 548	600, 646	0.03
4-9-1	422, 518, 553, 592, 650	656	0.22

4. 3 Conclusions

An efficient and convenient stepwise fragment-coupling approach to the synthesis of unsymmetrical architectures composed of porphyrins and hydrogen-bond functionalities anchored to an oxacalix[4]arene spacer is reported. Spectroscopic data and computer calculations indicate that these oxacalix[4]arene porphyrins adopt 1,3-alternating conformations. These novel, high-yield syntheses of unsymmetrical oxacalix[4]arenes will find applications in supramolecular chemistry and in molecular design.

4. 4 Experiment

4.4.1 General

Silica gel (32–63 mm) was used for flash column chromatography. All reactions were monitored by TLC using 0.25 mm silica gel plates with or without UV indicator (60F-254). ^{1}H and ^{13}C NMR spectra were obtained on either a DPX-250 or a ARX-300 Bruker spectrometer.

Chemical shifts (δ) are given in ppm relative to CDCl$_3$ (7.27), acetone-d$_6$ (2.05), DMSO-d$_6$ (2.50) or THF-d$_8$ (1.73) as indicated. Electronic absorption spectra were measured on a Perkin Elmer Lambda 35 UV–vis spectrophotometer in the 300–800 nm wavelength region with 0.1 nm accuracy. Fluorescence spectra were measured on a Perkin Elmer LS55 spectrometer in the 500–800 nm wavelength region with 1 nm accuracy. The fluorescence quantum yields were measured using the standard method and 5,10,15,20-tetraphenylporphyrin as the standard (quantum yield is 0.11), according to the literature[41]. Mass spectra were obtained on Applied Biosystems QSTAR XL spectrometer. High-resolution mass spectra were obtained on a Q-TOF2 eletrospray at the mass spectrometry facility of Ohio State University. All solvents were obtained from Fisher Scientific (HPLC grade, Houston, TX) and used without further purification unless indicated. Acetone (reagent plus, phenol free, > 99.5%) and DMSO (Biotech grade solvent, 99.8%) were purchased from Sigma–Aldrich and used without further purification. K$_2$CO$_3$ was ground and dried at 140 ^{o}C. Compounds **4-d**[42] and **4-3-1**[35] were synthesized according to literature procedures. Solvents were dried according to literature procedures[43]. The computational simulations used the AM1 semiempirical Hamiltonian method[44] incorporated into the quantum mechanical Spartan program[45]. The coordinates used to build the porphyrins in this study were based on the X-ray crystal structure of **4-5-1**[33].

4.4.2 Syntheses

4.4.2.1 Aryl-containing Linear Trimer 4-6-a.

3,5-Dihydroxybenzaldehyde (**4-a**) (276.7 mg, 2.0 mmol) was mixed with 1, 5-difluoro-2, 4-dinitrobenzene (816.5 mg, 4.0 mmol) and K$_2$CO$_3$ (561.4 mg, 4 mmol) in 10 mL of acetone at room temperature under air. When the reaction was complete, acetone was removed under vacuum. The resulting residue was purified by silica gel column chromatography using

DCM/ethyl acetate (v/v = 20/1) for elution. After removal of the solvent under vacuum and washing with hexane (2×10 mL), pure linear trimer **4-6-a** was obtained as a white solid in 85% yield (860.0 mg). ^{1}H NMR (300 MHz, CDCl$_3$) δ 10.03 (s, 1H), 8.98 (s, 1H), 8.95 (s, 1H), 7.58 (d, 2H, J = 2.25 Hz), 7.30 (s, 1H), 7.06 (s, 1H), 7.02 (s, 1H). ESI-MS Calcd. for C$_{19}$H$_8$F$_2$N$_4$O$_{11}$ m/z 506.3, found: 506.5.

4.4.2.2 Aryl Containing Linear Trimer 4-6-b.

Ethyl 3,5-dihydroxybenzoate (**4-b**) (182.0 mg, 1 mmol) was mixed with 1,5-difluoro-2,4-dinitrobenzene (408.0 mg, 2 mmol) and K$_2$CO$_3$ (560.0 mg, 4 mmol) in 10 mL of acetone at room temperature under air. When the reaction was complete, acetone was removed under vacuum. The resulting residue was purified by silica gel column chromatography using DCM for elution. After removal of the solvent and washing with hexane (2×10 mL), linear trimer **4-6-b** was obtained as a white solid in 82% yield (451.0 mg). ^{1}H NMR (300 MHz, CDCl$_3$) δ 8.94 (s, 1H), 8.91 (s, 1H), 7.74 (d, 2H, J = 2.34 Hz), 7.19 (s, 1H), 6.96 (s, 1H), 6.92 (s, 1H), 4.39 (q, 2H), 1.38 (t, 3H). Anal. Calcd for C$_{21}$H$_{12}$F$_2$N$_4$O$_{12}$: C, 45.83; H, 2.20; N, 10.18. Found: C, 45.79; H, 2.26; N, 9.98. ESI-MS Calcd for C$_{21}$H$_{12}$F$_2$N$_4$O$_{12}$ m/z 550.3, found: 549.8.

4.4.2.3 Aryl Containing Linear Trimer 4-6-c.

Compound **4-c** (510.4 mg, 2 mmol) was mixed with 1,5-difluoro-2,4-dinitrobenzene (1.63 g, 8.0 mmol) and K$_2$CO$_3$ (2.21 g, 16 mmol) in 20 mL of acetone at room temperature under air. When the reaction was complete, acetone was removed under vacuum. The residue was purified by silica gel column chromatography using DCM to the mixture solvents of DCM/ethyl acetate (v/v = 20/1) for elution. After removal of the solvent under vacuum and washing with hexane (2×10 mL), linear trimer **4-6-c** was obtained as a white solid in 75% yield (935.0 mg). ^{1}H NMR (300

MHz, acetone-d_6) δ 8.93 (d, 2H, J = 7.67 Hz), 7.93 (m, 4H), 7.69 (s, 1H), 7.65 (s, 1H), 7.60 (d, 2H, J = 2.21 Hz), 7.48 (s, 1H). ESI-MS calcd for $C_{26}H_{11}F_2N_5O_{12}$ m/z 623.4, found: 623.8.

4.4.2.4 Porphyrin Conatining Linear Trimer 4-4-1.

5-(3,5-Dihydroxyphenyl)triphenylporphyrin (**4-3-1**) (32.8 mg, 0.05 mmol) was mixed with 1,5-difluoro-2, 4-dinitrobenzene (81.6 mg, 0.2 mmol) and K_2CO_3 (56.0 mg, 0.4 mmol) in 20 mL of acetone at room temperature under air. After the reaction was complete, acetone was removed under vacuum. The resulting residue was purified by silica gel column chromatography using the mixture solvents of DCM/hexane (v/v = 10/1) for elution. Pure linear trimer **4-4-1** was isolated in 80% yield (40.6 mg) after recrystallization from hexane and DCM. ^{1}H NMR (250 MHz, CDCl3) δ 8.84 (m, 6H), 8.68 (d, 2H, J¼2.37 Hz), 8.19 (m, 8H), 7.73 (m, 11H), 7.05 (m, 1H), 6.80 (m, 2H), -3.03 (s, 2H). HRMS (MALDI-TOF) Calcd for [M+H]$^+$ $C_{56}H_{33}F_2N_8O_{10}$ m/z 1015.2288, found: 1015.2265. UV–vis (DCM) λmax (log ε) 417 (5.84), 513 (4.47), 548 (4.03), 590 (3.85), 646 (3.58) nm.

4.4.2.5 Porphyrin 4-5-a.

Linear trimer **4-6-a** (50.1 mg, 0.1 mmol) was mixed with **4-3-1** (64.1 mg, 0.1 mmol) and K_2CO_3 (60.3 mg, 0.44 mmol) in 20 mL of DMSO at room temperature under air for 1 h (until TLC showed the complete disappearance of starting material). HCl (0.1 M, 40 mL) was used to quench the reaction. The water layer was extracted with 100 mL of ethyl acetate, and the organic layer was washed once with water and dried over anhydrous Na_2SO_4. The residue was purified by silica gel column chromatography using DCM for elution. Pure porphyrin **4-5-a** was obtained as a purple solid in 83% yield (92.1 mg) after recrystallization from DCM /hexane. ^{1}H NMR (250 MHz, THF-d_8) δ 10.07 (s, 1H), 8.98 (s, 2H), 8.84 (m, 6H), 8.66 (s, 2H), 8.20–8.21 (m, 6H), 8.13 (d, 2H, J = 2.10 Hz), 8.00 (d, 2H, J = 2.16 Hz), 7.81–7.82 (m, 9H), 7.64 (s, 1H), 7.52 (s, 1H),

6.77 (s, 2H), -2.76 (s, 2H). MALDI-TOF Calcd for $[M+H]^+$ $C_{63}H_{37}N_8O_{13}$ m/z 1114.0, found: 1114.0. HRMS (ESI) Calcd for $[M+H]^+$ $C_{63}H_{37}N_8O_{13}$ m/z 1113.2480, found:1113.2501. UV–vis (DCM) λmax (log ε) 418 (5.88), 514 (4.50), 548 (4.11), 591 (3.93), 647 (3.72) nm.

4.4.2.6 Porphyrin 4-5-b.

Linear trimer **4-6-b** (55.0 mg, 0.1 mmol) was mixed with **4-3-1** (64.6 mg, 0.1 mmol) and K_2CO_3 (56.0 mg, 0.44 mmol) in 20 mL of DMSO at room temperature under air (the reaction was considered complete after TLC showed the complete disappearance of the starting material). HCl (0.1 M, 40 mL) was used to quench the reaction. The water layer was extracted with 100 mL of ethyl acetate, and the organic layer was washed once with water and dried over anhydrous Na_2SO_4. The resulting residue was purified by silica gel column chromatography using DCM for elution. Pure porphyrin **4-5-b** was obtained as a purple solid in 86% yield (100.1 mg) after recrystallization from DCM / hexane. ^{1}H NMR (250 MHz, CDCl3) d 8.93 (s, 2H), 8.82 (m, 6H), 8.41 (s, 4H), 8.16 (m, 6H), 8.04 (d, 2H, J = 2.22 Hz), 7.99 (d, 2H, J = 2.22 Hz), 7.71 (m, 9H), 6.43 (s, 2H), 4.01 (q, 2H), 1.11 (m, 3H), -2.88 (s, 2H). MALDI-TOF Calcd for $C_{65}H_{40}N_8O_{14}$ m/z 1157.058, found: 1159.198. HRMS (MALDI-TOF) Calcd for $[M+H]^+$ $C_{65}H_{41}N_8O_{14}$ m/z 1157.2742, found: 1157.2787. HRMS (ESI) Calcd for $[M+H]^+$ $C_{65}H_{41}N_8O_{14}$ m/z 1157.2742, found: 1157.2799. UV–vis (DCM) λmax (log ε) 418 (5.89), 513 (4.51), 548 (4.09), 591 (3.88), 649 (3.76) nm.

4.4.2.7 Porphyrin 4-5-c.

Linear trimer **4-6-c** (63.3 mg, 0.1 mmol) was mixed with **4-3-1** (65.7 mg, 0.1 mmol) and K_2CO_3 (60.0 mg, 0.43 mmol) in 10 mL of DMSO at room temperature under air for 3 h (until TLC showed the complete disappearance of starting material). HCl (0.1 M, 40 mL) was used to quench the reaction. The water layer was extracted with 100 mL of ethyl acetate, and the organic

layer was washed once with water and dried over anhydrous Na_2SO_4. The residue was purified by silica gel column chromatography using DCM for elution. Pure porphyrin **4-5-c** was obtained as a purple solid in 83% yield (102.0 mg) after recrystallization from DCM/hexane. ^{1}H NMR (300 MHz, THF-d_8) δ 8.98 (s, 2H), 8.90 (br s, 2H), 8.82 (br s, 4H), 8.20 (br s, 4H), 8.17 (s, 3H), 8.14 (s, 3H), 7.79–7.81 (m, 9H), 7.63 (s, 2H), 7.56 (s, 1H), 7.35 (s, 1H), 6.95 (d, 4H, J = 2.55 Hz), 6.70 (s, 2H), -2.84 (s, 2H). MALDI-TOF Calcd for $[M+H]^+$ $C_{70}H_{40}N_9O_{14}$ m/z 1230.3, found: 1230.8. HRMS (ESI) Calcd for $[M+H]^+$ $C_{70}H_{40}N_9O_{14}$ m/z 1230.2694, found: 1230.2700. UV–vis (DCM) λmax (log ε) 418 (5.57), 515 (4.20), 550 (3.79), 591 (3.49), 652 (3.43) nm.

4.4.2.8 Bisporphyrin 4-5-1.

This compound was synthesized and characterized as previously reported[33].

4.4.2.9 Porphyrin 4-5-e.

Linear trimer **4-6-e** (20.3 mg, 0.02 mmol) was mixed with **4-3-1** (2.5 mg, 0.02 mmol) and K_2CO_3 (11.0 mg, 0.08 mmol) in 5 mL of DMSO at room temperature under air for 40 min. HCl (0.1 M, 20 mL) was used to quench the reaction. The water layer was extracted with 50 mL of ethyl acetate, and the organic layer was washed once with water and dried over anhydrous Na_2SO_4. The residue was purified by silica gel column chromatography using THF/hexane for elution. Porphyrin **4-5-e** was obtained in 20% yield (4.5 mg). ^{1}H NMR (300 MHz, THF-d_8) δ 9.95 (br s,1H), 9.06 (d, 2H, J = 3.90 Hz), 8.93 (s, 2H), 8.84 (s, 4H), 8.71 (d, 2H, J = 2.0 Hz), 8.20–8.28 (m, 6H), 8.13 (d, 2H, J = 4.58 Hz), 7.79–7.81 (m, 9H), 7.61 (s, 1H), 6.86 (s, 2H), 6.75 (s, 1H), 6.70 (d, 2H, J = 6.93 Hz), -2.75 (s, 2H). MALDI-TOF Calcd for $[M+H]^+$ $C_{62}H_{36}N_8O_{13}$ m/z 1102.0, found: 1103.3. HRMS (ESI) Calcd for $[M+H]^+$ $C_{62}H_{37}N_8O_{13}$ m/z 1101.2480, found: 1101.2545. UV–vis (DCM) λmax (logε) 417 (5.75), 513 (4.37), 548 (3.92), 591 (3.71), 646 (3.43) nm.

4.4.2.10 Porphyrin 4-5-d.

Hydrolysis of **4-5-d** was obtained by dissolving **4-5-b** (24.6 mg, 0.02 mmol) in 10 mL of THF, followed by addition of 4 M HCl (20 mL). The reaction mixture was refluxed at 60 ^{o}C in an oil bath for 3 days. After completion of the reaction, the mixture was extracted with ethyl acetate and the organic layer washed with brine. The resulting residue was purified by silica gel column chromatography using DCM/ethyl acetate (v/v = 20/1) for elution. Pure porphyrin **4-5-d** was obtained in 95% yield (21.5 mg) after recrystallization from DCM/hexane. ^{1}H NMR (300 MHz, THF-d$_8$) δ 8.97 (s, 1H), 8.93 (d, 2H, J = 4.40 Hz), 8.83 (s, 6H), 8.77 (s, 2H), 8.21 (m, 6H), 8.14 (d, 2H, J = 1.98 Hz), 8.03 (d, 2H, J = 2.06 Hz), 7.79 (d, 9H), 7.53 (s, 1H), 7.49 (s, 1H), 6.87 (s, 2H), -2.74 (s, 2H). MALDI-TOF Calcd for [M+H]$^{+}$ $C_{63}H_{37}N_8O_{14}$ m/z 1129.2, found: 1130.2. HRMS (ESI) Calcd for [M+H]$^{+}$$C_{63}H_{37}N_8O_{14}$ m/z 1129.2429, found: 1129.2405. UV–vis (DCM) λmax (log 3) 418 (5.43), 514 (3.90), 548 (3.32) nm.

4.4.2.11 5-(3, 5-Dihoxylphenyl)-10,15,20-triphenylporphyrin 4-7-1.

5-(3,5-Dimethoxyphenyl)-10,15,20-triphenylporphyrin **4-7-3** (400 mg, 0.6 mmol) and pyridine hydrochloride (10.0 g, 86 mmol) were added to a 100 mL round-bottom flask and heated to 220 °C in an oil bath. Upon the melting of pyridium hydrochloride at 170 °C, the solution turned green in color. TLC indicated the formation of the target porphyrin after 2 h reaction. Stirring was continued for an additional 4 h, whereupon TLC indicated that most of the starting materials had been consumed. The reaction was stopped and the mixture was cooled to room temperature. Then the reaction mixture was poured into 400 mL cold water and extracted with 400 mL ethyl acetate. The aqueous layer was extracted with ethyl acetate until colorless. The combined organic layers were washed twice with 0.1 M HCl aqueous solution and once with aqueous saturated NaHCO$_3$. After drying over anhydrous Na$_2$SO$_4$, the solvent was removed under

vacuum. The residue was separated on a silica gel column using chloroform/ethyl acetate 1:1 as eluting solvent. The major fraction was collected and was further purified by recrystallization from DCM hexane. After filtration and removal of the solvent under vacuum, porphyrin **4-7-1** was obtained in 84 % yield (160 mg). HRMS (MALDI-TOF) *m/z* 645.2272, calculated for $C_{44}H_{28}N_4O_2$ 645.2290. ^{1}H-NMR (DMSO-d$_6$) δ 9.92 (s, 1H), 9.77 (s, 1H), 9.22 (d, 1H, *J* = 4.3 Hz), 8.54 (d, 1H, J = 4.9 Hz), 8.28 (d, 1H, J = 3.6 Hz), 8.24 (d, 1H, J = 3.6 Hz), 8.16 (d, 1H, *J* = 4.4 Hz), 8.12 (d, 1H, J = 4.5 Hz), 8.03 (m, 6H), 7.78 (m, 9H), 7.22 (s, 1H), 7.08 (s, 1H), 5.95 (s, 1H), -0.16 (s, 2H). UV-Vis (DCM) λmax (log ε) 422 (4.9), 455 (4.8), 486 (4.7), 583 (3.7), 640 (3.7), 683 (3.6) nm.

4.4.2.12 5,15-Di(3,5-dihydroxyphenyl)-10,20-di(3,5-ditert-butylphenyl)porphyrin 4-7-2.

3,5-Dimethylbenzaldehyde (0.83 g, 5.0 mmol), 3,5-di-tert-butylbenzaldehyde (1.09 g, 5.0 mmol), and pyrrole (0.70 mL, 10 mmol) were mixed in a 2 L flask. Dry DCM (1000 mL) was added and the solution was stirred for 10 min under argon before 0.4 mL of 2.5 M BF$_3$·OEt in DCM was added. The reaction mixture was stirred under argon and in the dark for 2 h. DDQ (1.64 g) was added and the mixture was stirred for 45 min. The reaction mixture was concentrated to give a residue that was purified by silica gel column chromatography using a mixture of hexane and DCM for elution. The third eluted purple fraction contained 5,15-di(3,5-dimethoxyphenyl)-10,20-di(3,5-di-tert-butylphenyl)porphyrin. The solvent was removed under vacuum to give 192 mg (7.9% yield) of this porphyrin **4-7-4** as a purple powder. MALDI-TOF Calcd for [M+H]$^+$ $C_{64}H_{71}N_4O_4$ m/z 960.25, found: 960.17. ^{1}H NMR (CDCl$_3$) d 9.07 (d, 4H, J = 4.70 Hz), 9.01 (d, 4H, J = 4.70 Hz), 8.20 (d, 4H, J = 1.68 Hz), 7.91–7.90 (m, 2H), 7.53 (d, 4H, J = 2.24 Hz), 6.97–6.99 (m, 2H), 1.63 (s, 36H), -2.63 (s, 2H). To a solution of 5, 15-di (3,5-dimethoxyphenyl)-10,20-di(3,5-di-tert-butylphenyl)porphyrin **4-7-4** (0.096 g, 0.1 mmol) in dry

DCM (20 mL) at -20 °C was added dropwise a solution of BBr$_3$ (0.3 mL, 3.1 mmol) in DCM (1 mL) with vigorous stirring under argon over a period of 30 min. The reaction mixture was stirred at room temperature for a period of 24 h and then poured into water and extracted with ethyl acetate (3×50 mL). The combined organic layers were washed successively with brine and aqueous NaHCO$_3$ solutions. The organic solution was dried over Na$_2$SO$_4$ and evaporated to dryness, giving the title porphyrin **4-7-2** as purple crystals in 91.6% yield (82.7 mg, 0. 092 mmol). MALDI-TOF Calcd for [M+H]$^+$ C$_{60}$H$_{63}$N$_4$O$_4$ m/z 904.14, found: 904.21. ^{1}H NMR (CD$_2$Cl$_2$) δ 9.04 (d, 4H, J = 4.80 Hz), 8.90 (d, 4H, J = 4.75 Hz), 8.70 (s, 4H), 8.15 (d, 4H, J = 1.81 Hz), 7.96–7.94 (m, 2H), 7.26 (d, 4H, J = 2.18 Hz), 6.84–6.82 (m, 2H), 1.56 (s, 36H), -2.75 (s, 2H).

4.4.2.13 Porphyrin 4-9-1.

5,15-Di(3,5-dihydroxyphenyl)-10,20-di(3,5-di-tert-butylphenyl)porphyrin **4-7-2** (36.1 mg, 0.04 mmol) was mixed with linear trimer **4-6-b** (44.0 mg, 0.08 mmol) and K$_2$CO$_3$ (33.6 mg, 0.24 mmol) in 10 mL of DMSO at room temperature under air for 3 h. Dilute HCl (0.1 M × 40 mL) was used to quench the reaction and ethyl acetate (2×25 mL) was used to extract the water layer. The resulting organic phase was dried over anhydrous Na$_2$SO$_4$ and purified by alumina column chromatography using DCM/ethyl acetate (v/v = 100/1) for elution. Porphyrin **4-9-1** was obtained in 84% yield (64.7 mg). ^{1}H NMR (250 MHz, CDCl$_3$) δ 8.95 (br s, 8H), 8.46 (br s, 4H), 8.09 (s, 4H), 8.05 (d, J = 1.86 Hz, 4H), 8.02 (d, J = 1.82 Hz, 4H), 7.92 (s, 2H), 7.25 (br s, 4H), 6.49 (s, 4H), 3.98–4.06 (m, 4H), 1.56 (s, 36H), 1.27 (t, 6H). MALDI-TOF Calcd for [M+H]$^+$ C$_{102}$H$_{83}$N$_{12}$O$_{28}$ m/z 1923.5, found: 1923.1. HRMS (ESI) calcd for [M+H]$^+$ C$_{102}$H$_{83}$N$_{12}$O$_{28}$ m/z 1923.5440, found: 1923.5460. UV–vis (DCM) λmax (log ε) 422 (5.79), 518 (4.40), 553 (4.08), 592 (3.87), 650 (3.85) nm.

4.4.2.13 Molecular Structures.

The crystal structure of linear trimer **4-6-b** was determined using data collected at T = 150 K to q =31.5 with Mo Ka radiation on a Nonius KappaCCD diffractometer. The X-ray crystallographic data for **3c** can be found in supplementary publication CCDC-626294 available from the Cambridge Crystallographic Data Centre.

4.5 References

1   Dismukes, G. C. *Science* **2001**, *292*, 447.

2   Tommos, C.; Babcock, G. T. *Acc. Chem. Res.* **1998**, *31*, 18.

3   Yocum, C. F.; Pecoraro, V. L. *Curr. Opin. Chem. Biol.* **1999**, *3*, 182.

4   (a) Dawson, J. H. *Science* **1988**, *240*, 433; (b) Sono, M.; Roach, M. P.; Coulter, E. D.; Dawson, J. H. *Chem. Rev.* **1996**, *96*, 2841.

5   Ozaki, S.-I.; Roach, M. P.; Matsui, T.; Watanbe, Y. *Acc. Chem. Res.* **2001**, *34*, 818.

6   Chang, C. J.; Chng, L. L.; Nocera, D. G. *J. Am. Chem. Soc.* **2003**, *125*, 1866.

7   Mims, M. P.; Porras, A. G.; Olson, J. S.; Noble, R.W.; Peterson, J. A. *J. Biol. Chem.* **1983**, *258*, 14219.

8   Rohlfs, R. J.; Mathaws, A. J.; Carver, T. E.; Olson, J. S.; Springer, B. A.; Egeberg, K. D.; Sligar, S. G. *J. Biol. Chem.* **1990**, *265*, 3168.

9   Momenteau, M.; Reed, C. A. *Chem. Rev.* **1994**, *94*, 659.

10 Chang, C. K.; Kondylis, M. P. *J. Chem. Soc., Chem. Commun.* **1986**, 316.

11 Chang, C. J.; Brown, J. D. K.; Chang, M. C. Y.; Baker, E. A.; Nocera, D. G. *Electron Transfer in Chemistry*; Balzani, V., Ed.; Wiley-VCH: Weinheim, Germany, **2001**; Vol. *3.2.4*, pp 409.

12 (a) Deng, Y.; Roberts, J. A.; Peng, S.-M.; Chang, C. K.; Nocera, D. G. *Angew. Chem., Int. Ed.* **1997**, *36*, 2124; (b) Cukier, R. I.; Nocera, D. G. *Annu. Rev. Phys. Chem.* **1998**, *49*, 337.

13 Chang, C. K.; Liang, Y.; Aviles, G. *J. Am. Chem. Soc.* **1995**, *117*, 4191.

14 Liu, S. Y.; Nocera, D. G. *J. Am. Chem. Soc.* **2005**, *127*, 5278.

15 (a) Yeh, C. Y.; Chang, C. J.; Nocera, D. G. *J. Am. Chem. Soc.* **2001**, *123*, 1513; (b) Chang, C. J.; Yeh, C. Y.; Nocera, D. G. *J. Org. Chem.* **2002**, *67*, 1403; (c) Chng, L. L.; Chang, C. J.; Nocera, D. G. *Org. Lett*. **2003**, *5*, 2421.

16 Zhang, X. X.; Lippard, S. J. *J. Org. Chem*. **2000**, *65*, 5298.

17 Liang, Y.; Chang, C. K. *Tetrahedron Lett*. **1995**, *36*, 3817.

18 Chang, C. K.; Bag, N.; Guo, B. M.; Peng, S. M. *Inorg. Chim. Acta* **2003**, *351*, 261.

19 Arimura, T.; Brown, C. T.; Springs, S. L.; Sessler, J. L. *Chem. Commun*. **1996**, 2293.

20 König, B.; Fonseca, M. H. Eur. J. *Inorg. Chem.* **2000**, 2303.

21 Lhoták, P. Eur. *J. Org. Chem.* **2004**, 1675.

22 Chambers, R. D.; Hoskin, P. R.; Kenwright, A. R.; Khalil, A.; Richmond, P.; Sandford, G.; Yufit, D. S.; Howard, J. A. K. *Org. Biomol. Chem.* **2003**, *1*, 2137.

23 Li, X.; Upton, T. G.; Gibb, C. L. D.; Gibb, B. C. *J. Am. Chem. Soc.* **2003**, *125*, 650.

24 (a) Wang, M.-X.; Yang, H.-B. *J. Am. Chem. Soc.* **2004**, *126*, 15412; (b) Wang, M.-X.; Zhang, X.-H.; Zheng, Q.-Y. *Angew. Chem., Int. Ed.* **2004**, *43*, 838.

25 Yang, F.; Yan, L.; Ma, K.; Yang, L.; Li, J.; Chen, L.; You, J. *Eur. J. Org. Chem.* **2006**, 1109.

26 Sommer, N.; Staab, H. A. *Tetrahedron Lett.* **1966**, *25*, 2837.

27 Lehmann, F. P. A. *Tetrahedron* **1974**, *30*, 727.

28 Gilbert, E. E. *J. Heterocycl. Chem.* **1974**, *11*, 899.

29 Bottino, F.; Foti, S.; Pappalardo, S. *Tetrahedron* **1976**, *32*, 2567.

30 (a) Katz, J. L.; Feldman, M. B.; Conry, R. R. *Org. Lett.* **2005**, *7*, 91; (b) Katz, J. L.; Geller, B. J.; Conry, R. R. *Org. Lett.* **2006**, *8*, 2755; (c) Katz, J. L.; Selby, K. J.; Conry, R. R. *Org. Lett.* **2005**, *7*, 3505.

31 Maes, W.; Rossom, W. V.; Hecke, K. V.; Meervelt, L. V.; Dehaen, W. *Org. Lett.* **2006**, *8*, 4161.

32 Konishi, H.; Tanaka, K.; Teshima, Y.; Mita, T.; Morikawa, O.; Kobayashi, K. *Tetrahedron Lett.* **2006**, *47*, 4041.

33 Hao, E.; Fronczek, F. R.; Vicente, M. G. H. *J. Org. Chem*. **2006**, *71*, 1233.

34 For reversibility in thiocalixarene formation by nucleophilic substitution, see: Freund, T.; Kübel, C.; Baumgarten, M.; Enkelmann, V.; Gherghel, L.; Reuter, R.; Müllen, K. Eur. *J. Org. Chem.* **1998**, *63*, 555.

35 Tanaka, T.; Endo, K.; Aoyama, Y. *Bull. Chem. Soc. Jpn*. **2001**, *74*, 907.

36 Lindsey, J. S.; Schreiman, I. C.; Hsu, H. C.; Kearney, P. C.; Marguerettaz, A. M. *J. Org. Chem.* **1987***, 52*, 827.

37 Jollife, K. A.; Langford, S. J.; Oliver, A. M.; Shephard, M. J.; Paddon-Row, M. N. *Chem.-Eur. J.* **1999**, *5*, 2518.

38 Parusel, A. *J. Mol. Model*. **1998**, *4*, 366.

39 Hermann, D. T.; Schindler, A. C.; Polborn, K.; Gompper, G.; Stark, S.; Parusel, A.; Grabner, G.; Kohler, G. *Chem.-Eur. J.* **1999**, *5*, 3208.

40 Odobel, F.; Suresh, S.; Blart, E.; Nichlas, Y.; Quintard, J.-P.; Janvier, P.; Questel, J.-Y.; Illien, B.; Rondeau, D.; Richomme, P.; Haupl, T.; Wallin, S.; Hammarstrom, L. *Chem.-Eur. J.* **2002**, *8*, 3027.

41 Fery-Forgues, S.; Lavabre, D. *J. Chem. Educ.* **1999**, *76*, 1260.

42 Thorn, M. A.; Denny, G. H.; Babson, R. D. *J. Org. Chem.* **1975**, *40*, 1556.

43 Perrin, D. D.; Armarego, W. L. F. *Purification of Laboratory Chemicals*, 3rd ed.; Pergamon: Oxford, **1988**.

44 Dewar, M. J. S.; Zoebisch, E. G.; Healy, E. F.; Stewart, J. J. P. *J. Am. Chem. Soc*. **1985**, *107*, 3902.

45 Spartan, version 2.0; Wavefunction: Irvine, CA, **2001**.

CHAPTER 5. TOTAL SYNTHESIS OF PORPHYCENES AND IMPROVED SYNTHESIS OF 2,2'-BIPYRROLES

5.1 Introduction

"Photofrin" is the only sensitizer that is approved by the FDA for use in PDT. As a sensitizer consisting of a mixture of hematoporphyrin-derivatives, it is hard to study the relationship between individual components and the overall activity[1]. Thus, many new porphyrin based photosensitizers have been developed and their PDT efficiency had been tested[2], many being in clinical trials. The major issue limiting the wide application of porphyrin based sensitizers in PDT is their weak absorptions in the phototherapeutic windows. Thus many chromophore-extended porphyrins have been developed to overcome this problem, as described in *Chapter 3*. Lately, modification of porphyrin backbone to generate its various isomers has also been widely studied[3]. Among those, porphycene (see *Figure 5-1*) has attracted increasing research interests.
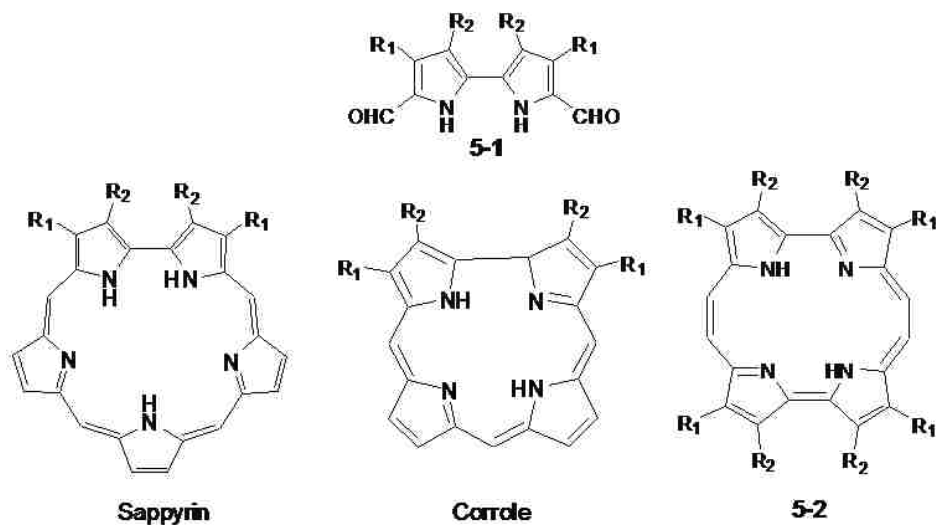
Figure 5-1. Chemical structure of 5,5'-diformyl-2,2'-bipyrrole (**5-1**), porphycene (**5-2**) sappyrin and corrole.

Porphycenes are isomeric with porphyrins. It was first synthesized by Vogel and coworkers as a novel aromatic macrocyle in 1986[4]. Soon after the first synthesis, it was found that porphycenes gave strong absorption bands above 600 nm, where light has the highest

penetration into tissue. Furthermore, porphycene can efficiently generate singlet oxygen upon radiation with light, in response to the generation of a photodynamic effect in tissues. Compared with porphyrins, the uptake of most available porphycenes shows high efficiency and is usually accomplished within 2 hours, while it can take between 24 to 48 hours for Photofrin be taken up[5]. Subsequent *in vivo* studies of the PDT efficiency of porphycenes was very successful. For example, the porphycenes tested were between 17 to 220 times more efficient than the currently approved sensitizer Photofrin[6], which made this type of porphyrin isomer very promising as photosensitizers in the PDT treatment of cancers.
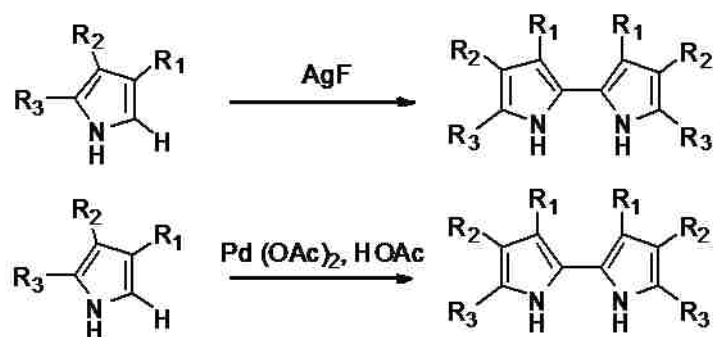
Scheme 5-1. Common oxidative coupling reactions to achieve 2,2'-bipyrroles.

The efficient synthesis of porphycenes remains a big challenge. Porphycene[6-8] synthesis involves the preparations of a key synthetic precursor - 5,5'-diformyl-2,2'-bipyrroles (**5-1**), which also serves as a key synthetic precursor in the preparation of sapphyrins[9] and other expanded porphyrin analogs[10]. Since the preparation of porphycene was achieved from the reductive coupling of **5-1** through one-step McMurry reaction[4,6-8], we envisioned that the efficient synthesis of **5-1** could lead to improved synthetic efficiency for porphycenes.

The 2,2'-bipyrrole motif occurs in a number of polypyrrole pigments, many of which have attracted increasing attention in coordination chemistry, medicinal chemistry and in material science[11]. Available synthetic methods for 2,2'-bypyrroles are limited[6,8-9,12-13] to

oxidative coupling and reductive coupling methodologies (see *Scheme 5-1*). Oxidative coupling[12] works only in a limited number of cases and often in low yield, so reductive couplings are preferred[6,8-9,13]. Among those, the Ullmann reaction are usually the most widely used method for access to 2,2'-bypyrroles. Due to the drastic conditions of the Ullmann coupling reaction, sensitive substituents (such as formyl groups), can not be carried through intact; thus, direct access to **5-1** (see *Figure 5-1*) is not possible. Since the original preparation of **5-1** by Vogel and coworkers[6,8] during their synthesis of porphycene **5-2**, only a few variants of the seminal synthetic methodology have been described[6,8,13]. All except one[14] are based on the Ullmann-type dimerization of a preformed halopyrrole (see *Scheme 5-1*).
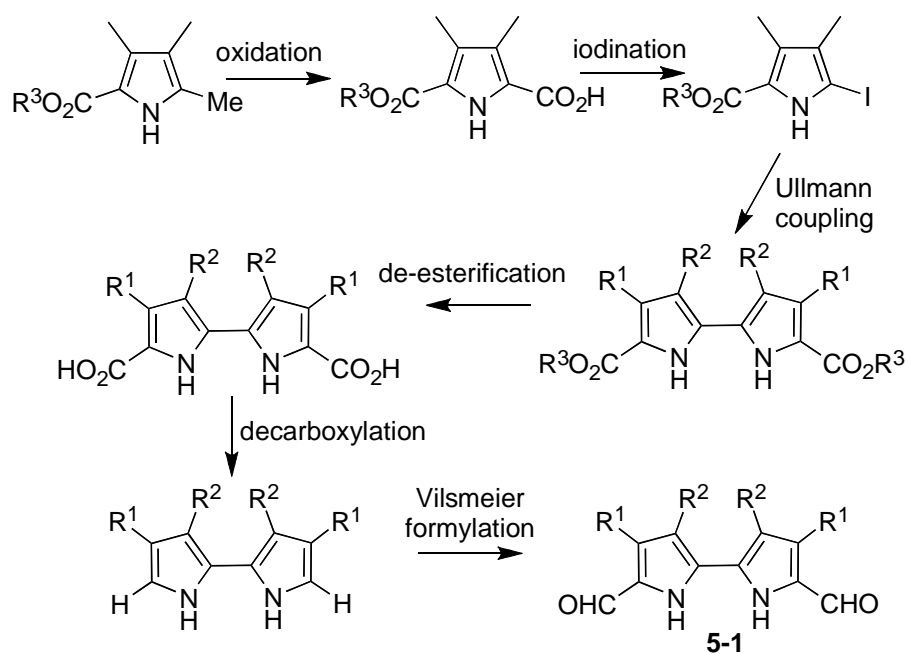
Scheme 5-2. Previous methodologies for synthesis of 5,5'-diformyl-2,2'-bipyrrole **5-1**.

Synthesis of **5-1**, as reviewed in detail in the literature[14], normally requires four key steps (see *Scheme 5-2*): (1) Ullmann coupling of a 2-iodopyrrole-5-carboxylic ester, (2) hydrolysis of the ester, (3) decarboxylation of the resulting 5-carboxylic acid, and (4) Vilsmeier-type

diformylation. The Ullmann synthesis of biaryls by the copper-induced reductive coupling of aromatic halides is of broad synthetic use[15a]. Although some substrates will undergo Ullmann reductive coupling under mild conditions, the typical Ullmann coupling is conducted at high temperature[15b]. Generally, Ullmann-type reductive coupling of pyrroles works well only when there is an electron-withdrawing group present; high temperature is usually required[15b].
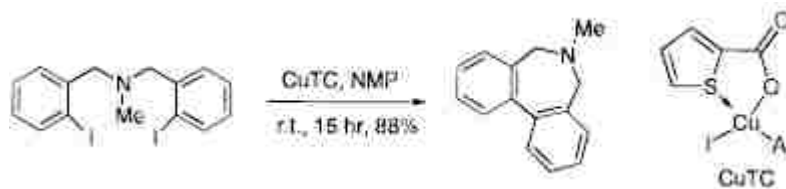
Scheme 5-3. Example of ambient temperature Ullmann-type coupling reaction.

Recently, Liebeskind and coworkers reported an ambient temperature Ullmann-type coupling reaction[15c], but the requirement of specific type of substrates or specific positions of the substitutent limits its synthetic application (see *Scheme 5-3*). They stated that "The most noticeable limitation of this process is the lack of reaction of aromatic halide substrates not possessing a coordinating ortho-substituent" [15c].

R_1	R_2	Yield (%)
Me	Me	65
Me	Et	78
CO_2Et	Me	83
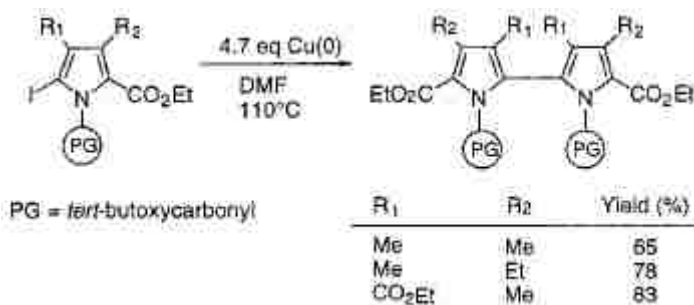
Scheme 5-4. Examples of akyl-substituted 2,2'-bipyrroles from a N-protected monopyrrole.

Sessler et al.[13a] developed an efficient procedure for the preparation of alkyl-substituted 2,2'-bipyrroles by protection of the pyrrole nitrogen atom before an Ullmann-type coupling reaction; this was followed by deprotection of the resulting N-substituted 2,2'-bipyrroles. Vogel[13b] et al. later improved the Sessler method by changing the solvent from DMF to toluene

(see *Scheme 5-4*). Meanwhile, the decarboxylation step – usually a sublimation - involved high temperature to which the unstable 2,2-di-unsubstituted bipyrrole was somewhat incompatible. This limited the scale up synthesis of the 5,5'-diformyl-2,2'-bipyrrole (the porphycene precursor). Although some improvements were made by avoiding the intermediate sublimation[6,8], still the precursor generated for Vilsmeier di-formylation is very unstable, and this has limited the generality of the reaction scheme. Since the nature of substituents on the pyrrole system greatly influences the performance of the literature reactions, thus precluding the synthesis of some attractive target compounds, the total number of compounds **5-1** is still very limited.

The above synthetic limitations encouraged us to develop new expedited methodology for the synthesis of compound **5-1**. The relatively harsh conditions required in the copper-catalyzed Ullmann type reaction prevented its wide application for the synthesis of functionalized bipyrroles. Inspired by the rapidly developing field of metal-catalyzed coupling reactions, and especially some recently developed palladium-catalyzed couplings of aryl halides under mild conditions[16-17], we decided to try different metals (other than copper) for coupling of iodopyrroles.
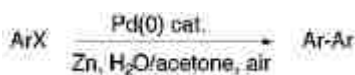
Scheme 5-5. Examples of room temperature Pd-C catalyzed biaryl coupling reaction in the presence of water.

The use of palladium-catalyzed reductive couplings in carbon-carbon bond forming reactions has attracted considerable attention in modern synthetic organic chemistry[18a-e]. These include the Stille coupling[18b], the Suzuki-coupling[18c], the Heck reaction[18d] and the Sonogashira coupling[18e] reactions, to name only a few. Early usage of Pd-C as the catalyst for the Ullmann coupling, under phase-transfer conditions, required refluxing at 100 °C, but the high temperature for this reaction limits its application in the synthesis of biaryls processing functional groups[18].

Recently, Pd-C co-catalyzed biaryl synthesis was reported to take place at room temperature (see *Scheme 5-5*) by simply adding water into the reaction system[17]. Meanwhile 2-formyl-5-iodopyrroles have been used in Sonogashira coupling reactions (see *Scheme 5-6*) with TMS-acetylene to build acetylenic and diacetylenic diformyldipyrroles[19].
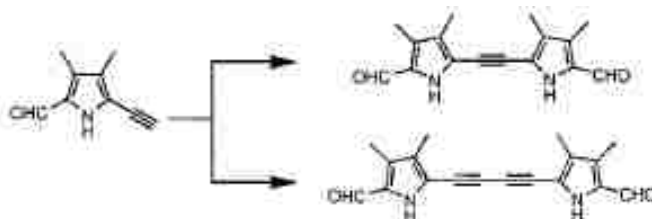
Scheme 5-6. Examples of 2-formyl-5-iodopyrroles directly used in the coupling reaction.

5.2 Results and Discussion

5.2.1 Total Synthesis of Porphycene (CpoTMPn)
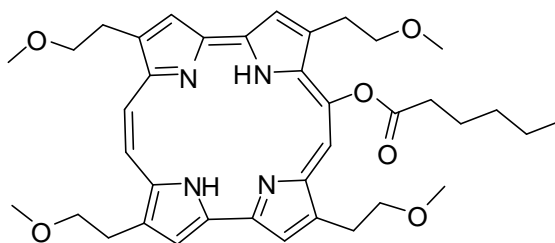
Figure 5-2. Chemical structure of CpoTMPn.

Porphycenes containing two or four methoxyethyl side chains, such as CpoTMPn (see *Figure 5-2*), are able to enhance and accelerate cellular uptake[6]. The membrane solubility of photosensitizers is assumed to be critical in their photodynamic efficiency. The presence of nonionic polar side chains in CpoTMPn was found to be able to strongly enhance cellular uptake and antitumor activity of porpycenes[3,6, 20].

The total synthesis followed the procedures reported by Vogel et al.[21] and Richert, et al.[6, 22] but with small modifications (see *Scheme 5-7* through *Scheme 5-10*). The synthesis of diketone **5-7-2** involved the preparation of activated metal zinc. The metal zinc activation was

achieved by adding 3M HCl ito the metal dust with stirring by glass rod. It was then poured into

a filter funnel and washed with water, ethanol and diethyl ether in that exact sequence. Then the

zinc dust was dried in an oven under vacuum. After crushing into fine powder, it was kept in the

oven under vacuum before use in subsequent reactions.
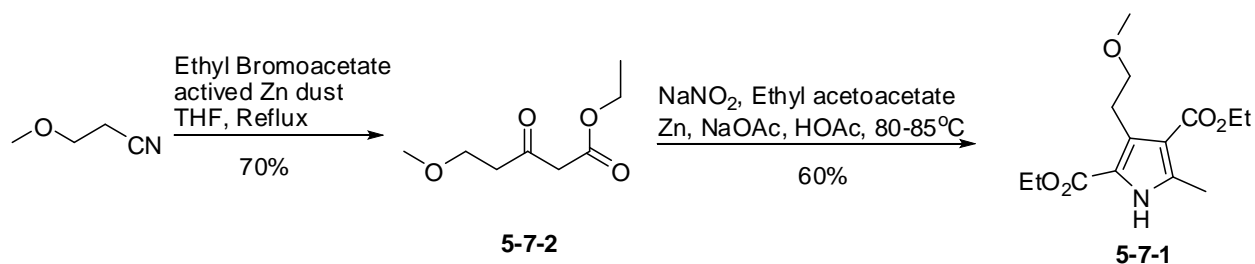
Scheme 5-7. Synthesis of pyrrole **5-7-1** from classical pyrrole synthesis – the Knorr reaction.

The preparation of **5-7-2** was achieved by reacting methoxylpropionitile with ethyl

bromoacetate in the presence of activated zinc powder in freshly distilled THF under argon (see

Scheme 5-7). After workup, the residue, a reddish liquid, was distilled under reduced pressure.

The desired compound **5-7-2** was collected in the 95~110°C temperature range in 70% yield as a

colorless aromatic liquid. It was found that high temperature should be avoided because the

desired compound was destroyed at high temperature, giving a highly sticky deep red gel.

Compound **5-7-1** was synthesized from **5-7-2** in two steps[23]: 1) the formation of oxime; 2)

the Knorr reaction to form pyrrole. The formation of the oxime was achieved from reacting of **5-7-2** with NaNO$_2$ in HOAc as solvent. This process needed to be extremely slow to avoid the

generation of toxic NOx gas. TLC is strongly recommended to follow this reaction. The TLC

eluting solvent was hexane/EtOAc (3/1). It should be noticed that the intermediate oxime was

more polar than desired **5-7-1**, which showed polarity similar to the starting material **5-7-2**. The

Knorr condensation reaction was performed at temperature between 80~85°C. A water bath was

strongly recommended rather than an oil-bath. The main reason was the thermal sensitivity of

this reaction and the strict temperature control required in order to achieve high yield. This

condensation reaction could release large amount of heat during a short period, the use of a hot water bath provided great control of the temperature by constant addition of ice during the reaction process. Also it was important to have zinc always in excess throughout the reaction, which was easily achieved by always allowing excess zinc powder in sight throughout the addition of oxime. When TLC indicated the disappearance of oxime, the reaction was stopped. Recrystalization from ethanol water gave **5-7-1** in 60% yield as a yellowish powder.
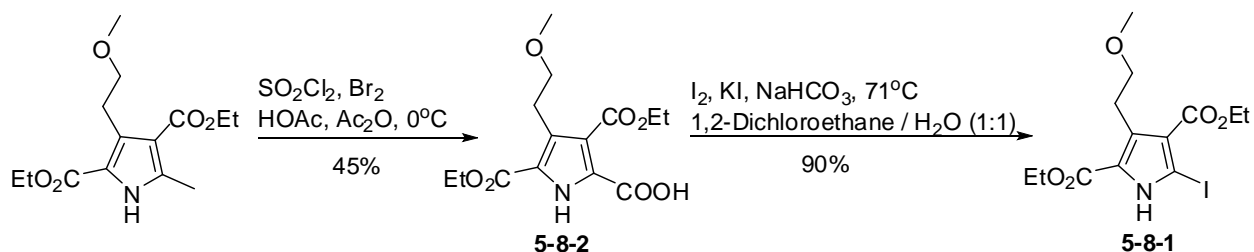
Scheme 5-8. Halogenation, hydrolysis, decarboxylative and iodination of monopyrrole to generate **5-8-1**.

The synthesis of **5-8-1** was achieved from the oxidation of **5-7-1** followed by iodination reaction as shown in *Scheme 5-8*[23a]. The preparation of **5-8-2** from **5-7-1** involved two steps: the oxidation and then the hydrolysis. In the oxidation step, the solution of **5-7-1** was placed in an ice-bath and stirred at 0 °C. If the temperature was higher than 0 °C, the intermediate would be hydrolyzed by HOAc during the oxidation process, which would resulted in incomplete oxidation and also ester formation, thus lowering the yield of the desired acid. In the hydrolysis step, the acetone/water (v/v = 4/1) was used as solvent and the reaction was performed at refluxing temperature. The use of this mixture solvent system gave advantages over the use of aqueous solution. With the evaporation of acetone, the remaining product was able to separate over the water layer as an oil form. Solid $NaHCO_3$ was added into the mixture solution for hydrolysis instead of saturated aqueous solution of it. After workup, the resulting fine solid was filtered and **5-8-2** was obtained in 45% yield. The iodination of **5-8-2** to generate **5-8-1** was

performed in the mixture solvents of 1,2-dichloroethane/water with the mixture of I_2/KI as the

iodination reagent. When the reaction was stopped, $Na_2S_2O_3$ was added to the reaction mixture in

portions to remove excess iodine. After removal of the solvent under vacuum, the desired

product **5-8-1** was achieved in 90% yield.
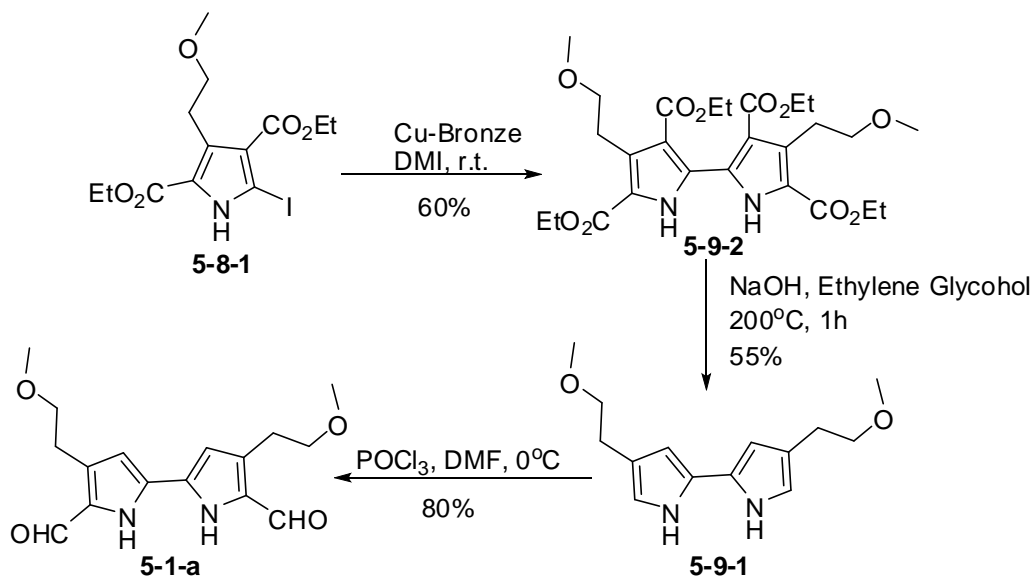
Scheme 5-9. Synthesis of 5,5'-diformyl-2,2'-bipyrroles **5-1-a**.

The preparation of **5-1-a** involved the 1) Ullmann-coupling reaction, 2) the

decarboxylation reaction and 3) Vilsmeier formylation reaction (see *Scheme 5-9*). The Ullmann-

coupling reaction was performed in DMI at room temperature with Cu-bronze as the coupling

reagent, under argon. The reaction mixture was a suspended solution with greenish-brown color.

TLC showed a strong blue luminous spot under UV-radiation (366 nm). After workup, the

solvents was removed under vacuum, the residue was recrystallized from ethanol. After filtration,

the desired **5-9-2** was obtained as colorless needles in 60% yield.Following the formation of **5-9-

2**, hydrolysis to form the carboxylic acid was performed in ethylene glycol at 200 °C with NaOH

as the base, under argon. TLC was used to follow the hydrolysis reaction. When TLC indicated

the completion of decarboxylation, the reaction mixture was poured into water and extracted

with DCM. The formylation reaction used dry DMF as solvent; thus it was in excess amount.

After workup, 44% of **5-1-a** was obtained from recrystallization from THF.
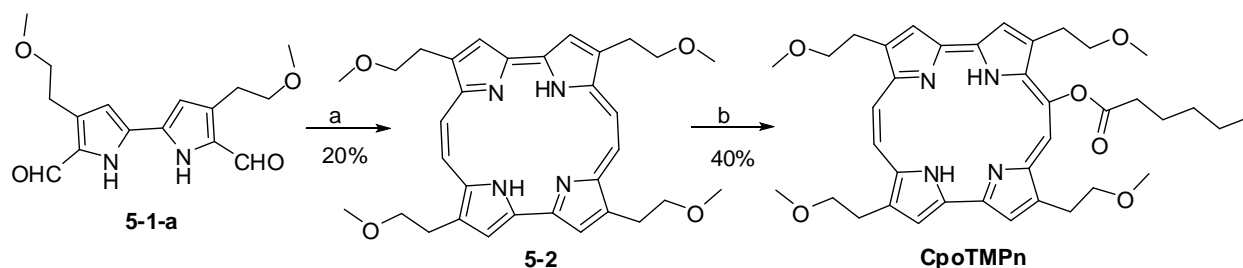
Scheme 5-10. Synthesis of CpoTMPn. Reaction conditions: a) TiCl$_4$, actived Zn dust, THF, reflux 10~15min; b) PbO$_2$, hexanoic acid, DCM.

The preparation of symmetrical porphycene **5-2** was achieved using the McMurry reductive coupling of **5-1-a**[6, 21-22] (see *Scheme 5-10*). Activated zinc metal and freshly distilled THF were used for this reaction. TiCl$_4$ was added via syringe into the system all at once. The solution turned black color, and then brown. TLC was used to strictly follow the reaction and DCM was used as eluting solvent. The desired **5-2** gave a strong red-fluorescence on TLC at 366nm (UV-radiation) and was obtained as a blue powder in 20% yield. The CpoTMPn synthesis was completed by reacting of **5-2** with hexanoic acid in dry DCM.

5.2.2 Improved Synthesis of 2,2'-Bipyrroles
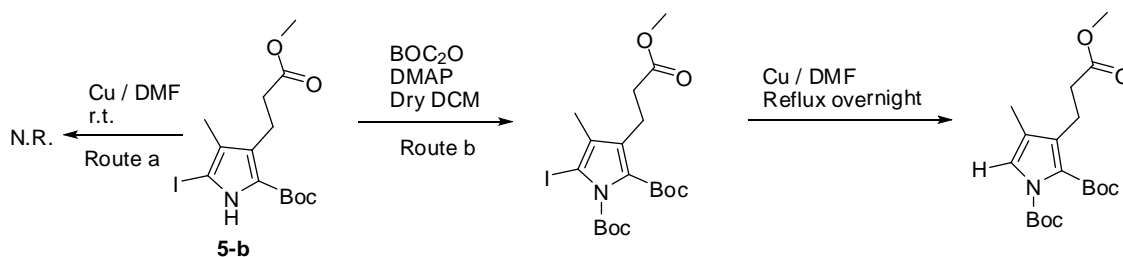
Scheme 5-12. Ullmann coupling reaction that failed to generate the desired 2,2-bipyrrole at both room temperature and under refluxing conditions.

Attracted by the importance role of 2,2'-bipyrrole played in the total synthesis of porphycenes and the fact that there exists limited access to these bipyrroles, we developed an

improved synthetic methodology. The whole idea to improve the 2,2'-bipyrrole synthesis came from difficulties experienced by one of our former group members who failed to produce 2,2'-bipyrrole from the Ullmann Coupling reaction of 2-iodopyrrole **5-b** as shown in *Scheme 5-12*.
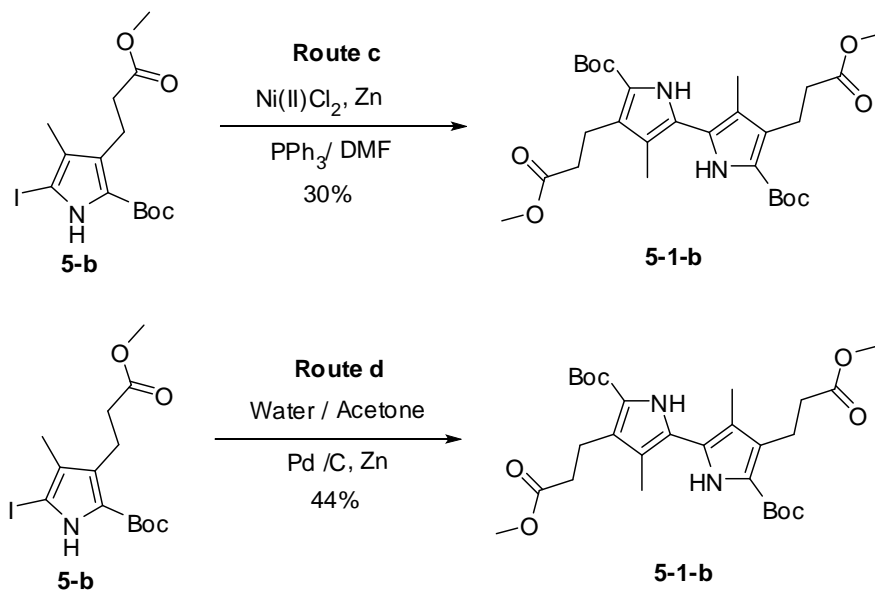
Scheme 5-13. Our improved synthetic method to the 2,2'-bipyrrole **5-1-b**.

n = b: $R_1 = R_2 = $ Me, $R_3 = $ Cbz;

n = c: $R_1 = CH_2CH_3$, $R_2 = CH_3$, $R_3 = $ Cbz;

n = d: $R_1 = CH_3$, $R_2 = CH_2CH_2CO_2CH_3$, $R_3 = $ Cbz;

n = e: $R_1 = CH_2CH_2CH_3$, $R_2 = CH_3$, $R_3 = $ Cbz;

n = m: $R_1 = CH_3$, $R_2 = CH_2CH_3$, $R_3 = $ Boc;

n = n: $R_1 = CH_3$, $R_2 = CH_2CH_2CO_2CH_3$, $R_3 = $ Boc;

n = o $R_1 = R_2 = CH_3$, $R_3 = CO_2Et$;
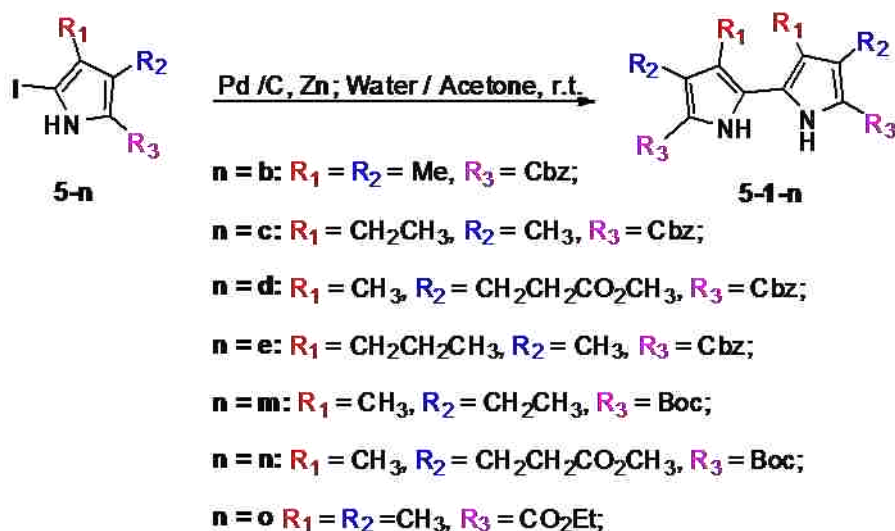
Scheme 5-14. Versatility of the Pd-C/zinc catalyzed coupling reaction.

The former group member even tried to protect the nitrogen atom of the pyrrole ring in compound **5-b** with a CO_2-t-Bu group coupling reaction at reflux temperatures, but still no

desired 2,2'-bipyrrole was obtained. In both cases, no desired product was generated from the coupling reaction. At room temperature, all the starting material was recovered. At refluxing temperatures, the only product was the protiodehalogenated product. This interesting result inspired enough curiosity to study this coupling reaction and search for the possible alternative ways to solve the coupling problem. As was mentioned in the introduction part (Chapter 1), transition metal catalyzed aryl homo-coupling reactions have been widely used lately to efficiently construct carbon-carbon bonds[17-19]. Thus we decided to change the common catalyst in the Ullmann Coupling reaction--copper to the other type of metals. We first tried the $Ni(II)Cl_2$ and Zn as a complex catalyst[24]. In this case, the coupling reaction was performed at the mixture solvent of toluene and DMF and using a temperature ranged between $50\sim60^oC$ for overnight (see Route c in *Scheme 5-13)*. The desired 2,2-bipyrrole was generated in 30% yield after separation. In the meanwhile, the usage of Pd /C and Zn as complex catalyst also gave good result[25]. In this catalyst system, the reaction was performed at the mixture solvent of acetone and water at room temperature under argon protection. The desired 2,2'-bipyrrole was achieved obtained in 44% yield after separation (see Route d in *Scheme 5-13)*. By compared the coupling results from the complex $NiCl_2$/Zn catalyst and that of Pd-C/Zn, we chose the later as catalyst system. Although it is expensive compared with the $NiCl_2$/Zn system, the Pd-C/Zn catalyst required only room temperature conditions and also provided a relatively higher yield, which made it even more attractive. After settling on Pd-C/Zn as catalyst, we used different types of monopyrroles to test the versatility of this coupling reaction (see *Scheme 5-14*). In this improved synthetic approach, the homocoupling reactions of 2-iodopyrrole were performed in acetone/water or toluene/water, at room temperature under argon. The combined Pd-C/Zn catalyst was used. The yields of this coupling reaction are summarized in *Table 5-1*. Functional groups at the α-position of

144

Table 5-1. Improved coupling of 2-iodopyrroles using the combined Pd/C and Zn as catalyst at room temperature under various conditions (P^{Me}= $CH_2CH_2CO_2Me$).

Comp	R_3	R_2	R_1	Product	Yields
5-b		Me	Me	**5-1-b**	75%
5-c	CO_2Bz	Me	Et	**5-1-c**	78%
5-d		Me	Pr	**5-1-d**	49%
5-e		P^{Me}	Me	**5-1-e**	51%
5-m	CO_2-t-Bu	Et	Me	**5-1-m**	32%
5-n		P^{Me}	Me	**5-1-n**	44%
5-p	CO_2Et	Me	Me	**5-1-p**	19%

Table 5-2. The influence of solvent in the Pd-C-Zn coupling reaction.

Entry	Solvents Ratio (v/v)	Major Product	Reaction Time	Yield Ratio (**5-1-o/5-o-H**)
1	Acetone / Water (1/1)	**5-o-H**	≤ 1 hour	0
2	Acetone / Water (1/0.1%)		≤ 1 hour	0
3	Acetone	**5-o**	1 week	--
4	Acetone / Water / Toluene (1/1/1)	**5-1-o/5-o-H**	≤ 2 hours	2 / 8
5	Toluene / Water (1/1)	**5-1-o**	≤ 6 hours	> 9 / 1
6	Toluene	**5-o**	1 week	--

iodopyrroles had important effects on the coupling reaction. Besides the steric hindrance effect, the presence of a benzyl ester group at the α-position of the pyrrole gave higher yields than pyrroles possessing other types of functional group at that same position. The solvent mixture of acetone/water worked well for the coupling reactions of pyrroles that possess a benzyl ester group at the α-position, and the yields were found to be excellent with up to gram scales. This result indicated that an aromatic ring system such as benzene might stabilize the coupling intermediate as described in the literature.[26a] Thus we believed the change of solvents from

145

acetone/water to toluene/water would be helpful for the coupling reaction of other type monopyrroles. Monopyrrole **5-o** was used as starting material for the coupling reaction because it was one the most reactive monopyrroles in the Ullmann-Coupling reaction. The results are shown in *Table 5-2*.

The addition of toluene really helped to improve the coupling reaction; however the real function served by benzene in the coupling reaction was still unknown. According to the disappearance of starting material on TLC, in acetone/water system, reaction took place very fast with pyrrole **5-o**. However, only trace amounts of the desired 2,2'-bipyrrole **5-1-o** could be generated, while the protiodehalogenated product **5-o-H** was obtained as the major product. When organic solvent was changed from acetone to toluene, the yield of **5-o-H** was dramatically reduced; meanwhile the desired 2,2'-bipyrrole **5-1-o** became the major product. Meanwhile, the reaction rate was reduced. Water was found to play an important role in this reaction: the presence of water increased the reaction rate and allowed room temperature performance of the reaction. Although **5-1-o** was one of the few example of 2,2'-bipyrroles that could be easily obtained from room temperature Ullmann-Coupling reaction, it usually took around 24~48 hours for this reaction to complete under Ullmann conditions. However, it usually took only several hours for the completion of coupling **5-o** under this improved condition. The absence of water, no coupling reaction was observed and only starting materials **5-o** was recovered even over a long period (up to 4 days). The simple addition of only 0.1% of water into the acetone solution of the reaction mixture led to the conversion of most starting material to **5-o-H** within 2 hours.

The previous preparation of 5,5'-diformyl-2,2'-bipyrrole (see *Figure 5-1*) was achieved from the Ullmann Coupling reaction in our group. Since it usually require high temperature, functional groups such as aldehyde do not survive the Ullmann-Coupling conditions. Thus

146
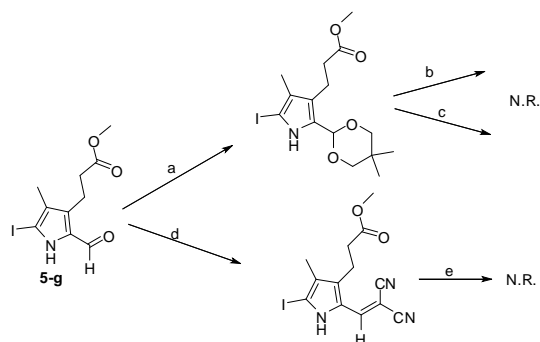
Scheme 5-15: Protected formylpyrrole **5-g** under various coupling conditions generated no products. Reaction conditions: a) Boc$_2$O, DMAP, DCM; b) Cu-bronze, r.t.; c) Cu-bronze, 100 ^{o}C; d) malononitrile, TEA, MeOH; e) Cu, DMF, refluxing temperature.
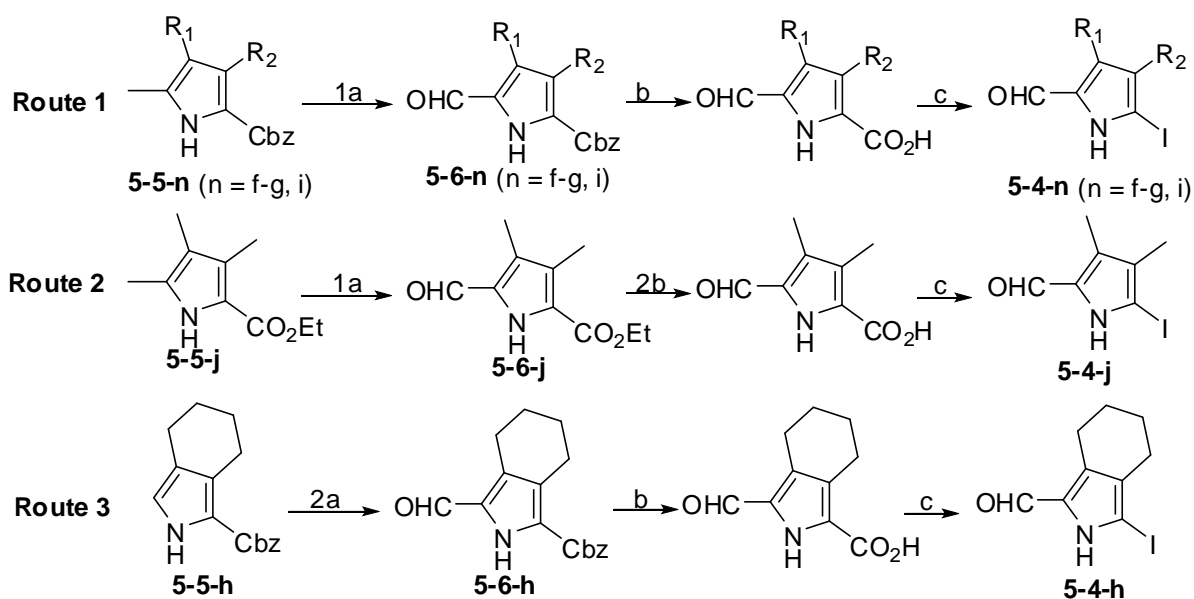
Scheme 5-16. Ready syntheses of 5-formyl-2-iodine pyrroles. Reaction condition: 1a) CAN, HOAc, THF/H$_2$O; 2a) POCl$_3$, DMF, DCM, AcONa; 1b) Pd-C, H$_2$, THF; 2b) LiOH, THF; c) KI, I$_2$, 1,2-dichloroethane/H$_2$O.
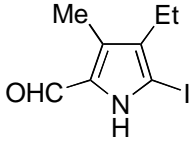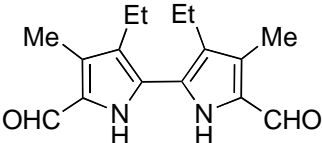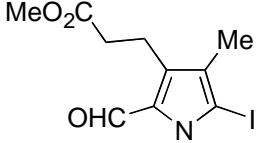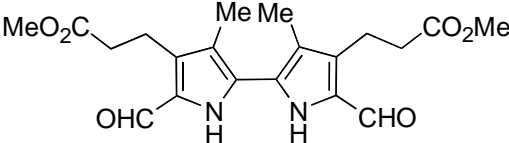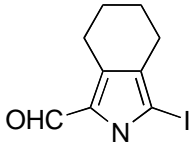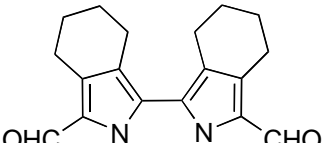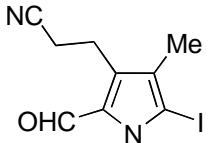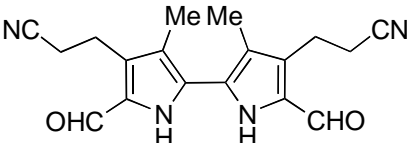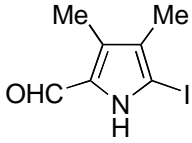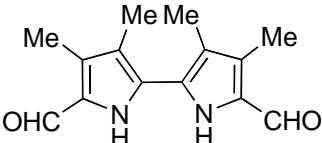
the literature preparation of 5,5'-diformyl-2,2'-bipyrroles involved the protection of functional groups before coupling and subsequently deprotection after coupling. Despite the requirement of these stepwise synthetic route to 5,5'-diformyl-2,2'-bipyrrole (see *Scheme 5-2*), one former group member still failed to generate the desired coupling product **5-1-g** under various conditions from **5-g** (*Scheme 5-15*). The success usage of our improved synthesis in the preparation of many other types of 2,2'-bipyrroles inspired us to apply it to the *direct* synthesis

147

of 5,5'-diformyl-2,2'-bipyrroles. We believed the mild reaction conditions made it possible for the directly coupling of formyl-containing monopyrroles without the troublesome protection and deprotection processes. On the other hand, the ready availability of 2-formyl-pyrroles from high yield reactions[26b] (see route 1~3 in *Scheme 5-16*) smoothed the application of this improved synthetic method in the preparation of 5,5'-diformyl-2,2'-bipyrroles. The key starting materials, 2-formyl-5-iodopyrroles **5-4-n** (n = f-j) are very easy to generate from **5-5-n** (n = f-j) in high yields over three steps (as shown in *Scheme 5-16*). It involved (1) Functionalization at the pyrrole α-position with an aldehyde group: this could involve regioselective oxidation of the α-methyl group of compound **5-5-n** (n = f-g, i-j)[27] using ceric ammonium nitrate[29a] to give a high yield of compound **5-6-n** (n = f-g, i-j)[29] (see route 1 and 3 in *Scheme 5-16*) or a Vilsmeier reaction on an unsubstituted pyrrole to generate compound **5-4-h** (92% yield)[27g] (see route 2 in *Scheme 5-16*); (2) hydrolysis of the ester without aldehyde protection: this could involve catalytic debenzylation of the benzyl esters with Pd-C in THF under H_2 (see route 1 and 3 in *Scheme 5-16*) or hydrolysis of alkyl esters using LiOH in THF (more than 90% yield) following a literature procedure (see route 2 in *Scheme 5-16*)[11], and (3) direct de arboxylative iodination to generate compound 5-**4-n** (n = f-j). The yield in each step is excellent and there is normally no need for chromatography. The overall yield for the three steps is generally more than 65%.
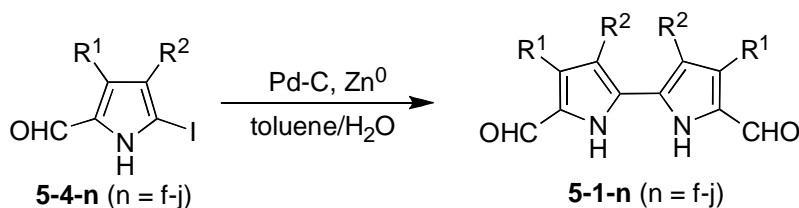
Scheme 5-17. New synthetic route to 5,5'-diformyl-2,2'-bipyrrole **5-1-n** (n = f-j).

Table 5-3. Reductive coupling of 2-iodopyrroles **5-4-n** (n =f-j) using 10% Pd-C and Zn at room temperature in toluene/water under argon.

Formyliodopyrrole	Diformylbipyrrole	Yield
5-4-f	**5-1-f**	35%
5-4-g	**5-1-g**	54%
5-4-h	**5-1-h**	41%
5-4-i	**5-1-i**	26%
5-4-j	**5-1-j**	40%

The aldehyde group was found to be able to survive from this mild coupling condition. Starting from 5-formyl-2-iodopyrroles **5-4-n** (n = f-j), using this improved method, compounds 5-**1-n** (n = f-j) were obtained from the direct coupling of **5-4-n** (n = f-j) in a single step (see *Scheme 5-17*). These coupling reactions were performed in toluene/water at room temperature under argon, with Pd-C/Zn as the catalyst. The reaction was readily followed by TLC, because the target bipyrroles display a very characteristic blue fluorescence under ultraviolet (366 nm) irradiation. The yields of this coupling reaction were moderate as shown in *Table 5-3*. However, the overcoming of the decarboxylation step during the synthesis and avoiding the formation of unstable intermediates will help the scaled-up syntheses of 5,5'-diformyl-2,2'-bipyrroles. As usual in these coupling reactions, the major byproduct was the protiodehalogenation product. Similar to the coupling of the other functional group substituent pyrroles, the substitution of toluene with acetone caused the ratio of dehalogenated product to increase.

Figure 5-3 shows the X-ray structure of 2,2'-bipyrrole **5-1-b**; the nitrogen atoms have the same orientations. Thus we envision that these 2,2'-bipyrroles might also be able to bind small ions.
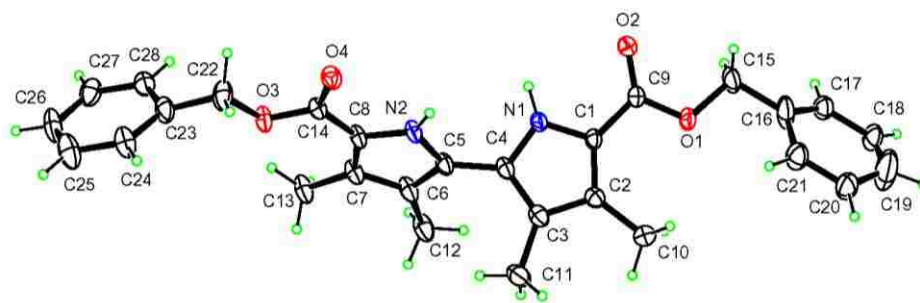
Figure 5-3. X-ray structure of 2,2'-bipyrrole **5-1-b**.

The photophysical properties of **5-1-n** (n = b-j, m-p) are summarized in *Table 5-4* and *5-5*. As shown in *Table 5-4,* most 2,2'-bipyrroles have a blue shift of the λmax in DMSO compared with DCM, except for **5-1-o**. All these bipyrroles are highly luminescent materials at room

temperature, similar to those described in the literature[30]. They also had high quantum yield, thus they may show potential use as bioprobes. The fluorescence quantum yields were measured according to the literature methods[31]. The absorption wavelengths were between 231~401 nm and they are strongly luminous at about 410 nm.

Table 5-4. UV-vis of **5-1-n** (n = b-j, m-p) in both DCM and DMSO at room temperature.

Bipyr role	Absorption λmax (nm) (log ε) DCM	Absorption λmax (nm) (log ε) DMSO	λmax(nm) shift
5-1-b	229 (4.17), 319 (4.46)	318 (4.31)	1
5-1-c	229 (4.11), 312 (4.26)	293 (4.44)	19
5-1-d	209 (3.97), 319 (4.37)	317 (4.31)	2
5-1-e	229 (3.85), 315 (3.95)	294 (4.12)	21
5-1-f	233 (4.08), 280 (3.90), 363 (4.32)	354 (4.26)	9
5-1-g	232 (4.21), 268 (4.00), 361 (4.41)	353 (4.43)	8
5-1-h	235 (4.27), 382 (4.59), 401 (4.58)	370 (4.25)	12
5-1-i	232 (4.04), 262 (3.82), 356 (4.24)	351 (3.94)	5
5-1-j	231 (3.79), 275 (3.64), 361 (4.05)	354 (3.96)	7
5-1-m	229 (4.10), 318 (4.31)	313 (4.06)	5
5-1-n	229 (4.02), 317 (4.22)	313 (4.38)	4
5-1-o	230 (4.47), 250 (4.56), 289 (4.32), 347 (4.48)	289 (4.31)	49
5-1-p	229 (4.00), 317 (4.27)	315 (4.35)	2

Table 5-4. Photophysical data for **5-1-n** (n = b-j, m-p) in degassed DCM at room temperature.

Comp	Emission λmax (nm)		Fluorescence[c] quantum yield		Stocks Shift(nm)	
	DCM	DMSO	DCM	DMSO	DCM	DMSO
5-1-b	386[a]	381[d]	0.519	0.717	67	63
5-1-c	387[a]	377[d]	0.451	0.561	75	84
5-1-d	387[a]	381[d]	0.564	0.671	68	64
5-1-e	387[a]	378[d]	0.523	0.487	72	84
5-1-f	410[b]	418[e]	0.356	0.226	37	64
5-1-g	410[b]	417[e]	0.321	0.191	49	64
5-1-h	415[b]	424[e]	0.411	0.398	14	54
5-1-i	408[b]	414[e]	0.326	0.175	52	63
5-1-j	410[b]	417[e]	0.320	0.212	49	54
5-1-m	384[a]	381[d]	0.502	0.705	68	68
5-1-n	384[a]	381[d]	0.577	0.622	67	68
5-1-p	382[a]	379[d]	0.550	0.652	65	64
5-1-o	401[a]	402[d]	0.559	0.579	84	87

a: excitation at 350 nm; b: calculated using quinine sulfate 5% H_2SO_4 solution as the standard.
For most of bipyrroles, there is large strong red stokes shifts at around 37~68 nm in DCM

and 54~84 nm in DMSO were observed, except for bipyrrole **5-1-h**, which has a smaller Stokes

shift around 14 nm and bipyrrole **5-1-o**, which had been previously synthesized. However **5-1-h**

also gave the highest quantum yield among all the compounds reported here. The initial tests of

these bipyrroles as bioprobe were begun by our group technician, Mr. Tim Jensen (see *Figure 5-*

4), and initial uptake results indicate good potential use of these bipyrroles in bioimaging.

Subsequently, the delocolization experiment was performed by using fluorescence light microscopy (see *Figure 5-5*). It was found that 2,2'-bipyrrole **5-1-o** gave strong blue fluorescence and it was mainly localized in the ER, some of it also was found in mitichron and lysosome.
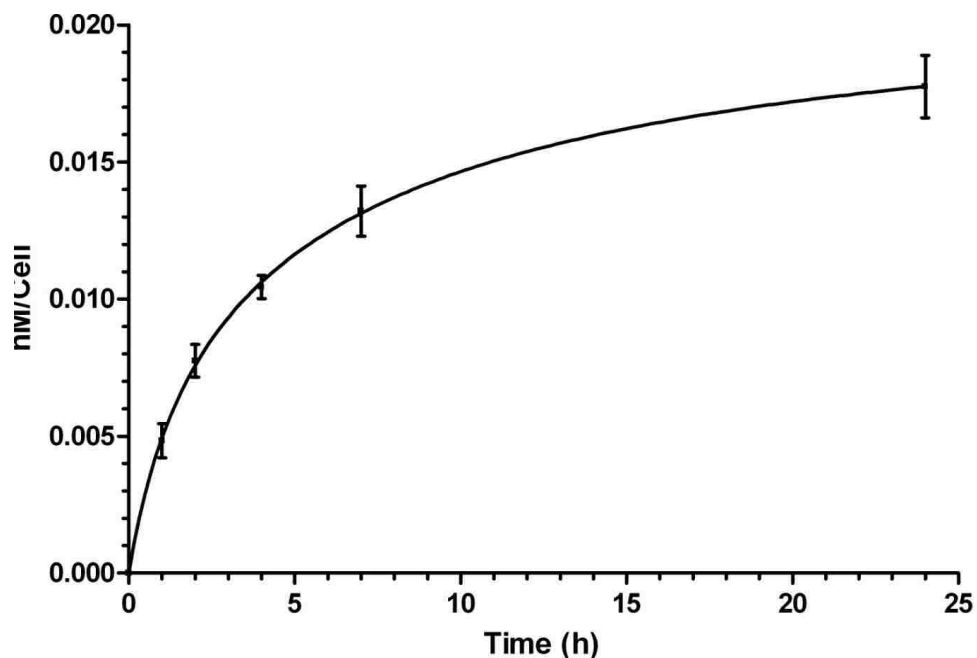
Figure 5-4. Time-dependent uptake of bipyrrole **5-1-o** at 10μm by human carcinoma HEp2 cells.

The initial binding study was performed with the 2,2'-bipyrroles based on their fluorescence quenching properties. It was a surprise to see that these bipyrroles were able to selectively bind to fluoride ions instead of bromide, chloride, phosphate or sulfide ions. Also, the binding behaviors of the bipyrroles were different (see *Figure 5-6*). For the bipyrroles that have benzyl esters (**5-1-b**) or Boc- (**5-1-m**) attached at the 5-position, the addition of n-Bu$_4$NF into a DMSO solution resulted mainly the reduction of the fluorescence intensity. However, for those bipyrroles have CHO-attached to the 5-position, there was a large shift of fluorescence emission. With the decreasing of the initial fluorescence intensity, there was an increasing intensity for the newly appeared fluorescence emission of this type of bipyrroles. The most interesting binding
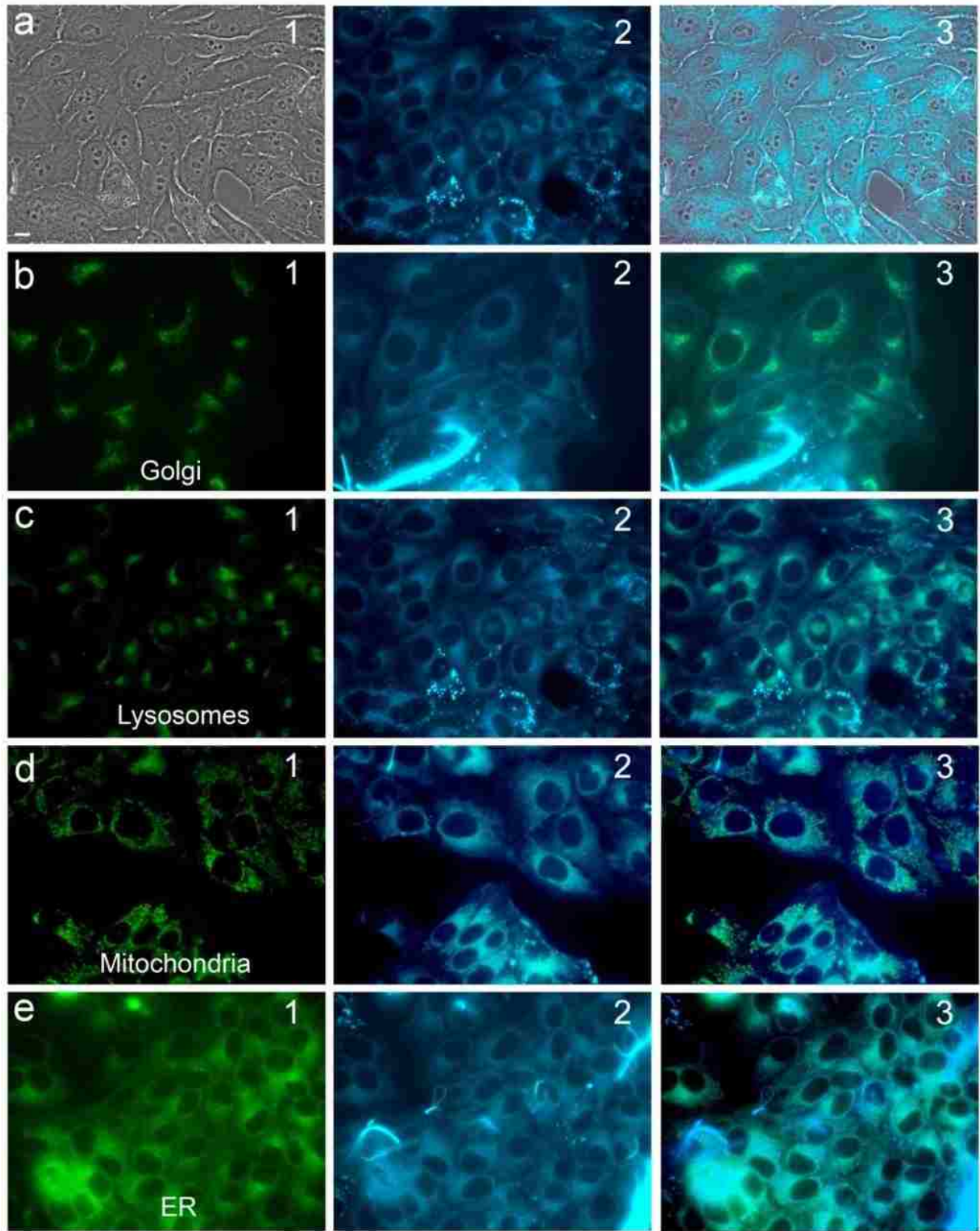
Figure 5-5. Fluorescence microscopy of **5-1-o.**
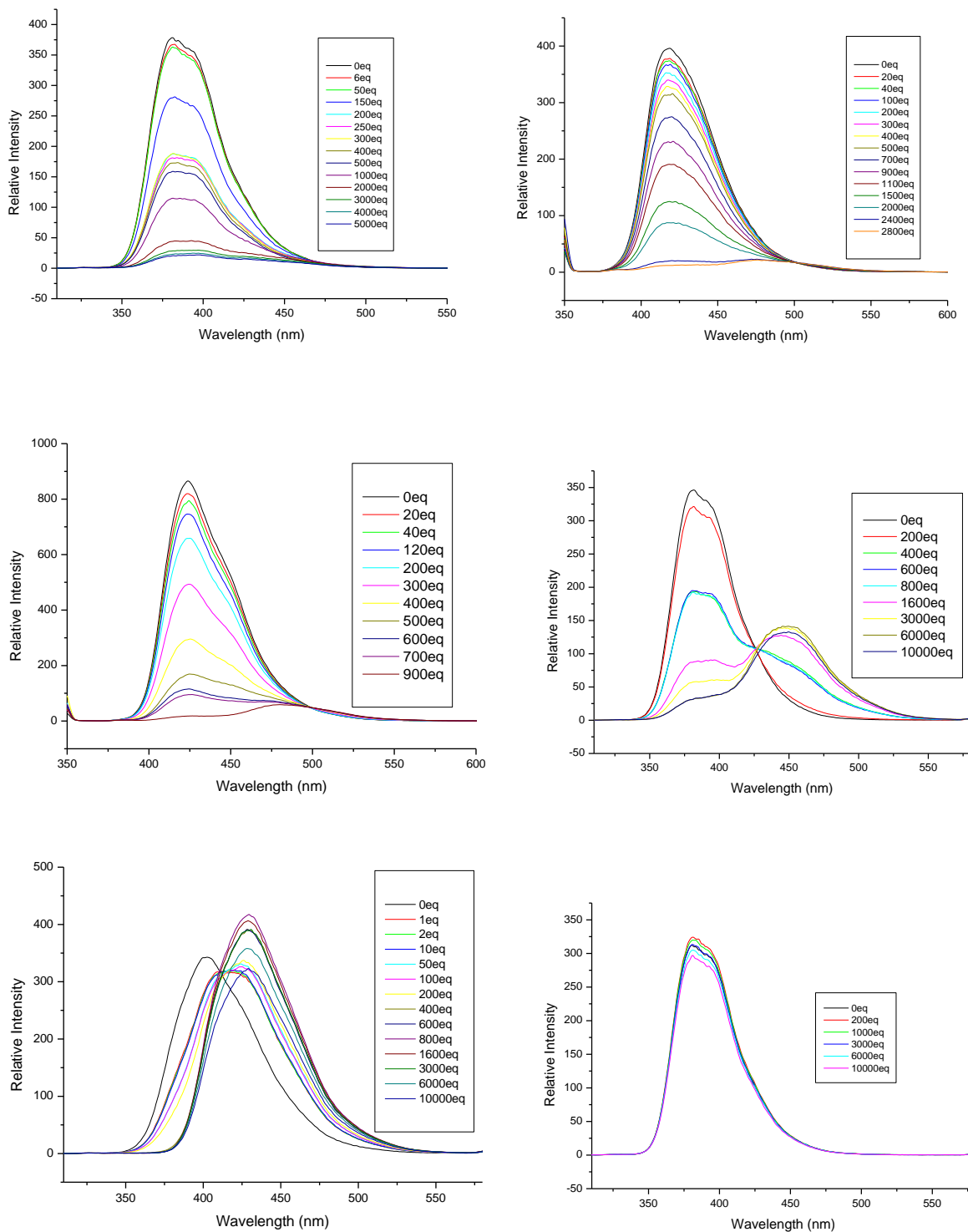
Figure 5-6. Fluorescence quenching upon addition of n-Bu$_4$NF to DMSO solutions of 2,2'-bipyrroles at r.t.. Top figures: **5-1-b** (left, benzyl ester series) and **5-1-m** (right, Boc series), middle figures: **5-1-h** (left) and **5-1-j** (right), both are CHO series; bottom figures: **5-1-o** (left, CO$_2$Et series), control experiment (right, no n-Bu$_4$NF added).

behavior was observed for **5-1-o**, which has an ethyl ester attached to the 5-position of the bipyrrole. There was also a shift of fluorescence emission wavelength similar to that of **5-1-h** and **5-1-j**, but there was an increase of the fluorescence intensity instead of quenching for this compound. The exact reason for this different fluorescence quenching behavior is still under investigation. But it seems to be reasonable that besides the binding of bipyrrole to the fluoride ion, a protonation/deprotonation process as described in the literature might also be involved. In different bipyrrole systems, these two processes might have different contributions to the final appearance of the fluorescence emission, which might result the different "binding" behaviors shown in *Figure 5-6*.

5.3 Conclusions and Future Work

In summary, we have developed an improved method for synthesis of 2,2'-bipyrroles based on a Pd-C/zinc catalyzed homo-coupling in toluene/water at room temperature under argon. The presence of water in the reaction system is critically important. These mild reaction conditions allow functional groups such as aldehyde and nitrile to be carried through the sequence intact. These bipyrroles are strongly luminescent and the new approach should provide a ready access to new materials for light-emitting devices and bioimaging.

5.4 Experiment

5.4.1 General

All commercially available solvents and starting materials were used without further purification. Silica gel (32-63 μm) was used for flash column chromatography. All reactions were monitored by TLC using 0.25 mm silica gel plates with or without UV indicator (60F-254). Acetone (reagent plus, phenol free, ≥ 99.5%) and toluene (HPLC grade, Houston, TX) were

purchased from Sigma-Aldrich without further purification. Palladium, 10% on activated carbon, reduced, dry powder was purchased from Strem Chemicals. Zinc dust, < 10 micron, 98+%, was purchased from Sigma-Aldrich and activated according to the literature. ^{1}H- and ^{13}C-NMR spectra were obtained on a DPX-250 or an ARX-300 Bruker spectrometer; chemical shifts (δ) are given in ppm relative to CDCl$_3$ (7.26 ppm), acetone-d$_6$ (3.58 ppm, or DMSO-d$_6$ (2.54 ppm). MALDI-TOF mass spectra were obtained on an Applied Biosystems QSTAR XL. Electronic absorption spectra were measured on a Perkin Elmer Lambda 35 UV-Vis spectrophotometer in the 200-800 nm wavelength regions with 0.1 nm accuracy. Fluorescence spectra were measured on a Perkin Elmer LS55 spectrometer in the 360-800 nm wavelength region with 1 nm accuracy. Fluorescence quantum yields were measured using the standard method and quinine sulfate in 5% H$_2$SO$_4$ aqueous solution as the standard (quantum yield is 0.55), according to the literature.[31] Monopyrroles used to make 2-iodopyrroles were synthesized according to the literature.[27] Pyrrole **5-6-h** was prepared in the same way as described in the literature[27g] through a Vilsmeier reaction on pyrrole **5c**, the synthesis of which has been reported in the literature.[27b] Pyrroles **5-4-j** were prepared from **5-6-j** according to the literature.[19] Pd-C (10%) was purchased from Strem Chemicals. All the spectral data for CpoTMPn were in agreement with the literature[6,21-22]. For more information about these compounds, see scanned spectra at the end of this Chapter.

5.4.2 Total Synthesis of CpoTMPn

Preparation of 5-7-2

The preparation of **5-7-2** was achieved from the reaction of methoxypropionitrile (34 g, 0.4 mol), ethyl bromoacetate (267.2 g, 1.6 mol) and activated zinc (104.7 g, 1.6 mol) in 500 ml freshly distilled THF under argon condition. A vacuum was pulled over zinc dust for approximately 1 hour before adding freshly distilled THF. Then the reaction mixture was heated to reflux

temperature while stirring. To the refluxing solutions was added ethyl bromoacetate in a dropwise manner through an addition funnel. Upon the appearance of a slightly green color in the reaction mixture (usually around 0.8~1.0 mol), methoxypropionitrile (34 g, 0.4 mol) was added all at once (through a syringe for small amount or through an addition funnel for large amount). Then the rest of the ethyl bromoacetate was added to the reaction mixture in a dropwise manner over a period of 1 hour. During this period, the color of the solution changed from green to brown. Keeping adding until all the ethyl bromoacetate had been added into the reaction mixture. After finishing addition of ethyl bromoacetate, the reaction mixture was left refluxing for an additional 30 minutes. After cooling down to room temperature, the reaction mixture was filtered through a Celite plug to get rid of any unreacted zinc powder. The solvent was then removed under vacuum. The residue was deep yellow in color and was dissolved into EtOAc, and subsequently 3M HCl (400 mL) was added. It was stirred at room temperature for a period of 30 minutes. When stirring was stopped, EtOAc (400 mL) was added into the mixture to extract the target compound from the aqueous solution. The organic phase was subsequently washed with water, then with concentrated aqueous $NaHCO_3$, and saturated NaCl solution. After drying over anhydrous Na_2SO_4, the solvent was removed under vacuum. The residue, a reddish liquid, was distilled under reduced pressure. The desired compound **5-7-2** was collected in the 95~110°C temperature range in 70% yield (52.6 g, 0.28 mol) as a colorless aromatic liquid. It was found that high temperature should be avoided because the desired compound was destroyed at high temperature, giving a highly sticky deep red gel.

Preparation of 5-7-1

Compound **5-7-1** was synthesized from **5-7-2** in two steps[23]: 1) the formation of oxime; 2) the Knorr reaction to form pyrrole. Oxime was generated from the reaction of **5-7-2** (33.2 g, 0.18

mol) with NaNO$_2$ (13.34 g, 0.19 mol) in 143 mL HOAc. Dissolving **5-7-2** (33.2 g, 0.18 mol) in ice-cold 143 mL HOAc and left it stir in ice-bath. Meanwhile, saturated aqueous NaNO$_2$ (13.34 g, 0.19 mol) was prepared and placed into the ice-bath before adding into the ice-cool solution of **5-7-2** (through pipette for small amount and addition funnel for large amount). This addition process needed to be extremely slow to avoid the generation of toxic NOx gas. An addition funnel was also connected to a bubble flask through tubes to control addition rate. After finishing addition of NaNO$_2$ solution, the ice-bath was removed and the reaction was continued to stir for a period of 2 hours at room temperature. TLC is strongly recommended to follow this reaction. The TLC eluting solvent was hexane/EtOAc (3/1). It should be noticed that the intermediate oxime was more polar than desired **5-7-1**, which showed polarity similar to the starting material **5-7-2**. When TLC indicated the disappearance of oxime, the reaction was stopped. The resulting solution was ready for the use in the next step—Knorr condensation to prepare **5-7-1**. The Knorr condensation reaction was performed in a three-necked large flask at temperature between 80~85°C. A water bath was strongly recommended rather than an oil-bath. The main reason was the thermal sensitivity of this reaction and the strict temperature control could help the achievement of high yield since large amount of heat was released over a short period. Water bath provided great control of the temperature through constant addition of ice during the reaction process. Ethyl acetoacetate (26.4 g, 0.16 mol) was dissolved in 26 mL HOAc in a three-necked flask and the solution was heated to 80~85°C in a hot water bath. Activated zinc (25.4 g, 0.39 mol) was mixed well with NaOAc (31.8 g, 0.39 mol). This solid mixture was then added slowly and frequently in small portion to the refluxing solution through funnel. The addition of this mixed solid was alternated with the addition of oxime. Oxime was added to the mixture over a period of 30 minutes, while the mixed solid was added over a period of 40 minutes. It was

important to have zinc always in excess throughout the reaction, which was easily achieved by always allowing excess zinc powder in sight throughout the addition of oxime. After adding all the reagents, the reaction mixture was stirred at 80~85°C for an additional period of 0.5~1 hour. TLC was used to follow this reaction. When TLC indicated the disappearance of oxime from the reaction mixture, the reaction was stopped. Recrystalization from ethanol water gave **5-7-1** in 60% yield (30.6 g, 0.11 mol) as a yellowish powder.

Preparation of 5-formyl-2-iodine-pyrrole

The synthesis of 5-formyl-2-iodopyrrole was achieved from the oxidation of **5-7-1** followed by iodination reaction as shown in *Scheme 5-8*[23a]. The preparation of **5-8-2** from **5-7-1** involved two steps: the oxidation and then the hydrolysis. In the oxidation step, **5-7-1** (5g, 0.02 mol) was dissolved in HOAc/Ac$_2$O (16.6 ml/3.4 ml). The solution was placed in an ice-bath and stirred at 0 $^{\circ}$C. Under these conditions, Br$_2$ (2.82 g, 0.91 mL) was added to the solution all at once. Subsequently, SO$_2$Cl$_2$ (7.56g, 4.55 mL) was added slowly through addition funnel in the dark over a period of 2 hours. Once half of the SO$_2$Cl$_2$ (2.5 mL) had been added, acetone was added to the ice-bath to ensure the temperature remained below 0°C before addition of the rest of the SO$_2$Cl$_2$. If the temperature was higher than 0 $^{\circ}$C, the intermediate would be hydrolyzed by HOAc during the oxidation process, which would resulted in incomplete oxidation and also ester formation, thus lowering the yield of the desired acid.

After adding all of the SO$_2$Cl$_2$, the reaction mixture was refrigeratorated for a period of 4 hours. Then water at room temperature was added to the reaction mixture in a dropwise manner until no more violent reaction could be observed. Then additional water was added very quickly. The temperature was raised to 60 $^{\circ}$C and kept there for a period of 30 minutes. Then the mixture was poured it into cold water and set aside overnight. After filtration, it was ready for the

subsequent hydrolysis. In the hydrolysis step, the filtration residue was dissolved into 120 mL mixture of acetone/water (v/v = 4/1) and heated to refluxing temperature. PH-paper indicated the solution rapidly changed into acidic at around a period of 20 minutes refluxing. Then solid NaHCO$_3$ was added into the mixture solution; the generation of CO$_2$ can be observed during this process. Addition of solid NaHCO$_3$ was stopped when no more CO$_2$ was generated from the reaction mixture. With the evaporation of acetone, the remaining product was separated over the water layer as an oil form. Once the formation of two layers was observed in the refluxing flask, the mixture was poured very slowly with constantly stirring into 100 mL cold water. Then let the reaction mixture was occasionally stirred with glass rod for a period of 1 hour to ensure complete precipitatation. After filtration, the solution was neutralized with 6 M HCl slowly under vigorous stirring condition before keeping it at 0°C for a period of 8 hours at refrigerator. The resulting fine solid was filtered and **5-8-2** was obtained in 45% yield (2.8 g, 0.009 mol). The iodination of **5-8-2** to generate **5-8-1** was performed in the mixture solvents of 1,2-dichloroethane/water with the mixture of I$_2$/KI as the iodination reagent. First NaHCO$_3$ (2.96 g, 0.035 mol) was dissolved into 16.5 mL water and heated to 50 ^{o}C. To this basic solution was added **5-8-2** (2.59 g, 0.008 mol) rapidly in several portions. When most of **5-8-2** was completed dissolved, 1,2-dichloroethane (16.5 mL) was added and the temperature was raised to 71 ^{o}C. Then the saturated aqueous solution of I$_2$/KI (2.96 g/ 3.73 g) was added into the mixture over several minutes. The reaction mixture was refluxed for an additional 40 minutes. Then Na$_2$S$_2$O$_3$ was added to the reaction mixture in portions to remove excess iodine. After separation and removal of the solvent under vacuum, the desired product **5-8-1** was achieved in 90% yield (3.20 g, 0.008 mol).

Preparation of 5-1-a

The preparation of 5,5'-diformyl-2,2'-bipyrrole **5-1-a** involved the 1) Ullmann-coupling reaction, 2) the decarboxylation reaction and 3) Vilsmeier formylation reaction. The Ullmann-coupling reaction was performed in DMI at room temperature with Cu-bronze as the coupling reagent, under argon. To a round flask was added **5-8-1** (2.97 g, 0.0075 mol), vacuum was pulled over the flask and then argon was applied to the system. After that, DMI (15.7 mL) was added. Subsequently, Cu-bronze (2.82 g, 0.044 mol) was added into the reaction mixture all at once. Then let the reaction to perform at room temperature over a period of 24~48 hours. The reaction mixture was a suspended solution with greenish-brown color. TLC showed a strong blue luminous spot under UV-radiation (366 nm). After adding water, the reaction mixture was filtered through a Celite plug to remove precipitate and then washed with hot chloroform. The organic phase was washed with aqueous 20% HNO_3, water, and saturated $NaHCO_3$. After removing the solvents under vacuum, the residue was recrystallized from ethanol. After filtration, the desired **5-9-2** was obtained as colorless needles in 60% yield (2.42 g, 0.0045 mol).

Following the formation of **5-9-2**, hydrolysis to form the carboxylic acid was performed in ethylene glycol at 200 ^{o}C with NaOH as the base, under argon. To ethylene glycol (130 mL) was added **5-9-2** (2.42 g, 0.0045 mol) and NaOH (2.15 g, 0.05 mol). After NaOH was completely dissolved, the reaction mixture was heated to 100 ^{o}C under argon. The mixture was stirred at this temperature for a period of 30 minutes to achieve the hydrolysis of **5-9-2**. TLC was used to follow the hydrolysis reaction. Upon the disappearance of **5-9-2** and with the appearance of a very polar new spot, the temperature was quickly raised to 200 ^{o}C for a period of 1 hour. When TLC indicated the completion of decarboxylation from the disappearance of the polar spot, the reaction mixture was poured into water and extracted with DCM. The organic phase was

quickly washed 8 times with water. After drying over Na_2SO_4, the solvent was removed and the residue was put under vacuum for the subsequent use in the formylation reaction. The formylation reaction used dry DMF as solvent; thus it was in excess amount. First, phosphoryl chloride (6.14 g, 1.7 mL, 0.036 mol) was added into DMF (50 mL) under argon at 0 ^{o}C, and the mixture was stirred at this temperature for a period of 15 minutes before adding the DMF solution of the hydrolysis product (2.48 g, 0.01 mol). Then the temperature was raised to 60 ^{o}C and the mixture was refluxed for 1 hour. It was then poured it into the aqueous NaOAC solution and stirred at 85°C for 1 hour. The formation of a yellowish precipitate was observed. After cooling down to room temperature and filtration, the residue was washed with cold water. After drying over P_4O_{10} under vacuum, after further recrystallization from THF, **5-1-a** was obtained 44% yield (1.34 g, 0.0044 mol).

Preparation of 5-2

The preparation of symmetrical porphycene **5-2** was achieved using the McMurry reductive coupling of **5-1-a**[6, 21-22]. Activated zinc metal (20g, 0.31 mol) was put into a flask and vacuum was pulled over the flask, argon was then filled the system. Freshly distilled 800 mL THF was then added. $TiCl_4$ (16.5 mL, 0.15 mol) was added via syringe into the system all at once. The solution turned blacking, and then brown. The reaction mixture was refluxed for a period of 3 hours. Then the THF solution of **5-1-a** (1.85 g, 6 mmol) was added to the reaction mixture in a dropwise manner over a period of 10 minutes. TLC was used to strictly follow the reaction and DCM was used as eluting solvent. The desired **5-2** gave a strong red-fluorescence on TLC at 366nm (UV-radiation). After cooling to 0 ^{o}C, 300 mL 50% aqueous ammonium solution was added over a period of 1 hour. After adding 600 mL DCM to the reaction mixture, continued stirring for additional 15 minutes. Then the solution was poured into a Celite cake and

200 mL DCM was used to wash the cake. The organic layer was washed with water (300 mL).

After drying over Na_2SO_4, solvent was removed under vacuum and **5-2** obtained as blue powder

in 20% yield (325 mg, 0.6 mmol). The CpoTMPn was synthesized using PbO_2 (40 mg, 0.167

mmol) as catalyst and reacting **5-2** (100 mg, 0.184 mmol) with hexanoic acid (2 mL, 0.016 mol)

in 15 mL dry DCM at room temperature under argon. After workup, CpoTMPn was obtained in

19.8% yield (24 mg, 0.037 mmol).

5.4.3 General Procedure for 2-Iodopyrrole 5-4-n (n = b-e, m-p)

Starting material pyrrole **5-5-n** (n = b-e, m-p) was synthesized according to the

literature[27]. **5-4-n** (n = b-e, m-p) were obtained in two steps. *Step 1*. Hydrolysis: Pd-C (0.066 g, 6

mmol %) was added into a round bottom flask, to which was added the freshly distilled dry THF

10 mL to form a suspended solution of Pd-C. The mixture was stirred under a hydrogen

atmosphere for 20 minutes for the activation of Pd-C catalyst. Finally, **5-5-n** (n = b-e, m-p) (1

mmol) was dissolved into freshly distilled dry THF 50 mL and added into the above solution

through syringe. After finishing adding all the reagents, the reaction mixture was left under a

hydrogen gas atmosphere for a period of 6-12 hours while TLC was used to follow this reaction.

The reaction was stopped when all starting material was consumed and a very polar spot was

observed on TLC. After finishing the reaction, the reaction mixture was passed through a Celite

cake to remove Pd-C and subsequently washed with THF several times. After drying over

anhydrous Na_2SO_4, solvent was removed under vacuum and the resulting carboxylic acid

pyrroles were ready for the next step without further characterization. *Step 2*. Iodination:

$NaHCO_3$ (302.4 mg, 3.6 mmol) was added to 5 mL water and the solution was sonicated and

heated to 50°C in oil bath. After dissolving of $NaHCO_3$, **5-5-n** (n = b-e, m-p) (1 mmol) in 5 mL

1,2-dichloroethane was added and the reaction temperature was quickly raised to 70 °C. Shortly

after reaching 70 °C, a mixture of I$_2$/KI (279 mg, 1.1 mmol)/ (367 mg, 2.2 mmol) was dissolved into 3 mL water and added into the reaction mixture all at once. Let it continue to stir at refluxing conditions for a period of 1 hour. Upon completion of the reaction, it was cooled to room temperature and sodium thiosulfate was added to the mixture in small portion under stirring condition. Then the reaction mixture was poured into a separatory funeral and the organic layer was collected. After drying over anhydrous Na$_2$SO$_4$, solvent was removed under vacuum and the residue was recrystallization using methanol or ethanol/water.

Benzyl 5-iodo-3,4-dimethyl-pyrrole-2-carboxylate 5-4-b[28g]**:** 81 % yield. mp 127-129 °C [lit[28g] mp 126-128 °C]. ^{1}H NMR (400 MHz, CDCl$_3$) δ 8.90 (s, 1H), 7.43-7.35 (m, 5 H), 5.33 (s, 2H), 2.29 (s, 3H), 1.97 (s, 3H). ESI-MALDI Calcd for [C$_{14}$H$_{14}$INO$_2$] m/z, 355.01, found: 355.10.

Benzyl 5-iodo-3-(3-methoxy-3-oxopropyl)-4-methyl-pyrrole-2-carboxylate 5-4-d[28b]**:** 87 % yield. mp 110-112 °C [lit[28b] mp 110-111 °C]. ^{1}H NMR (250 MHz, CDCl$_3$) δ 8.80 (s, 1H), 7.40-7.38 (m, 5H), 5.30 (s, 2H), 3.64 (s, 3H), 3.10-3.04 (m, 2H), 2.53-2.47 (m, 2H), 2.00 (s, 3H). ESI-MALDI Calcd for [C$_{17}$H$_{19}$INO$_2$ + Na]+ m/z, 450.03, found: 449.97.

Benzyl 5-iodo-3-methyl-4-propyl-pyrrole-2-carboxylate 5-4-e[28c]**:** 79 % yield. mp 118-120 °C [lit[28c] mp 119-120 °C]. ^{1}H NMR (250 MHz, CDCl$_3$) δ 9.01 (s, 1H), 7.45-7.34 (m, 5H), 5.32 (s, 2H), 2.37-2.32 (m, 5H), 1.52-1.43 (m, 2H), 0.97-0.91 (m, 3H). ^{13}C NMR (250 MHz, CDCl$_3$) ppm 160.77, 136.58, 131.23, 129.02, 128.66, 127.66, 123.82, 74.13, 66.33, 28.86, 23.84, 14.27, 11.40. ESI-MALDI Calcd for [C$_{16}$H$_{18}$INO$_2$] m/z, 383.22, found: 383.29.

Tert-butyl 3-ethyl-5-iodo-4-methyl-pyrrole-2-carboxylate 5-4-m[28e]: 77 % yield. mp 105-107 °C [lit[28e] mp 105-107 °C]. ^{1}H NMR (250 MHz, CDCl$_3$) δ 9.49 (s, 1H), 3.68 (s, 3H), 3.06-2.99 (m, 2H), 2.54-2.47 (m, 2H), 1.97 (s, 3H), 1.56 (s, 9H). ^{13}C NMR (250 MHz, CDCl$_3$) ppm 173.39,

159.88, 128.34, 125.49, 124.82, 81.27, 73.10, 51.43, 34.79, 28.34, 21.27, 11.69. ESI-MALDI Calcd for $C_{14}H_{20}INO_4$ m/z, 393.04, found: 392.90.

Diethyl 3-(2-ethoxyethyl)-5-iodo-pyrrole-2,4-dicarboxylate 5-4-o[28h]: 83 % yield. mp 148-150 °C [lit[28h] mp 150 °C]. ^1H NMR (250 MHz, CDCl$_3$) δ 9.30 (s, 1H), 4.40-4.33 (m, 4H), 3.55-3.52 (m, 2H), 3.44-3.41 (m, 2H), 3.37 (s, 3H), 1.43-1.36 (m, 6H). ESI-MALDI Calcd for $C_{14}H_{20}INO_4$ m/z, 393.04, found: 329.90.

Tert-butyl 3-ethyl-4,5-dimethyl-pyrrole-2-carboxylate 5-5-n[28e]: 77 % yield. mp 105-107 °C [lit[28e] mp 105-107 °C]. ^1H NMR (300 MHz, CDCl$_3$) δ 9.38 (s, 1H), 7.40-7.34 (m, 5H), 5.32 (s, 2H), 3.67 (s, 3H), 3.03-2.98 (m, 2H), 2.53-2.48 (m, 2H), 2.29 (s, 3H), 1.57 (s, 9H). ^{13}C NMR (250 MHz, CDCl$_3$) ppm 173.39, 159.88, 128.34, 125.49, 124.82, 81.27, 73.10, 51.43, 34.79, 28.34, 21.27, 11.69. ESI-MALDI Calcd for $C_{14}H_{20}INO_4$ m/z, 393.04, found: 392.90.

5.3.3 General Procedure for Syntheses of Pyrrole 5-6-n (n = f-i): The following description used pyrrole **5-5-i** as a representative example for the preparation of pyrrole 5-**6-n** (n = f-g, i). Pyrrole **5-5-i** (2.0 g, 0.006 mole) was dissolved in THF (63 mL), and followed by addition of HOAc(16 mL) and H$_2$O (16 mL). Then 8.6 equiv of ceric ammonium nitrate (28.2 g, 0.052 mole) was added to the mixture all in once. The reaction mixture was stirred at room temperature while TLC was used to follow reaction progress. When there remained no starting material left, the mixture was poured into 150 mL of water and extracted with DCM (100 mL) three times. The organic layer was washed with water (100 mL) three times followed by saturated aqueous NaHCO$_3$ (100 mL). Then the organic extracts were combined and dried over anhydrous Na$_2$SO$_4$. Finally the solution was concentrated under vacuum to remove the solvents. Recrystallization from DCM/hexane gave a slight yellowish fine powder of **5-6-i** in 89% yield (1.76 g).

Benzyl 3-Ethyl-5-formyl-4-methylpyrrole-2-carboxylate 5-6-f.[27h,29b] 91 % yield. Mp 86-87 °C (lit.[27h] mp 86-87 °C). ^{1}H NMR (250 MHz, CDCl$_3$) δ 9.76 (s, 1H), 9.53 (s, 1H), 7.44-7.33 (m, 5H), 5.34 (s, 2H), 2.79-2.70 (m, 2H), 2.30 (s, 3H), 1.23-1.17 (m, 3H). ^{13}C NMR (250 MHz, CDCl$_3$) ppm 179.80, 161.25, 137.21, 135.97, 129.06, 128.49, 128.93, 128.84, 127.10, 124.80, 67.04, 17.24, 16.84, 10.14. ESI-MS Calcd for C$_{16}$H$_{17}$NO$_3$ m/z, 271.12, found: 271.18.

Benzyl 5-Formyl-4-(2-methoxycarbonylethyl)-3-methylpyrrole-2-carboxylate 5-6-g.[27e,f,i] 89% yield. Mp 79-80 °C (lit.[2i] mp 80-81 °C). ^{1}H NMR (300 MHz, CDCl$_3$) δ 9.81(s, 1H), 9.52 (s, 1H), 7.43-7.35 (m, 5H), 5.33 (s, 2H), 3.65 (s, 3H), 3.08-3.03 (m, 2H), 2.59-2.54 (m, 2H), 2.31 (s, 3H). ^{13}C NMR (250 MHz, DMSO- d^6) ppm 180.49, 173.21, 161.20, 135.92, 132.36, 130.73, 128.99, 128.91, 128.76, 127.33, 124.75, 67.04, 52.08, 35.28, 19.25, 10.26. ESI- MS Calcd for C$_{18}$H$_{19}$NO$_5$ m/z, 329.13, found: 329.17.

Benzyl 4-(2-Cyanoethyl)-5-formyl-3-methylpyrrole-2-carboxylate 5-6-i. 87% yield. Mp 111-113 °C. ^{1}H NMR (250 MHz, CDCl$_3$) δ 10.38 (s, 1H), 9.77 (s, 1H), 7.40-7.31 (m, 5H), 5.35 (s, 2H), 3.10-3.04 (m, 2H), 2.62-2.57 (m, 2H), 2.33 (s, 3H). ^{13}C NMR (250 MHz, CDCl$_3$) ppm 180.27, 161.19, 135.73, 130.84, 129.43, 129.11, 128.96, 128.81, 127.68, 124.93, 119.36, 67.34, 20.25, 19.11, 10.35. ESI- MS Calcd for C$_{17}$H$_{16}$N$_2$O$_3$ m/z, 296.12, found: 296.15.

Benzyl 3:4-Butano-5-formylpyrrole-2-carboxylate 5-6-j. The starting material is readily available pyrrole **5c**. The procedure for the preparation of pyrrole **6c** was different from the other pyrroles **6**. The Vilsmeier complex was prepared by adding 2 mL phosphoryl chloride to 20 mL of dry DMF. Then benzyl 3:4-butanopyrrole-2-carboxylate **5c** (2.55 g, 0.01 mol) was dissolved in 20 mL of dry DMF and added slowly to the reaction mixture through a syringe under ice-bath cooling conditions. The ice-bath was then removed and the mixture was refluxed for 45 min. Then, 250 mL of aqueous NaHCO$_3$ was added slowly until the pH reached 8. Stirring was

continued at 30°C until TLC indicated the complete hydrolysis of the intermediate imine salt. The solution was extracted with DCM (100 mL) three times, and washed with water (100 mL) three times, and finally dried over anhydrous Na_2SO_4 before removing the solvent under vacuum to give the title compound **5-6-h** as slightly yellow powder in 92% yield (2.61 g, 0.009 mol). Mp 111-112 °C. ^{1}H NMR (250 MHz, CDCl$_3$) δ 9.71 (s, 1H), 9.58 (s, 1H), 7.41-7.34 (m 5H), 5.34 (s, 2H), 2.84-2.81 (m, 4H), 1.80-1.78 (m, 4H). ^{13}C NMR (250 MHz, CDCl$_3$) ppm 178.98, 160.68, 135.51, 131.91, 129.17, 128.86, 128.63, 128.42, 128.32, 123.19, 66.57, 22.72, 22.57, 22.36, 20.89. HRMS (ESI) Calcd for $C_{17}H_{18}NO_3$ [M+H]$^+$ 284.1281, found: 284.1209.

5.4.4 General Procedure for Synthesis of Pyrroles 5-4-n (n = f-i)

Pyrroles **5-4-n** (n = f-j) were obtained in two steps from pyrroles **5-6-n** (n = f-i). A typical preparation procedure involved two steps: hydrolysis and iodination. The hydrolysis was monitored by TLC, there was a big polarity differences between the starting material and the product. The following description using **5-4-g** as a typical example to illustrate the general procedure; the other 5,5'-diformyl-2,2'-bipyrroles were prepared in a similar manner.

5-Formyl-2-iodo-4-(2-methoxycarbonylethyl)-3-methylpyrrole 5-4-g. *Step 1*. Hydrolysis: Pd-C (180 mg, 6%) was added into a 50 mL round bottom flask and 3 mL of freshly distilled dry THF was added to form a suspension. This was stirred under a hydrogen atmosphere capped with a balloon at room temperature for 20 min to active the Pd-C. Then, benzyl 5-formyl-4-(2-methoxycarbonylethyl)-3-methylpyrrole-2-carboxylate **5-6-g** (500 mg, 1.52 mmol) was dissolved in 6 mL freshly distilled dry THF and added into the above solution through a syringe. The mixture was stirred under the hydrogen atmosphere at room temperature for 6-12 h, using TLC to follow the reaction; it was stopped when all the starting material has been transformed into very polar spot on TLC. Upon completion of the reaction, the mixture was passed through a

Celite plug to remove Pd-C, followed by washing with THF (50 mL) three times. After removing the combined solvent under vacuum, a grayish white powder of 5-formyl-4-(2-methoxycarbonylethyl)-3-methylpyrrole-2-carboxylic acid was obtained in 97% yield (348.1 mg); it was used directly for the next iodination step without characterization. *Step 2.* Iodination: NaHCO$_3$ (453.6 mg 5.4 mmol) was added to 25 mL of water, into which the carboxylic acid pyrrole (348.1 mg) obtained from the previous step was added, followed by sonication. Then the reaction mixture was placed into a 50°C oil bath. Once carboxylic acid pyrrole was completely dissolved, 25 mL of DCM was added to the reaction mixture and the temperature was quickly raised to 70°C. Then, I$_2$ (410.8 mg, 1.6 mmol) and KI (488.2 mg, 2.9 mmol) were dissolved in 15 mL of water and added to the reaction mixture all at once. The mixture was refluxed for 1 h, using TLC to follow the reaction. The mixture was cooled and excess sodium thiosulfate was added into the reaction mixture in small portions with stirring to remove excess iodine. The reaction mixture was poured into a separatory funeral and the organic layer was collected. After drying over anhydrous Na$_2$SO$_4$, the organic solvent was removed under vacuum. After recrystallization from MeOH, a slightly yellow powder of **5-4-g** was obtained in 85% yield (401.4 mg). The overall yield of 5-**4-g** from **5-6-g** was 82% (400mg, 1.25 mmol).

3-Ethyl-5-formyl-2-iodo-4-methylpyrrole 5-4-f.[29b] 85% yield. Mp 118-120 °C (lit.[29b] mp 118-120 °C). ^{1}H NMR (250 MHz, CDCl$_3$) δ 10.77 (s, 1H), 9.41 (s, 1H), 2.76-2.70 (m, 2H), 1.99 (s, 3H), 1.22-1.16 (m, 3H). ^{13}C NMR (250 MHz, CDCl$_3$) ppm 176.53, 138.35, 133.38, 126.17, 83.80, 18.14, 16.89, 11.93. ESI- MS Calcd for C$_8$H$_{10}$INO m/z, 262.98, found: 263.05.

5-Formyl-2-iodo-4-(2-methoxycarbonylethyl)-3-methylpyrrole 5-4-g.[29c] 82% yield. Mp 91-92 °C (lit.[29c] mp 92 °C). ^{1}H NMR (300 MHz, CDCl$_3$) δ 10.66 (s, 1H), 9.41 (s, 1H), 3.64 (s, 3H), 3.06-3.00 (m, 2H), 2.57-2.51 (m, 2H), 1.96 (s, 3H). ^{13}C NMR (250 MHz, DMSO- d^6) ppm

176.45, 172.63, 133.28, 132.84, 125.87, 82.60, 51.69, 35.06, 19.47, 11.46. ESI- MS Calcd for $C_{10}H_{12}INO_3$ m/z, 320.99, found: 321.06.

3:4-Butano-5-formyl-2-iodopyrrole 5-4-h. 84% yield. Mp 165-167 °C. ^{1}H NMR (250 MHz, CDCl$_3$) δ 9.48 (br, 1H), 9.34 (s, 1H), 2.84-2.80 (m, 2H), 2.39-2.34 (m, 2H), 1.84-1.76 (m, 4H). ^{13}C NMR (250 MHz, CDCl$_3$) ppm 175.45, 133.53, 132.39, 128.57, 79.05, 23.01(2C), 22.66, 20.92. HRMS (ESI) Calcd for $C_9H_{11}N_2OI$ [M+H]$^+$ 275.9879, found: 275.9878.

4-(2-Cyanoethyl)-5-formyl-2-iodo-3-methylpyrrole 5-4-i. 81% yield. Mp 143-145 °C. ^{1}H NMR (250 MHz, CDCl$_3$) δ 9.76 (s, 1H), 9.47 (s, 1H), 3.14-3.08 (m, 2H), 2.64-2.58 (m, 2H), 2.05 (s, 3H). ^{13}C NMR (250 MHz, CDCl$_3$) ppm 175.81, 133.55, 129.49, 126.47, 118.58, 82.5, 20.41, 19.12, 11.64. HRMS (ESI) Calcd for $C_9H_{10}N_2OI$ [M+H]$^+$ 288.9832, found: 288.9834.

5.4.5 General procedure for reductive coupling of 5-4-n to generate 5-1-n (n =b-j, m-p)

Activated zinc was obtained by washing zinc dust with 3 M HCl and then filtering through filter paper, after which it was washed successively with water, ethanol, and diethyl ether, and then dried under vacuum. **5-4-b** was used as an example to describe the general procedure for reductive coupling of compounds **5-4-n** (n = b-j, m-p). A mixture of Pd-C (10.0mg, 10%) and activated zinc powder (100 mg, 1.5 mmol) were placed in a dry 50 mL round bottom flask. After removing air under vacuum, the flask was filled with argon. After that, 2 mL of toluene was added to the reaction mixture which was stirred at ambient temperature under argon protection for 15 mins before adding 2-iodopyrrole **5-4-b** (132 mg, 0.5 mmol) dissolved in 8 mL of toluene. Then 10 mL distillated water was added through a syringe into the reaction flask. The reaction mixture was stirred vigorously at room temperature under argon. It is worth mention that the Pd-C purchased from the other source or old catalyst would reduce the yield and in some case even no reaction occurs. Also strict air-free and solvent adding sequence will also affect the

coupling yield. TLC was used to follow reaction, all of the five 5,5'-diformyl-2,2'-bipyrroles **5-1-b** display a characteristic blue fluorescence under UV irradiation (around 366 nm) on silica gel TLC plates. Their DCM, acetone, DMSO and THF solutions also show strong blue luminescent properties under the same wavelength illumination at ambient conditions, unlike the starting material **5-4-b**. Stop the reaction upon the disappearance of the starting material. DCM (40 mL) was added and it was sonicated to form two layers. After removing the water layer, the remained solution was filtered through a Celite plug, followed by washing with DCM (100 mL) three times. The organic solvents were collected and dried over anhydrous Na_2SO_4, before evaporation under vacuum. The pure target compounds were obtained by using silica gel column to separate and eluted with EtOA /hexane (1: 2). Further purification could be performed by recrystallization from DCM/hexane, or from ethanol.

5,5'-Bis(benzyoxyl)-3,3',4,4'-tetramethyl-2,2'-bipyrrole-2,2'-bipyrrole   5-1-b[32]:   After recrystalizing from MeOH/DCM and washing with hexane (2 × 2 ml), pure 5-**1-b** was obtained as a milk-white solid in 78 % yield (89.0 mg, 0.195 mmol). mp 218-220 ^{o}C [lit[32] mp 220 ^{o}C]. ^{1}H NMR (250MHz, CDCl$_3$) δ 9.08 (s, 2H), 7.39-7.34 (m, 10 H), 5.25 (s, 4H), 2.31 (s, 6H), 2.02 (s, 6H). ^{13}C NMR (250 MHz, CDCl$_3$) ppm 161.42, 136.25, 128.51, 128.07, 128.03, 127.90, 124.90, 119.87, 119.00, 65.78, 10.67, 9.89. HRMS (ESI) Calcd for $C_{28}H_{29}N_2O_4$ [M+H]$^+$: 457.2127, found 457.2124.

5,5'-Bis(benzyoxyl)-3,3'-diethyl-4,4'-dimethyl-2,2'-bipyrrole 5-1-c: After recrystallizing from DCM/hexane and washing with hexane (2 × 2 ml), pure **5-1-c** was obtained as a milk-white solid in 80 % yield (96.9 mg, 0.20 mmol). ^{1}H NMR (300 MHz, CDCl$_3$) δ 9.65 (s, 2H), 7.98 (s, 10H), 5.85 (s, 2H), 3.06-2.94 (m, 10H), 1.65 (s, 6H). ^{13}C NMR (300 MHz, CDCl$_3$) ppm 161.35, 136.23,

128.50, 128.02, 127.08, 126.82, 124.18, 119.04, 65.74, 17.69, 15.42, 10.59. HRMS (ESI) Calcd for $C_{30}H_{33}N_2O_4$ [M+H]$^+$: 485.2440, found 485.2444.

5,5'-Bis(benzyoxyl)-4,4'-bis(3-methoxy-3-oxopropyl)-3,3'-dimethyl-2,2'-bipyrrole   5-1-d: After recrystallizing from DCM/hexane and washing with hexane (2 × 2 ml), pure **5-1-d** was obtained as a milk-white solid in 65 % yield (97.5 mg, 0.16 mmol). ^{1}H NMR (250 MHz, CDCl$_3$) 9.21 (s, 2H), 7.37-7.33 (m, 10H), 5.23 (s, 4H), 3.63 (s, 6H), 3.07-3.01 (m, 4H), 2.54-2.47 (m, 4H, 2.05-2.00 (m, 6H). ^{13}C NMR (250 MHz, CDCl$_3$) ppm 173.89, 161.28, 136.28, 130.82, 128.98, 128.75, 128.66, 125.30, 120.14, 119.45, 66.56, 51.91, 35.07, 21.11, 10.16. HRMS (ESI) Calcd for $C_{34}H_{37}N_2O_8$ [M+H]$^+$: 601.2550, found 601.2540.

5,5'-Bis(benzyloxy)-4,4'-dimethyl-3,3'-dipropyl-2,2'-bipyrrole 5-1-e: After recrystallizing from MeOH/DCM and washing with hexane (2 × 2 ml), pure **4b** was obtained as a milk-white solid in 27 % yield (34.6 mg, 0.068 mmol). ^{1}H NMR (250 MHz, CDCl$_3$) 8.73 (s, 2H), 7.44-7.33 (m, 10H), 5.31 (s, 4H), 2.44-2.33 (m, 10H), 1.49-1.39 (m, 4H), 0.89-0.83 (m, 6H). ^{13}C NMR (250 MHz, CDCl$_3$) ppm 161.09, 136.24, 128.56, 128.13, 127.64, 124.85, 124.44, 118.90, 65.80, 29.70, 26.56, 24.07, 13.95, 10.65. HRMS (ESI) Calcd for [M+H] $C_{32}H_{37}N_2O_4$ [M+H]$^+$: 513.2753, found 513.2759.

Di-tert-butyl   4,4'-diethyl-3,3'-dimethyl-2,2'-bipyrrole-5,5'-dicarboxylate   5-1-m: After separating by using a silica gel column eluted with ethyl acetate and hexane, pure target **5-1-m** was obtained as a milk-white solid in 31% (32.3 mg, 0.078 mmol). ^{1}H NMR (250 MHz, CDCl$_3$) δ 8.66 (s, 2H), 2.81-2.72 (m, 4H), 2.05 (s, 6H), 1.58 (s, 18H), 1.19-1.13 (m, 6H). ^{13}C NMR (250 MHz, CDCl$_3$) ppm 161.37, 133.51, 124.49, 120.30, 118.95, 81.10, 28.85, 18.84, 15.52, 10.08. HRMS (ESI) Calcd for $C_{24}H_{37}N_2O_4$ [M+H]$^+$: 417.2753, found 417.2737.

5,5'-Di-4,4'-bis(2-methoxycarbonylethyl)-3,3'-dimethyl-2,2'-bipyrrole **5-1-n**: After separating by using a silica gel column eluted with ethyl acetate and hexane, pure target **11b** was obtained as a milk-white solid in 44% (58.5 mg, 0.11 mmol). ^{1}H NMR (250 MHz, CDCl$_3$) δ 8.75 (s, 2H), 3.67 (s, 6H), 3.08-3.01 (m, 2H), 2.60-2.54 (m, 2H), 2.05 (s, 6H), 1.56 (s, 18H). ^{13}C NMR (250 MHz, CDCl$_3$) ppm 173.59, 160.66, 128.92, 123.98, 120.55, 119.12, 81.12, 51.48, 34.90, 29.67, 20.77, 9.68. HRMS (ESI) Calcd for C$_{28}$H$_{41}$N$_2$O$_8$ [M+H]$^+$: 533.2862, found 533.2854.

3,3',5,5'-tetracarboxylatethylester-4,4'-bis(2-ethoxyethyl)-2,2'-bipyrrole **5-1-o**: After recrystallization from DCM/hexane and washing with hexane (2 × 2 ml), pure **5-1-o** was obtained as a milk-white solid in 69% yield (92.5 mg, 0.17 mmol). ^{1}H NMR (250 MHz, CDCl$_3$) δ 9.42 (s, 2H), 4.49-4.37 (m, 8H), 3.54-3.48 (s, 8H), 3.38 (s, 6H), 1.47-1.40 (s, 12H). FAB MS Calcd for C$_{26}$H$_{36}$N$_2$O$_{10}$ m/z, 536.24, found: 536.30. MALDI-TOF MS Calcd for C$_{26}$H$_{36}$N$_2$O$_{10}$ m/z, 536.24, found: 536.41.

3,3',4,4'-tetramethyl-5,5-dicarboxylatethylester -2,2'-bipyrrole 5-1-p: After separating by using a silica gel column eluted with ethyl acetate and hexane, pure target **5-1-p** was obtained as a milk-white solid in 19% (63.1 mg, 0.19 mmol). ^{1}H NMR (250 MHz, CDCl$_3$) δ 8.97 (s, 2H), 4.34-4.25 (m, 4H), 2.31 (s, 6H), 2.05 (s, 6H), 1.38-1.32 (m, 6H). ^{13}C NMR (250 MHz, CDCl$_3$) ppm 161.70, 127.42, 124.55, 119.60, 119.25, 60.02, 14.47, 10.51, 9.87. MALDI-TOF MS Calcd for C$_{18}$H$_{24}$N$_2$O$_4$ m/z, 332.17, found: 332.34.

3,3'-Diethyl-5,5-diformyl-4,4'-dimethyl-2,2'-bipyrrole 5-1-f[9c]. After using the silica gel column for the separation the title compound was obtained as a milk-white solid in 35% yield (23.7 mg, 0.087 mmol). Mp 240-242 °C (lit. [9c] mp 241-242 °C). ^{1}H NMR (250 MHz, CDCl$_3$) δ11.71(s, 2H), 9.61 (s, 2H), 2.74-2.71 (m, 4H), 1.95 (s, 6H), 1.56-1.10 (m, 6H). ^{13}C NMR (250

MHz, CDCl$_3$) ppm 177.80, 135.93, 128.89, 128.18, 119.19, 16.93, 16.08, 9.31. HRMS (ESI) Calcd for C$_{16}$H$_{21}$N$_2$O$_2$ [M+H]$^+$ 273.1597, found 273.1601.

5,5'-Diformyl-4,4'-bis(2-methoxycarbonylethyl)-3,3'-dimethyl-2,2'-bipyrrole 5-1-g. After separating by using the silica gel column the title compound was obtained as a milk-white solid in 54% yield (52.4 mg, 0.13 mmol). Mp >330 °C (dec.). ^{1}H NMR (250 MHz, DMSO-d$_6$) δ 11.7 (s, 2H), 9.60(s, 2H), 3.57 (s, 6H), 3.00-2.95 (m, 4H), 2.58-2.48 (m, 4H), 1.93 (s, 6H). ^{13}C NMR (250 MHz, CDCl$_3$) ppm 178.30, 172.61, 131.69, 129.32, 127.79, 119.70, 51.30, 34.51, 19.22, 9.30. HRMS (ESI) Calcd for C$_{20}$H$_{25}$N$_2$O$_6$ [M+H]$^+$ 389.1707, found 389.1707.

3:4, 3':4'-Bisbutano-5,5'-diformyl-2,2'-bipyrrole 5-1-h. After separating by using the silica gel column the title compound was obtained as a milk-white solid in 41% yield (30.3 mg, 0.10 mmol). Mp >310 °C (dec.). ^{1}H NMR (300 MHz, DMSO-d$_6$) δ 11.50 (s, 2H), 9.54 (s, 2H), 2.80 (m, 4H), 2.50 (m, 4H), 1.67 (br, 8H). ^{13}C NMR (250 MHz, DMSO-d$_6$) ppm 177.26, 128.38 (2C), 126.85, 121.55, 22.94, 22.37, 21.76, 21.22. HRMS (ESI) Calcd for C$_{18}$H$_{21}$N$_2$O$_2$ [M+H]$^+$ 297.1597, found 297.1605.

4,4'-Bis(2-cyanoethyl)-5,5'-diformyl-3,3'-dimethyl-2,2'-bipyrrole 5-1-i. After separating by using the silica gel column the title compound was obtained as a milk-white solid in 26% yield (20.9 mg, 0.065 mmol). Mp >330 °C (dec.). ^{1}H NMR (250 MHz, acetone-d$_6$) δ 9.71 (s, 2H), 9.65 (s, 2H), 3.18-3.12 (m, 4H), 2.71-2.65 (m, 4H), 2.18 (s, 6H). ^{13}C NMR (250 MHz, acetone-d$_6$) ppm 178.86, 131.00, 130.71, 128.28, 121.43, 120.21, 20.79, 18.99, 9.72. HRMS (ESI) Calcd for C$_{18}$H$_{19}$N$_4$O$_2$ [M+H]$^+$ 323.1502, found 323.1504.

5,5'-Diformyl-3,3',4,4'-tetramethyl-2,2'-bipyrrole 5-1-j[9a]. After separating by using the silica gel column the title compound was obtained as a milk-white solid in 40% yield (24.4 mg, 0.10 mmol). Mp >307°C (dec.) [lit.[9a] mp 305-307 °C (dec.)]. ^{1}H NMR (250 MHz, DMSO-d$_6$) δ 11.66

(s, 2H), 9.61 (s, 2H), 2.25 (s, 6H), 1.91 (s, 6H). ^{13}C NMR (250 MHz, DMSO-d$_6$) ppm 177.86, 129.53(2C), 128.06, 119.89, 9.44, 9.00. HRMS (ESI) Calcd for C$_{14}$H$_{17}$N$_2$O$_2$ [M+H]$^+$ 245.1284, found 245.1289.

5.5 References

1   Dougherty, T. J. *Photochem. Photobiol.* **1987**, *46*, 569.

2   Gomer, C. J. *Photochem. Photobiol.* **1991**, *54*, 1093; b) Morgan, A. R.; Rampersaud, A.; Garbo, G. M.; Keck, R. W.;Selman, S. H., *J. Med. Chem.* **1989**, *32*, 904.

3   Kadish, K. M.; Smith, K. M.; Guilard, R. Eds., In *Porphyrin Handbook*, Academic Press, San Diego, San Francisco, New York, Boston, London, Sydney, Tokyo, Volume 2, **2000**.

4   Vogel, E.; Köcher, M.; Schmickler, H.; Lex, J. *Angew. Chem. Int. ed. Engl.* **1986**, *25*, 257.

5   Aramendia, P. F.; Redmond, R. W.; Nonell, S.; Schuster, W.; Braslavsky, S. E.; Schaffner, K. *Photochem. Photobiol.* **1986**, *44*, 555.

6   Richert, C.; Wessels, J. M.; Müller, M.; kisters, M.; benninghaus, T.; Goetz, A. E. *J. Med. Chem.* **1994**, *37*, 2797.

7   Vogel, E.; Kocher, M.; Schmickler, H.; Lex, J. *Angew. Chem., Int. Ed. Engl.* **1986**, *25*, 257; b) Sessler, J. L.; Weghorn, S. J. *Expanded, Contracted and Isomeric Porphyrins*, Pergamon: New York, 1997.

8   Vogel, E.; Balci, M.; Kakumanu, P.; Kogh, P.; Lex, J.; Ermer, O. *Angew. Chem., Int. Ed. Engl.* **1987**, *26*, 928; b) Nonell, S.; Bou, N.; Borrell, J. I.; Teixido, J.; Villanueva, A.; Juarranz, A.; Canete, M. *Teterhedron Lett.* **1995**, *36*, 3405; c) Gavalda, A.; Borrell, J. I.; Teixido, J.; Nonell, S.; Arad, O.; Grau, R.; Canete, M.; Juarranz, A.; Villanueva, A.; Stockert, J. C. *J. Porphyrins Phthalocyanines* **2001**, *5*, 846; d) Hayashi, T.; Dejima, H.; Matsuo, T.; Sato, H.; Murata, D.; Hisaeda, Y. *J. Am. Chem. Soc.* **2002**, *124*, 11226; e) Hayashi, T.; Nakashima, Y.; Ito, K.; Ikegami, T.; Aritome, I.; Suzuki, A.; Hisaeda, Y. *Org. Lett.* **2003**, *5*, 2845.

9   Bauer, V. J.; Clive, D. L. J.; Dolphin, D.; Paine III, J. B.; Harris, F. L.; King, M. M.; Loder, J.; Wang, S-W. C.; Woodward, R. B. *J. Am. Chem. Soc.* **1983**, *105*, 6429; b) Broadhurst, M. J.; Grigg, R.; Johnson, A. W. *J. Chem. Soc., Perkin Trans. 1* **1972**, 2111; c) Sessler, J. L.; Cyr, M. J.; Lynch, V.; McGhee, E.; Ibers, J. A. *J. Am. Chem. Soc.* **1990**, *112*, 2810; d) Schevchuk, S. V.; Davis, J. M.; Sessler, J. L. *Tetrahedron Lett.* **2001**, *42*, 2447.

10 Sessler, J. L.; An, D.; Cho, W-S.; Lynch, V. *Angew. Chem., Int. Ed. Engl.* **2003**, *42*, 2278; b) Setsune, J.-I.; Tsukajima, A.; Watanabe, J. *Tetrahedron Lett.* **2006**, *47*, 1817; c) Geier, G. R. III.; Grindrod, S. C. *J. Org. Chem.* **2004**, *69*, 6404; d) Decréau, R. A.; Collman, J. P. *Tetrahedron Lett.* **2003**, *44*, 3323.

11 *The Porphyrin Handbook,* Kadish, K. M.; Smith, K. M.; Guilard, R., Eds.; Academic Press: San Diego, **2000**; Vol 6; b) Gale, P. A.; Anzenbacher, P., Jr.; Sessler, J. L.; *Coord. Chem. Rev*. **2001**, *222*, 57; c) Kleemann, A.; Engl, J.; Kutscher, B.; Reichert, D. *Pharmaceutical Substance: Synthesis, Patents, Applications,* 4th ed.; Georg Thieme: Stuttgart, **2001**.

12 Ceacareanu, D. M.; Gerstenberger, M. R. C.; Haas, A. *J. Heterocycl. Chem.* **1985**, *22*, 281; b) Wasserman, H. H.; Petersen, A. K.; Xia, M.; Wang, J. *Tetrahedron Lett.* **1999**, *40,* 7567; c) Oda, K.; Sakai, M.; Ohno, K.; Machida, M. *Heterocycles* **1999**, *40*, 277; d) Dohi, T.; Morimoto, K.; Maruyama, A.; Kita, Y. *Org. Lett.* **2006**, *8*, 2007.

13 Sessler, J. L.; Hoehner, M. C.; *Synlett* **1994**, *3*, 211; b) Vogel, E.; Deponte, R. *US Patent*, 5,756,724; c) Skowronek, P.; Lightner, D. A. *Monatsh. Chem.* **2003**, *134*, 889; d) Furstner, A.; Radkowski, K.; Peters, H. *Angew. Chem., Int. Ed. Engl.* **2005**, *44*, 2777.

14 Arad, O.; Morros, J.; Batllori, X.; Teixido, J.; Nonell, S.; Borrell, J. I. *Org. Lett.* **2006**, *8*, 847.

15 Hassan, J.; Sevignon, M.; Gozzi, C.; Schulz, E.; Lemaire, M. *Chem. Rev*. **2002**, *102*, 1359. (b) Grigg, R.; Johnson, A. W.; Wasley, J. W. F. *J. Chem. Soc*. **1963**, 359. (c) Zhang, S.; Zhang, D.; Liebeskind, L. S. *J. Org. Chem*. **1997**, *62*, 2312.

16 Hassan, J.; Sevigon, M.; Gozzi, C.; Schulz, E.; Lemaire, M. *Chem. Rev.* **2002**, *102*, 1359; b) Shezad, N.; Clifford, A. A.; Rayner, C. M. *Green Chem.* **2002**, *4*, 64.

17 Venkatraman, S.; Li, C-J. *Org. Lett.* **1999**, *1*, 1133 ; b) Venkatraman, S.; Li, C-J. *Tetrahedron Lett.* **2000**, *41,* 4831.

18 Trost, B. M. *Accounts Chem. Res.* **1990**, *23*, 34; b) Stille, J. F. *Angew. Chem. Int. Ed. Engl.* **1986**, *75*, 508; c) Miyaura, N.; Suzuki, A. *Chem. Rev.* **1995**, *95*, 2457; d) Heck, R. H. *Accounts Chem. Res*. **1979**, 12, 146; e) Sonogashira, K. In *Comprehensive Organic Synthesis*; Trost, B. M., Ed.; Pergamon; Oxford, **1991**; f) Bamfield, P.; Quan. P. M. *Synthesis*, **1978**, 537.

19 Cho, D. H.; Lee, J. H.; Kim, B. H. *J. Org. Chem*. **1999**, *64*, 8048.

20 Tolendano, H.; Edrei, R.; Kimel, S., *J. Photochem. Photobiol, B: Biology,* **1998**, *42*, 20.

21 Vogel, E.; Emanuel, M.; Martin, H.; Otto, C.; Alexander, D., US patent: WO/1996/031452, **1996**.

22 Szeimies, R.-M.; Karrer, S.; Abels, C.; Steeinbach, P.; Fickweiler, S.; messmann, H.; Baeumler, W.; Landthaler, M. *J. Photochem. Photobiol. B,* **1996**, *34*, 67.

23 Jones, R. A.;Bean, G. P., In *The chemistry of pyrroles*, Academic Press, London, New York, **1977**; b) Dolphin, D., In *The Porphyrins*, Academic Press, New York, **1978**.

24 Dorff, P. H.; Chiu, G.; Goldstein, S. W.; Morgan, B. P. *Tetrahedron Lett.* **1998**, *39*, 3375.

25 Venkatraman S.; Li, C.-J. *Org. Lett.* **1999**, *1*, 1133.

26 Itahara, T. *J. Org. Chem.* **1985**, *50*, 5272.

27 Kleinspehn, G. G. *J. Am. Chem. Soc.*, **1955**, *77*, 1546; b) John, K. D.; Pearce, W. A.; Pyke, S. M. *J. Porphyrins Phthalocyanines*, **2002**, *6*, 661; c) Takaya, H.; Kojima, S.; Murahashi, S. - I. *Org. Lett.*, **2001**, *3*, 421; d) Smith, K. M.; Martynenko, Z.; Pandey. R. K.; Tabba, H. D. *J. Org. Chem.*, **1983**, *48*, 4296; e) Smith, K. M.; Milgrom, L. R.; Kenner, G. W. *J. Chem. Soc., Perkin Trans. 1,* **1981**, 2065; f) Smith, K. M.; Pandey, R. K. *J. Chem. Soc., Perkin Trans. 1* **1987**, 1229; g) Smith, K. M.; Minnetian, O. M. *J. Org. Chem.* **1985**, *50*, 2073; h) Jackson, A. H.; Kenner, G. W.; Warburton, D. *J. Chem. Soc.* **1965**, 1328; i) Ringuet, M.; Gagnon, J. *Can. J. Chem.* **1985**, *63*, 2420.

28   (a) Smith, K. M.; Minnetian, O. M. *J. Org. Chem.* **1985**, *50*, 2073-2080. (b) Cox, M. T.; Jackson, A. H.; Kenner, G. W. *J. Chem. Soc. C*, **1971**, 1974-1981. (c) Al-Hazimi, H. M. G.; Jackson, A. H.; Knight, D. W.; Lash, T. D. *J. Chem. Soc. Perkin Trans 1*, **1987**, 265. (d) Jackson, A. H.; Kenner, G. W.; Smith, K. M. *J. Chem. Soc. C,* **1971**, 502. (e) Clelow, P. J. *J. Chem. Soc. Perkin Trans 1,* **1990**, 1925. (f) Paine, J. B. III. In The porphyrins; Dolphine, D. Ed.; Academic; New York, **1978**; Vol. 1, Chapter 4, pp101-234. (g) Grigg, R.; Jackson, A. W. *J. Chem. Soc.* **1964**, 3315. (h) Richert, C.; Wessels, J. M.; Müller, M.; Kisters, M.; Benninghaus, T.; Goetz, A. E. *J. Med. Chem.* **1994**, *37*, 2797.

29 (a) Thyrann, T.; Lightner, D. A. *Tetrahedron Lett.* **1995**, *36,* 4345. (b) Tu, B.; Lightner, D. A. *J. Heterocycl. Chem.* **2003**, *40,* 707; b) Jacobi, P. A.; Pippin, D. *Org. Lett.* **2001**, *3*, 827.

30 Kuo, W.-J.; Chen, Y-H.; Jeng, R.-J.; Chan, L.-H.; Lin, W-P.; Yang, Z.-M. *Tetrahedron*, **2007**, *63*, 7086; b) Che, C-M.; Wan, C-W.; Lin, W-Z.; Yu, W-Y.; Zhou, Z-Y.; Lai, W. -Y.; Lee, S. -T. *Chem. Commun.* **2001**, 721.

31 Fery-Forgues, S.; Lavabre, D. *J. Chem. Ed.* **1999**, *76*, 1260.

32 Heinz, F. *Monatshefte Fuer Chemie*, **1988**, *119(2),* 247-252.

CHAPTER 6. THE UNIQUE REGIOCHEMISTRY OF MONO-(L)-ASPARTYLCHLORIN-E$_6$

6.1 Introduction

PDT is a binary cancer therapy that relies on the selective uptake of a photosensitizer into tumor tissues, followed by generation of singlet oxygen and other cytotoxic species upon irradiation with light of an appropriate wavelength[1-3]. Photofrin® (porfimer sodium) has been commercially developed and approved in more than 40 countries as a 1st generation photosensitizer. It has limited application in the PDT treatment of cancers, due to the following factors: it has low absorption of light within the "therapeutic window" (600-800 nm) and it is slow to clear from skin, resulting in residual patient photosensitivity[4]. To extend the application of photosensitizers in PDT, so-called 2nd-generation photosensitizers, such as LS-11 (**6-10**) has been developed recently. LS-11 is the latest name for mono-(L)-aspartylchlorin-e$_6$, which previously had been also known as Talaporfin sodium, NPe6 and MACE. As a chlorophyll derivative, LS-11 has been used in advanced-stage clinical trials for PDT. LS-11 has a strong characteristic absorption maximum at 666 nm (solvent dependent), ability to generate cytotoxic singlet oxygen in high yields upon irradiation, and enjoys rapid clearance from normal tissue[4-5]. Moreover, it has increased stability and amphiphilicity compared with many synthetic chlorins tested as PDT sensitizers.

A patent search identifies LS-11 (at that time "NPe6" or Talaporfin sodium) as the 17^3-aspartyl derivative, though the option for a mixture with other regioisomers was left open in the patent itself[6]. Surprisingly, in 1998 a very thorough 2D NMR study was published claiming that LS-11 is actually the 15^2-regioisomer[7] (**6-10**). Unfortunately, the conclusions in this paper were not universally accepted due to the ambiguous NMR spectra of the aggregated compound[8] in

water. Additionally, the result was counter-intuitive from a mechanistic perspective since the propionic side chain is the most reactive and also the least steric hindered position compared with the acetic and formic analogs. Although this paper also reported the syntheses and spectroscopic evaluation of the 17^3- and 13^1-positional isomers of 15^2-LS-11, the yields were low and the synthetic routes to these regioisomers were ambiguous. As a result, most papers ever since 1998 reported LS-11 to be either the 15^2-or the 17^3-aspartyl derivatives, most often the latter. The identity of LS-11 has remained a matter of conjecture and the distributors appear to have remained silent on the critically important structural issue raised by Gomi et al.[7]. Meanwhile, subsequent to the initial patent, our group had also synthesized and biologically studied this molecule as well as an over-reacted di-(L)-aspartylchlorin-e_6 ("DACE") that was correctly identified as the $17^3,15^2$-diaspartyl compound (**6-8**)[9]. Recently, our group also reported the unambiguous improved syntheses of the 13^1-, 15^2- and 17^3-aspartyl regioisomers of LS-11, as their tetramethyl esters[10]. The transfer of free acids into esters provided good solubility and avoided the formation of aggregates in solution; thus monomeric NMR spectra were obtained. In the meanwhile, we were also able to obtain the X-ray structure of the tetramethyl ester of authentic LS-11, which was prepared from the coupling of commercially available chlorin-e_6 with aspartic acid derivatives using peptide coupling reagents, such as DCC. Our results are in agreement with the recent, though unaccepted, report[7] that aspartyl group is attached to the 15^2-side chain position in chlorin-e_6. With the absence of carboxylic protecting groups during the synthesis of the commercial material, which is formed clearly as one pure regioisomer, it is really surprising to see such a highly regioselective coupling to form uniquely the 15^2-positional LS-11 derivative (**6-10**). Considering the fact that chlorin-e_6 possesses no less than three carboxylic acid functional groups, all of which are able to undergo amino-acid coupling reactions,

179

if there is selective formation of one unique regioisomer, then it should be the 17^3-regioisomer of LS-11 instead of 15^2-aspartyl isomer. However, the regioisomer isolated from experiment is indeed the 15^2-positional LS-11[7, 10] instead of that at 17^3. It seems to us that the reaction should have an unknown complexity in the pathway which guides the efficient coupling of amino acid at the specifically unfavorable 15^2-position. To discover this pathway, we designed reactions and explored MALDI-TOF and NMR techniques. In the meanwhile, we achieved a key improvement in synthesizing the 15^2-positional LS-11, in which organic base was found to play an important role during the coupling.

When using H-Lys (Boc)-OtBu instead of L-aspartic acid, the 15^2-positional Lys-substituted chlorin-e_6 was also achieved in good yield with high regio-selectivity.

6.2 Results and Discussion

We hypothesized that the highly regioselective formation of the 15^2-positional regioisomer was due to the formation of a seven-member anhydride ring intermediate, which has high reactivity and can easily undergo a ring opening reaction upon addition of a nucleophilic reagent, such as the L-aspartic acid dimethy lester in the absence of a peptide coupling agent (see *Scheme 6-1*). To substantiate our rationale, first we designed a reaction to prove that cyclic anhydride ring do form for **6-1** under the coupling condition *before* the addition of nucleophilic reagent. The designed reaction was performed by coupling pure chlorin-e_6 with the peptide coupling reagent DCC[6,10]. In this coupling reaction, 1 equivalent of chlorine-e_6 was suspended in dry DCM solution under an argon atmosphere. One equivalent of DCC and 1 equivalent of DMAP were dissolved in dry DCM and were added to a DCM solution of chlorin-e_6 at room temperature under an argon atmosphere. It took around 5-10 minutes for chlorin-e_6 to become completely dissolved after adding DCC/DMAP. In the meanwhile, the solution changed into a

brown color. It took a round 30 minutes before TLC indicated the formation of two new spots, which changed color on the TLC plate upon standing. The initial color was brown and subsequently it changed into green. The minor of the two products has R_f value at 0.8 and the major product has R_f value at 0.4 when 10% acetone/DCM was used as the eluting solvent. MALDI mass spectra of the reaction mixture gave two peaks at MW 785 and 578 (see *Figure 6-1*).
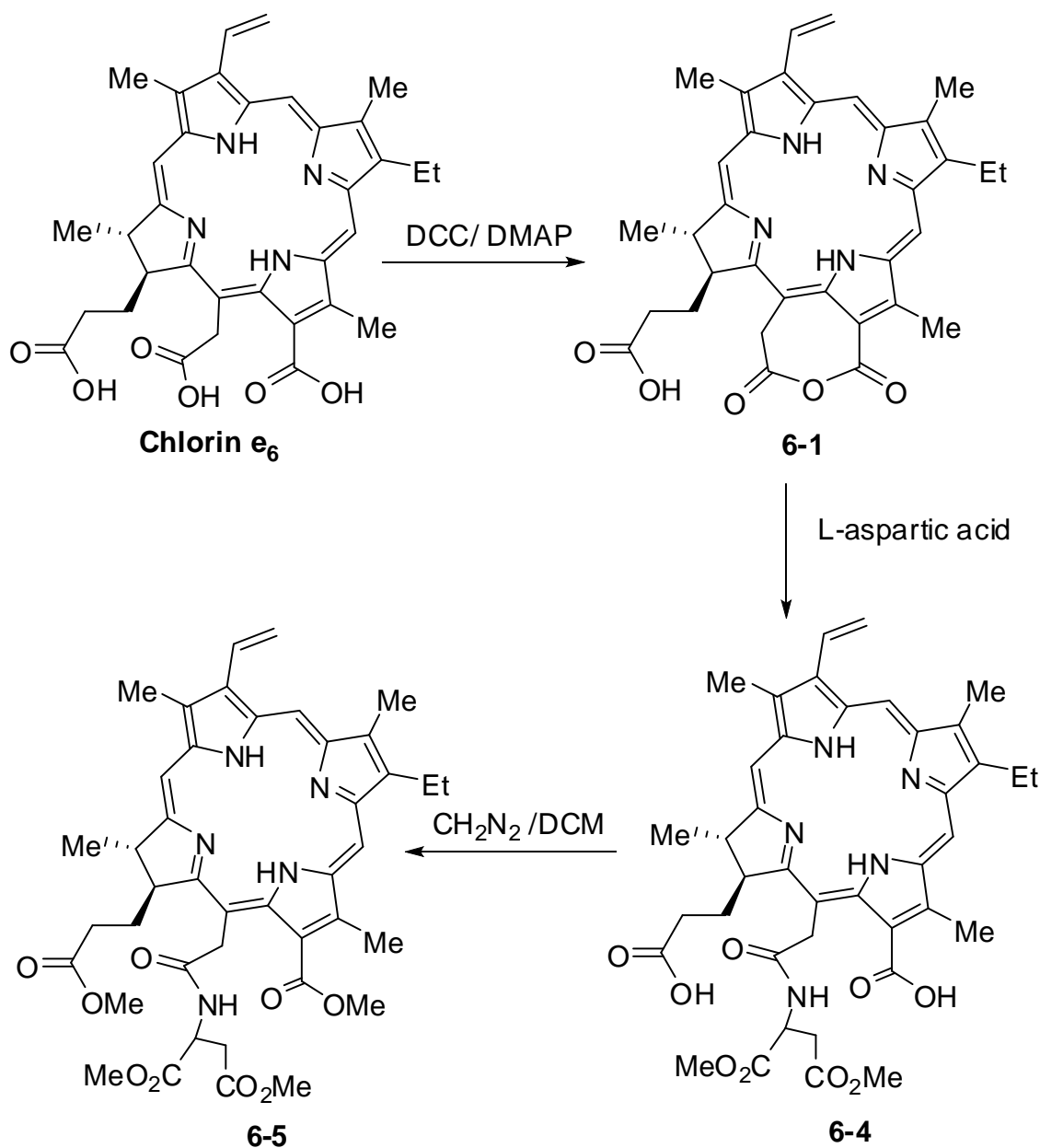
Scheme 6-1. Rationale for the unique formation of **6-5**.
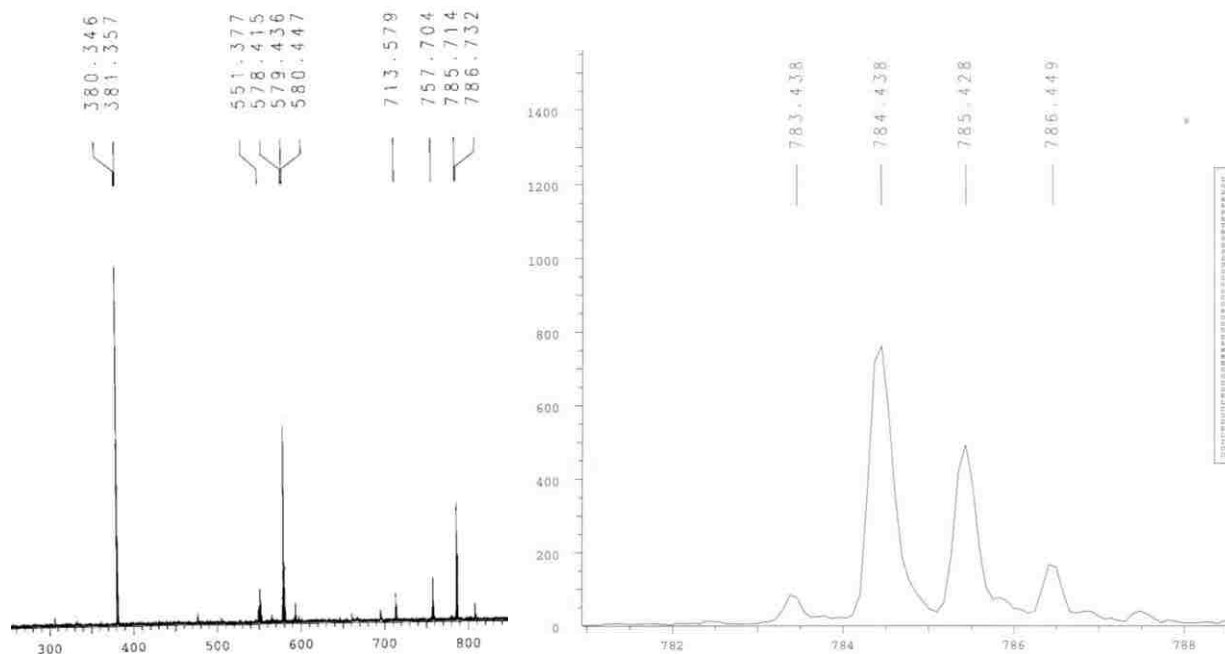
Figure 6-1. MALDI-TOF mass spectrum of the reaction mixture (left) and **6-2** (right) with CCA.
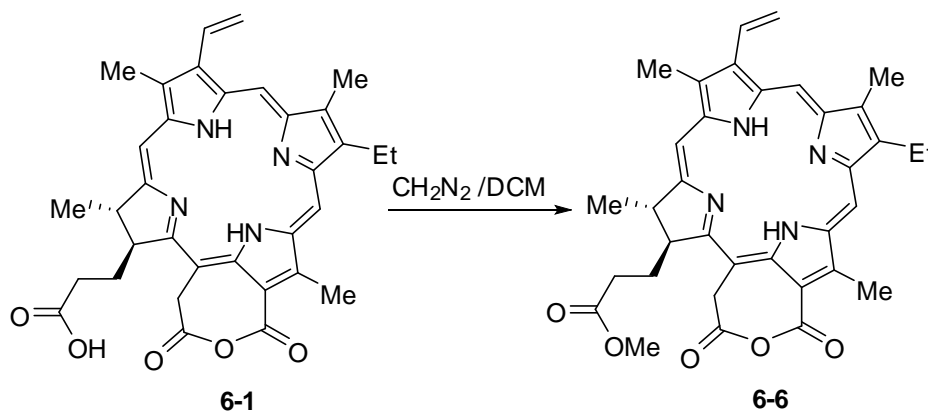
Scheme 6-2. Methylation of **6-1** using diazomethane in DCM to generate **6-6**.

The separation was performed using silica gel TLC, with 10% acetone/DCM as the eluting solvent. However, due to their high reactivity, only tiny amount of pure products could be isolated. Thus only MALDI and UV-vis studies were performed with them. The MALDI-TOF spectrum gave a peak at 578 for the isolated polar compound, which matched with the formation

of **6-1**. MALDI-TOF spectroscopy also gave a peak at 785 for the less polar compound, which matches with the formation of **6-2**. Due to the high reactivity and the ready aggregation behavior associated with the presence of free acids in **6-2**, decent NMR spectra were not possible. In order to obtain good NMR spectra, esterification was performed on **6-1** using excess diazomethane gas under strictly moisture free and nucleophile free conditions (see *Scheme 6-2*).Due to the high reactivity associated with the coupling mixture, the esterification reaction was performed directly
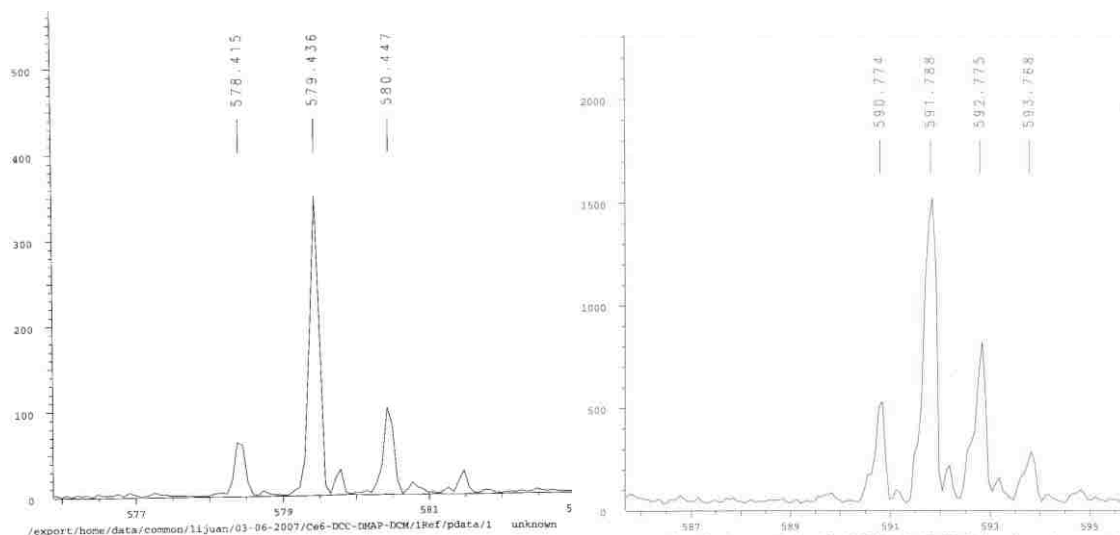
Figure 6-2. MALDI-TOF mass spectra of **6-1** (left) and **6-6** (right) with CCA as matrix.
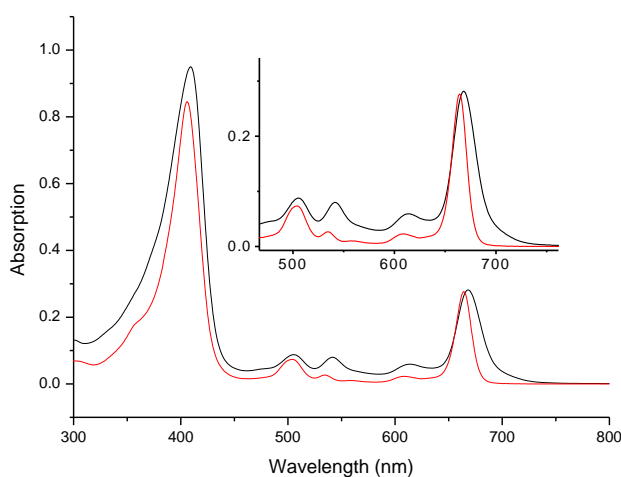
Ce_6	406, 504, 534, 608, 664 nm	Green
6-6	409, 505, 541, 614, 668 nm	Purple

183
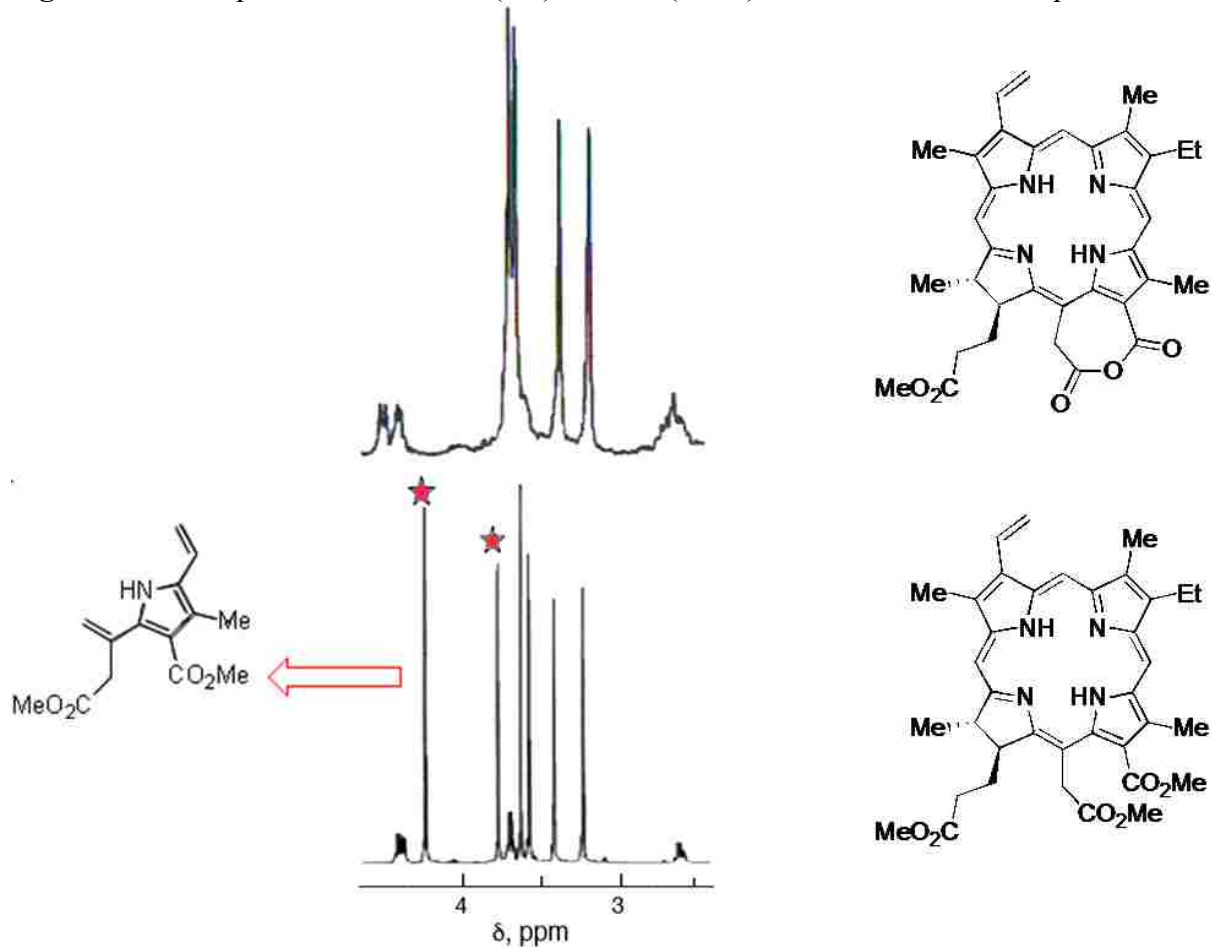
Figure 6-4. Stacked NMR spectra of **6-6** (top) and chlorin-e$_6$ trimethyl ester (bottom).

following the coupling reaction of chlorin-e$_6$ without workup or purification of the coupling mixture. The preparation of **6-6** was performed by blubbing excess amounts of diazomethane gas through the reaction mixture under a N$_2$ atmosphere. As indicated by TLC, the methylation was completed within a couple of minutes. The formation of **6-6** was indicated on TLC as the appearance of a major brown spot. However, after isolation from silica gel TLC plate with 10% acetone/DCM, only a small amount of pure **6-6** was obtained. We attribute this to the high reactivity of anhydride seven-membered-ring of **6-6**. Upon applying it to a silica gel TLC plate, the anhydride ring of **6-6** could easily be opened to form very polar free acids. This, on the other

hand, also supports our rationale that once the anhydride intermediate was formed, the ring opening with a nucleophilic reagent would be extremely efficient. Although **6-6** was quickly removed from the silica TLC plate still no practical way was found to generate a large amount of pure **6-6**. Pure **6-6** was however fully characterized by NMR, MALDI and UV-vis spectra.
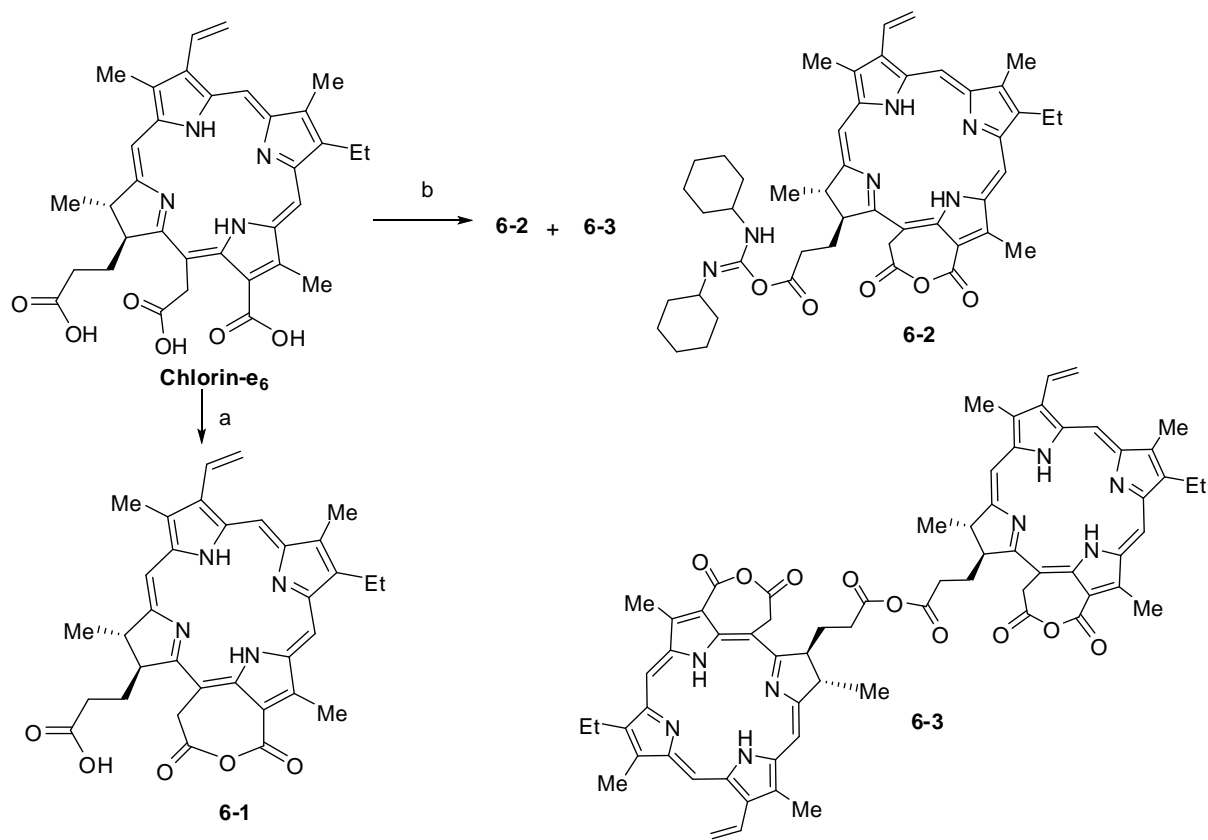
Scheme 6-3. Anhydride ring formation, and byproducts, in chlorin-e$_6$ derivatives. Reaction conditions: a) 1 equiv DCC DMAP, dry DCM, argon, room temperature; b) 1 equiv DCC, dry DCM, argon, room temperature.

MALDI gave a peak at MW 592 for the formation of **6-6** (see *Figure 6-2*). Comparing its UV-vis spectra with that of chlorin-e$_6$ in DMSO, **6-6** showed a red-shift of around 3-7 nm (see Figure 6-3). In our previous report[10], the ring-opening of the isocyclic ring of methyl pheophorbide-*a* to form the trimethyl ester of chlorin-e$_6$ had resulted in a blue shift of around 2-

10 nm in DCM. Contrasting to the ring-opening of pheophorbide-a, the red-shift in this case is attributable to the anhydride ring formation.

We compared the NMR spectra of **6-6** with those in the literature[10] reported for 15^2-LS-11 and also with chlorin-e$_6$ trimethyl ester (see *Figure6-4*). It was found that the methyl ester had been definitely been added at the 17^3-position, while the other two free acids (13^1- and 15^2-positional acids) had been fused to form the anhydride seven-membered-ring. The clear disappearance of two methyl ester peaks in chlorin-e$_6$ trimethylester is shown in Figure *6-4*. While **6-6** was purple in the solid state, it gave a reddish-brown color when dissolved in both DCM and DMSO.

It is worth noticing that base (DMAP) plays an important role in this coupling reaction. When only DCC was used without DMAP, under the same reaction condition there was no formation of the desired product **6-1** (see *Scheme 6-3*). In the absence of DMAP, and increasing DCC up to 5 equivalents, the coupling of chlorine-e$_6$ only generated two undesired products, with **6-2** as a relative major product and **6-3** in a very small amount. MALDI-TOF mass spectra showed two peaks, at MW of 783 for **6-2** and MW of 1138 for **6-3** (*Figure 6-5*).
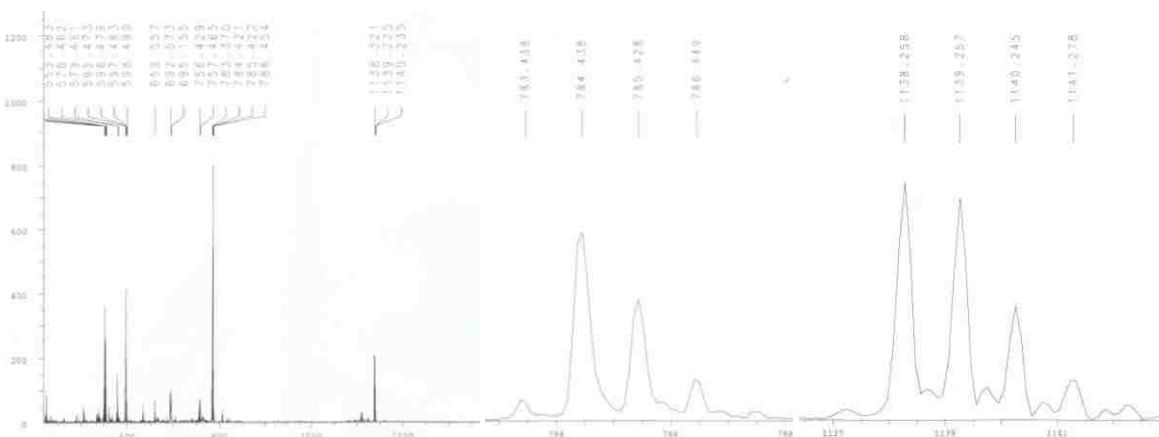
Figure 6-5. MALDI-MS of the reaction mixture (left), **6-2** (middle) and **6-3** (right) with CCA as matrix.

On the other hand, small amounts of DMAP (0.32 equivalent) were enough to efficiently assist the generation of **6-1**, which we believed to be the key intermediate in the generation of **6-6** in our rationale. Also, it was found that increasing the amount of DMAP was helpful to improve the yield of **6-1** based to TLC, but the reaction became slower as a result.
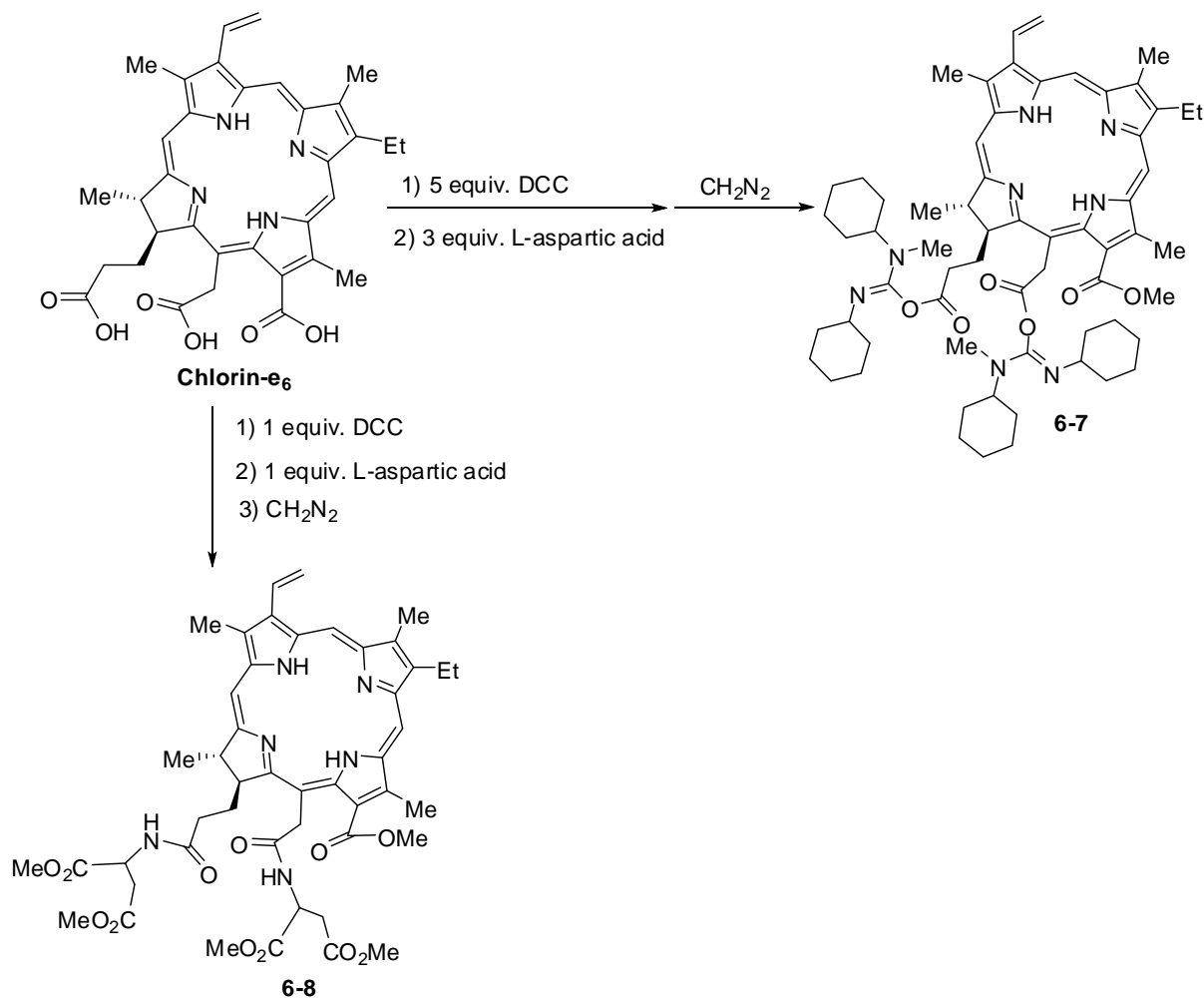
Scheme 6-4. Organic base DMAP plays an important role in the coupling reaction.

The major product generated under these conditions possessed a similar polarity to that of chlorin-e_6 trimethy ester and in turn less polar than **6-10**. There were also several un-isolated low yield byproducts. Moreover, the isolated product was very stable and the purification was performed using a silica gel column, with 20-30% EtOAc/DCM as eluting solvent. After

removing the solvent in vacuum, the major product was obtained as a solid in 24% yield. Based

on MALDI and NMR spectra, we hypothesize it might be the isomer of **6-7**[12]. MALDI-TOF

mass spectra gave a peak at MW 1051 for the major product which matches with the chemical

structure of **6-7** (see *Figure 6-6*). In solution it gave a very intense green color with a slight blue

tinge, which is attributed to the ring-opening of anhydride ring. The unexpected stability of **6-7**

is attributed to the relatively basic media induced by the presence of triethylamine. Also, the

addition of a methyl group to the free base amine in the DCC backbone might be a possible

reason for the high stability. Most of reported coupling reactions are performed undser slightly
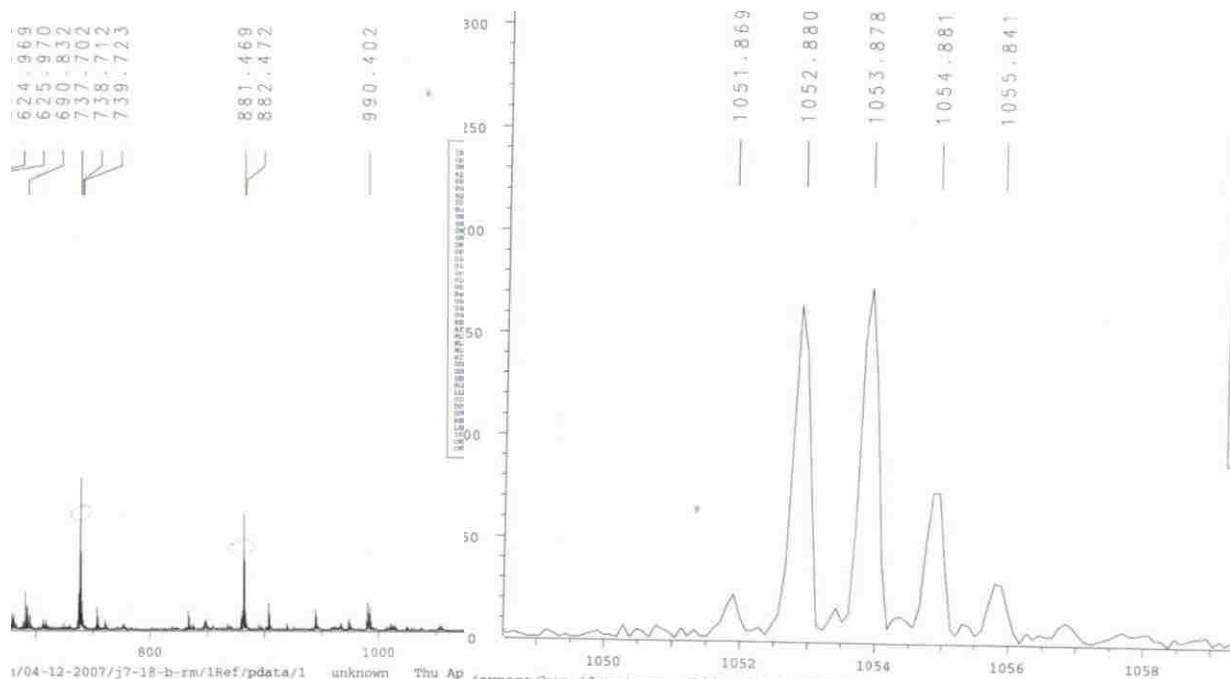
Figure 6-6. MADLI-TOF mass spectra of the coupling reaction mixture in the absence of DMAP before diazomethane esterification (left) and **6-7** (right).

basic or neutral conditions. If the isolated product was the isomer of **6-7**, then the rationale of **6-6**

formation through the seven-member-ring intermediate would also be supported. It should also

be noticed that the use of HBTU instead of DCC/DMAP as the coupling reagent provided only

chlorin-e_6 trimethyl ester, despite the use of different solvents. We attributed this to either the poor solubility of HBTU in organic solvents or the survival problem of the seven-membered anhydide ring of **6-1** in the presence of HBTU, as described in literature[10].
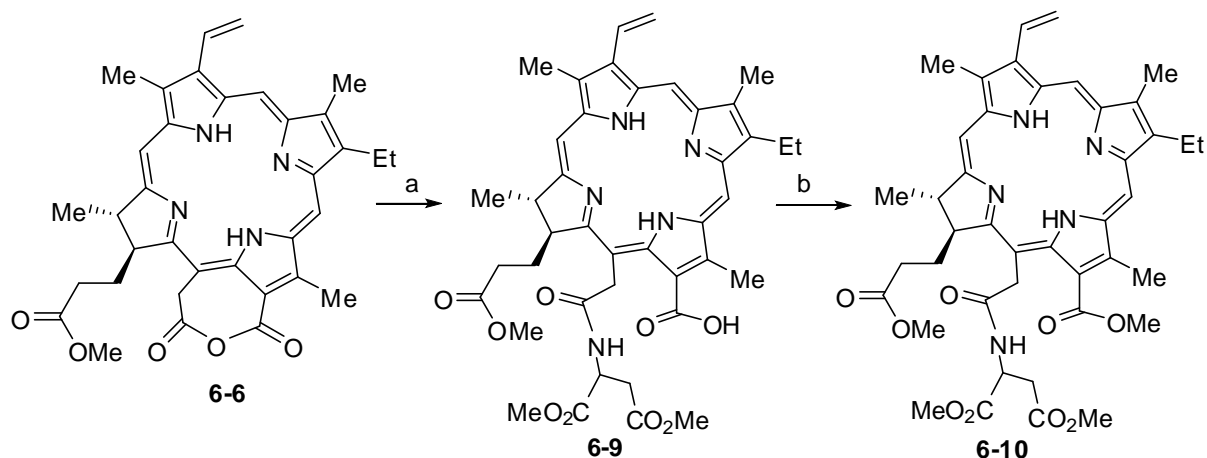
Scheme 6-5. Ring-opening of the anhydride ring. Reaction conditions: a) 1 equi of L-aspartic acid dimethyl ester hydrochloride, 1 equiv triethylamine, dry DCM, room temperature, argon; b) excess diazomethane.
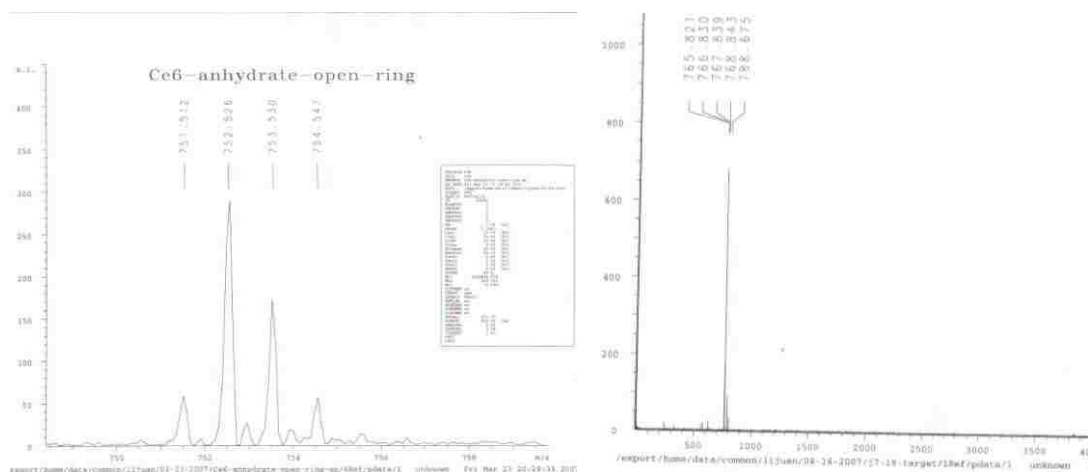
Figure 6-7. MALDI-TOF of **6-9** (left) and **6-10** (right) with CCA as matrix.

After proving the formation of the seven-membered anhydride ring, and finding it to be highly reactive in the presence of nucleophiles, we next needed to prove that the ring opening reaction was occurring exactly at the 15^2-position instead of at 13^1-position. The amino-acid was

189

generated *in situ* from L-aspartic acid dimethyl ester by mixing L-aspartic acid dimethyl ester hydrochlorid with triethylamine in dry DCM, followed by sonication. The coupling reaction mixture of chlorin-e$_6$ with the mixture of DCC/DMAP in dry DCM was used directly for the ring-opening reaction (see *Scheme 6-5*). After most of the chlorin-e$_6$ was converted into **6-6** as indicated by TLC and MALDI-TOF spectra, the freshly prepared L-aspartic acid was added. MALDI-TOF spectra showed the reaction mixture to have a major peak at MW 751 for **6-9**[13].
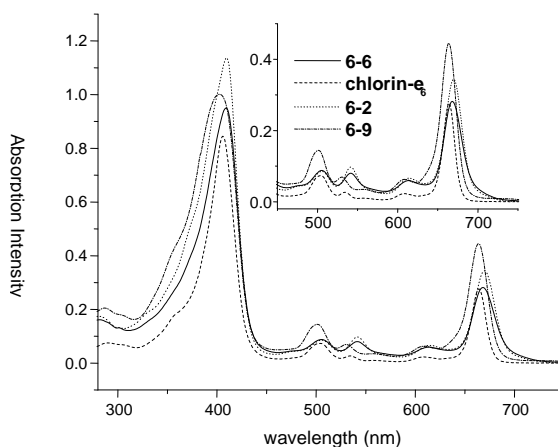
Fig 6-8. The stacked UV-vis spectra in SOLVENT of **6-2**, **6-6**, **6-9** and **chlorin-e$_6$**.

After methylation with excess diazomethane gas in dry DCM, **6-10** was obtained. After isolation from a silica gel column eluted with 30% EtOAc/DCM and removal of solvent under vacuum, pure **6-10** was obtained as a solid in 75% yield. MALDI-TOF spectra gave a peak at MW 765 for **6-10**. After comparing with the literature[10], **6-10** was assigned to be 15^2-positional LS-11. Thus by using MALDI-TOF spectroscopy to follow the reaction and NMR spectroscopy to characterize the key intermediate, we were finally convinced of the underlying anhydride mechanism for the unique formation of "less reactive" 15^2-regioisomer of LS-11. *Figure 6-8*

shows the stacked UV-vis spectra of **6-2**, **6-6**, **6-9** and the starting material chlorin-e_6. The small red-shift presented in both **6-2** and **6-6** is attributed to the formation of the seven-membered anhydride ring intermediate which was absent in both **6-9** and chlorin-e_6.

Chlorin-e_6   **6-11**

Scheme 6-7. Formation of a lysine derivative of chlorin-e_6. Reaction condition: a) 1 equiv DCC/DMAP (1/1), dry DCM, argon, room temperature; b) 1 equiv H-Lys (Boc)-OtBu.HCl, 1 equiv triethylamine, dry DCM, argon, room temperature.

After discovering the underlying mechanism for the unique formation of the 15^2-regioisomer of chlorine-e_6, we also improved its synthesis based on a two-step one-pot reaction. In this improved synthetic route, MALDI-TOF spectra and TLC were used to detect the formation of anhydride intermediate before addition of L-aspartic acid dimethyl ester. By dividing the previous one-step one-port reaction[6,10] into a two-step one-port reaction, the selectivity of the coupling was improved. We also used H-Lys(Boc)-OtBu hydrochloride in place of L-aspartic acid dimethyl ester hydrochloride to test of the versatility of the mechanism and of our improved synthesis (see *Scheme 6-6*). The reaction was performed by using 1 equivalent of DCC and 1 equivalent of DMAP as the coupling reagent to react with chlorin-e_6 in

DCM, subsequently adding amino-acid and esterifying with excess amounts of diazomethane gas. After a silica gel column separation (eluting with 30% EtOAc/DCM), pure **6-11** was obtained in 65% yield. MALDI-TOF spectra gave a peak at MW 907 for the formation of **6-11** (see *Figure 6-9*).
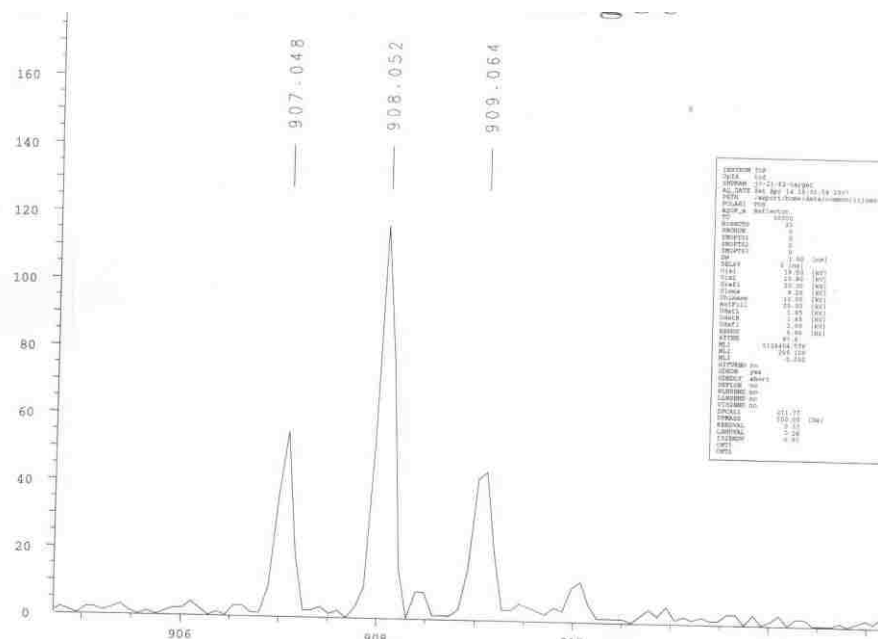
Figure 6-9. MALDI-TOF mass spectrum of **6-11** with CCA as matrix.

The selectivity of this coupling reaction was very high; the only byproduct generated was chlorin-e_6 trimethyl ester.

6.3 Conclusion

In summary, there is a unique-selective formation of the 15^2-positional chlorin-e_6 derivativs when subjecting cghlorin-e_6 to a reaction using a peptide coupling reagent, such as DCC/DMAP. The underlying mechanism for this unique selectivity was shown to involve the intermediacy of a seven-membered anhydride ring derivative. The organic base DMAP was found to play an important role in this unique coupling reaction. Based on this discovery, an

improved synthesis of 15^2-positional chlorin-e_6 was developed, namely a two-step one-pot process and the yield was good. The versatility of this coupling reaction was also tested.

6.4 Experiment

6.4.1 General

Silica gel (32–63 mm) was used for flash column chromatography. All reactions were monitored and some highly reactive compounds were separated by TLC using 0.25 mm silica gel plates with or without UV indicator (60F-254). ^{1}H NMR spectra were obtained on either a DPX-250, ARX-300 or Varian VS-700 spectrometer. Chemical shifts (δ) are given in ppm relative to CD_2Cl_2 (5.32), $CDCl_3$ (7.27) or DMSO-d_6 (2.50) as indicated. Mass spectra were obtained on an Applied Biosystems QSTAR XL instrument. All solvents were obtained from Fisher Scientific (HPLC grade, Houston, TX) and were used without further purification unless indicated. DMSO (Biotech grade solvent, 99.8%) was purchased from Sigma–Aldrich and used without further purification.

6.4.2 Preparation of diazomethane gas (small scale)

The apparatus consists of a Buckner-type conical flask (**A**), which was equipped with a magnetic bar and a rubber stopper, and another Erlenmeyer flask (**B**), which was connected to the conical flask (**A**) through polythene tubing. The stopper on the conical flask (**A**) has two holes, the first one is closed with a rubber septum and the second one is used to hold polythene tubing for the connection to Erlenmeyer flask (**B**). For example, the typical preparation of approximately 59 mmol diazomethane preceeds as follows: Diazald (18g, 84 mmol) was weighed directly into flask (**A**) and ethanol (110 mL, 5 times its weight of diazald) was added. The flask was cooled to 0 ^{o}C by using an ice-bath. Flask (**B**) has the reaction mixture readily for the methylation reaction in dry DCM. There must be a good stream of nitrogen gas continuously pasings through the

whole system. Concentrated aqueous solution of sodium hydroxide was added dropwise through a plastic pipette inserted into the hole on the rubber stopper of flask (**A**). Upon the complete dissolving of diazald, sodium hydroxide was added at a rate of 1 mL every 30 sec. After a few seconds yellow diazomethane gas can be found to pass into flask (**B**), where the desired methylation reaction occured. Continuing adding sodium hydroxide solution until the disappearance of yellow colour in flask (**A**) is observed. TLC monitoring of the solution in flask (**B**) showed complete methylation of the acid. The methylation reaction could complete within couple of minutes.

6.4.3 Preparation of 6-2 and 6-3

Ce_6 (60 mg, 0.1 mmol) was suspended in dry DCM 25 mL under Argon. Concentrated DCC (1 equiv) in dry DCM 5 mL was added into the reaction mixture. After 5-10 minutes, chlorin-e_6 became completely dissolved and the solution showed a brown color. 30 Minutes later, when using TLC to follow the reaction, two new brown spots (initial brown in color, later changing to green) appeared at R_f 0.9 (**6-3**, minor) and 0.8 (**6-2**, major) (as indicate from MALDI-MS spectroscopy) when 10% acetone/DCM was used as eluting solvent. Extending the reaction time (it usually took 3-4 hours), only a small amount of chlorin-e_6 remained according to TLC used to follow the reaction. The MALDI spectrum of the reaction mixture gave a major peak at MW 784 for **6-2** and minor peak at MW 1138 for **6-3**.

6.4.4 The preparation of 6-1 and 6-6

Chlorin-e_6 (60 mg, 0.1 mmol) was suspended in dry DCM 25 mL under argon. Concentrated DCC (1 equiv) in dry DCM solution 5 mL and DMAP (0.32 equivalent) were added into the reaction mixture. After 4 h, TLC (10% acetone/DCM as eluting solvent) showed two major brown sports: the first one at R_f 0.8 (**6-2**, minor) and a second one at 0.4 (**6-1**, major). In

agreement with TLC, the MALDI spectrum of the reaction mixture gave two major peaks, at 578 (**6-1**, major) and 785 (**6-2**, minor). No anhydride dimer (**6-3**) was detected under these conditions. The separation of **6-1** and **6-2** from the reaction mixtures was performed on TLC plates (silica gel) very quickly. Small amounts of each substance were obtained and identified by MALDI mass spectra. However, the separation yield was very low due to decomposition of the compounds. Both UV-vis spectra of the DCC-adduct and anhydride-acid showed several nm red-shifts compared with chlorin-e$_6$ trimethyl ester, due to the formation of an extra seven-membered ring on the chlorin.

The methylation of **6-1** to form **6-6** was performed by bubbling diazomethane gas into the DCM reaction mixture of **6-1**. TLC gave a major brown spot for **6-6**. Separation was performed on TLC plates (silica gel). The desired **6-6** was fully characterized by MALDI-TOF, NMR and UV-vis spectroscopy.

6-6: MALDI-TOF Calcd for C$_{35}$H$_{36}$N$_4$O$_5$, 592.7. Found 592.8. UV-Vis (λmax nm/DMSO): 409, 505, 541, 614, 668; ^{1}H-NMR (CDCl$_3$, 300 MHz) δ 9.57 (1H, s), 9.29 (1H, s), 8.58 (1H, s), 7.98-7.93 (1H, m), 6.35 (1H, dd, J = 17.5 Hz), 6.18-6.16 (1H, dd, J = 11.9 Hz), 5.43 (2H, br), 4.53 (1H, t, J = 8.4 Hz), 4.44 (1H, tr J = 14.7), 3.70-3.67 (8H, m), 3.38 (3H, s), 3.18 (3H, s), 2.70-2.67 (1H, m), 2.60-2.59 (1H, m), 2.38-2.36 (1 H, m), 1.99-1.97 (1H, m), 1.75-1.74 and 1.70-1.68 (6H, m), -0.42 (1H, s), -0.52 (1H, s).

6-7: MALDI-TOF Calcd for C$_{63}$H$_{86}$N$_8$O$_6$,1051.4. Found 1051.9. ^{1}H-NMR (DMSO-d$_6$, 300 MHz) δ 9.74 (1H, s), 9.41 (1H, d, J = 6.0 Hz), 9.13 (1H, t, J = 9.72), 8.20-8.11 (3H, m), 6.41(1H, d, J = 17.8 Hz), 6.13 (1H, d, J = 11.4 Hz), 4.56 (1H, d, J = 6.8 Hz), 4.06 (1H, tetra, J = 7.11 Hz), 3.96 (2H, d, J = 11.0 Hz), 3.84 (2H, s), 3.67-3.62 (6H, d, J = 13.7 Hz), 3.50-3.47 (3H, d, J = 9.8

Hz), 3.38 (3H, s), 3.14 (3H, s), 2.53 (3H, s), 2.01 (2H, s), 1.82-1.71 and 1.63-1.59 (10 H, br), 1.34-1.05 (10H, br), -1.08-1.13 (2H, m).

6-8: MALDI-TOF Calcd for $C_{63}H_{86}N_8O_6$, 1051.4. Found 1051.4. ^{1}H-NMR (CD_2Cl_2, 400 MHz) δ 9.74 (1H, s), 9.41 (1H, s), 9.13-9.09 (1H, m), 8.19-8.11 (3H, m), 6.41 (2H, d, J = 18 Hz), 6.13 (1H, d, J = 12 Hz), 3.96-3.92 (1H, m), 3.83 (2H, s), 3.67-3.62 (2H, m), 3.47 (2H, s), 3.38 (6H, s), 3.14 (3H, s), 2.53 (3H, s), 1.82 (2H, s), 1.60-1.59 (12H, m), 1.22-1.17 (10H, s), -1.08- -1.13 (2H, m).

6-9: MALDI-TOF Calcd for $C_{41}H_{47}N_5O_9$, 753.8. Found 753.5. UV-Vis (λmax nm/DMSO): 402, 501, 530, 609, 664.

6-10: MALDI-TOF Calcd for $C_{42}H_{49}N_5O_9$, 767.9. Found 767.9. ^{1}H-NMR (CD_2Cl_2, 400 MHz) δ 9.71 (1H, s), 9.56 (1H, s), 8.79 (1H, s), 8.07-8.02 (1H, m), 6.36 (1H, d, J = 16 Hz), 6.15 (1H, d, J = 12 Hz), 5.30 (1H, s), 4.89 (1H, s), 4.53-4.50 (2H, m), 4.32 (2H, s), 3.80-3.77 (2H, m), 3.60 (5H, m), 3.48 (2H, s), 3.43 (2H, m),3.30 (2H, s), 3.13 (2H, s), 2.90 (2H, s), 2.33 (2H, s), 2.07 (1H, s), 1.78-1.71 (6H, m), 1.30-1.29 (2H, m), -1.26 (1H, s), -1.38 (1H, s).

6-11: MALDI-TOF Calcd for $C_{51}H_{68}N_6O_9$, 909.1. Found 909.1. ^{1}H-NMR ($CDCl_3$, 300 MHz) δ 9.73 (1H, s), 9.58 (1H, s), 8.78 (1H, s), 8.10-8.01 (1H, m), 6.39 (1H, d, J = 17.8 Hz), 6.17 (1H, d, J = 11.4 Hz), 5.22 (2H, s), 4.53 (3H, s), 4.27 (3H, s), 3.80 (2H, s), 3.59 (3H, s), 3.49 (3H, s), 3.30 (2H, s), 2.91 (2H, s), 2.58 (1H, s), 2.22 (1H, s), 2.06 (2H, s), 1.88 (6H, s) 1.44 (9H, s), 1.29 (9H, s), -1.30 (1H, s), -1.43 (1H, s).

6.5 References

1   Dougherty, T. J.; Gomer, C. J.; Henderson B. W.; Jori, G.; Kessel D.; Korbelik, M.; Moan, J.; Peng, Q. *J. Natl. Cancer Inst*. **1998**, *90*, 889-905.

2   Pandey, R. K.; Zheng, G. In *The Porphyrin Handbook*, Kadish, K. M., Smith, K. M., Guilard, R., Eds.; Academic Press, Boston; **2000**, Vol. 6, pp 157.

3   Vicente, M. G. H. *Current Medicinal Chemistry, Anti-Cancer Agents 1*, **2001**, 175.

4   Spikes, J. D.; Bommer, J. C. In *Chlorophylls*, Scheer, H., Eds; CRC Press, Boston; **1996**, pp 1181.

5   Song, L. -M. W.; Wang, K. K.; Zinsmeister, A. R. *Cancer*, **1998**, *82*, 421.

6   Bommer, J. C.; Ogden, B. F. *U. S. Patent*, **1987**, 4,693,885.

7   Gomi, S.; Nishizuka, T.; Ushiroda, O.; Uchida, N.; Takahashi, H.; Sumi, S. *Heterocycles*,**1998**, *48*, 2231.

8   Abraham, R. J.; Rowan, A. E. In *Chlorophylls*; Scheer, H., Eds.; CRC Press: Boston; **1996**, pp 797.

9   Roberts, W. G.; Shiau, F. -Y.; Nelson, J. S.; Smith, K. M.; Berns, M. W. *J. Natl. Cancer Inst.* **1988**, *80*, 330.

10 Hargus J. A.; Fronczek, F. R.; Vicente, M. G. H.; Smith, K. M. *Photochem. Photobio.* **2007**, *83*, 1006.

APPENDIX: LETTERS OF PERMISSION

From: Lijuan Jiao [mailto:ljiao1@lsu.edu]

Sent: 09 July 2007 17:11

To: CONTRACTS-COPYRIGHT (shared)

Subject: Ask for permission to use my publication for my dissertation

Dear Sir/ Madam:

I am a graduate student from Louisiana State University and I am graduating this summer. I am writing to ask for the permission to use the materials described in my publication for the usage in my dissertation. The Title of the publication is "Benzoporphyrins via an olefin ring-closure metathesis methodology" and it was published in 2006 in the Journal "Chem. Commun." The page number is from 3900-3902.

Thanks for your time and your help.

Sincerely:

Lijuan Jiao

Dear Lijuan Jiao:

The terms and conditions of granting you permission to include the paper in you thesis are given below.

The Royal Society of Chemistry (RSC) hereby grants permission for the use of your paper(s) specified below in the printed or microfilm version of your thesis. You may also make available the PDF version of your paper(s) that the RSC sent to the corresponding author(s) of your paper(s) upon publication of the paper(s) in the following ways: in your thesis via any restricted internal website that your university may have for the deposition of theses, via your university's Intranet or via your own personal website. We are unable to grant you permission to include the paper(s) in any publicly available database/website, including the *ProQuest Dissertation Abstracts Database*. The Royal Society of Chemistry is a signatory to the STM Guidelines on Permissions (available on request).

Please note that if the material specified below or any part of it appears with credit or acknowledgement to a third party then you must also secure permission from that third party before reproducing that material.

Please ensure that the published article states the following:

Reproduced by permission of The Royal Society of Chemistry

Regards

Gill Cockhead

Contracts & Copyright Executive

Gill Cockhead (Mrs), Contracts & Copyright Executive

Royal Society of Chemistry, Thomas Graham House

Science Park, Milton Road, Cambridge CB4 0WF, UK

Tel +44 (0) 1223 432134, Fax +44 (0) 1223 423623

http://www.rsc.org and http://www.chemsoc.org

From: Lijuan Jiao [mailto:ljiao1@lsu.edu]

Sent: 09 July 2007 17:36

To: Rights and Permissions (ELS)

Subject: Request the permission to use my publications for my dissertation

Dear Sir/ Madam:

   I am a graduate student from the Chemistry Department of Louisiana State University and I am graduating this summer. I am writing to request the permission to use the materials described in the following two papers (I am the first author for both of papers) for the usage in my dissertation.

Paper 1: "Syntheses and properties of functionalized oxacalix[4]arene porphyrins", published in the Journal "Tetrahedron" in 2007, and the volume is 63 and page numbers are from 4011-4017.

Paper 2: "beta-beta Linked cofacial bis-porphyrins", published in the Journal "tetrahedron Letters" in 2006. The Volume number is 47 and the page numbers are from 501-504.

Thanks for your time and your kind help.

Sincerely:

Lijuan Jiao

From: "Rights and Permissions (ELS)" <Permissions@elsevier.com>

To: "Lijuan Jiao" <ljiao1@lsu.edu>

Subject: RE: Request the permission to use my publications for my dissertation

Date: 2007 年 7 月 11 日 4:53:06

Dear Lijuan Jiao

Thank you for your e-mail.

Elsevier is pleased to announce our partnership with Copyright Clearance Center's Rightslink service. With Rightslink ® it's faster and easier than ever before to obtain permission to use and republish material from Elsevier.

In this instance the link to the requested material is http://dx.doi.org/10.1016/j.tetlet.2005.11.065

For future requests simply visit: http://www.sciencedirect.com/ and locate your desired content.

Click on Permissions within the table of contents or in the tool-box to the right of the online article to open the following page:

1. Select the way you would like to reuse the content

2. Create an account if you haven't already

3. Accept the terms and conditions and you're done

Please contact Rightslink Customer Care with any questions or comments concerning this service:

Copyright Clearance Center

Rightslink Customer Care

Tel (toll free): 877/622-5543

Tel: 978/777-9929

E-mail: mailto:customercare@copyright.com

Web: http://www.rightslink.com

VITA

Lijuan Jiao was born on December 10, 1977, in Guoyang county, Anhui province, China. She enrolled in Shandong Univeristy, Jinan, China, in 1996. From Shandong University, she earned her Bachelor of Science degree in chemistry in June of 2000. For her master degree study in chemistry, she enrolled in University of Science &Technology of China, Hefei, China, where she earned her Master of Science degree in chemistry in June of 2003. In August of 2003, with the financial support from the Department of Chemistry of Louisiana State Univeristy (LSU), she came to LSU to begin her doctoral degree study in chemistry and soon joined Professor Kevin M. Smith's research group to begin doing research in porphyrin chemistry.